THE
PHYSICAL REVIEW

A journal of experimental and theoretical physics established by E. L. Nichols in 1893

SECOND SERIES, VOL. 73, NO. 10 MAY 15, 1948

Fission of Elements from Pt to Bi by High Energy Neutrons

E. L. KELLY AND CLYDE WIEGAND
Radiation Laboratory, Department of Physics, University of California, Berkeley, California
(Received February 9, 1948)

The neutron beam of the 184-inch cyclotron has been used to produce fission in elements from Pt to Bi. The atomic fission yields relative to thorium for 84-Mev neutrons are bismuth 0.019, lead 0.0055, thallium 0.0032, mercury 0.0023, gold 0.0020, and platinum 0.0009. Yield curves for reduced neutron energies were determined. Significant differences in the fission yields of the abundant lead isotopes were found. With 84-Mev neutrons the maximum fission fragment ionization relative to thorium was 0.8 for bismuth and ranged down to about 0.7 for gold.

I. INTRODUCTION

THE fast neutron fission of U^{238} and Th^{232} suggests that with neutrons of sufficiently high energy fission can occur in elements of lower atomic number. Several attempts to detect the fission of bismuth and lead have been made. Broda and Wright[1] bombarded bismuth and lead with neutrons of maximum energy of about 14 Mev produced by 900-kev deuterons on lithium. They then made chemical separations in an attempt to detect any radio-iodine, which might have been formed as a fission product. They could find no positive evidence of fission and concluded that for neutrons from their deuterons on lithium reaction the ratio of cross sections of lead to U^{238} was less than 1.3×10^{-5} and that the ratio of cross sections of bismuth to U^{238} was less than 5×10^{-5}. Broda also exposed photographic plates containing lead and bismuth salts to neutrons from the same Li-D source and could find no tracks ascribable to the fission of these elements. J. G. Hamilton and H. York (unpublished) have looked for fission in bismuth with neutrons from 20-Mev deuterons on lithium, with negative results. Chemical identification of fission products in bismuth and lead bombarded with neutrons from the 184-inch cyclotron has been reported by I. Perlman *et al.*[2]

In this paper we shall describe experiments which have demonstrated the fission of bismuth, lead, thallium, mercury, gold, and platinum in the intense neutron beam of the 184-inch Berkeley cyclotron. We have also measured the relative fission yields of these elements at various neutron energies. The method of investigation was the detection of the ionization produced by the recoil fission fragments from a sample placed in an argon filled ionization chamber. The chamber was exposed to the neutron beam as indicated in Fig. 1. The individual pulses from electron collection in the argon were fed into a linear amplifier and the amplified pulses were recorded by a scaling circuit and a mechanical register.

[1] Broda and Wright, Nature **158**, 871 (1946).

[2] I. Perlman, R. H. Goeckermann, D. H. Templeton, and J. J. Howland, Phys. Rev. **72**, 352 (1947).

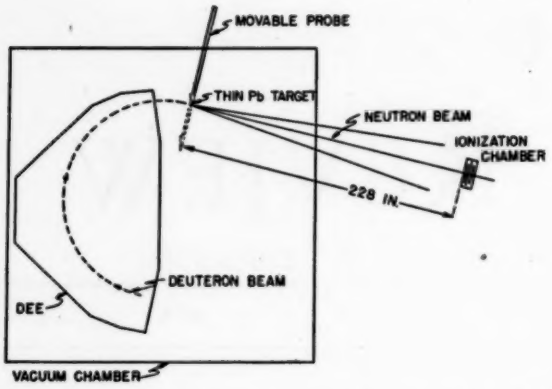

FIG. 1. Experimental arrangement showing the position of the internal target of the cyclotron, the direction of the neutron beam, and the position of the ionization chamber.

A double ionization chamber was chosen in order that the fission pulses from a comparison sample could be observed at the same time and in the same position in the beam as the element under investigation. Thorium was used as a monitor because it does not undergo fission by slow neutrons. The use of electron collection and fast amplifiers was essential in distinguishing between fission fragment ionization and the background ionization produced by the pulsed beam of the synchro-cyclotron.

2. NEUTRON BEAM

The neutron beam used in this experiment was produced by bombardment of a thin internal target of lead with accelerated deuterons. With deuterons of an estimated energy of 190 Mev the neutron beam has a total angular width at half-maximum of about 10°.[3] According to Serber[4] the narrow beam of high energy neutrons is largely produced by a process in which the proton is stripped off the deuteron while the neutron proceeds with approximately the velocity of the incident deuteron. The mean energy of the emergent neutrons is given by the equation

$$E_n=\tfrac{1}{2}(E_d-E_b-E_t),$$

where E_d is the energy of the bombarding deuteron, E_b the energy required by a deuteron to penetrate the Coulomb field of a target nucleus (12 Mev for Pb), and E_t is the average energy lost by a deuteron in the target before being stripped. Thus it is possible to vary the energy of the neutron beam by varying the energy of the bombarding deuterons. This is accomplished by intercepting the deuteron beam in the cyclotron at suitable radii. A schematic diagram of the general arrangement is shown in Fig. 1. The energy of the deuteron beam as a function of its radius has been calculated from measured values of cyclotron magnetic field strength. Values of E_d, E_t, E_n, and ΔE_n at various radii are given in Table I. ΔE_n is the total width at half-maximum of the energy distribution curve for a thin target. According to Serber, ΔE_n in the forward direction, and for an opaque nucleus is given by

$$\Delta E_n=1.030(\epsilon_d E_d)^{\frac{1}{2}},$$

where ϵ_d is the binding energy of the deuteron (2.18 Mev). This does not include uncertainties in energy due to the finite thickness of the target.

TABLE I. Neutron energies in Mev at various cyclotron target radii. E_d is the calculated deuteron energy; E_t is the average energy lost by a deuteron in the target; E_n is the calculated energy of the emergent neutrons; and ΔE_n is the total energy width at half-maximum of the energy distribution curve, which takes into account only neutrons in the forward direction.

Target radius in inches	E_d	E	E_n	ΔE_n
81	190	10	84.0	20.9
75	168	11	72.5	19.7
70	150	12	63.0	18.6
65	132	13	53.5	17.4
60	114	14	44.0	16.2
55	97	16	34.5	15.0
50	81	19	25.0	13.7

3. APPARATUS

The double ionization chamber consisted of three insulated parallel plates mounted in a steel housing. The parallel plates had an area of 100 cm² each and were separated by a distance of 1.5 cm. The center plate was maintained at a potential of −800 volts supplied by a dry cell battery pack and the chamber was filled with argon at atmospheric pressure. The comparison sample was mounted on one side of the center plate and the sample to be studied was mounted on the opposite side of the center plate. The two outer plates were the collecting electrodes and together with the center plate formed two separate parallel plate ionization chambers. A linear amplifier was connected to each collecting electrode and the output of each

[3] A. C. Helmholtz, E. M. McMillan, and D. C. Sewell, Phys. Rev. **72**, 1003 (1947).
[4] R. Serber, Phys. Rev. **72**, 1008 (1947).

amplifier was fed into the pulse height discriminator of a scaling circuit. The amplifiers had a time of rise of 0.2 microsecond and a decay time constant of 5 microseconds; the bias of the discriminator circuits could be adjusted to reject pulses below any specified height. The number of pulses passed by each discriminator was recorded by a mechanical register and the interpolation system of the scaling circuit. A cathode-ray oscillograph provided continuous visual inspection of the amplified fission pulses.

Two samples of bismuth were prepared by evaporating bismuth upon a backing of aluminum. One bismuth sample was thin compared to the range of fission fragments (0.2 mg cm^{-2}) and the other was thick (10 mg cm^{-2}). Two samples of thorium were used, one thick and one thin compared to the range of fission fragments. The thin sample was composed of about one mg cm^{-2} of ThO_2 deposited on an aluminum backing over an area of 44 cm^2 and contained 32 mg of thorium metal; the thick sample was a foil of thorium metal having an area of 2.93 cm^2 and a weight of 120 mg cm^{-2}. The samples of platinum, gold, and ordinary lead were commercially available foils and the thallium was rolled into foil; these were thick compared to the range of fission fragments. The mercury sample was a pool of liquid mercury. Lead enriched in Pb^{208} was electroplated upon a copper support forming a deposit which weighed 10 mg cm^{-2}. A similar sample was prepared from radiogenic Pb^{206}. Except for the thorium, each sample had an area of 80 cm^2.

4. EXPERIMENTAL PROCEDURE AND RESULTS

The operating amplifier gain and scaling circuit discriminator bias were determined by counting fission pulses from a thin bismuth sample at various bias settings. The thin bismuth sample was placed in one side of the double chamber and the thin thorium comparison foil was placed in the other side. During the time that the bismuth fissions were counted the neutron beam was monitored by recording with fixed bias the fissions from the thorium foil. A plot of these data gives the number *versus* bias curve shown in Fig. 2. Fission pulses from the thorium sample also were counted at various bias settings of the thorium channel discriminator while the neutron beam was monitored by recording with fixed bias the fissions from the bismuth sample. The resulting number *versus* bias data are plotted in Fig. 3. The curves of Figs. 2 and 3 indicate suitable operating biases. The arbitrary units of the bias scales in these figures were made equal by inter-calibrating with signals from a pulse generator. The bias curves are affected by the pulses of ionization produced by the neutrons crossing the ionization chamber during the output times of the cyclotron.

The working conditions of the ionization chambers could be checked at any time by observing the natural alpha-particle pulses from the thorium and the pulses from a small source of polonium placed adjacent to the sample under investigation. The pulse height of the alpha-particles also served as a rough calibration of the fission pulse height.

With the cyclotron target at 81 inches radius (neutron energy 84 Mev) fission counts from each of the thick samples were measured relative to the fission counts of the comparison foil of thick thorium. Differences in the counting efficiencies of channels 1 and 2 were minimized by counting the sample under investigation with channel 1

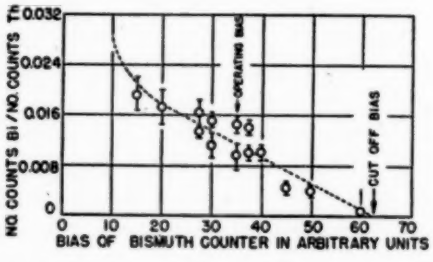

FIG. 2. Number of counts of fission in Bi as a function of bias, monitored with a Th fission counter kept at constant bias.

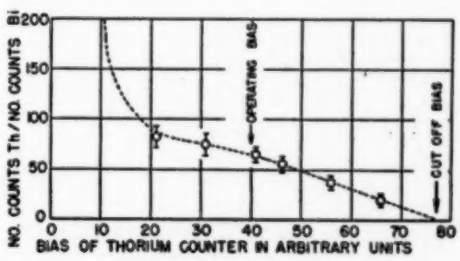

FIG. 3. Number of counts of fission in Th as a function of bias, monitored with a Bi fission counter kept at constant bias.

TABLE II. Fission yields relative to thorium for neutron energy of 84 Mev.

Element	Bi	Pb	Tl	Hg	Au	Pt	Background
Fission yield per atom relative to Th	0.019	0.0055	0.0032	0.0023	0.0020	0.0009	0.00005

and the thorium with channel 2 and then interchanging the leads to the chamber so that channel 2 counted the sample under investigation and channel 1 counted the thorium. The geometric mean of the ratios so obtained was used for computing the yields relative to thorium. The values listed in Table II are corrected for the difference in area of the thorium comparison foil and the thick samples tested.

Fission counts of the thick samples of bismuth, ordinary lead, thallium, mercury, gold, and platinum were measured at various neutron energies using the thin thorium foil as a beam monitor only. The arbitrary yield scales of the excitation curves obtained in this manner were adjusted so that the values at 81 inches radius coincided with those given in Table II. The data of Fig. 4 represent thick target fission yields relative to bismuth. It should be remarked that

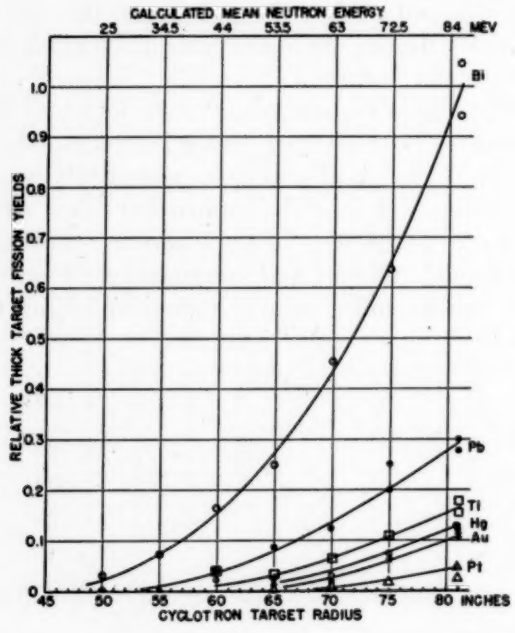

FIG. 4. Relative fission yields as a function of the mean energy in the neutron beam.

TABLE III. Fission yields of three samples of lead differing in isotopic composition and the calculated yields of the abundant isotopes. The neutron energy was 84 Mev.

Lead sample	Isotopic composition 206	207	208	Observed fission yield relative to Th	Pure Pb isotope	Calculated yield relative to Th
1	0.93	0.07	0	0.0071±0.0004	206	0.0070±0.0005
2	0.02	0.08	0.90	0.0036±0.0001	207	0.0101±0.002
3	0.25	0.23	0.52	0.0055±0.0003	208	0.0028±0.0003

these curves are distorted by the spread in neutron energies (ΔE_n in Table I). Thus, even though a true excitation curve might rise abruptly from zero yield at a certain energy, this threshold point would be obscured by the spread in energy of the neutron beam.

Actually, the number of fissions recorded is clearly proportional to

$$\int \sigma(E)N(E)dE,$$

where (E) is the cross section as a function of energy, $N(E)$ is the flux of neutrons with energy between E and $E+dE$ and the integral is extended over the whole neutron spectrum. It is not inconceivable that the main contribution to the integral may come from the high energy tail of the neutron distribution because even if $N(E)$ is small $\sigma(E)$ may have become so large as to overcompensate for the smallness of $N(E)$.

A rough check on the value given in Table II (0.019) of the fission yield of bismuth relative to that of thorium for the neutron distribution obtained with the maximum energy deuterons can be determined from the number *versus* bias curves of Figs. 2 and 3 and the weights of the thin samples. The result is 0.022 ± 0.006.

The fission yields of three samples of lead differing in isotopic composition were measured at the maximum neutron energy by the compensating method previously described. The composition of the samples together with the observed and computed yields are presented in Table III. The errors given in the yield values are standard erros based upon internal consistency and should be reliable for comparison purposes. The samples were checked for uranium and thorium impurities by counting fissions at reduced neutron energies. The reduced yields

were those expected from the lead excitation curve of Fig. 4.

An effort was made to determine the maximum fission fragment ionization of bismuth, thallium, and gold relative to that of thorium by finding the ratios of the maximum pulse heights. The maximum pulse heights were determined by the cut-off bias of the number *versus* bias curves. Figures 2 and 3 indicate that bismuth produces 0.8 of the ionization of thorium fission. From Fig. 5 gold and thallium appear to give 0.7 as much ionization as thorium. Visual observations with the oscillograph are in agreement with these values.

The use of thick samples in the measurement of fission yields causes the observed yields to depend upon pulse height, which in turn depends upon the ionization released by the recoil fission fragment. With the operating conditions used in our experiment this means that the thick sample yield values probably are uncertain by as much as 20 percent. It is unlikely, however, that this introduces any appreciable error into the ratio of the lead isotope yields listed in Table III.

An interesting application of the preceeding work is the construction of neutron counters sensitive only to very high energy neutrons. Such instruments have been built and are currently used in the Radiation Laboratory. They will be described elsewhere.

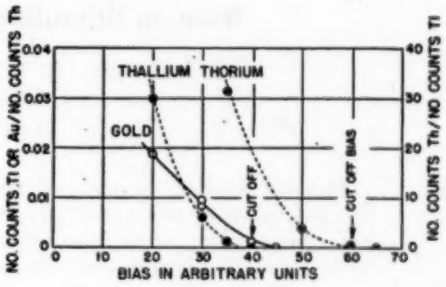

FIG. 5. Ratio of the number of fission counts in a chamber with variable bias *versus* a monitor held at constant bias. In the curves labeled thallium and gold a thorium monitor has been used. In the curve labeled thorium a thallium monitor was used.

ACKNOWLEDGMENTS

The authors wish to thank Professors Ernest O. Lawrence, Edwin M. McMillan, and Emilio Segrè for their interest and helpful discussions; Dr. E. H. Huffman and L. J. Beaufait for the preparation of the lead isotope samples; and the crew of the 184-inch cyclotron for their fine cooperation. This paper is based on work performed under Contract No. W-7405-Eng-48, with the Atomic Energy Commission, in connection with the Radiation Laboratory, University of California, Berkeley, California.

Note on Stimulated Decay of Negative Mesons

S. T. EPSTEIN, R. J. FINKELSTEIN, AND J. R. OPPENHEIMER
Institute of Advanced Study, Princeton, New Jersey

(Received February 5, 1948)

Theories in which the decay of negative mesons is accelerated by electrostatic fields are investigated. Such theories always give radiative decay for free mesons. The competition of radiationless decay of negative mesons increases with Z^5, and the two rates become equal for a value of Z, which depends somewhat on the choice of coupling, but which, for one simple form, is 12. Experimental evidence probably disproves theories of this kind.

VALLEY and Rossi[1] have reported their studies of the decay of mesons in aluminum. They find that the lifetime of negative mesons in that material is about $\frac{1}{3}$ that of positive mesons. They also refer to the suggestion* that the shortened lifetime may be interpreted, not in terms of competing nuclear capture of mesons, but by the acceleration of the decay process itself, presumably because of the strong electric fields acting on negative mesons when they are bound in atomic states. If this were true, we should clearly have a natural interpretation of the regular and marked decrease of observed delayed coincidences from negative mesons as the effective intensity of the electric field increases with atomic number.

One general feature of any theory which provides for appreciable acceleration of meson decay by electric fields needs first to be noted. In effect, even in the absence of matter, fluctuating electric fields, ascribable to the vacuum fluctuations, will always be present. These will in turn lead to stimulated decay accompanied by the emission of light quanta. Thus, in all theories of this kind, the decay of mesons in free space must, at least frequently, be accompanied by γ-ray emission. When negative mesons are trapped in matter, the electrostatic fields of the nuclei compete with the fluctuation fields, giving rise to processes in which no quanta are emitted, and whose probability may be expected to increase markedly with atomic number.

We wish to report briefly some typical calculations bearing on this point. However, we need to note, in a preliminary way, that the evidence[2] as it stands is probably not compatible with the view that normal meson decay involves light quantum emission. It need hardly be pointed out that the results of Anderson[3] and his collaborators in which a decay positron has an observed energy of 25 Mev *could* readily be explained in these terms.

For the calculations we have assumed that the spin of the meson is 0 (it cannot be greater than $\frac{1}{2}$); it then does not affect these results whether the meson field is scalar or pseudoscalar.

One might at first take, as a simple interaction which promises to account for a stimulated decay, the coupling

$$g\varphi_n^+\gamma^\mu\varphi_e\partial_\mu U+\text{complex conjugate}, \qquad \text{(A)}$$

where φ_n, φ_e, and U are the neutrino, electron, and meson wave functions and $\partial_\mu=(\partial/\partial x_\mu)-(ie/\hbar c)A_\mu$. As is well known, the free disintegration of a meson into electron and neutrino is highly forbidden with this coupling, and one might suppose that electromagnetic fields would circumvent the selection rule. That this is not true follows from the remark of Nelson,[4] that, in fact, the coupling (A) is for these purposes equivalent to the scalar coupling

$$g(m/\mu)\varphi_n^+\varphi_e U, \qquad \text{(A')}$$

(with m the electron, μ the meson, masses) except for terms of higher order in g, which do not enter here. Estimates based on these couplings indicate that the decay rate in aluminum

[1] G. Valley and B. Rossi, Phys. Rev. **73**, 177 (1948).

* These questions were discussed at the Ram Island Conference sponsored by the National Academy of Sciences, June, 1947.

[2] For example, R. D. Sard, and E. J. Althaus (to be published).

[3] Anderson, Adams, Lloyd, and Rau, Phys. Rev. **72**, 724 (1947).

[4] E. C. Nelson, Phys. Rev. **60**, 830 (1941).

is not changed by more than 1 percent from the rate for free mesons.

We have, therefore, examined more complex coupling schemes, such as are obtained by adding to the Lagrangian one of the four following forms

$$gF_{\mu\nu}\varphi_n^{+}\gamma^{\mu}\gamma^{\nu}\varphi_e U, \tag{B}$$

$$gF_{\mu}{}^{\nu}\varphi_n^{+}\gamma^{\mu}\varphi_e\partial_{\nu}U, \tag{C}$$

$$gF_{\mu}{}^{\nu}U\partial_{\nu}(\varphi_n^{+}\gamma^{\mu}\varphi_e), \tag{D}$$

$$gF_{\mu}{}^{\nu}U\varphi_n^{+}\gamma^{\mu}\partial_{\nu}\varphi_e. \tag{E}$$

Of these, we have examined only (B) and (C) in detail. The result of the calculation can be expressed in terms of the ratio λ_s/λ_f where λ_f is the rate of ternary free decay, and λ_s is the rate of binary stimulated decay for a negative meson trapped in its atomic K-shell. These ratios are completely fixed by the coupling, and of course independent of the value of g. The results are

$$\lambda_s/\lambda_f=(256/3)(e^2/\hbar c)^4Z^5 \text{ for (B)},$$
$$=1280(e^2/\hbar c)^4Z^5 \text{ for (C)}.$$

The general character of these results can be understood by a simple argument. The vacuum fluctuations leading to the emission of quanta of energy $\sim\mu c^2$ can be characterized by an electric field of the order

$$E_f=(\hbar c)^{\frac{1}{2}}/(\hbar/\mu c)^2.$$

On the other hand, the electric field acting on a meson in the K-shell is

$$E_k=Ze/[(\hbar/\mu c)(\hbar c/e^2)Z^{-1}]^2.$$

Hence, for the ratio of the two rates

$$(E_k/E_f)^2=Z^6(e^2/\hbar c)^5. \tag{1}$$

Detailed calculation shows, however, that in these high energy disintegrations the effective distance of the meson from the nucleus is

$$(\hbar/\mu c)(Ze^2/\hbar c)^{-\frac{1}{2}}$$

rather than the K-radius

$$(\hbar/\mu c)(Ze^2/\hbar c)^{-1},$$

as assumed above. This alters the ratio (1) to

$$Z^5(e^2/\hbar c)^4. \tag{2}$$

We can compare these results with the findings of Valley and Rossi by asking for what value of Z we get a λ_s twice the value of λ_f. Valley and Rossi find $Z\sim13$; (B) gives $Z=24$; (C) gives $Z=14$. This latter result would clearly be consistent with experiment. Because of the unlikelihood that the basic mechanisms here proposed are realized in nature, we have not examined the cases (D) and (E) in detail.

It is, of course, conceivable that the acceleration of decay would have to be ascribed, not to the electric fields of nuclei, but to the charge density itself. In this case, free decay would not involve γ-ray emission, though it would involve pair emission. It has not seemed profitable to explore these complex alternatives.

The Disintegration of Antimony 124

BERNARD D. KERN, DANIEL J. ZAFFARANO, AND ALLAN C. G. MITCHELL
Indiana University, Bloomington, Indiana

(Received February 5, 1948)

The radiations from antimony bombarded by slow neutrons have been investigated with the help of a magnetic lens spectrometer. Compton electrons, ejected from a copper radiator, and photoelectrons ejected from a thin lead radiator, were measured. Gamma-rays of the following energies were found: 2.062, 1.708, 0.714, 0.650, and 0.603 Mev. The beta-ray spectrum was measured and found to be complex. An analysis according to the Fermi theory gives the possibility of resolving the spectrum into five groups with the following end-point energies and relative abundances: 2.37 Mev, 21 percent; 1.62 Mev, 8 percent; 1.00 Mev, 9 percent; 0.65 Mev, 44 percent; 0.48 Mev, 18 percent. An internal conversion line was detected corresponding to a gamma-ray of 0.603 Mev. A gamma-ray attributed to Sb^{122}(2.8d) was found to have an energy of 0.568 Mev.

1. INTRODUCTION

THE nuclear radiations from antimony have been studied by a number of investigators during the past several years with somewhat discordant results. Since some of the early work on antimony[1] was performed in this laboratory, it was thought wise to make a careful investigation of Sb^{124} using the several different types of spectrometers now available to us. Accordingly, this paper and the two associated papers from this laboratory—one by Cook and Langer, using a large 180° magnetic spectrometer, and one by Jurney and Mitchell on coincidence work—give the results of the work. The two investigations of the energy of beta- and gamma-rays, one with the 180° spectrometer and one with the magnetic lens, were carried on independently and the results compared after the observations were completed. The satisfactory agreement between the two sets of observations gives a nice check on the calibration of the apparatus used. This paper will embody the results obtained using the magnetic lens spectrometer.

Antimony has two stable isotopes, Sb^{121} and Sb^{123}, from which the well-known radioactive isotopes Sb^{122} (2.8 days) and Sb^{124} (60 days) can be formed from neutron capture.[2] In addition, several short lived radioactive isomers have recently been discovered by Der Mateosian, Goldhaber, Muehlhause, and McKeown.[3] Of these, the ones with period of 1.3 min. and 21 min. are ascribed to Sb^{124}, and that of 3.5 min. is ascribed to Sb^{122}. These isomers, however, are not disturbing factors in the work reported in this paper.

The radiations from Sb^{124} have been variously described. Amaki and Sugimoto[4] found a beta-ray end point, by absorption, of 1.64 Mev. Mitchell, Langer, and McDaniel using similar methods obtained an end point of 1.53 Mev. Hales and Jordan,[5] using a beta-ray spectrograph, found the spectrum to be complex and resolvable into two groups with end points at 0.74 and 2.45 Mev, while Miller and Curtiss,[6] using similar apparatus, found end points at 0.53 and 2.25 Mev. Jnanananda,[7] using a magnetic lens, found one group at 0.654 and a higher energy group.

The gamma-rays have been investigated by several observers. Measurements on the range of Compton electrons produced in aluminum were made by Mitchell, Langer, and McDaniel, with the help of coincidence counting techniques, and yielded a value for the most energetic gamma-ray of 1.82 Mev. In addition, they presented some evidence for the existence of radiation of a much lower energy. Meyerhoff and Scharff-Goldhaber[8] using similar techniques found gamma-rays at

[1] A. C. G. Mitchell, L. M. Langer, and P. W. McDaniel, Phys. Rev. **57**, 1107 (1940).
[2] J. T. Livingood and G. T. Seaborg, Phys. Rev. **55**, 414 (1939); *ibid.*, Rev. Mod. Phys. **12**, 30 (1940).
[3] E. Der Mateosian, M. Goldhaber, C. O. Muehlhause, and M. McKeown, Phys. Rev. **72**, 1271 (1947).
[4] T. Amaki and A. Sugimoto, Inst. Phys. and Chem. Research, Tokyo, Sci. Paper No. 853, 1656 (1938).
[5] E. B. Hales and E. B. Jordan, Phys. Rev. **64**, 202 (1943).
[6] L. C. Miller and L. F. Curtiss, Phys. Rev. **70**, 983 (1946).
[7] S. Jnanananda, Phys. Rev. **72**, 1124 (1947).
[8] W. E. Meyerhoff and G. Scharff-Goldhaber, Phys. Rev. **72**, 273 (1947).

approximately 1.7 and 0.6 Mev. Kruger and Ogle[9] measured the energy of pairs formed in a cloud chamber and observed a gamma-ray of 1.70 ±0.04 Mev, while Feister and Curtiss,[10] using a magnetic lens, found a gamma-ray energy of 0.6 Mev. Rall and Wilkinson[11] measured photoelectrons in a magnetic lens and concluded that there was a gamma-ray of energy 1.72 Mev. Several investigators have made experiments on the energy of neutrons produced by the gamma-rays of Sb^{124} on Be. The results obtained by the various investigators are: 1.75±0.04, by Klaiber and Scharff-Goldhaber,[12] 1.73±0.04 by O'Neal,[13] 1.67 by Wattenberg,[14] 1.704±0.012 by Hughes and Eggler.[15] Out of this group, no one investigator measured both the beta-ray spectrum and the energy of the gamma-ray lines in an instrument of high resolving power.

2. APPARATUS

The apparatus used was a magnetic lens of rather conventional design.[16] A detailed description will be given elsewhere, but the main features are shown in Fig. 1. The vacuum housing is a brass tube 7 in. in O.D. and 7 ft. long. The magnetic field, along the axis, is furnished by the coil *C*, which consists of 4124 turns of No. 14 wire. The inside and outside radii of the coil are 10.0 and 28.9 cm, respectively; the thickness is 10 cm and the field along the axis at the center of the coil is 141 gauss/amp. The baffle system is mounted on longitudinal "stringers" and slides into the tube from the end *E*. The annular opening through which the electrons are accepted is defined by the fixed baffle *Bf* of 14.75-cm inside diameter and the movable baffle *Bm* of 10-cm outside diameter. The annular opening can be changed by moving the baffle *Bm* with the help of a rod through a Wilson seal to the outside (not shown). Thus the resolving power can be changed when the focal length is kept constant. The baffles denoted by *Bs* are used to prevent scattering.

The source *S* is mounted on a Lucite holder at the end of a long brass tube which may be slid into the system through a gate valve *G* and Wilson seal. The source holder itself is positioned by the Lucite guide, *H*, securely mounted on the baffle system. The source *S* and counter *D* are surrounded with lead shielding which serves to cut down the gamma-ray background. A lead cone 25 cm long was mounted on the axis of the lens to attenuate the direct gamma-ray beam reaching the counter. The counter *D* was of the usual end window type. In the experiments to be described the window was of mica, having a surface density of 4 mg/cm².

The instrument has been used so far at a focal length setting of 25 cm. It was calibrated at this setting with the help of annihilation radiation from a Cu^{64} target. Assuming that the energy of the annihilation radiation is 0.511 Mev, the calibration constant of the instrument was found to be 1547±5 gauss-cm/amp.

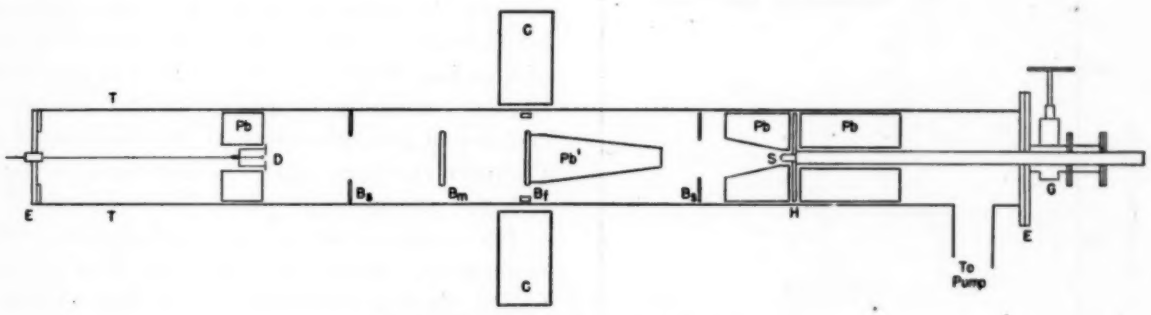

FIG. 1. Schematic diagram—magnetic lens.

[9] P. G. Kruger and W. E. Ogle, Phys. Rev. **67**, 273 (1945).
[10] I. Feister and L. F. Curtiss, see reference 8.
[11] W. Rall and R. G. Wilkinson, Phys. Rev. **71**, 321 (1947).
[12] G. S. Klaiber and G. Scharff-Goldhaber, Phys. Rev. **61**, 733(A) (1942).
[13] R. D. O'Neal, Phys. Rev. **70**, 1 (1946).
[14] A. Wattenberg, Phys. Rev. **71**, 497 (1947).
[15] D. J. Hughes and C. Eggler, Phys. Rev. **72**, 902 (1947).
[16] See M. Deutsch, L. G. Elliott, and R. D. Evans, Rev. Sci. Inst. **15**, 178 (1944).

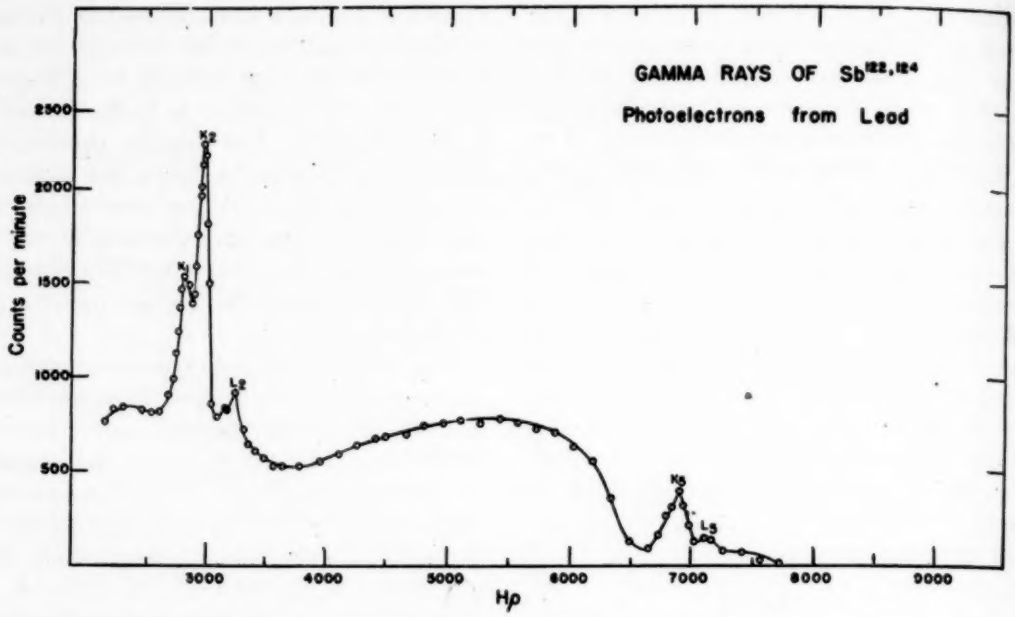

FIG. 2. Photoelectrons ejected from lead by gamma-rays of antimony 124 and 122. (K_1—0.568 Mev Sb^{122}); (K_2—0.603 Mev Sb^{124}); (K_3—1.708 Mev Sb^{124}).

The antimony source used in the experiment was obtained from the Oak Ridge pile of the U. S. Atomic Energy Commission. The active material, in the form of antimony powder, was dissolved and purified chemically. Especial attention was paid to the removal of tellurium. The material was finally brought down as Sb_2S_5, in which form it was used in these experiments.

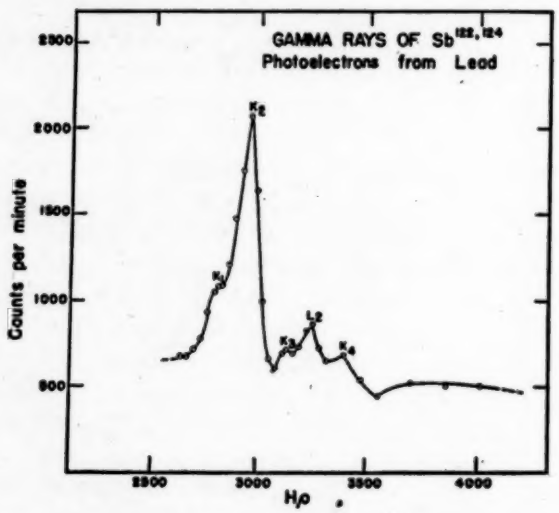

FIG. 3. Photoelectrons ejected from lead by gamma-rays of antimony 124 and 122. (K_1—0.568 Mev Sb^{122}); (K_2—0.603 Mev Sb^{124}); (K_3—0.652 Mev Sb^{124}); (K_4—0.714 Mev Sb^{124}).

3. GAMMA-RAY MEASUREMENTS

In order to measure the energy of the gamma-rays, two methods were used. The first was to measure the photoelectrons produced in a lead radiator by the gamma-rays and the second was to measure the distribution of Compton electrons from a copper radiator. For this purpose the antimony salt was placed in a cylindrical copper capsule 1 cm in diameter. The walls and flat end of the cylinder were just thick enough to stop the most energetic beta-rays produced by antimony. A lead sheet 1 cm in diameter and of a surface density of 26 mg/cm² was placed on the flat end of the copper capsule to serve as a radiator of photoelectrons. If the distribution of Compton electrons was to be measured, the lead radiator was omitted.

The measurements of the photoelectrons were made many times, over an interval of several weeks. Figure 2 shows the first of these measurements which was taken at a time at which an appreciable amount of the 2.8-d Sb^{122} was still present. There is a peak at 2829 $H\rho$ corresponding to a photoelectron ejected from the K shell by a gamma-ray of 0.568 Mev; K and L peaks at 2980 $H\rho$ and 3255 $H\rho$ corresponding to a gamma-ray of energy 0.603 Mev, and K and L

peaks at 6900 $H\rho$ and 7120 $H\rho$ corresponding to a gamma-ray of energy 1.708 Mev. Figure 3 shows a detail of the region around 3000 $H\rho$ taken four days after the data of Fig. 2. It will be seen at once that the peak at 2829 $H\rho$ dies away rather rapidly with time and is therefore to be attributed to Sb^{122} (2.8 days). In addition, weak lines appear at 3148 $H\rho$ and 3370 $H\rho$. These correspond to K peaks from lines at 0.652 Mev and 0.714 Mev, respectively.

The distribution of the Compton electrons is shown[17] in Fig. 4, in which $N/H\rho$ is plotted against $H\rho$. It will be seen at once that there is a low intensity, high energy gamma-ray. The energy of the gamma-ray, computed from the Compton electron distribution, is 2.072 Mev. Evidence for the other gamma-rays is also shown on this curve. Upon finding the high energy gamma-ray in the Compton electron distribution, a search was made to find a photoelectron peak corresponding to it. Such a peak was indeed found at 8090 $H\rho$, which gives for the gamma-ray energy the value 2.056 Mev. In addition to locating some of the lines by use of the Compton electron distribution, the relative intensities of the various gamma-rays were determined by integrating under the curves.[17]

TABLE I. Gamma-rays of Sb.

$H\rho$	$E\gamma$ (Mev)	Remarks
	(a) Sb^{124}	
7660	2.072	Compton electrons
8090	2.056	K-photo peak
6900	1.708	K-photo peak
3387	0.714	K-photo peak
3148	0.650	K-photo peak
2980	0.603	K-photo peak
	Sb^{122}	
2829	0.568	K-photo peak

(b) Beta-ray spectrum of Sb^{124}	
End-point energy (Mev)	Percent abundance
2.37	21
1.62	8
1.00	9
0.65	44
0.48	18

(c) Internal conversion line	
E_{elect} (Mev)	$E\gamma$ (Mev)
0.580	0.603

The results of the measurements on the en-

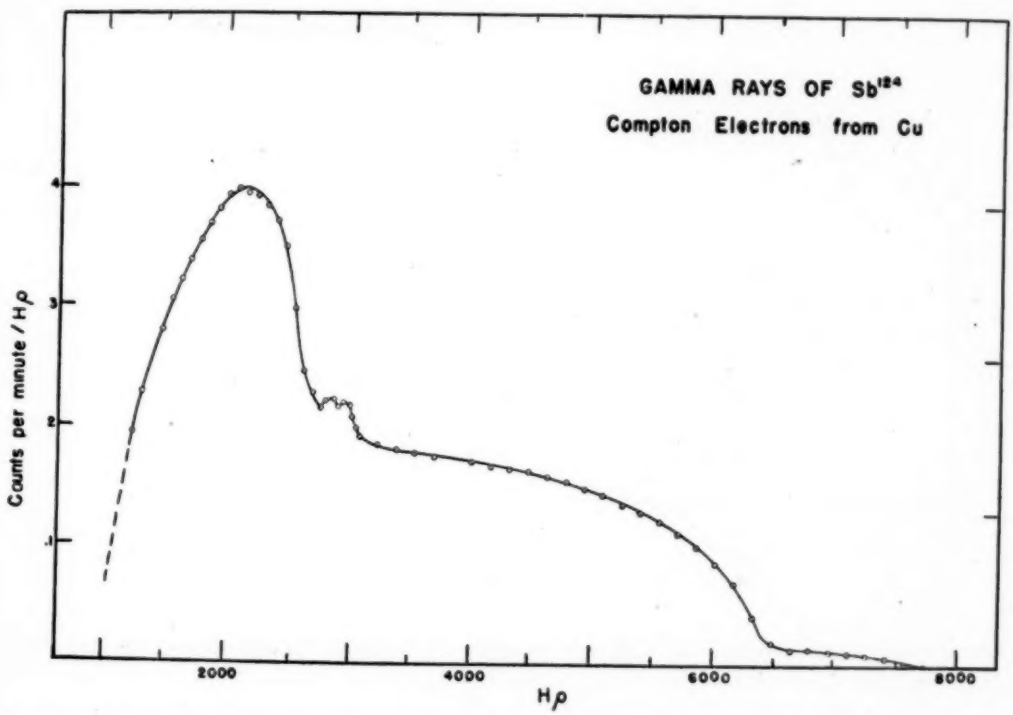

FIG. 4. Distribution of Compton electrons ejected from a copper radiator by the gamma-rays of Sb^{124}.

[17] For a discussion of the method of measuring gamma-rays from a study of the Compton electron distribution see K. Siegbahn, Proc. Roy. Soc. **A188**, 541 (1947).

ergy and relative intensities of the gamma-rays are shown in Table I and Fig. 7.

4. MEASUREMENT OF THE BETA-RAY SPECTRUM

In order to measure the distribution of the beta-rays, a source of Sb_2S_5 was spread upon a thin aluminum foil. The surface density of the beta-ray source was 5.5 mg/cm² and that of the backing 1 mg/cm². The results of this investigation are shown in Fig. 5, in which the number of counts per min. is plotted against $H\rho$ (gauss-cm.). It will be seen at once that there is an internal conversion line which appears at 3170 $H\rho$. This value corresponds to that of electrons ejected from the K shell of Te^{124} by a gamma-ray of 0.603 Mev.

A Kurie[18] plot was made of these data, in which the number of electrons per unit $H\rho$ interval, divided by the distribution function $F(Z,\eta)$ is plotted against $(1+\eta^2)^{\frac{1}{2}}$. Here

$$\eta = H\rho/1700.$$

The result is shown in Fig. 6. The spectrum is clearly not simple but can be broken up into five groups. The end-point energies and relative abundances of these groups are also shown in Table I. The ft values of the groups have been calculated and show that the three higher energy groups belong to the second forbidden class, and the two lower energy groups are first forbidden.

The ratio of the number of internal conversion electrons in the internal conversion line to the total number of disintegration electrons was determined by integrating under the line and under the distribution curve for the electrons and was found to be 0.00210. In addition to this line, Cook and Langer[19] have found another internal conversion line produced by a gamma-ray of

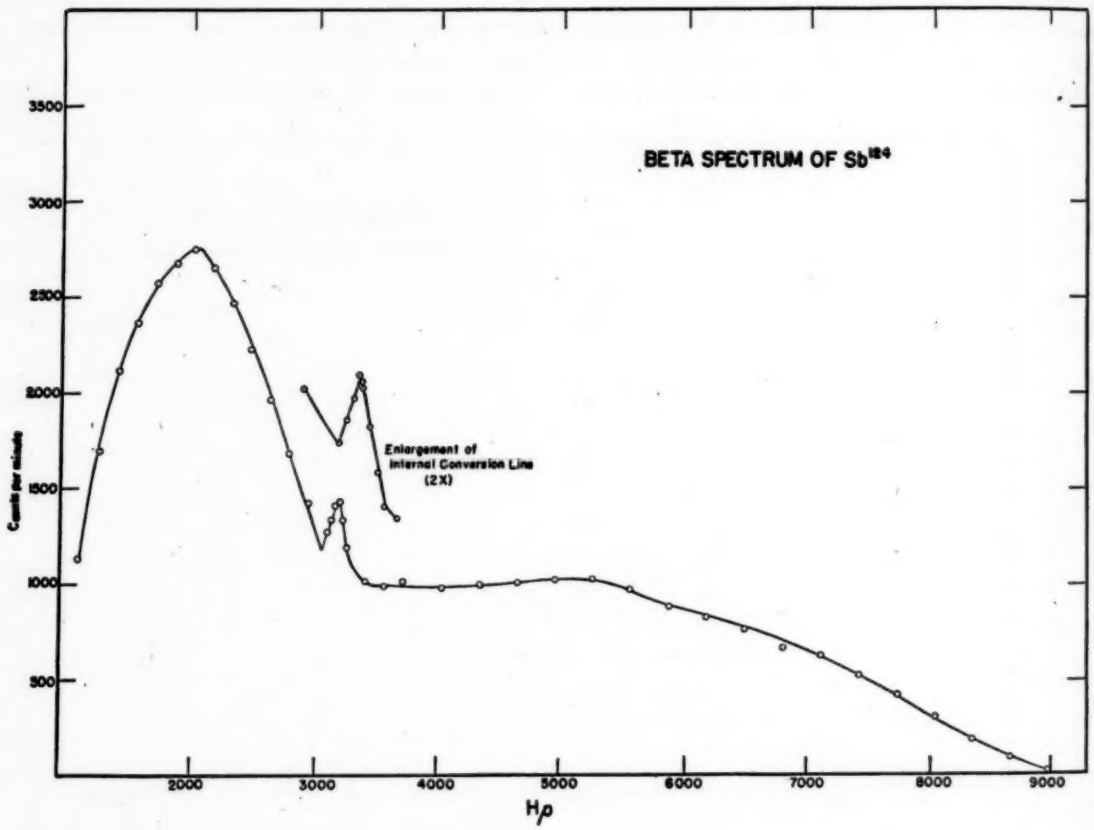

FIG. 5. Beta-ray spectrum of Sb^{124}.

[18] F. N. D. Kurie, J. R. Richardson, and H. C. Paxton, Phys. Rev. 48, 167 (1935).
[19] C. S. Cook and L. M. Langer, see the other papers in this group.

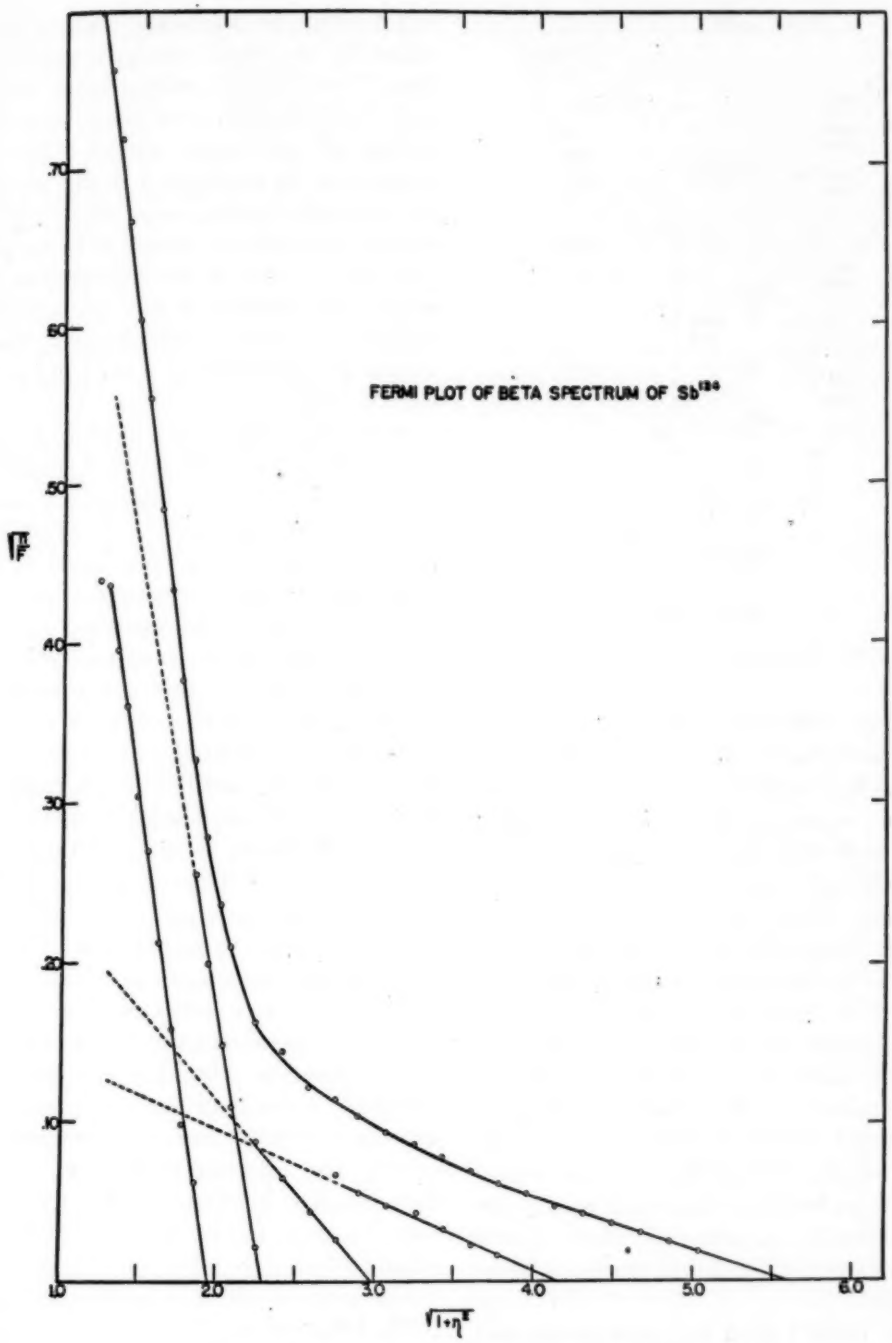

FIG. 6. Fermi plot of beta-ray spectrum of Sb^{124}.

energy 0.121 Mev. The best estimate that we have been able to make of the disintegration scheme appears to show that the 0.603-Mev line follows all beta-ray transitions and leads to the ground state of Te^{124}. If this be the case, the ratio of the number of internal conversion electrons under this line to the total number of disintegration electrons is essentially the internal conversion coefficient of the 0.603-Mev line.

Mr. J. R. Pruett has calculated the internal conversion coefficients to be expected on the basis of electric dipole, electric quadrupole, and

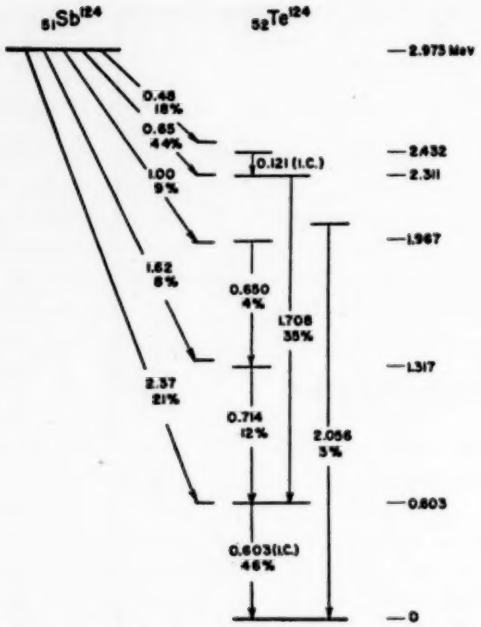

FIG. 7. Tentative disintegration scheme for Sb^{124}.

magnetic dipole radiation, and has found the following values: electric dipole, 0.000269; electric quadrupole, 0.00623; magnetic dipole, 0.00213. The experimental value of 0.0021 agrees quite well with the value calculated for magnetic dipole radiation.

The question arises as to whether a satisfactory energy level scheme for the disintegration of Sb^{124} can be determined from the information in Table I. It should be pointed out at once that the evidence presented here shows that the disintegration scheme is much more complicated than that proposed by Meyerhoff and Scharff-Goldhaber[8] based on the results of their coincidence experiments. The authors do not believe that with the techniques employed up to the present, coincidence experiments alone would be sufficient to work out a disintegration scheme for this element.

The data in Table I show six gamma-rays and five beta-ray groups. The gamma-ray energies are probably known to better than one percent. The beta-ray energies, on the other hand, are not known to anywhere near this accuracy, especially the lower energy groups, since these depend on several subtractions in the Kurie plot. It is possible that there may be beta-ray groups of still lower energy than the lowest found here. In addition, it is also possible to miss low intensity gamma-rays. For this reason any energy level scheme which may be proposed at this time is open to considerable doubts and is subject to revision if and when additional information is found. Nevertheless the tentative scheme proposed in Fig. 7 fits most of the experimental data.

In the first place, this scheme gives a good fit as regards the energies given in Table I. The two strongest lines in the gamma-ray spectrum are those of 0.603 Mev and at 1.708 Mev. The relative intensity of these two lines, as determined from the Compton distribution curves, is $I_{0.603}/I_{1.708}=1.45$. An estimate of the relative intensity can also be obtained from the photoeffect data. To do this the Compton electron background must be subtracted and the area under the lines, plotted as $N/H\rho$ *vs.* $H\rho$, obtained. This gives the number of photoelectrons produced by each line. The efficiency for production of photoelectrons is then obtained using the curves of Gray.[20] The relative intensity obtained by this method is $I_{0.603}/I_{1.708}=1.15$. The relative intensity to be expected from the scheme of Fig. 7 would be $I_{0.603}/I_{1.708}\sim 1.5$.

There are two objections to the tentative scheme proposed. It would seem that the attempt to associate the 2.06-Mev gamma-ray with the 1.97-Mev level may not be correct, since the difference between these two energies is probably outside the experimental error. Secondly, one does not like to place the 0.121 internally converted gamma-ray so high up in the energy level scheme.

The authors wish to express their appreciation to the Office of Naval Research for their support of this work through Contract N6ori-48, Task Order I.

[20] L. H. Gray, Proc. Camb. Phil. Soc. **27**, 103 (1931).

Energies of the Beta- and Gamma-Rays from Antimony

C. SHARP COOK AND LAWRENCE M. LANGER
Indiana University, Bloomington, Indiana
(Received February 5, 1948)

The radiations from antimony bombarded by slow neutrons have been investigated in a large, high resolution, shaped-field magnetic spectrometer. The beta-spectrum of Sb^{124} (60 d.) was measured with a relatively thin source and with a thin window counter. The spectrum is found to be complex. By means of the Fermi theory, it is possible to resolve the distribution into at least five groups having the following end points and intensities: 2.37 Mev, 21 percent; 1.50 Mev, 7 percent; 0.98 Mev, 7 percent; 0.68 Mev, 26 percent; 0.50 Mev, 39 percent.

An internal conversion line was detected corresponding to a gamma-ray of 0.121 Mev.

Measurements on the Compton and photoelectrons ejected from a thin Pb radiator yield additional gamma-ray energies of 0.608, 0.654, 0.732, 1.708, and 2.04 Mev.

Measurements made while the short period activity was still present indicate that a gamma-ray of 0.568 Mev is associated with the 2.8-day activity of Sb^{122}.

I. INTRODUCTION

SINCE there appeared to be considerable disagreement among the results obtained by previous measurements for the energies of the radiations from Sb^{124} (60 d), it was thought desirable to reinvestigate the problem with the aid of a new, high resolution, shaped-field magnetic spectrometer. A similar investigation was undertaken simultaneously and independently at this laboratory by Kern, Zaffarano, and Mitchell, using a thin magnetic lens. Their results are reported in another paper in this journal. That paper gives a detailed discussion of the background of the problem and refers to the pertinent literature. The general agreement in the measurements made with these two instruments gives additional assurance of the accuracy of the results. The apparent complexity of the disintegration process in Sb^{124} makes more understandable the disagreement among the previous results obtained by low resolution methods.

II. EXPERIMENTAL METHOD

The magnetic spectrometer used for these measurements is described in detail elsewhere,[1] and has been used recently for the precise determination of the shape of the beta-spectra of Cu^{64}.[2] The instrument employs a radially inhomogeneous magnetic field in order to obtain higher order focusing at 180° from the source. The nominal value of the radius of curvature is 40 cm. When used with a thin source 0.4 cm wide, the full width at half-maximum for an internal conversion line is 0.5 percent. The instrument is free from spurious scattering effects.

The source used in these measurements was obtained by neutron bombardment of antimony metal in the Oak Ridge pile.

Sources for the measurement of gamma-ray energies were prepared by inserting the sample in a copper box whose front face was covered by a thin Pb radiator 0.4 cm wide by 2.5 cm high and 26.3 mg/cm² thick. The thickness of the copper walls of the box was chosen so as to prevent any nuclear beta-rays from escaping. The momentum of the photoelectrons and Compton electrons ejected from the Pb by the gamma-rays were measured in the spectrometer.

The source for the measurement of the beta-spectrum was prepared by electroplating a thin deposit of Sb less than 1 mg/cm² thick onto a 0.010-in. graphite backing. Distortion of the distribution caused by a source and backing of such thickness should be negligible for almost the entire spectrum.

For the region below $H\rho = 2500$ gauss-cm the beta-particles were detected by an end window G-M counter having a Zapon lacquer window with an electron range of 2.0 kev. For the upper end of the spectrum, and for the gamma-ray measurements, a mica window counter of 2.83 mg/cm² was employed.

[1] L. M. Langer and C. S. Cook, Rev. Sci. Inst. **19**, 257 (1948).
[2] C. S. Cook and L. M. Langer, Phys. Rev. **73**, 601 (1948).

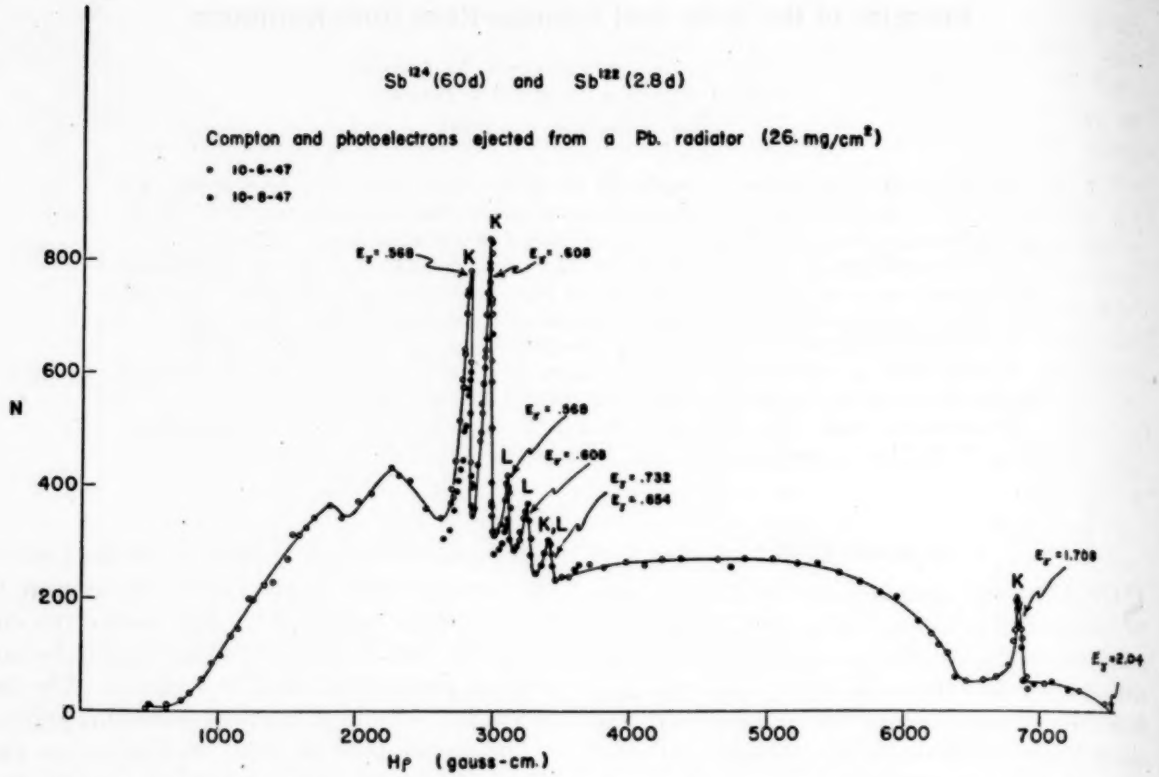

FIG. 1. Compton and photoelectrons ejected from a 26.3-mg/cm² Pb radiator by the gamma-rays of Sb^{124} and Sb^{122}. The number of counts detected is plotted against the momentum. The data represented by the solid circles were taken after a lapse of two days and show the decay of the K and L lines due to the 2.8-day Sb^{122}.

Relative measurements of magnetic field strength were made by means of a flip coil and ballistic galvanometer. The absolute calibration of the instrument is in terms of the 0.5108-Mev radiation from the annihilation of Cu^{64} positrons.

Whenever possible, the energies of gamma-rays are determined from the steep back edge of the K lines. Because of the multiplicity of the L levels, the back edge of these lines is not so clearly defined.

III. RESULTS

Figure 1 shows the momentum distribution of Compton and photoelectrons obtained from the Sb source just after it was received from Oak Ridge. The number of counts per minute are plotted against the momentum. The solid circles are for data taken after a lapse of two days and clearly identify the K and L lines of a gamma-ray of 0.568 Mev with the 2.8-day activity of Sb^{122}.

Associated with the 60-day Sb^{124}, photo lines are shown corresponding to gamma-ray energies of 0.608, 0.732, 0.654, and 1.708 Mev. In addition, the high energy Compton edge corresponds to a gamma-ray of 2.04 Mev. The superposition of the K line corresponding to the 0.732-Mev gamma-ray and the L line for the 0.654-Mev gamma-ray is more clearly shown in Fig. 2. This run was taken after the short period activity had died out and after chemical separation, particularly from any possible tin or tellurium impurities. Here the K line corresponding to the 0.654-Mev gamma-ray is clearly resolved.

Figure 3 shows the distribution of the beta-rays of Sb^{124} obtained with a chemically separated source and after all short period activities had died out. Here the number of counts, normalized by dividing by $H\rho$, is plotted against the momentum. From this curve it is obvious that the spectrum is complex and consists of at least two groups. In addition, a line of conversion electrons is observed having an energy of 89 kev. If these electrons are from the K level of tellurium, then they correspond to an Sb^{124} gamma-ray of 121 kev.

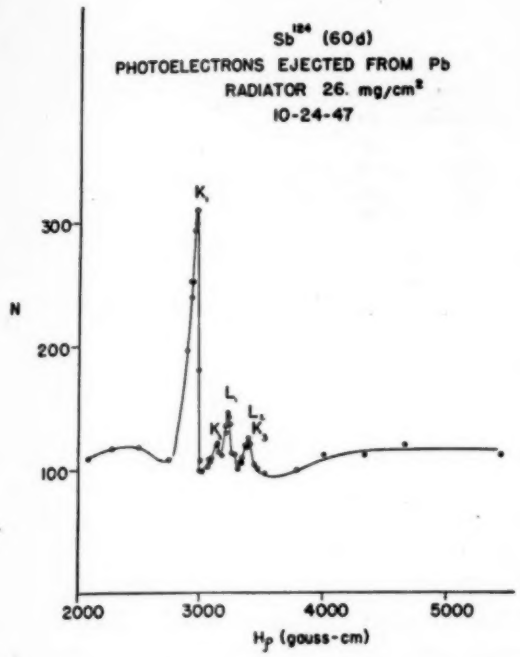

FIG. 2. Compton and photoelectrons ejected from a 26.3-mg/cm² Pb radiator by the gamma-rays of Sb^{124}. The source was chemically separated and all 2.8-day activity had died out.

If one assumes that the Fermi theory correctly describes the distribution of the beta-particles and if one assumes that on a Kurie plot[3] the component spectra should be straight lines, then one can resolve the complex experimental spectrum into five groups. The results of such an analysis are shown in Fig. 4. The maximum energies and the relative intensities of the five components are also shown. The validity for performing such an analysis is somewhat questionable in this case, inasmuch as some of the groups would belong to the so-called second forbidden class and do not necessarily have to follow straight line Kurie plots. Because of the number of subtractions involved, the values for the end-point energies of the inner groups are probably not good to better than 5 percent.

The Fermi plot for the lowest energy group does not yield a perfect straight line, but curves gently up at low energies. The *possibility* of a sixth low energy group is therefore not excluded. It would, however, be meaningless to try to resolve such a group by means of this analysis, for the following reasons: (a) there are indications that the Fermi theory may not be correct at low energies;[3] (b) the thickness of the source and backing may be introducing some distortion; (c) with additional subtractions, the errors multiply and the statistics become poorer at low energies.

IV. CONCLUSION

The disintegration of Sb^{124} has been observed to be quite complex. The beta-spectrum consists of at least two groups and may very well be

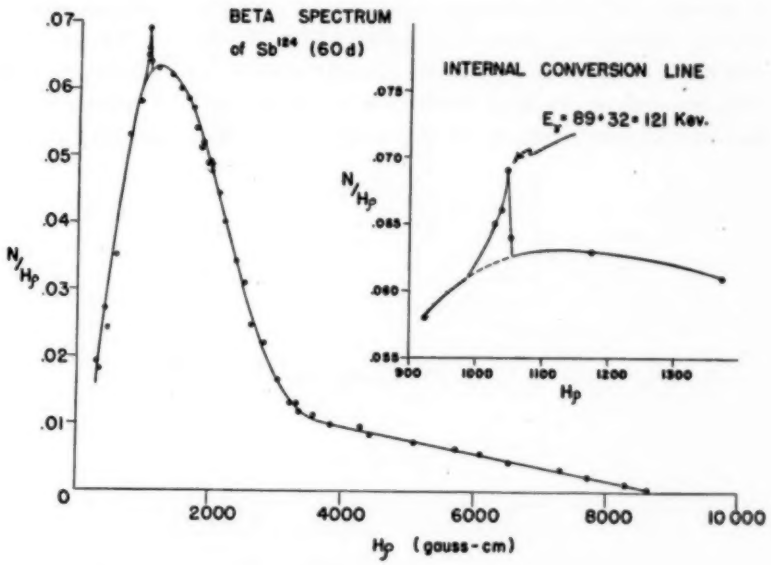

FIG. 3. Beta-spectrum of Sb^{124}.

[3] F. N. D. Kurie, J. R. Richardson, and H. C. Paxton, Phys. Rev. **48**, 167 (1935).

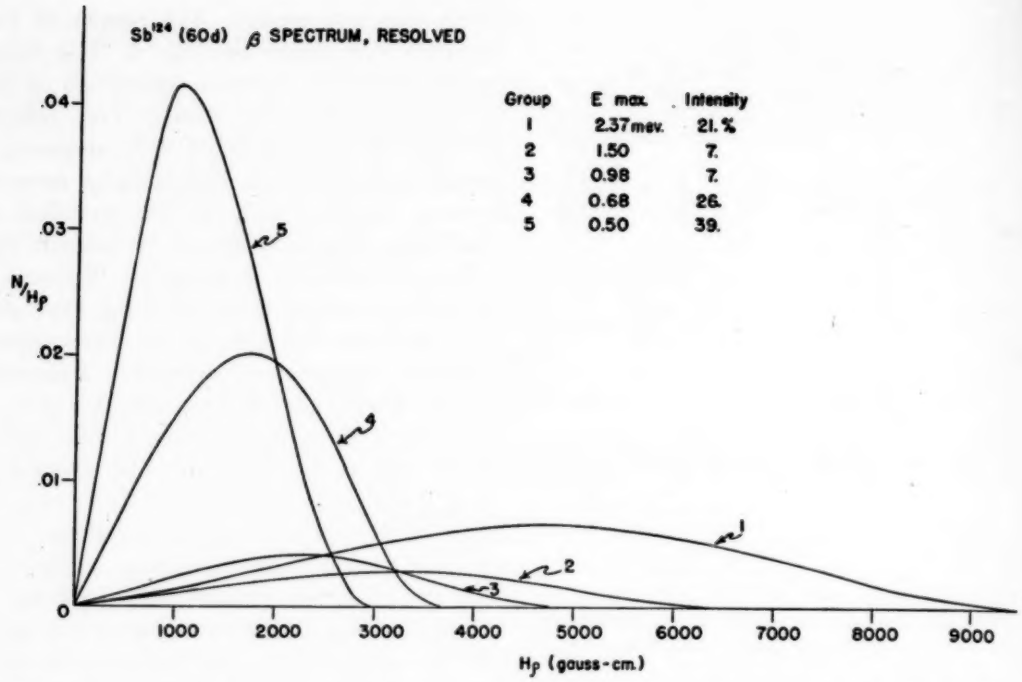

FIG. 4. The complex beta-spectrum of Sb^{124} resolved into five groups by means of the Fermi theory.

composed of five or six groups. The energies of six gamma-rays accompanying the disintegration of Sb^{124} have been measured.

An attempt can be made to fit the present data into a consistent energy level scheme. It is felt, however, that the data are still not sufficiently complete to ensure the uniqueness of such a scheme. Additional weak gamma-rays and low energy conversion lines may exist which would not have been observed in the present investigation because of the high resolution employed and because of the strength of the source. It is also possible that one or more of the gamma-rays which have been observed may be associated with a K capture process and therefore be characteristic of the levels of tin rather than those of tellurium. It is probable that only by beta-gamma coincidences in a spectrometer could one be completely certain of which gamma-ray follows which beta-particle group.

This work was supported by a grant from the Frederick Gardner Cottrell Fund of the Research Corporation and by the Office of Naval Research under Contract N6ori-48, T.O. I.

Coincidence Experiments in Antimony 124

E. T. JURNEY AND ALLAN C. G. MITCHELL
Physics Department, Indiana University, Bloomington, Indiana

(Received February 5, 1948)

The radiations from Sb^{124} (60 d.) have been measured with the help of coincidence counting methods. The beta-ray absorption curve was measured and analyzed by the method of Bleuler and Zünti. Two groups of electrons were found with end points at 2.24 and 0.51 Mev. Gamma-gamma and beta-gamma coincidences were measured. A plot of the number of beta-gamma coincidences per recorded beta-particle indicates that the spectrum is complex. Two low energy groups were found with end points at 0.75 and 0.47 Mev.

1. INTRODUCTION

COINCIDENCE counting techniques have been employed on several occasions to study the radiations from Sb^{124} (60 d.). The first attempt was made by Mitchell, Langer, and McDaniel,[1] who measured gamma-gamma and beta-gamma coincidences in this element. Later Meyerhoff and Scharff-Goldhaber,[2] Wiedenbeck and Chu,[3] and Scherb and Mandeville,[4] made a reinvestigation of Sb^{124} and found results somewhat different from those originally obtained by MLM. In order to clear up the differences between the earlier work of MLM and that of MSG, the authors have repeated some coincidence experiments in Sb^{124} as a part of a program carried on in this laboratory designed to work out in more detail the disintegration scheme of Sb^{124}. The other papers, dealing with the determination of gamma-ray and beta-ray energies will be found in this issue of the Physical Review.

2. APPARATUS

An end-window counter, having a window thickness of 6 mg/cm² of mica, was used to count beta-particles. To improve the efficiency[5] for counting gamma-rays, especially those with energy under one Mev, a cylindrical, lead cathode counter was used. During the experiment the source was situated between the two counters, 4.5 cm from the window of the beta-ray counter and 4.0 cm from the central axis of the gamma-

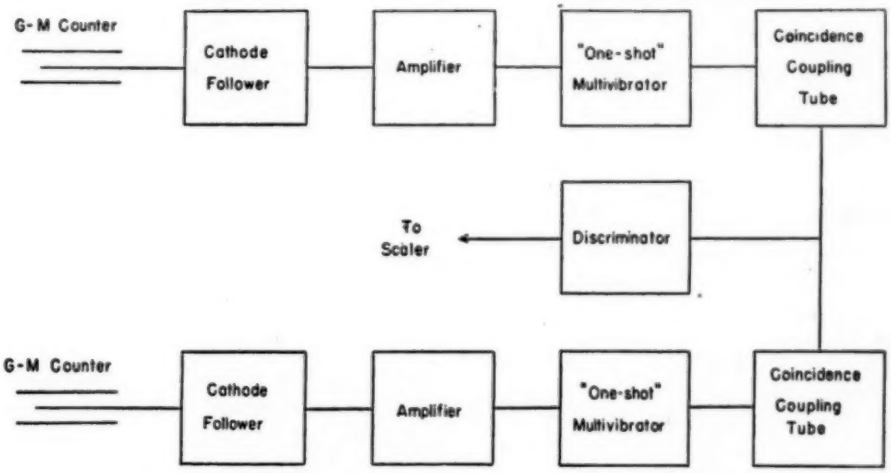

FIG. 1. Block diagram of the coincidence counting apparatus.

[1] A. C. G. Mitchell, L. M. Langer, and P. W. McDaniel, Phys. Rev. **57**, 1107 (1940), herein referred to as MLM.
[2] W. E. Meyerhoff and G. Scharff-Goldhaber, Phys. Rev. **72**, 273 (1947), herein referred to as MSG.
[3] M. L. Wiedenbeck and K. Y. Chu, Phys. Rev. **72**, 1164 (1947).
[4] M. V. Scherb and C. E. Mandeville, Bull. Am. Phys. Soc. **23**, No. 2, 40 (1948).
[5] H. Bradt, P. C. Gugelot, O. Huber, H. Medicus, P. Preiswerk, and P. Scherrer, Helv. Phys. Acta **19**, 77 (1946).

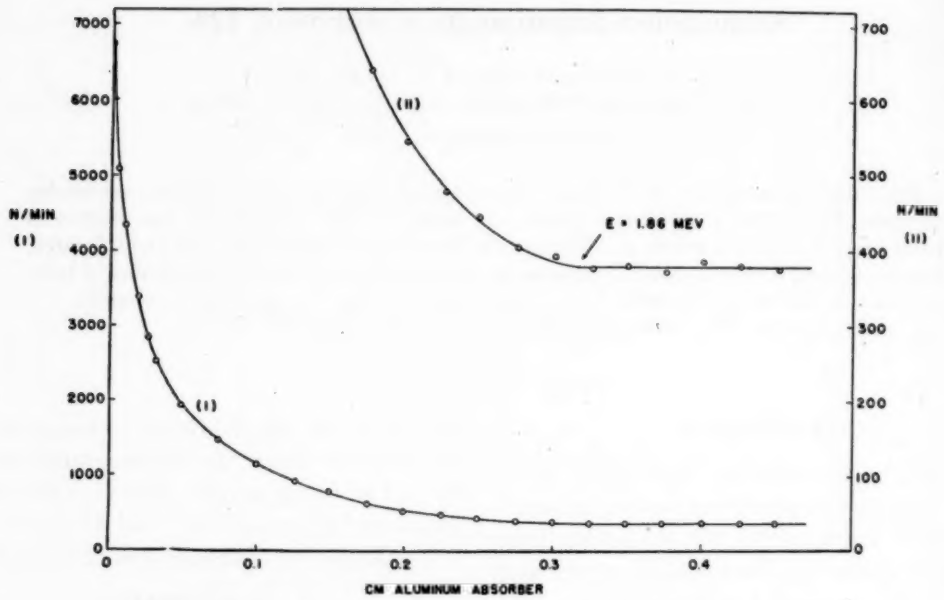

FIG. 2. Absorption of Sb^{124} beta-rays in aluminum.

ray counter. This type of arrangement is essentially that used by other investigators.[1–4]

A block diagram of the coincidence amplifier is shown in Fig. 1. The bias setting on the final discriminator tube can be adjusted for counting either coincidental pulses from both counters or for counting the individual pulses from a single counter.

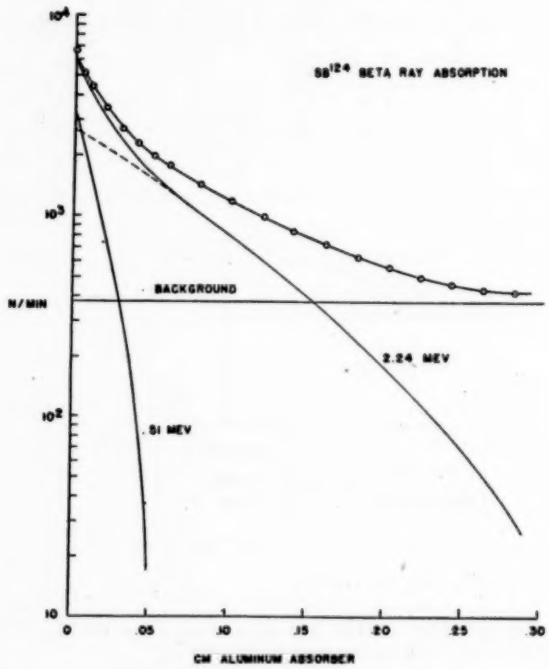

FIG. 3. Logarithmic plot of the beta-ray intensity as a function of aluminum absorber thickness.

The pulses which are applied to the grids of the Rossi-type coincidence circuit are formed by a "one-shot" multivibrator in each channel. This procedure insures a constant resolving time, independent of pulse height from the counters. The resolving time was determined from the usual relation

$$N_{ch}=2n_1n_2t,$$

which gives the rate of chance coincidences as a function of individual counting rates in two counters which are counting particles from independent sources when the circuit resolving time is t. The resolving time was found to remain constant at 4.5 microseconds over a period of about three months.

3. RESULTS

Using the thin window counter and a thin source (under 10 mg/cm²) mounted on Scotch tape, an absorption curve was run on the beta-rays. Figure 2 shows the usual method of plotting absorption curves, in which the number of counts per min. is plotted against the thickness of absorber. The "inspection" end point appears to be at 0.86 g/cm² corresponding to a range of 1.86 Mev. This value is much lower than the end points determined with the help of beta-ray

spectrographs,[6] but is somewhat higher than that determined originally by MLM or that obtained later by Scherb and Mandeville.

If one makes an analysis of these data by the method of Bleuler and Zünti,[7] the beta-ray spectrum can be resolved into two groups with end points at 2.24 Mev and 0.51 Mev. Figure 3 shows the data plotted with $\log R$ as ordinate (R = number of counts/min.) against the thickness of aluminum as abscissa. The circles show the experimental points. After the gamma-ray background is subtracted, the remaining curve can be broken down into two components. The relative abundance of the two groups is approximately equal, with the lower energy group showing a slightly higher abundance. Actually, the beta-ray spectrum consists of five groups,[6] with energies at 2.37, 1.62, 1.00, 0.65, and 0.48 Mev. The three higher energy groups comprise about 35 percent of the total intensity and the two lower energy groups about 65 percent. The end point for the lower energy component as obtained from the Bleuler and Zünti analysis probably represents the two high intensity, low energy groups. The fact that the "inspection" end point is much too low is clearly caused by the low intensity of the high energy groups.

Coincidence experiments were carried out in the usual way using, however, the lead lined counter as the gamma-ray counter and the thin window counter as the beta-ray counter. The gamma-gamma coincidence rate was obtained by placing an aluminum absorber 0.45 cm thick between the source and the beta-ray counter. This thickness is sufficient to stop all beta-particles. After corrections for cosmic-ray and chance coincidences, the gamma-gamma coincidence rate was determined. This rate can be referred either to the counting rate in the gamma-ray counter or to the gamma-ray counting rate in the beta-ray counter; that is, in the lead lined counter or the end window counter. The values were found to be $(N_{\gamma\gamma}/N_\gamma)_{\text{gamma}}=0.29 \pm 0.017\times10^{-3}$ and $(N_{\gamma\gamma}/N_\gamma)_{\text{beta}}=0.87\pm0.05 \times10^{-3}$. Since the lead lined counter is more efficient for counting gamma-rays, the single count in this counter for a given source strength is higher than that in the end-window type, which accounts for the difference in the observed $N_{\gamma\gamma}/N_\gamma$ ratio. Naturally, the values of these ratios should not agree with any values found in previous experiments in which different types of counters were used. Since the efficiency of neither the lead lined nor the end-window type counter has been measured, the ratios $N_{\gamma\gamma}/N_\gamma$ will not be used in the calculation.

The number of beta-gamma coincidences was next investigated. To this end, the absorber thickness between the source and the end-window counter was varied, and the number of beta-

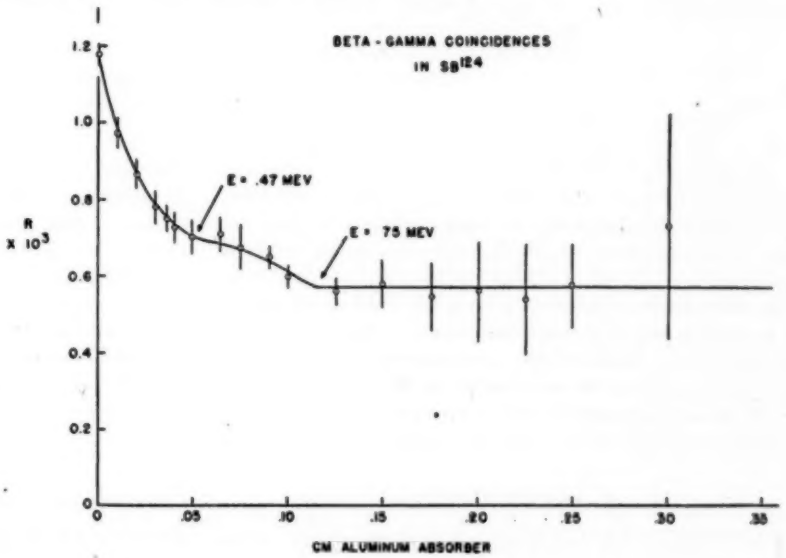

FIG. 4. Number of beta-gamma coincidences per recorded beta-ray as a function of beta-ray absorber thickness.

[6] See the preceeding papers in this issue.
[7] E. Bleuler and W. Zünti, Helv. Phys. Acta 19, 375 (1946).

gamma coincidences determined. Figure 4 shows a plot of $R=N_{\beta\gamma}/N_{\beta}$, the number of beta-gamma coincidences per recorded beta-particle as a function of the absorber thickness. From this graph it will be seen that, beyond a thickness of 0.12 cm Al (the range corresponding to beta-rays of 0.75-Mev energy) the curve is parallel to the axis. Below 0.12 cm the curve rises and there is an additional sharp break at 0.05 cm of aluminum, corresponding to a beta-particle energy of 0.47 Mev.

One would infer from Fig. 4 that there are at least three groups of electrons and that there are more gamma-rays associated with the lower energy groups than with the high energy ones. These experiments are in good agreement with the tentative energy level scheme which has been proposed as a result of the investigation of the beta- and gamma-ray spectrum in the magnetic lens.[8] One of the high intensity groups as proposed by these authors has an end point of 0.65 Mev. The first break in the $N_{\beta\gamma}/N_{\beta}$ curve comes at 0.75 Mev which is in reasonable agreement with the magnetic lens data. In addition, another group appears at 0.47 Mev, which is just at the position of the second break in the coincidence curve. Since the high energy part of the beta-ray spectrum, beyond 1 Mev contains very few electrons, it is difficult to measure coincidences in the neighborhood of the end point, 2.37 Mev. It cannot, therefore, be definitely inferred from these experiments that the highest energy group does or does not lead to the ground state of Te^{124}.

The work reported in this paper is essentially in agreement with that of MSG, with the exception that an additional low energy group has been found here. The work of MLM failed to detect any low energy groups, probably because the counters used at that time had walls which were too thick to transmit those groups. In conclusion, the authors would like to point out that, for an element with a decay scheme as complicated as that of Sb^{124}, it is not possible to work out a detailed disintegration scheme on the basis of coincidence experiments alone.

The authors wish to express their appreciation to the Office of Naval Research for their support of this work through Contract N6ori-48.

[8] See preceding paper by Kern, Zaffarano, and Mitchell.

PHYSICAL REVIEW VOLUME 73, NUMBER 10 MAY 15, 1948

X-Ray Yield Curves for $\gamma-n$ Reactions

G. C. BALDWIN AND G. S. KLAIBER*
General Electric Company, Schenectady, New York

(Received February 5, 1948)

Yield curves for the reactions $C^{12}(\gamma,n)C^{11}$ and $Cu^{63}(\gamma,n)Cu^{62}$ have been taken with x-rays up to 100 Mev. The induced radioactivity at each energy is plotted per unit x-ray intensity as measured by a r-meter thimble jacketed by $\frac{1}{4}$ in. of Pb. Both yield curves are similar to the photo-fission yield curves, the x-ray yield increasing to a maximum and then slowly decreasing as the x-ray energy is increased. With simple assumptions regarding the generation of ionizing secondaries in the Pb walls of the monitor and assumption of a constant intensity x-ray spectrum, these curves can be analyzed. The relative cross section is found to have a maximum at approximately 22 Mev for Cu^{62} and 30 Mev for C^{11}, decreasing to negligible values at high quantum energies. This decrease in cross section can be attributed to competition from multiple disintegrations. These reactions provide detectors sensitive only to part of the x-ray spectrum. Absorption curves have been taken in Pb using uranium photo-fission and in Cu and Pb using the $Cu^{63}(\gamma,n)Cu^{62}$ reaction as detectors. The resulting absorption coefficients compare favorably with theoretical values.

1. INTRODUCTION

INVESTIGATIONS which can be made with high energy quanta include measurements of cross section for photo-nuclear processes as a function of the energy of the absorbed quantum. In studying such processes with continuous x-rays generated by an electron accelerator, one

* Now at the University of Buffalo, Buffalo, New York.

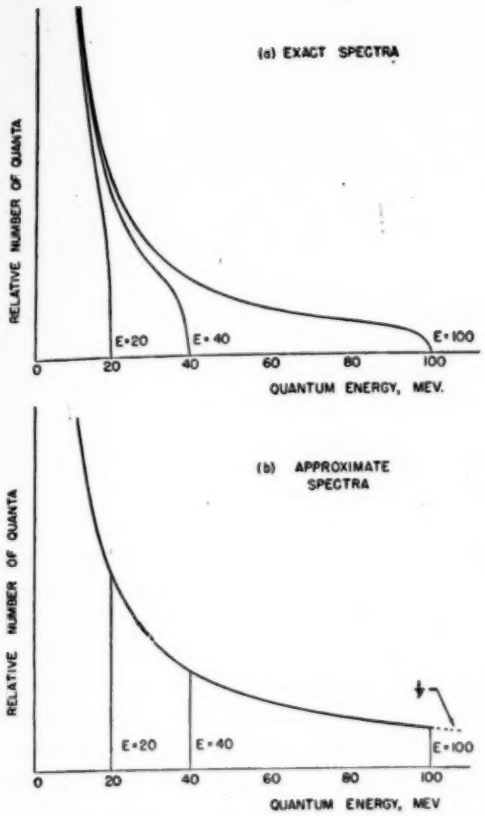

FIG. 1. Theoretical thin target bremsstrahlung spectra.

irradiates specimens of the substance concerned together with some sort of monitor at different x-ray energies, and obtains a "yield curve" in which the ratio of the yield of the process in question to the yield of the monitoring process is plotted against the x-ray energy; i.e., the maximum energy in the x-ray spectrum. To interpret such data, one must know the spectrum of the radiation and the response of the monitoring process to this spectrum at different x-ray energies.[1]

The curves in Fig. 1a are theoretical thin-target x-ray spectra given by the theory of bremsstrahlung.[2] The ordinates are relative numbers of quanta per unit energy interval, normalized to coincide at 10 Mev. The curves in Fig. 1b represent the distribution of quanta in "rectangular" spectra having equal intensity in every energy interval, the approximation used in cascade theory; even at these energies it will be seen by comparison with Fig. 1a that it is a good approximation. It will be noted that, were irradiations at various x-ray energies E so adjusted that all the respective spectra were normalized as in the figure, the difference between effects observed for neighboring values of E would be very nearly caused only by the action of those quanta whose energies, γ, lie between these values of E. To obtain the cross section as a function of γ from the yield curve, one differentiates the yield curve and divides it by the envelope of the spectrum curves.

In practice one cannot, of course, insure that the condition of normalization is satisfied.

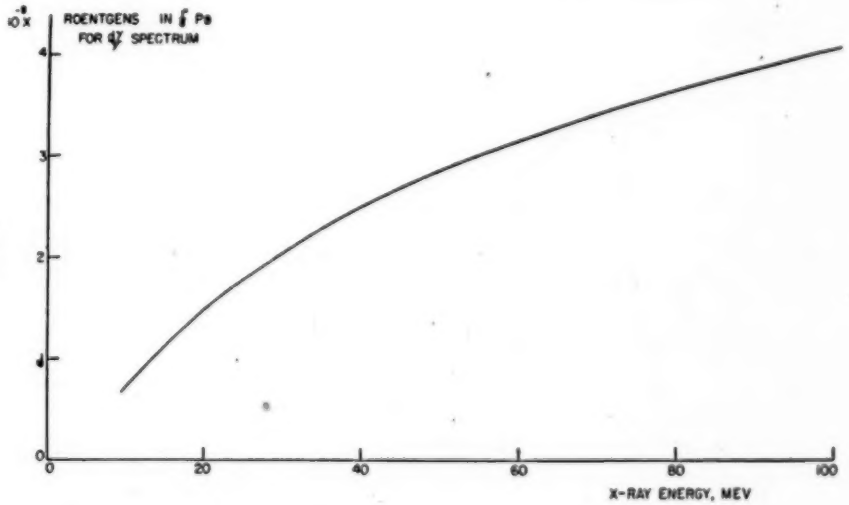

FIG. 2. Calculated sensitivity to the x-ray spectra of Fig. 1b of the monitor employed in these experiments.

[1] G. C. Baldwin and G. S. Klaiber, Phys. Rev. **71**, 3 (1947).
[2] B. Rossi and K. Greisen, Rev. Mod. Phys. **13**, 254 (1941).

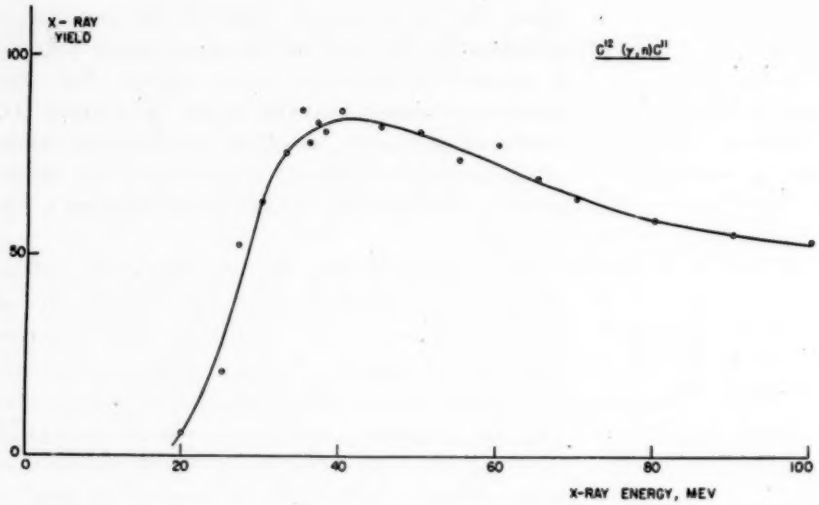

FIG. 3. X-ray yield of C^{11}.

Instead a monitor is employed. A Victoreen thimble r-meter surrounded by $\frac{1}{8}$-in. Pb forms a convenient if not perfect monitor. A more accurate monitor has been recently proposed but has not been tested experimentally.[3] The response of the former monitor to the approximate spectra of Fig. 1b as a function of E has been calculated,[1] assuming it to be due to ionization by electron secondaries generated by pair production, scattering and photo-effect, proceeding mainly in the forward direction and not generating an appreciable number of cascade processes in the $\frac{1}{8}$-in. Pb wall of the monitor. This response is shown in Fig. 2. If the experimentally obtained yield curve is multiplied by the monitor response curve, $r(E)$, the product is the yield curve for a normalized family of spectra, and can be analyzed by differentiation and division by the spectrum envelope, $1/\gamma$, as explained above.

We have previously reported measurements of the x-ray yields of fission of uranium and thorium, which indicated that the photo-fission cross section rises to a maximum at approximately 16 Mev, decreasing at higher energies to become negligibly small above 30 Mev. This effect was ascribed to the competition of other types of photo-disintegration[4] that can occur at higher energies. It has seemed worthwhile to

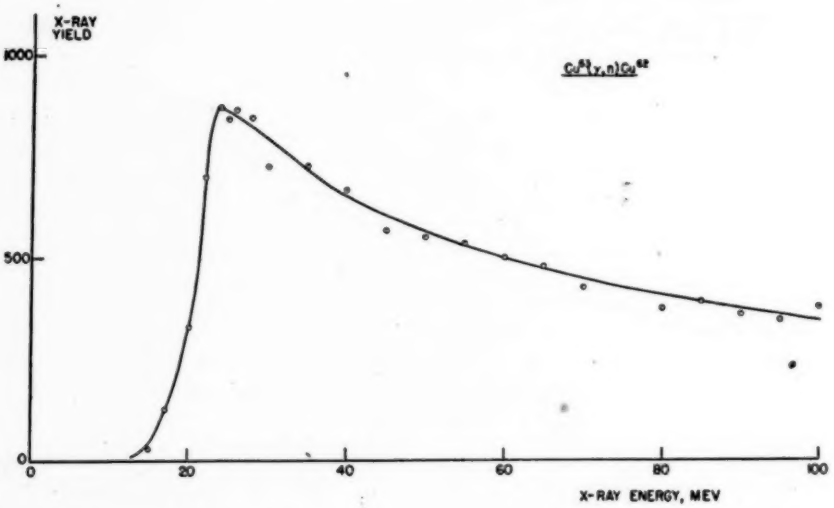

FIG. 4. X-ray yield of Cu^{62}.

[3] M. Lax, Phys. Rev. **72**, 61 (1947).
[4] G. C. Baldwin and G. S. Klaiber, Phys. Rev. **70**, 259 (1946).

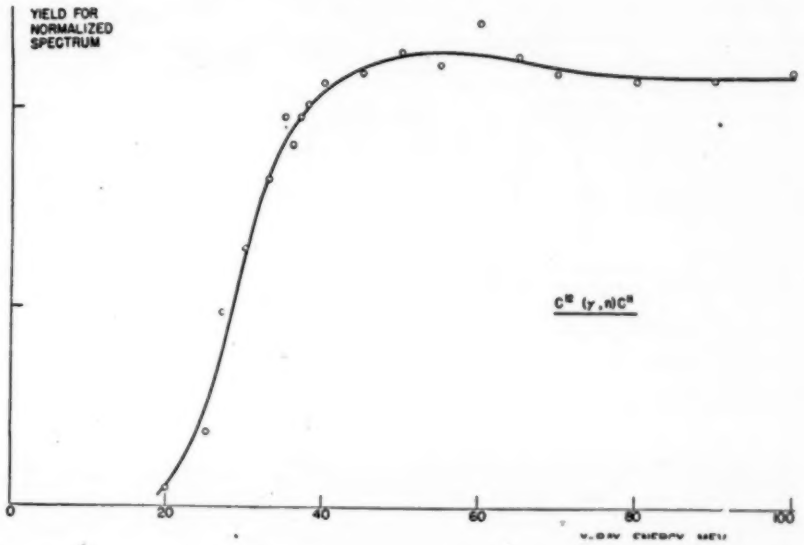

FIG. 5. Product of the curves of Figs. 2 and 3.

extend these measurements to other processes. It was also desired to obtain confirmatory evidence to support the validity of the method of analysis used and conclusions reached.

2. (γ,n) YIELD MEASUREMENTS

The reactions investigated were $C^{12}(\gamma,n)C^{11}$ and $Cu^{63}(\gamma,n)Cu^{62}$. The carbon samples were polythene sheets, 2 in. square by 0.03 in. thick; the copper foils 2 in. square by 0.003 in. thick. A special clamp held each sample for irradiation at a reproducible position 67 in. from the target in the center of the x-ray beam from the 100-Mev betatron, the lead-jacketed r-meter thimble being clamped immediately behind the sample. Decay curves were first taken which established that no activity other than C^{11} or Cu^{62} gave appreciable contribution to the measured activity for the irradiation time of 20 minutes. The samples were then irradiated at various x-ray energies, transferred to a G-M counter and counted in a standard position for two half-lives. Corrections were made for background and for losses at fast rates of counting, the latter taking account of the fourfold variation in counting rate over the measurement period. The resulting yield curves for C^{11} and Cu^{62} are shown in Figs. 3 and 4. The ordinates are ratios of the saturation initial activity in counts per minute per gram of sample to the number of roentgens per minute registered

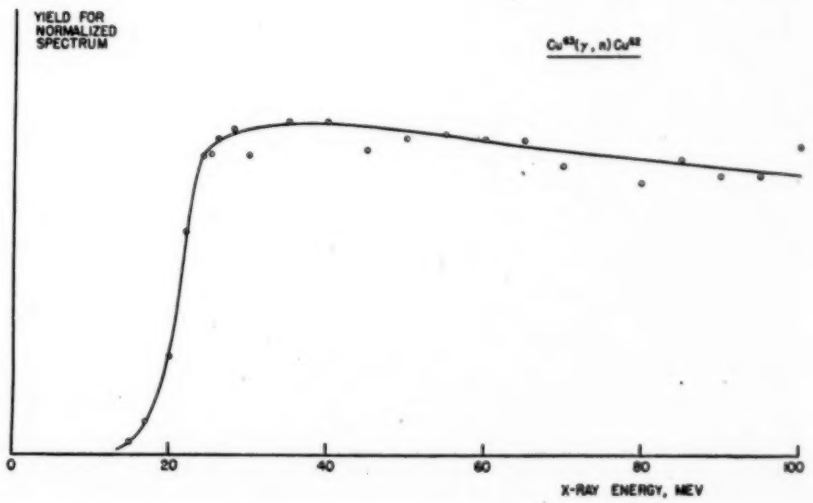

FIG. 6. Product of the curves of Figs. 2 and 4.

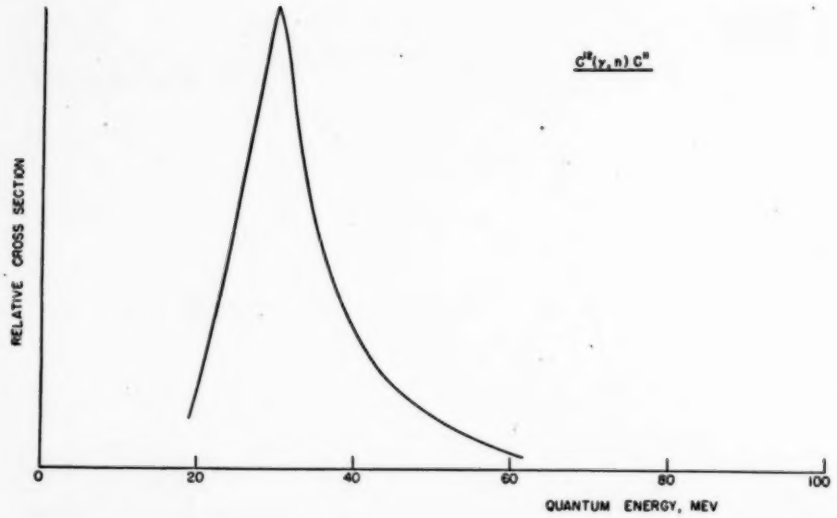

FIG. 7. Approximate cross section for $C^{12}(\gamma,n)C^{11}$, arbitrary units.

by the monitor. Both curves show the same behavior as the x-ray yield for photo-fission—a steep rise from threshold to a maximum, followed by a gradual decrease in yield at higher x-ray energies. The maxima occur at 40 Mev for $C^{12}(\gamma,n)$ and at 24 Mev for $Cu^{63}(\gamma,n)$. The maximum x-ray yield for $U(\gamma,f)$ was at 18 Mev, for $Th(\gamma,f)$ at 20 Mev.[1]

The respective yield curves for production by a normalized family of spectra, obtained by multiplying each yield curve by the function in Fig. 2 are shown in Figs. 5 and 6. From these as in the case of fission, it is apparent that the decreasing x-ray yield at energies above that corresponding to the maximum is in both cases probably due to rising sensitivity of the monitor and that quanta of high energies do not induce the reaction.[5]

The approximate cross sections, shown in Fig. 7 and Fig. 8, have maxima near 30 Mev for C^{11}, 22 Mev for Cu^{62}.

This behavior of the (γ,n) cross section is to be expected as a result of the competition of multiple disintegration processes once these become energetically possible. In Table I are given several photo-nuclear reactions on C^{12} together with their thresholds calculated from mass and

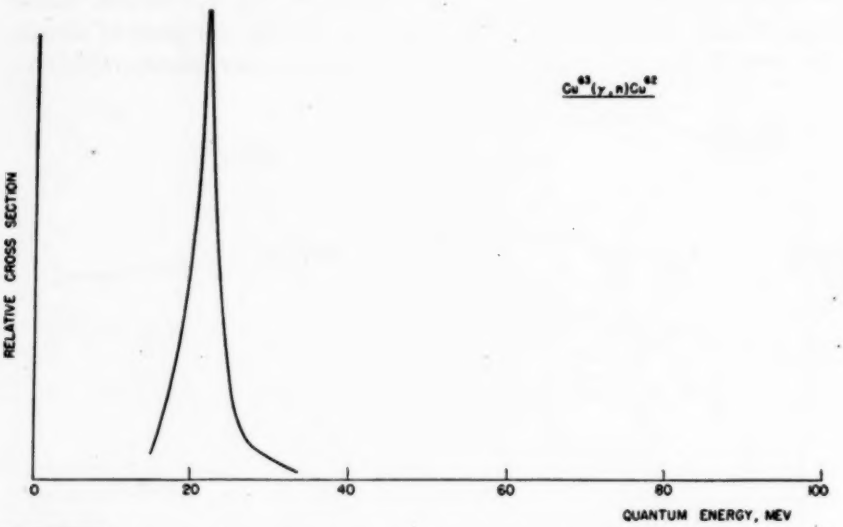

FIG. 8. Approximate cross section for $Cu^{63}(\gamma,n)Cu^{62}$, arbitrary units.

[5] The slight negative slope still present in these curves probably indicates that the true monitor sensitivity rises slightly faster with x-ray energy than the function in Fig. 2. This is probably owing to cascade processes in the lead wall of the monitor, neglected in the calculation; the error is not serious.

beta-decay energies. It is evident that above 27 Mev many alternative disintegration processes can compete with the single-neutron process. The latter, involving a relatively improbable concentration of the entire excitation energy on a single particle or on the latter and a gamma-ray, will be relatively rare.

That "star" processes, similar to the last entry of Table I, occur at fairly low photon energies is evidenced by the star shown in Fig. 9 produced in a 12-in. air-filled cloud chamber with 100-Mev x-rays. This may be a carbon disintegration of this type, but it is believed more likely that it is a disintegration of N^{14} into three alphas, a proton, and a neutron. On this assumption the data of Table II are deduced from measurements

TABLE I. Photo-nuclear thresholds for C^{12}.

Reaction	Threshold (Mev)
$C^{12}(\gamma,p)B^{11}$	15.9
$C^{12}(\gamma,n)C^{11}$	18.6
$C^{12}(\gamma,2p)Be^{10}$	27.0
$C^{12}(\gamma,pn)B^{10}$	27.2
$C^{12}(\gamma,2n)C^{10}$	32.3
$C^{12}(\gamma,2pn)Be^{9}$	33.6
$C^{12}\xrightarrow{\gamma}2\alpha+2p+2n$	35.4

FIG. 9. Tracks of a nuclear evaporation photographed in a 12-in. air-filled cloud chamber; the analysis is given in Table II. The x-ray beam enters from below in the direct (lower) image.

TABLE II. Analysis of the "star" of Fig. 9. Reaction: $_7N^{14}+\gamma\rightarrow{}_1H^1+3\,{}_2He^4+{}_0n^1$.

Particle	$_1H^1$	$_2He^4$	$_2He^4$	$_2He^4$	$_0n^1$
Data	$H\rho=4.3\times10^5$	$R=2.35$ cm.	$R=1.25$ cm.	$R=1.35$ cm.	
Energy, Mev	9.4	3.8	2.4	2.5	2.5
Angle to beam	96°	82°	75°	68°	145°
Azimuth	262°	76°	76°	248°	260°

Calculated threshold = 20 Mev
Total kinetic energy of products = 21 Mev
Energy of incident quantum = 41 Mev

of range or curvature and directions of emission. All of the particles are of low energy, the 40-Mev excitation dividing about equally between binding energy and kinetic energy.

The conclusion that the (γ,n) cross sections become small at high energies is consistent with the observations of Perlman and Friedlander on relative yields at 50 and 100 Mev of several (γ,n) reactions.[6]

3. ABSORPTION MEASUREMENTS

Additional support for this conclusion is found when the absorption of quanta is measured using the photo-nuclear reaction as a detection process.

In Fig. 10 is shown an absorption curve in which the detection process is uranium photofission. The ionization chamber[1] was placed in the 100-Mev x-ray beam and fission counts taken with the beam passing through absorbing slabs of lead to reach the chamber. The activity induced in a Cu foil ahead of the Pb was used to monitor each run. The exponentials drawn for comparison have slopes corresponding to theoretical absorption coefficients in Pb for quanta of the energies indicated.[7]

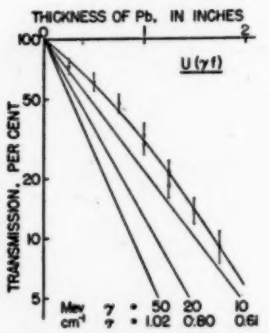

FIG. 10. Absorption of fission-producing component of 100-Mev x-rays.

Figures 11 and 12 present absorption curves taken in Cu and Pb, respectively, with 100-Mev x-rays using the $Cu^{63}(\gamma,n)Cu^{62}$ reaction as detector. A pair of Cu foils, 2 in. square by 0.003 in. thick were placed, one just ahead of a 4-in. ×4-in. ×10-in. block of the absorbing material and the other at a variable depth, x, in the block. These were irradiated simultaneously, then transferred to G-M counters. Each foil's activity was counted for a standard period of one half-life, then the samples were interchanged and the count repeated. From ratios of the three possible products by pairs of the recorded counts was obtained the ratio of sample activities, ratio of counter efficiencies, and ratio of average activity of either sample in the first to that in the second counting period. The latter two data, being constants, provided checks on each run to insure against mistakes or other errors.[8]

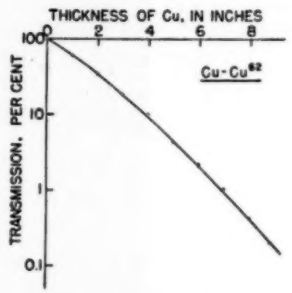

FIG. 11. Absorption in copper of that component of 100-Mev x-radiation which produces the reaction $Cu^{63}\rightarrow Cu^{62}$.

[6] M. L. Perlman and G. Friedlander, Phys. Rev. **72**, 1272 (1947).

[7] W. Heitler, *The Quantum Theory of Radiation* (Oxford University Press, New York, 1944), second edition, Chapter V.

[8] It will be noted from Fig. 12 that deep in the absorber a constant background is present, arising from the reaction $Cu^{63}(n,2n)Cu^{62}$ induced by photo-neutrons in the Pb absorbing block. Since this background is less than 0.1 percent of the Cu^{62} activity observed at the surface of the

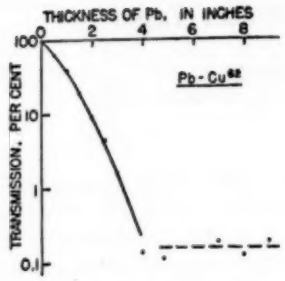

FIG. 12. Absorption in lead of that component of 100-Mev x-radiation which produces the reaction $Cu^{63} \rightarrow Cu^{62}$.

The results are summarized in Fig. 12, which gives the absorption coefficient as a function of depth in the absorbing block, together with theoretical absorption coefficients for radiation of various energies.[7] The experimental curves are, of course, not exponential because:

1. Cascade shower processes build up quanta in the lower energy region of the spectrum.

2. Compton scattering processes in which the energy of the scattered photon remains above the Cu^{62} threshold do not appear as absorption, and, in fact, may appear as a generation of quanta to a detector sensitive only to the lower energy portion of the x-ray spectrum. This effect becomes less important as the spectrum is degraded by passing through increasing thicknesses of absorber.

absorber, it is legitimate to consider the Cu^{62} yield in Fig. 4 to be induced by quanta alone. That this is also true of the photo-fission yields reported in reference 1 is indicated by observations that the fission yield is unaffected by changing the surrounding material from aluminum and brass to graphite and polystyrene, that the fission yield is proportional to the thickness for small thicknesses of the uranium target, that the fission-producing radiation is confined to a beam of 3° half-angle coaxial with the x-ray beam and is absorbed like gamma-radiation (Fig. 10).

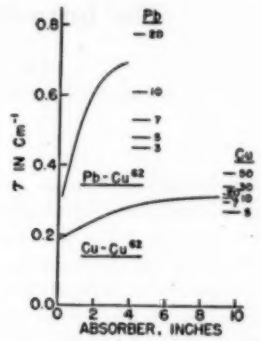

FIG. 13. Summary of absorption data of Figs. 11 and 12. Theoretical absorption coefficients of Cu and Pb are also given for various quantum energies in Mev.

3. The detecting process does not respond only to a single quantum energy but to a band of energies, within which the absorption coefficient varies by an appreciable extent.

Asymptotically, however, the absorption curve should approach an exponential of slope corresponding to the most penetrating component within the energy region in which the detector responds. It will be evident from Fig. 12 that this limiting value of the absorption coefficient compares favorably with that expected theoretically for quanta in the energy region where, according to the analysis of the x-ray yield curves, the detecting reaction has an appreciable cross section.

4. ACKNOWLEDGMENT

We wish to express our appreciation to Mr. C. E. Pickert for his assistance in taking the experimental data and the calculations, to Mr. R. H. Groncznack for assistance with the cloud chamber, and to the operating staff of the 100-Mev betatron.

The Infra-Red Spectrum of Heavy Water Vapor

FRED P. DICKEY AND HARALD H. NIELSEN
Mendenhall Laboratory of Physics, Ohio State University, Columbus, Ohio

(Received January 23, 1948)

The vibration-rotation bands ν_2 and ν_3 in the heavy water vapor (D_2O) spectrum have been remeasured. An analysis of the rotational structure has been carried out. From the interpretation of the data the values of the normal frequencies have been determined as well as the values of the reciprocals of inertia effective in these two vibration states. The frequency ν_2 is found to be 1178.30 cm^{-1}, and the frequency ν_3, 2787.23 cm^{-1}. For the state ν_2 the effective reciprocals of inertia are $A(V)=16.60$ cm^{-1}, $B(V)=7.35$ cm^{-1}, $C(V)=4.84$ cm^{-1}. For the state ν_3, $A(V)=14.88$ cm^{-1}, $B(V)=7.24$ cm^{-1}, $C(V)=4.84$ cm^{-1}.

I. INTRODUCTION

THE vibration-rotation spectrum of water vapor has probably been studied more extensively than that of any other molecule. The fine structure is quite extensive since the moments of inertia are small and the rotational energies large. The rotational structure is, moreover, quite irregular since no two moments of inertia of the molecule are equal and thus the molecule is an asymmetric rotator. The spectrum of heavy water vapor is equally as extensive as that of ordinary water vapor. The band centers of the vibration-rotation bands occur at somewhat lower frequencies than the corresponding water vapor bands, however, because the reduced masses of the molecule are increased by the substitution of deuterium for hydrogen.

The far infra-red spectrum of heavy water vapor (D_2O), corresponding to transitions between the rotational energy levels only, has been measured by Fuson, Randall and Dennison[1] and term values have been assigned. Two of the fundamental vibration-rotation bands, ν_2 and ν_3, have been measured by Barker and Sleator.[2] Their resolution of the lines was not good enough to enable them to make any analysis of the rotational structure beyond the identification of a few lines in the band ν_2. The third fundamental vibration band, ν_1, has been observed by Bender[3] as a Raman line.

The incompletely resolved band ν_2 as given by Barker and Sleator has recently been interpreted by King,[4] who has used a punch card system to obtain the band contour which most resembles that obtained experimentally. From the most satisfactory fit he has obtained values for the moments of inertia.

The potential constants of H_2O have been evaluated by Bonner[5] from the observed frequencies and from the dimensions for the molecule given by Mecke.[6] Using this information, Bonner has predicted the fundamental vibration frequencies of D_2O. More recently Darling and Dennison,[7] using more complete data, have evaluated the normal frequencies of H_2O and D_2O together with values for the moments of inertia of the molecule in many of the vibrational states. The recent measurements by Nielsen[8,9] corroborate essentially the values given by them.

II. EXPERIMENTAL

The absorption spectrum of heavy water vapor was examined with a prism grating spectrometer. The absorption cell which contained the D_2O vapor was 2.54 cm in diameter and 8 cm long. Built onto one side of the cell, and connecting to it, was a small reservoir which contained a sample of liquid D_2O. The windows of the cell were silver chloride. By using this material for the windows there were no etching effects on them due to the heavy water vapor. The windows were sealed onto the cell with red glytal.

[1] N. Fuson, H. M. Randall, and D. M. Dennison, Phys. Rev. **56**, 982 (1939).
[2] E. F. Barker and W. W. Sleator, J. Chem. Phys. **3**, 660 (1935).
[3] D. Bender, Phys. Rev. **47**, 252 (1935).
[4] G. W. King, J. Chem. Phys. **15**, 85 (1947).
[5] L. G. Bonner, Phys. Rev. **46**, 458 (1934).
[6] R. Mecke, Zeits. f. Physik **81**, 313 (1933).
[7] B. T. Darling and D. M. Dennison, Phys. Rev. **55**, 128 (1940).
[8] H. H. Nielsen, Phys. Rev. **59**, 565 (1941).
[9] H. H. Nielsen, Phys. Rev. **62**, 422 (1942).

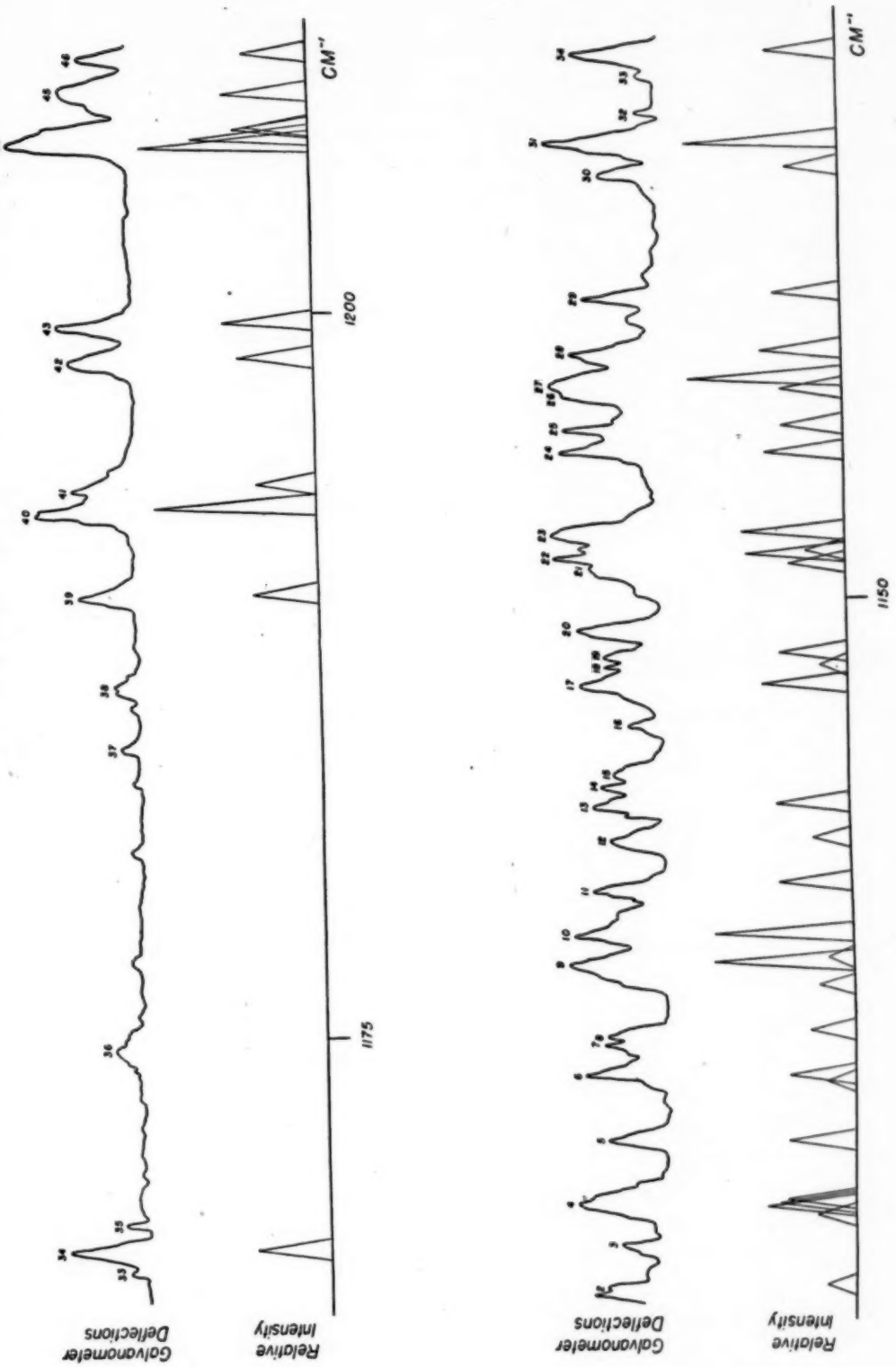

FIG. 1. Absorption band ν_2 for D_2O.

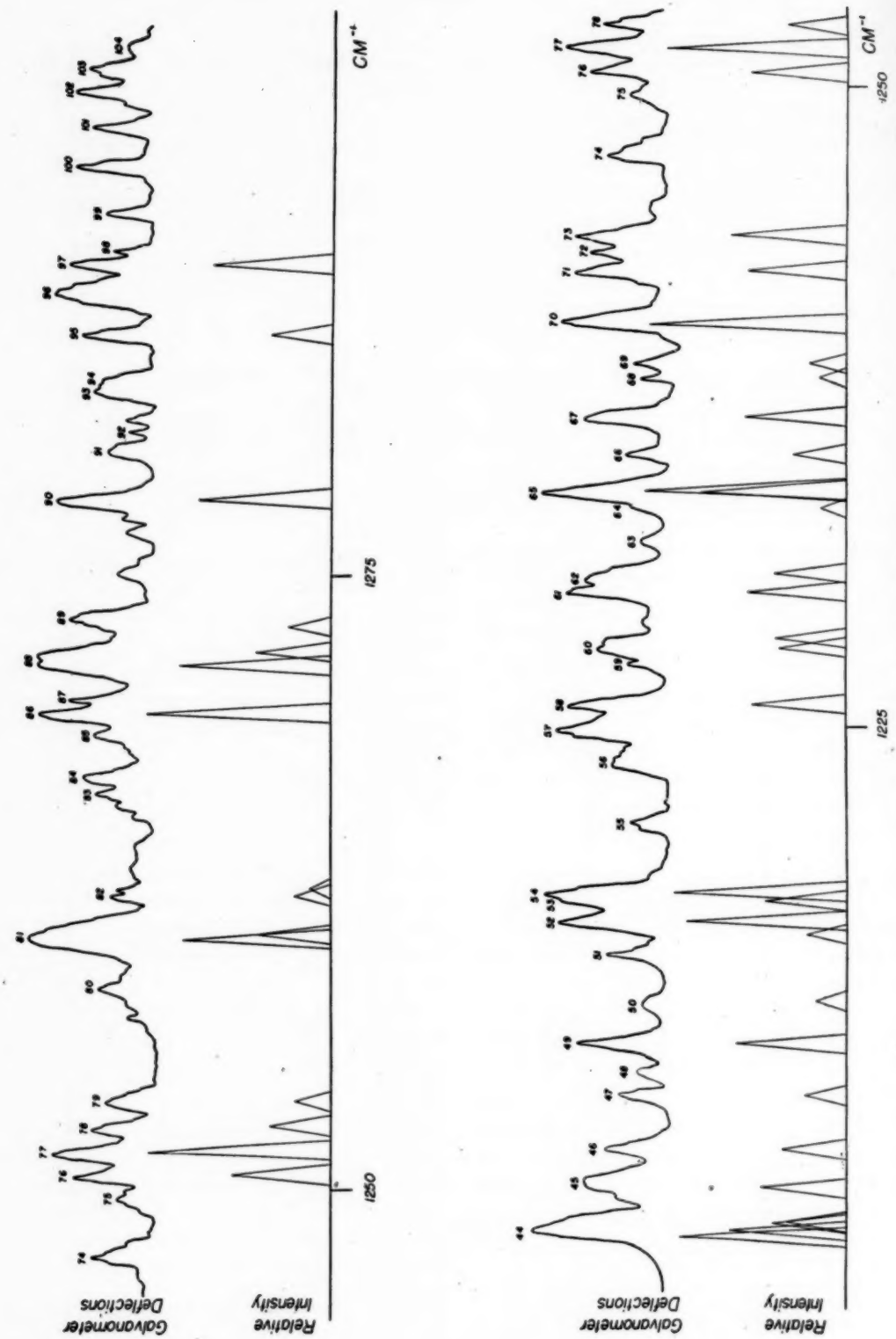

FIG. 2. Absorption band ν_2 for D_2O.

The sample of heavy water used was obtained from the Stuart Oxygen Company and contained a minimum of 99.9 percent D_2O. The sample was introduced into the reservoir of the cell through a stopcock and then frozen by immersing the reservoir in liquid air. The cell was then evacuated and the stopcock closed. When the reservoir was removed from the liquid air, the heavy water melted, and heavy water vapor filled the cell. To prevent the vapor from condensing on the windows, and a resulting loss in the amount of transmitted energy, the windows of the cell were kept slightly warmer than the rest of the cell.

The gratings used for these measurements were replicas made by R. W. Wood. The one used in measuring the band ν_2 was a grating ruled with 3600 lines per inch. The one used in measuring the band ν_3 was ruled with 7200 lines per inch. The grating constants were determined by observing lines of the mercury spectrum in high orders. The position of the lines in wave numbers were reduced to their values in vacuum, and thus the corrected wave numbers are strictly proportional to the oscillation frequencies, the more fundamental figure, since these are not changed when the medium is changed.

The fundamental vibration-rotation band ν_2 was observed in the region between 1125 cm^{-1} and 1300 cm^{-1} with the effective slit width of the spectrometer set to 0.35 cm^{-1}. Readings of the transmitted energy were made and recorded for every five seconds of arc of the grating circle. The results of the measurements may be seen by referring to the upper curves of Figs. 1 and 2. The numbers appearing over the various lines are arbitrary numbers assigned to them. These numbers are useful in quickly picking out any one line. Frequencies in wave numbers, corrected to vacuum, for the lines are given in Table I.

The fundamental vibration-rotation band ν_3 was observed in the region between 2650 cm^{-1} and 2900 cm^{-1}. The effective slit width was 0.35 cm^{-1}, and readings of the transmitted energy were made and recorded for every five seconds of arc of the grating circle. The results of these measurements may be seen by referring to the upper curves of Fig. 3. Frequencies in wave numbers, corrected to vacuum, for these lines are given in Table II.

After these measurements were taken and an analysis of the bands carried out, the automatic recording vacuum spectrometer described by

TABLE I. Frequency positions and identifications of heavy water vapor lines in ν_2.

Line No.	Obs. $\nu_{(vac)}$ (cm^{-1})	Transition
1	1128.66	
2	1128.89	4_2-4_4
3	1130.14	
4	1131.43	$3_{-3}-4_{-3}$
		$5_{-4}-5_{-2}$
		$6_{-6}-6_{-4}$
5	1133.78	$5_{-2}-5_0$
6	1135.41	$4_{-1}-4_{-3}$
		$4_{-1}-5_{-3}$
7	1136.27	
8	1136.54	3_0-3_2
9	1138.78	$3_{-2}-4_{-4}$
		3_1-3_3
		$4_{-3}-4_{-1}$
10	1139.72	$2_{-2}-3_{-2}$
11	1141.10	4_0-4_2
12	1142.63	$5_{-5}-5_{-3}$
13	1143.71	$3_{-2}-3_0$
14	1144.31	
15	1144.69	
16	1146.27	
17	1147.54	$6_{-2}-6_0$
18	1148.07	$2_{-1}-2_1$
19	1148.42	$1_{-1}-2_{-1}$
20	1149.09	
21	1151.26	$2_{-1}-3_{-3}$
22	1151.74	3_0-4_{-2}
		$6_{-4}-6_{-2}$
23	1152.22	$4_{-4}-4_{-2}$
24	1154.94	2_0-2_2
25	1155.65	$5_{-3}-5_{-1}$
26	1156.80	$3_{-1}-3_1$
27	1157.16	$4_{-2}-4_0$
28	1158.10	0_0-1_0
29	1159.91	$3_{-3}-3_{-1}$
30	1163.95	1_0-2_{-2}
31	1164.94	$2_{-2}-2_0$
32	1165.89	
33	1167.10	
34	1167.80	$1_{-1}-1_1$
35	1168.80	
36	1174.56	
37	1184.74	
38	1187.04	
39	1190.29	1_1-1_{-1}
40	1193.28	2_0-2_{-2}
41	1194.06	$2_{-2}-1_0$
42	1198.53	$3_{-1}-3_{-3}$
43	1199.80	1_0-0_0
44	1206.41	$3_{-3}-2_{-1}$
		3_1-3_{-1}
		$4_{-2}-4_{-4}$
		4_0-4_{-2}
45	1207.93	2_2-2_0
46	1209.38	$2_{-1}-1_{-1}$
47	1211.36	$4_{-2}-3_0$
48	1212.21	
49	1213.26	$6_{-2}-6_{-4}$
50	1214.73	2_1-2_{-1}
51	1216.57	
52	1217.84	$3_{-2}-2_{-2}$
		$5_{-3}-5_{-5}$
53	1218.58	3_0-3_{-2}
54	1218.91	$4_{-4}-3_{-2}$
55	1221.46	
56	1223.85	
57	1225.08	
58	1225.95	$4_{-2}-3_{-3}$
59	1227.54	
60	1228.50	$5_{-2}-5_{-4}$
		$6_{-4}-6_{-6}$
61	1230.23	$5_{-5}-4_{-3}$
62	1231.16	$5_{-2}-5_{-4}$
63	1232.30	
64	1233.44	3_2-3_1
65	1234.12	2_1-1_1
		4_2-4_0
		$5_{-4}-4_{-4}$
66	1235.52	3_2-3_0
67	1236.97	2_2-1_0
68	1238.45	$6_{-2}-6_{-5}$
69	1239.02	4_1-4_{-1}
70	1240.65	$6_{-6}-5_{-4}$
71	1242.68	$6_{-5}-5_{-5}$
72	1243.46	
73	1243.98	3_0-2_0
74	1247.24	
75	1249.64	
76	1250.46	$7_{-7}-6_{-5}$
77	1251.47	$7_{-7}-6_{-6}$
78	1252.39	$4_{-1}-3_{-1}$
79	1253.45	3_1-2_{-1}
80	1258.06	
81	1259.98	$8_{-8}-7_{-6}$
		$8_{-7}-7_{-7}$
82	1261.90	4_4-4_2
		4_4-4_1
83	1266.09	
84	1266.73	
85	1268.40	
86	1269.27	$9_{-9}-8_{-7}$
		$9_{-8}-8_{-8}$
87	1270.00	
88	1271.64	3_2-2_2
		3_2-2_1
89	1273.29	4_0-3_{-2}
90	1278.13	$10_{-10}-9_{-8}$
		$10_{-9}-9_{-9}$
91	1280.31	
92	1281.00	
93	1282.63	
94	1283.20	
95	1285.21	4_1-3_{-3}
96	1287.14	
97	1288.27	4_2-3_0
98	1288.92	
99	1290.57	
100	1292.52	
101	1294.19	
102	1295.81	
103	1296.58	
104	1297.78	

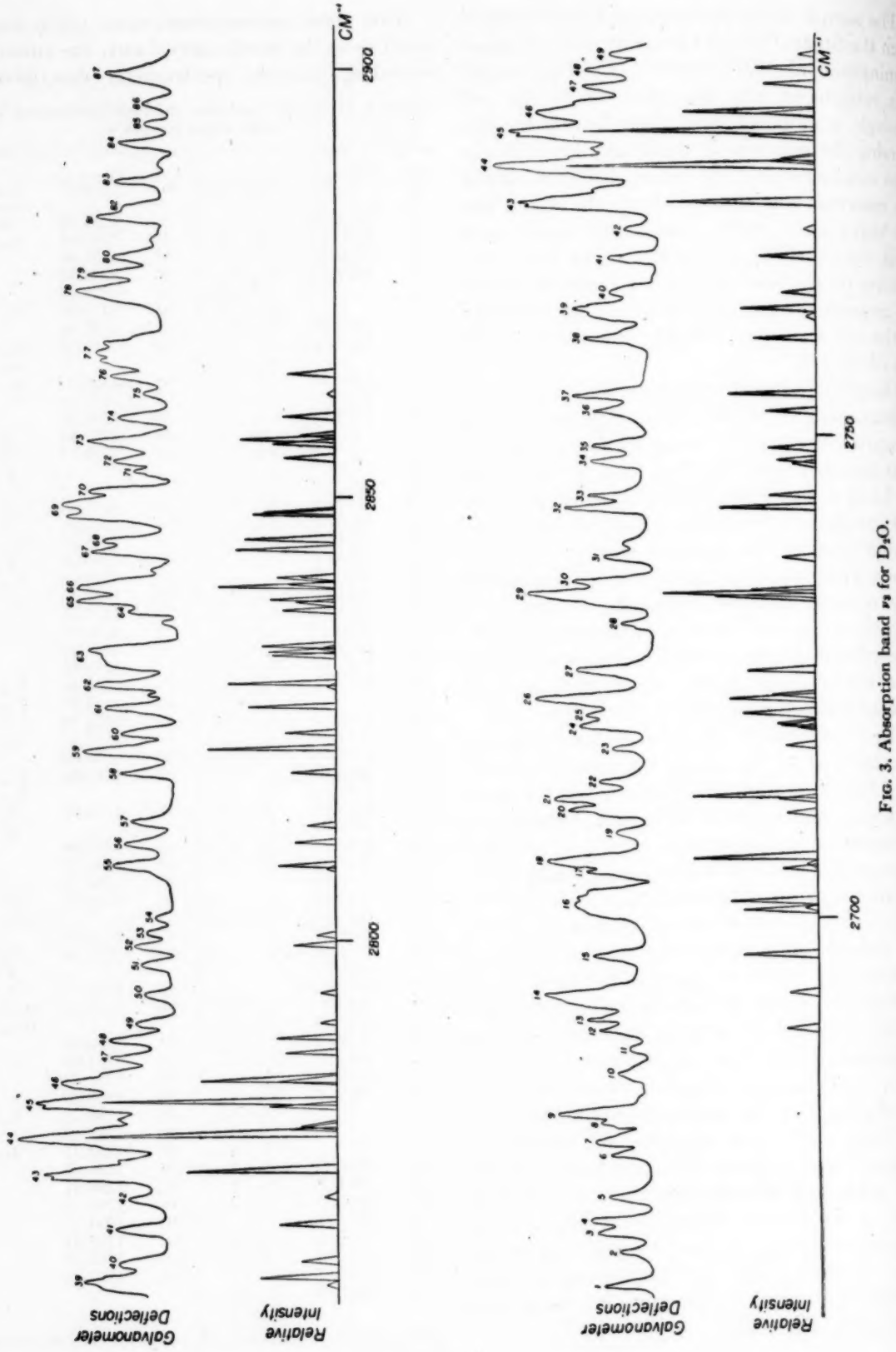

FIG. 3. Absorption band ν_3 for D_2O.

TABLE II. Frequency positions and identifications of heavy water vapor lines in ν_3.

Line No.	Obs. $\nu_{(vac)}$ (cm^{-1})	Transition
1	2663.78	
2	2666.96	
3	2668.80	
4	2669.85	
5	2672.10	
6	2676.33	
7	2677.78	
8	2679.44	
9	2680.47	
10	2684.32	
11	2686.50	
12	2688.60	
13	2689.75	6_0-7_{-1}
14	2692.26	$6_{-2}-7_{-3}$
15	2696.15	5_0-6_{-1}
		$6_{-1}-7_{-2}$
16	2700.69	$5_{-1}-6_{-2}$
		5_4-6_3
		5_3-6_4
	2701.33	5_1-6_0
		$6_{-4}-7_{-5}$
	2701.96	
	2702.49	
17	2704.82	5_2-6_1
		5_3-6_2
18	2705.88	$5_{-3}-6_{-4}$
		$6_{-3}-7_{-4}$
19	2708.65	
20	2710.89	$5_{-2}-6_{-3}$
21	2712.28	$6_{-6}-7_{-7}$
		$6_{-3}-5_{-4}$
22	2713.99	
23	2717.41	4_3-5_2
		4_4-5_3
24	2719.77	$4_{-2}-5_{-3}$
		4_0-5_{-1}
		4_2-5_1
25	2720.95	$4_{-2}-5_{-3}$
		4_1-5_1
26	2722.56	$5_{-3}-6_{-4}$
		$5_{-4}-6_{-5}$
27	2725.48	$1_{-1}-2_2$
		$4_{-1}-5_{-2}$
28	2730.25	
29	2733.40	$3_{-1}-4_{-2}$
		3_1-4_0
		3_2-4_1
		3_3-4_2
		$4_{-4}-5_{-5}$
		$4_{-3}-5_{-4}$
30	2734.48	
	2734.71	
31	2737.32	3_0-4_{-1}
32	2742.35	$3_{-3}-4_{-4}$
33	2743.67	$3_{-2}-4_{-3}$
34	2747.30	2_0-3_{-1}
		2_2-2_{-1}
		$3_{-3}-3_0$
35	2748.90	2_1-3_0
36	2752.82	$2_{-3}-3_{-3}$
37	2754.26	$2_{-1}-3_{-2}$
38	2760.36	1_1-2_0
39	2762.81	$4_{-3}-4_{-2}$
	2763.79	$1_{-1}-2_{-2}$
40	2765.38	1_0-2_{-1}
41	2768.74	6_5-6_6
	2769.30	6_6-6_5
42	2772.11	$3_{-2}-3_{-1}$
43	2774.70	
	2775.15	0_0-1_{-1}
		5_4-5_5
		5_5-5_4
		6_3-6_4
		6_4-6_3
	2776.27	
44	2779.21	$2_{-1}-2_0$
		$4_{-1}-4_0$
		4_3-4_4
		4_4-4_3
		5_3-5_3
		5_3-5_2
		6_1-6_2
		6_2-6_1
45	2782.50	
	2782.95	3_0-3_1
		3_2-3_3
		3_3-3_2
		4_1-4_2
		4_2-4_1

TABLE II.—*Continued.*

Line No.	Obs. $\nu_{(vac)}$ (cm^{-1})	Transition
46	2784.77	1_0-1_1
		2_1-2_2
		2_2-2_1
47	2787.62	3_1-3_0
48	2789.44	1_1-1_0
49	2791.27	4_0-4_{-1}
50	2794.30	2_0-2_{-1}
51	2797.57	
52	2799.63	$1_{-1}-0_0$
53	2800.90	$3_{-1}-3_{-2}$
54	2802.52	
55	2808.53	$2_{-1}-1_0$
		$4_{-2}-4_{-3}$
56	2811.09	$2_{-2}-1_{-1}$
57	2813.41	2_0-1_1
58	2819.13	$3_{-2}-2_{-1}$
59	2821.36	$3_{-3}-2_{-2}$
		3_0-2_1
60	2823.24	2_1-2_{-2}
		3_1-2_2
61	2826.16	$3_{-1}-2_0$
62	2828.89	$4_{-3}-3_{-2}$
		$4_{-1}-4_{-4}$
63	2830.89	
	2831.13	$4_{-4}-3_{-3}$
	2831.91	4_1-3_2
		5_0-4_1
	2832.19	4_2-4_3
	2832.77	
	2832.90	$4_{-1}-3_0$
64	2836.93	$4_{-2}-3_{-1}$
65	2838.36	4_0-3_1
		$5_{-4}-4_{-3}$
66	2839.90	$5_{-3}-4_{-4}$
	2840.80	$5_{-2}-4_{-1}$
		5_1-4_2
		5_2-4_3
		5_3-4_4
67	2844.00	$5_{-3}-4_{-2}$
68	2845.15	$5_{-1}-4_0$
69	2847.90	$6_{-5}-7_{-6}$
		$6_{-4}-5_{-5}$
	2849.34	
70	2850.66	
71	2853.07	
72	2854.26	6_1-5_2
		6_2-5_3
73	2856.44	$6_{-3}-5_{-2}$
		$6_{-1}-5_0$
		6_0-5_1
74	2859.34	$6_{-4}-5_{-3}$
75	2861.40	3_1-2_{-2}
76	2864.06	$6_{-2}-5_{-1}$
77	2865.29	
	2865.88	
	2866.74	
	2867.96	
78	2872.95	
	2874.18	
79	2876.02	
80	2877.79	
81	2882.90	
82	2884.01	
83	2886.85	
84	2891.43	
85	2893.54	
86	2896.25	
87	2899.77	

Bell, Noble, and Nielsen[10] became available at the laboratory, and as a matter of interest, the bands were remeasured on this instrument. The results of these measurements of the band ν_2 are shown in Fig. 4. It should be noted that the gain was increased on the high frequency side of the band. The measurements of the band ν_3 are shown in Fig. 5. Here the gain was reduced over the region occupied by the strong central lines of the Q branch, that is lines 42 to 50, and was somewhat different over the region occupied by lines 51 to 79. A section of the automatic recorded spectrum tracing may be seen in Fig. 6. This includes the region from the center of the band ν_2 to line 67.

[10] E. E. Bell, R. H. Noble, and H. H. Nielsen, Rev. Sci. Inst. 18, 48 (1947).

III. IDENTIFICATION OF THE OBSERVED LINES

The identification of the lines measured in the two bands was made by following the method used by Nielsen[8,9] in identifying the lines in the spectrum of water vapor. Each line in one of the bands ν_i is due to the molecules making a transition from a rotation level in the normal vibration state to a rotation level in the vibration state ν_i, and the frequency of such a line will be the difference between a term value in ν_i and one in the normal state. The selection rules governing what transitions may take place have been given by Dennison.[11]

Term values for the normal state have been determined experimentally by Fuson, Randall

[11] D. M. Dennison, Rev. Mod. Phys. 3, 280 (1931).

FIG. 4. ν_3 for D_2O measured with automatic recording spectrometer.

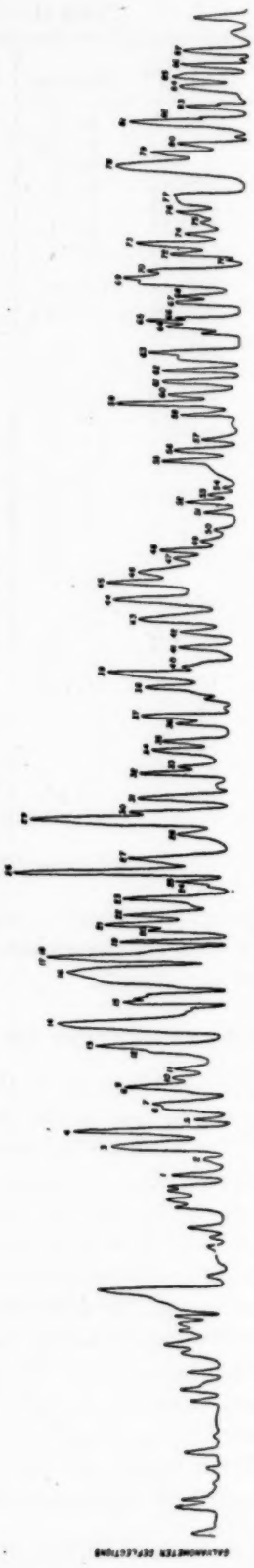

FIG. 5. ν_3 for D_2O measured with automatic recording spectrometer.

and Dennison.[1] Term values for the state ν_i will be the sum of the vibrational energy plus the rotational energy. Shaffer and Nielsen[12] have given the following expression for the rotational energies of the non-linear triatomic molecule:

$$E(V,J,\tau)=J(J+1)\tfrac{1}{2}(A(V)+B(V)) +\rho_1-J^2(J+1)^2\rho_2+\epsilon_\tau, \quad (1)$$

where ρ_1 and ρ_2 are constants; $A(V)$, $B(V)$, and $C(V)$ are the reciprocals of inertia; V_1, V_2 and V_3 are the vibrational quantum numbers, J is the quantum number of total angular momentum, and ϵ_τ is one of the $2J+1$ roots of the secular determinant which is used to diagonalize the rotational part of the Hamiltonian. Nielsen[1] has expanded this determinant for all values of J up through $J=6$, and given the algebraic relations for ϵ_τ. Constants which occur in (1) may be evaluated by first identifying, by trial and error, enough lines in the spectrum of ν_1 to enable the determination of the term values for $J=0$, $J=1$, and $J=2$. When these term values are known, enough relationships of (1) will be available to permit an evaluation of the constants for the state ν_i. For example, if a line is identified as being due to the transition 1_1-1_{-1}, then the term value for 1_1 in the state ν_i will be equal to the frequency of the line plus the term value for 1_{-1} in the normal state. The correctness of these term values may be checked by using them, together with the term values in the normal state and the selection rules, to see if lines which would occur from such values are actually found in the measured spectrum.

Once the constants of (1) are known, rotational energies and then term values for $J=3$ may be calculated. These term values will give rise to additional spectral lines. A check is then made of the measured spectrum to see if such lines occur. Once these lines are located in the measured spectrum new term values for $J=3$ may be determined from the experimental data. The new term values may be used to improve the values of the constants of (1). The process is then repeated for still higher values of J.

In an attempt to evaluate the centrifugal stretching coefficients from the data of Fuson, Randall, and Dennison[1] by fitting the energy

[12] W. H. Shaffer and H. H. Nielsen, Phys. Rev. 56, 188 (1939).

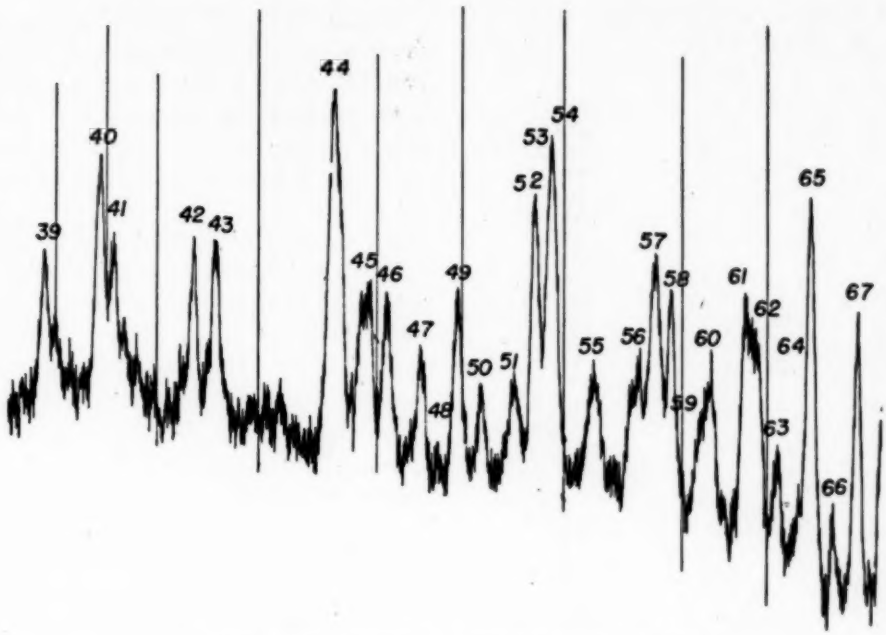

FIG. 6. Section of record of absorption band ν_2 for D_2O.

relations up to $J=6$ to their term values, no consistant values could be obtained. This was interpreted to mean that the effect of the centrifugal stretching on these levels was so small that it was less than the experimental accuracy. Since our evaluation of the moments of inertia of the molecule is made from transitions where J is not greater than 6, the effect of centrifugal stretching has been neglected. It may, in fact, be seen by reference to the relations (39) and (42) of the work of Shaffer and Nielsen[12] that the centrifugal stretching might here be expected to be approximately $\frac{1}{16}$ the magnitude of those for H_2O.

As a further aid in identifying the lines of the spectrum, the relative intensities of the lines have been calculated by using the line strengths given by Cross, Hanier, and King.[13] That is:

$$\sum_{X'Y'Z'}\sum_{M''}\sum_{M'}|(\phi_{F_0}{}^A)_{J''\tau''M'';\ J'\tau'M'}|^2, \qquad (2)$$

where ϕ_{F_0} represents the direction cosine element of the asymmetric rotator and $X'Y'Z'$ are the space fixed Cartesian coordinates. Their values are for various parameters of asymmetry. That is:

$$K=\frac{2B(V)-A(V)-C(V)}{A(V)-C(V)}, \qquad (3)$$

The values used were those tabulated for $K=-0.5$, since the parameter of asymmetry of D_2O in the normal state is -0.54, in the state ν_2 -0.57, and in the state ν_3 -0.53.

Term values determined in this manner for the frequencies ν_2 are tabulated in Table III.

TABLE III. Vibration-rotation term values for the frequencies ν_2.

J_τ	ν_2	J_τ	ν_2
0_0	1178.30 cm^{-1}	4_0	1347.51 cm^{-1}
1_1	1202.37	4_{-1}	1341.16
1_0	1199.75	4_{-2}	1321.16
1_{-1}	1190.39	4_{-3}	1296.20
2_2	1257.15	4_{-4}	1293.56
2_1	1256.70	5_{-2}	1401.19
2_0	1229.00	5_{-3}	1386.12
2_{-1}	1221.50	5_{-4}	1348.83
2_{-2}	1214.20	5_{-5}	1348.60
3_3	1345.44	6_{-2}	1492.79
3_2	1345.33	6_{-3}	1471.05
3_1	1295.39	6_4	1460.43
3_0	1293.18	6_{-5}	1411.56
3_{-1}	1268.79	6_{-6}	1410.61
3_{-2}	1253.55	7_{-6}	1483.39
3_{-3}	1248.67	7_{-7}	1483.06
4_4	1468.00	8_{-7}	1565.30
4_3	1468.00	8_{-8}	1565.22
4_2	1398.06	9_{-8}	1657.07
4_1	1397.29	9_{-9}	1657.02

[13] P. C. Cross, R. M. Hanier, and G. W. King, J. Chem. Phys. 12, 210 (1944).

TABLE IV. Vibration-rotation term values for the frequencies ν_3.

J_τ	ν_3	J_τ	ν_3
0_0	2787.23 cm^{-1}	5_5	3186.33 cm^{-1}
1_1	2809.58	5_4	3186.33
1_0	2807.36	5_3	3110.05
1_{-1}	2799.57	5_2	3110.05
2_2	2859.10	5_1	3046.64
2_1	2858.71	5_0	3037.68
2_0	2836.05	5_{-1}	3009.18
2_{-1}	2828.78	5_{-2}	2998.50
2_{-2}	2823.14	5_{-3}	2985.40
3_3	2939.40	5_{-4}	2955.63
3_2	2939.39	5_{-5}	2954.61
3_1	2897.42	6_6	3351.00
3_0	2895.00	6_5	3351.00
3_{-1}	2875.36	6_4	3260.56
3_{-2}	2861.04	6_3	3260.56
3_{-3}	2857.11	6_2	3185.20
4_4	3048.27	6_1	3184.95
4_3	3048.27	6_0	3126.60
4_2	2988.71	6_{-1}	3122.79
4_1	2988.36	6_{-2}	3094.53
4_0	2949.97	6_{-3}	3073.91
4_{-1}	2943.00	6_{-4}	3065.33
4_{-2}	2925.72	6_{-5}	3017.80
4_{-3}	2903.47	6_{-6}	3017.10
4_{-4}	2901.37	—	——

Term values for the frequencies ν_3 are tabulated in Table IV. The identification of lines is given in the third columns of Tables I and II. Immediately below the measured spectrum shown in Figs. 1, 2, and 3 is shown a spectrum which one would expect using the term values given in Tables III and IV. The lines are drawn as triangles, where the base is twice the equivalent slit width and the height is proportional to the relative intensity, which was determined in the manner described. The term values given for the state ν_2 with values of J higher than 6 were not determined in the manner discussed but rather from the characteristics of the spectrum and the calculated relative intensities.

The term values up to $J=6$ have been employed to calculate the values of the reciprocals of inertia $A(V)$, $B(V)$, and $C(V)$. The values which seem most consistent with the term values given in Tables I and II are stated in Table V. In the same table are stated the values of the corresponding effective moments of inertia I_A, I_B, and I_C for the normal state and the states ν_2 and ν_3.

Darling and Dennison[7] have shown that the quantity $\Delta=I_C-I_A-I_B$ is one which, for planar molecules, is independent of the coefficients of the anharmonic part of the potential energy. Its value may therefore be computed from a knowledge of the normal frequencies and the shape of the molecule. The values of Δ for the states ν_2 and ν_3 computed with the aid of the relation of Darling and Dennison, are also given in Table V, together with the experimentally determined values. It is somewhat disappointing that the computed value of Δ for the state ν_2 seems to differ appreciably from the measured value.

The data of Barker and Sleator[2] has been analyzed by King,[4] using a punch card method developed by them. His values for the moments of inertia, which were originally chosen to obey the Δ condition, vary slightly from the values given by us. The values of the moments of inertia chosen by King are such as to give the best over-all agreement with the contour of the incompletely resolved absorption pattern reported by Barker and Sleator. The values are therefore those which fit the term values of high J values best. No compensation has been made by him for centrifugal stretching. While the centrifugal stretching is much smaller here than in the case of ordinary water vapor, it can probably not be neglected for the higher values of J.

We have, of course, never employed the

TABLE V. Values of $A(V)$, $B(V)$, $C(V)$, I_A, I_B, I_C, and Δ.

	Normal state*	ν_2	ν_3
$A(V)$	15.38 cm^{-1}	16.60 cm^{-1}	14.88 cm^{-1}
$B(V)$	7.25	7.35	7.24
$C(V)$	4.83	4.84	4.84
I_A	1.820×10^{-40} g cm^2	1.686×10^{-40} g cm^2	1.881×10^{-40} g cm^2
I_B	3.860×10^{-40}	3.808×10^{-40}	3.866×10^{-40}
I_C	5.794×10^{-40}	5.782×10^{-40}	5.782×10^{-40}
$\Delta_{obs.}$	0.114×10^{-40}	0.288×10^{-40}	0.035×10^{-40}
$\Delta_{calc.}$	0.105×10^{-40}	0.327×10^{-40}	0.084×10^{-40}

* See reference 1.

method of King and are, therefore, not really qualified to criticize it. We do know, however, that his values of the moments of inertia do not yield lines at positions which fit our data as well as the values of the moments of inertia which we have given in Table V. We believe this to be because his values are chosen so as to give the best agreement at considerable distances from the center of the band where the centrifugal distortion is of considerable significance. They must, therefore, deviate from the values which would give the best fit near the center of the band. In our determination, compensation for centrifugal stretching has also been neglected. The values of the moments of inertia were, however, determined from term values of small J value where the centrifugal stretching is small and may be neglected. Since the lines which have been used to determine these term values are known accurately to about 0.05 cm^{-1}, we believe the values obtained by us for the moments of inertia are somewhat more reliable.

The authors wish to acknowledge with gratefulness grants-in-aid from The American Philosophical Society and The Research Corporation in New York City.

PHYSICAL REVIEW VOLUME 73, NUMBER 10 MAY 15, 1948

The Conservation of Momentum in the Beta-Decay of Y^{90}*

CHALMERS W. SHERWIN
University of Illinois, Urbana, Illinois
(Received January 27, 1948)

Monolayer sources of yttrium (90) are formed by evaporation in a vacuum of 10^{-7} mm of Hg. The momentum of individual recoil ions is measured by timing their flight in a field free space. The positively charged Zr (90) recoils appear to lose about 6-electron volts energy as they escape from the surface. If a 6-electron volt correction is made to the observed recoil spectra, there is good agreement regarding shape and absolute amplitude with those recoil spectra calculated on the assumption of a neutrino-electron angular correlation function of $(1-\beta\cos\theta)^2$. For this function the most probable angle between the neutrino and the electron is $\sim 135°$. These results are in agreement, within experimental error, with earlier data obtained with P^{32}. The exact limits of error due to chemical effects at the surface cannot yet be assigned, so it is not possible to make a definite selection of the form of the neutrino-electron angular correlation function.

1. INTRODUCTION

IN earlier experiments[1] the momentum spectra of the recoil ions from monolayer sources of P^{32} ($E_{max}=1.72$ Mev, half-life, 14.3d) were measured. It was concluded that momentum is not conserved between the electron and the recoil nucleus. If one assumes the existence of a neutrino, which is most probably emitted in the opposite hemisphere from the electron, one accounts for the experimentally observed recoil momentum spectra. The experiments reported here measure the recoil momentum spectra of yttrium (90) ($E_{max}=2.16$ Mev, half-life, 62 hr.). These experiments permit a rather critical test of the previous results, since the Zr^{90} recoil ion from Y^{90} is very different from the S^{32} recoil ion from P^{32}. The recoil ions in these two cases differ appreciably regarding (1) maximum velocity, (2) maximum energy, (3) maximum momentum, (4) mass, (5) ionization potential (S = 10.3 volts, Zr = 6.92 volts), and (6) the fraction of the recoils that escape in the charged state. If one assumes a $(1-\beta\cos\theta)^2$ neutrino-electron angular correlation function for both cases, about 8 percent of the sulfur, and about 87 percent of the zirconium recoils escape charged.

In addition, the nature of the freshly evaporated foundation surface on which the monolayer is deposited is different. P^{32} was deposited on

* This work was supported by the Office of Naval Research under Contract No. N6ori-71, Physics Task No. 1.

[1] C. W. Sherwin, Phys. Rev. **73**, 216 (1948).

quartz, NaF, and LiF. Y^{90} was deposited on quartz and tungsten. In all these cases, except for a 6-electron volt energy loss of the Zr ions, the recoil spectra are quite similar.

Only by varying the conditions at the surface over the widest possible range can estimates of the errors caused by surface effects be made. Changing the type of beta-active material as well as the type of foundation surface provides a method of distinguishing between nuclear effects and chemical effects.

2. THE EXPERIMENTAL METHOD

The apparatus is substantially the same as in the earlier experiments.[1] The velocity of the ionized recoil nucleus is measured by timing its flight over a field free path of 7.6 cm. The nucleus is accelerated (to 3000 volts) between two parallel grids, and then detected by an electron multiplier. This latter process takes a calculated time of 0.42 microsecond, which is essentially constant for all the recoil ions. The beta-particles are detected at 180°, 135°, 90°, and 45° with respect to the direction of the recoil ions. The beta-particles are detected in a 10 degree half-angle cone and the recoils in a 3 degree half-angle cone for all four directions.

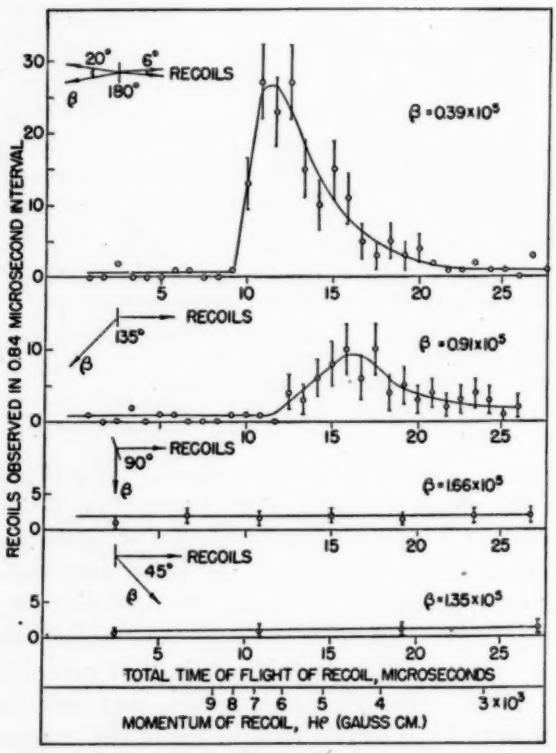

FIG. 1. *Observed time of flight distributions for the recoil ions from* Y^{90}. The yttrium, probably in the form of YO, is deposited on a freshly evaporated surface of tungsten. The angular apertures, for the detection of the beta-particles and the recoils, are the same for all four angles. The number equated to β is the total number of beta-particles detected by the Geiger counter during the collection of the recoil data. The failure to observe recoils, above background, at 90° and 45° is consistent with the neutrino hypothesis.

The Y^{90} is separated from the parent Sr^{90} (obtained from the Clinton Laboratories) by the method of J. D. Kurbatov and M. N. Kurbatov.[2] In this method, with the two radioactive materials in a pH 9 solution, most of the Y^{90} is absorbed on a filter paper while the Sr^{90} filters through the paper. Only about 1 percent of the activity of the final, carrier free, Y^{90} solution is due to Sr^{90}. The specific activity of this final solution (0.1 N HCl) is estimated to be less than one milligram of non-volatile matter per millicurie of Y^{90}.

The Y^{90} is evaporated (at about 2000°C) from a clean 10-mil tungsten wire bent in the form of a small hairpin. The catching surface, made of mica or thin glass, has a thickness ranging from 1.8 to 0.5 mg/cm². When quartz is used, the mica (or glass) is first coated with a thin gold surface to reduce the effect of electrostatic charges due to the escape of the excess number of beta-particles over the number of charged recoils. Recently it has been shown by Robley C. Williams[3] that polished or fire glazed glass surfaces have irregularities of the order of 5 angstroms. Thus, even when approaching the atomic scale, the blown glass films used in some of the experiments with Y^{90} are not very rough.

The catching surface, freshly coated with a few atomic layers of tungsten or quartz, is exposed to the evaporating Y^{90} for about 15 or 20 seconds when the 10-mil filament is at the most favorable temperature. In determining this temperature, it was observed in an auxiliary system that 90 percent of the Y^{90} activity evaporated from the 10-mil tungsten wire in about 60 seconds when the current was increased from 4.5 amperes to 4.8 amperes. Up to the 4.5-ampere point practically none of the Y^{90} evaporated. Even with the aid of this calibration,

[2] J. D. Kurbatov and M. N. Kurbatov, J. Phys. Chem. 46, 441 (1942).
[3] R. C. Williams (to be published).

only five out of sixteen surfaces showed the characteristic time of flight distributions which are interpreted as being due to monolayer surfaces. Figure 1 shows an example of these data, for which the best statistics were obtained. The eleven "bad" or "thick" surfaces showed a large number of low momentum recoils, and were in all respects identical to the "good" surfaces after they were five or six hours old. The "good" surfaces required anywhere from 20 to 100 minutes to begin to show signs of contamination. Both quartz and tungsten foundation surfaces gave the same time of flight distributions.

Studies with the mass spectrograph[4] have shown that yttrium evaporates from a tungsten surface as positively charged YO ions. Therefore, in these experiments, the yttrium is probably deposited on the catching surface as YO. This means that the recoil ion Zr^+, must break a bond with an oxygen atom in order to escape from the monolayer surface as a free ion. It is shown later that there is definite evidence of loss of about 6-electron volts energy by the recoil Zr^+ ion as it escapes the surface. The breaking of the oxygen bond may be the principle cause of this energy loss. This "work function" effect did not appear to be present in the P^{32} experiments, although it could have been obscured by the larger experimental error (due principally to the shorter time of flight).

To be certain that the recoil ions observed in Fig. 1 are really mass 90, their mass was measured by the same method used in the P^{32} experiments. A fine mesh, grounded grid was placed 3 millimeters in front of the monolayer surface. The surface was then placed successively at 0, 50, 100, 160, and 235 volts negative with respect to ground, thus adding different amounts of energy to the initial energy of the recoil ions. Time of flight spectra were observed at each of these voltages. The minimum time of flight was observed for each spectra, and from this time the maximum velocity of the recoil ions was calculated. These measured velocities all agree very well with an initial maximum energy of about 36 electron volts, and a mass of 90 ± 5. The possibility that the recoil ion is mass 106 (ZrO^+) is definitely ruled out. A careful examination of these results also sets the limit of the zero error in the time of flight measurements at 0.1 microsecond.

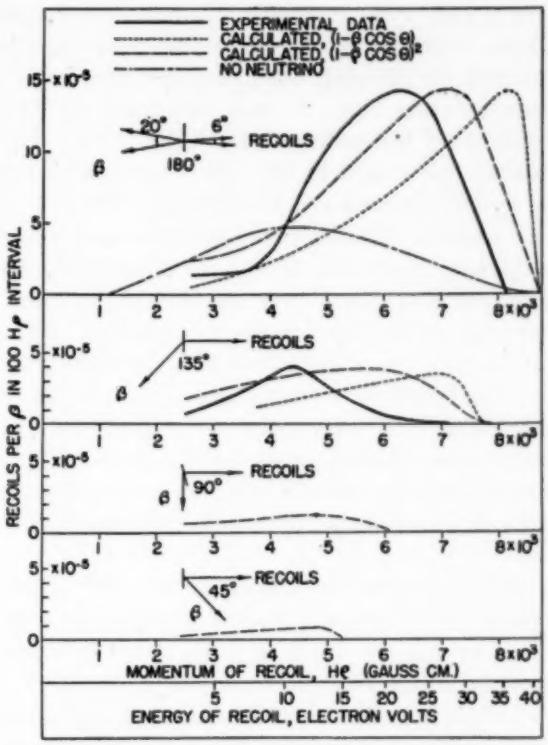

FIG. 2. *Comparison of observed recoil momentum spectra with those calculated from the neutrino hypothesis.* The 6-electron volt displacement of the observed spectra with respect to the calculated spectra is assumed to be due to the binding energy of the Zr^+ recoil ion to the surface. The calculated spectra for the $(1-\beta\cos\theta)^2$ and the $(1-\beta\cos\theta)$ neutrino-electron angular correlation functions were multiplied by 0.87 and 0.56, respectively, before plotting. This normalizes the amplitudes of the calculated 180° curves to the amplitude of the curve observed at 180°. The "no neutrino" calculated curve, which is just the spectrum of the detected electrons, is multiplied by 1/50 before plotting. The 90° and 45° calculated spectra for both the $(1-\beta\cos\theta)^2$ and the $(1-\beta\cos\theta)$ cases are nearly indistinguishable on the scale of the figure, so only one case is plotted.

3. INTERPRETATION OF THE DATA, AND COMPARISON WITH THEORY

The time of flight diagrams in Fig. 1 are plotted as momentum spectra in Fig. 2. Also plotted in Fig. 2 are the momentum spectra calculated on the following three assumptions:

(a) There is no neutrino. Recoils should appear only for the 180° case. These recoils should have the same shape spectrum as the electrons detected by the Geiger counter, and they should

[4] R. J. Hayden, private communication.

have a very high intensity. In fact, one should observe a recoil for every tenth beta-particle detected. In plotting the calculated recoil spectrum for this case, it was necessary to first multiply all the ordinates by 1/50. It has been assumed here, and in the following cases, that the original beta-particle spectrum for Y^{90} is that given by the Fermi theory for an allowed transition. That this is not an improbable assumption is shown by the cloud-chamber measurements by Stewart, Lawson, and Cork.[5] The end point is taken to be 2.16 Mev, or 8730-gauss cm. This predicts a maximum recoil energy of 40.7 electron volts for mass 90 recoil atoms. The spectrum as plotted in the 180° curve in Fig. 2 is corrected for the 15 mg/cm² total absorber between the monolayer source and the Geiger tube.

(b) A neutrino is assumed to exist whose probability of entering a solid angle element $d\Omega$, which makes an angle θ with respect to the direction of the electron, is $3/16\pi(1-\beta\cos\theta)^2 d\Omega$. For this function, the most probable angle between the electron and the neutrino is about 135°. This can be called a "backward" neutrino as contrasted to a "forward" neutrino such as is predicted by a $(1+\beta\cos\theta)$ function.

(c) A neutrino is assumed to exist whose probability of entering a solid angle element $d\Omega$, which makes an angle θ with respect to the direction of the electron, is $1/4\pi(1-\beta\cos\theta)d\Omega$. For this function, the most probable angle between the electron and the neutrino is about 120°. This function is predicted by both the scalar and pseudoscalar forms of the Fermi theory for an allowed transition.

β is the ratio of the velocity of the electron to the velocity of light.

The neutrino is assumed to share the total energy of 2.16 Mev with the electron, to have a mass small compared to the mass of the electron, and to have a momentum of E_ν/c. The electron multiplier is assumed to have 100 percent efficiency for 3000 volt ions.

Before plotting the calculated momentum spectra, for the $(1-\beta\cos\theta)^2$ case in Fig. 2, all the ordinates were multiplied by 0.87, which normalizes the amplitude of the 180° curve to the observed one. This means that about 87 percent of the recoil ions escape charged if this angular correlation function is correct. However, since the exact solid angle subtended by the "sensitive" area of the electron multiplier and the multiplier efficiency are not precisely known, the fraction of recoils escaping charged could be anywhere from 50 to 100 percent. A significant point here is the comparison of the 87 percent figure with the corresponding figure of 3 to 8 percent for the sulfur recoils from P^{32} (for the same neutrino-electron correlation function). In other words, per beta-particle, one observes about 10 times as many recoils from Y^{90} as from P^{32}.

In the $(1-\beta\cos\theta)$ case, all the calculated curves were normalized to the 180° observed curve by the factor 0.56.

Other recoil momentum spectra calculated on the basis of more "forward" neutrinos are plotted in the earlier paper. Since both the Y^{90} and P^{32} electrons are assumed to have about the same shape spectra, with E_{max} considerably in excess of mc^2, the recoil momenta spectra will have similar shapes. The very sharp high momentum peaks in the 180° curves predicted by both the "random" and also the "forward" neutrinos were never observed for either P^{32} or Y^{90}.

The most noticeable discrepancy between the observed and calculated recoil spectra is that the observed spectra (for both 180° and 135°) fall short of the maximum theoretical energy by about 6 electron volts. This is a real effect, and is definitely outside experimental error estimated to be ±3-electron volts in this part of the spectrum. A possible explanation of this energy loss is the binding energy of the Zr^+ ions to the surface and to the oxygen atom to which they are probably attached. The abnormally low number of recoils below about 10-electron volts energy for both the 180° and 135° cases substantiates this explanation. If all of the ions whose initial energy was less than 6 electron volts failed to escape the surface, the whole low momentum region of the observed recoil spectrum would be lowered in intensity.

The second discrepancy between the observed and calculated recoil spectra is the failure to observe any recoils above background for the 90° and 45° cases. This is expected on the neu-

[5] D. W. Stewart, J. L. Lawson, and J. M. Cork, Phys. Rev. 52, 901 (1937).

trino hypothesis, since the predicted amplitude of these recoil momentum spectra is only about twice the random background. The statistics are not good enough to permit the detection of this small an effect. Also, a 6-electron volt energy loss would strongly attenuate these spectra, making their detection still more difficult. This situation is considerably different from the P^{32} case where too many low energy recoils were observed at both 90° and 45°.

It is evident from Fig. 2, if a 6-electron volt binding energy correction is made, that a $(1-\beta\cos\theta)^2$ neutrino-electron angular correlation function accounts in an almost quantitative manner for the observed spectra. The $(1-\beta\cos\theta)$ function cannot definitely be ruled out. However, the "random" neutrino, the "forward" neutrino, and "no neutrino" predict curves of very different shape (see Fig. 5 in earlier paper), and of very different amplitudes (factors of 5 to 50), compared to observations. It does not seem possible to reconcile these cases with the observations.

The conclusion, that $(1-\beta\cos\theta)^2$ gives an adequate explanation of the observations, is in agreement with the data of P^{32}. The earlier paper pointed out that in many respects the observed P^{32} data fitted the $(1-\beta\cos\theta)^2$ function as well as the slightly favored $(1-\beta\cos\theta)$ function.

These results are in disagreement with the very tentative conclusions which Jacobsen[6] drew from his measurements on the recoil energy spectrum of Kr^{88} (2.4 Mev, 2.7 hrs.). In this experiment there were some correction factors, whose direction was known, but whose magnitude was uncertain. A careful examination of Figs. 11 and 13 in Jacobsen's paper, suggests that, if the corrections are not too large, his data can be reconciled to the conclusion reached here.

The conclusion that a "backward" neutrino is adequate to explain the observations on both Y^{90} and P^{32} is probably in disagreement with the Fermi beta-decay theory,[7] since neither of these two nuclei would ordinarily be considered as "allowed" cases. In particular, the function $(1-\beta\cos\theta)^2$ is not even a possibility in the present formulation of the theory.

[6] J. C. Jacobsen and O. Kofoed-Hansen, Mat. Fys. Medd. **23**, No. 12 (1945).
[7] D. R. Hamilton, Phys. Rev. **71**, 456 (1947).

4. CONCLUSIONS

It is assumed that a 6-electron volt binding energy correction can be made to the Y^{90} data.

(a) The "no neutrino," "forward" neutrino, and "backward" neutrino assumptions all predict recoil momentum spectra whose shapes are in strong disagreement with the observations, and whose amplitudes are in disagreement with observations by factors of 5 to 50.

(b) If a $(1-\beta\cos\theta)^2$ neutrino-electron correlation is assumed, the shape of the predicted spectra agree rather well with the shape of the observed spectra. Furthermore, the absolute amplitudes (assuming 100 percent of the recoils escape charged) of both the 180° and 135° calculated spectra agree to within about 20 percent with the amplitudes of the observed spectra. The failure to observe recoils above the background at 90° and 45° is consistent with this neutrino assumption (as well as with the others mentioned above).

(c) The Y^{90} data is in agreement, within estimated experimental error, with the earlier data from P^{32}, except in absolute intensity. Only about 8 percent of the high ionization potential recoil ions from P^{32} appear to escape charged.

(d) No exact limits of error due to chemical effects at the surface can be set at the present time. The reproducibility of the recoil spectra for different chemical combinations at the surface, and the systematic disappearance of high momentum recoils at 135°, 90°, and 45°, suggest that the surface effects do not seriously interfere with their behavior as predicted by the neutrino hypothesis. These qualitative arguments must be replaced by exact measurements of surface effects before a final selection of the neutrino-electron correlation function is possible.

5. ACKNOWLEDGMENTS

The author is particularly indebted to Professor R. B. Duffield for pointing out the possibility of using Y^{90} for this experiment, and to Mr. Louis M. Smith for preparing several carrier free samples of Y^{90}.

Collision and Saturation Broadening in Microwave Spectra*

HARTLAND S. SNYDER AND PAUL I. RICHARDS
Brookhaven National Laboratory, Upton, Long Island, New York

(Received January 30, 1948)

A theory of spectral line shape is presented for the case of a low pressure gas where only two energy levels (or several pairs of independent levels) are active in producing absorption. In Section I, an approximate set of differential equations is derived; these are solved in Section II. The method of approximation is shown to be consistent in Section III, and the final results are obtained in Section IV. A definite broadening of the lines in addition to that due to molecular collision is predicted as saturation is approached. The incident power needed for a given effect is proportional to the square of the pressure, and the maximum attenuation factor multiplied by the square of the half-width should be independent of incident power.

INTRODUCTION

IN spectroscopic work, it is generally appreciated that, owing to the limited population of states, a given amount of material can absorb no more than a certain maximum power independent of the electromagnetic power incident on the sample. Recent work in the microwave region has made it possible to reach values of incident flux sufficiently high to exhibit saturation effects. There has been some discrepancy[1-3] as to whether this saturation is accompanied by a broadening of the resonance absorption over and above that due to molecular collision alone. We shall present below a theory of spectral line shape which, it will be seen, definitely predicts additional broadening due specifically to saturation.

This theory is based on the following assumptions. The phenomena involved have three important characteristic times: the duration of a molecular collision T, the period of the incident radiation $1/\omega$, and the mean time between collisions τ. (a) It will be assumed that $T \ll 1/\omega \ll \tau$. (b) Only two energy levels are active in producing absorption. (c) Molecular collision restores a Boltzmann population.

Assumption (b) can be slightly relaxed to the extent that no energy level shall make a transition to more than one other level. In this latter case, the absorptions produced by the independent pairs of active levels can safely be added to give the total effect of the several lines. The results, however, must be expected to hold only in the near vicinity of a single line or group of independent lines.

Assumption (c) essentially states that the effects of molecular collision are to be independent of the presence of the electromagnetic field. A collision is to be regarded as a "violent" event compared to the action of the field.

Assumption (a) implies that the pressure must be low. In particular, the collision diameter must be negligible compared to the mean free path.

SECTION I

For any assemblage of quantum-mechanical systems, the density matrix, ρ, satisfies the following differential equation (superior dots indicate differentiation with respect to time).

$$i\hbar\dot{\rho} = [H, \rho]. \tag{1}$$

In our problem, the Hamiltonian matrix H is given by

$$H = H_0 + V \sin\omega t, \tag{2}$$

where the field-free Hamiltonian H_0 and the parameter V are independent of t. Choosing a representation in which H_0 is diagonal and letting

$$\rho_{nm} = e^{-i\omega_{nm}t} c_{nm}; \quad \omega_{nm} = (E_n^0 - E_m^0)/\hbar,$$

we obtain from (1):

$$i\hbar\dot{c}_{nm} = \sin\omega t \sum_l (V_{nl} e^{i\omega_{nl}t} c_{lm} - c_{nl} V_{lm} e^{i\omega_{lm}t}).$$

In accordance with the "two-level" assumption (b) above, we shall retain in these equations

* Research done at the Brookhaven National Laboratory under the auspices of the Atomic Energy Commission.

[1] C. H. Townes, Phys. Rev. **70**, 665 (1946).
[2] W. V. Smith and R. L. Carter, Phys. Rev. **72**, 638 (1947).
[3] T. A. Pond and W. F. Cannon, Phys. Rev. **72**, 1121 (1947).

only the terms involving c_{11}, c_{12}, c_{21}, c_{22}. If several independent pairs of levels are active, we obtain corresponding sets of equations for each pair; these sets can be independently treated by the method used below. With the definition

$$D=c_{22}-c_{11}=\rho_{22}-\rho_{11}, \tag{3}$$

these equations become:

$$\begin{aligned} i\hbar\dot{D}&=2\sin\omega t[V_{21}e^{i\omega_{21}t}c_{12}-c_{21}V_{12}e^{i\omega_{12}t}],\\ i\hbar\dot{c}_{12}&=\sin\omega t[V_{12}e^{i\omega_{12}t}D+c_{12}(V_{11}-V_{22})], \qquad (4)\\ i\hbar\dot{c}_{21}&=-\sin\omega t[V_{21}e^{i\omega_{21}t}D+c_{21}(V_{11}-V_{22})]. \end{aligned}$$

In view of assumption (a) above, we shall neglect rapidly varying terms inasmuch as their effects might be expected to be practically self-cancelling over the comparatively long time periods between collisions. We shall see in Section III that this approximation can be shown to be consistent. Writing $\sin\omega t$ in complex form and retaining only slowly varying parts, we obtain finally

$$\dot{D}=-(1/\hbar)[V_{12}c_{21}e^{i\delta t}+V_{21}c_{12}e^{-i\delta t}], \tag{5a}$$

$$\dot{c}_{12}=(1/2\hbar)V_{12}De^{i\delta t}, \tag{5b}$$

$$\dot{c}_{21}=(1/2\hbar)V_{21}De^{-i\delta t}, \tag{5c}$$

where we have chosen the following conventions:

$$\omega_{12}=-\omega_{21}>0; \quad \delta=\omega_{12}-\omega. \tag{6}$$

SECTION II

Equations (5) can be solved rigorously. Differentiation of (5a) and substitution from (5b, c) gives:

$$\ddot{D}=-(1/\hbar^2)|V_{12}|^2D - (i\delta/\hbar)[V_{12}c_{21}e^{i\delta t}-V_{21}c_{12}e^{-i\delta t}].$$

Again differentiating, substituting from (5b, c) and finally using (5a), we obtain

$$\dddot{D}=-\{(|V_{12}|/\hbar)^2+\delta^2\}\dot{D}.$$

The general integral of this equation is

$$D=\alpha\cos\Omega(t-T)+\beta, \tag{7}$$

where

$$\Omega^2=(|V_{12}|/\hbar)^2+\delta^2$$

and α, β, T are (real) constants. If the last collision occurred at $t=t_0$, our assumption that a collision restores the Boltzmann population requires the following boundary conditions on the density matrix

$$\left.\begin{matrix} c_{12}=0=c_{21}\\ D=D_0 \end{matrix}\right\} \text{ at } t=0, \tag{8}$$

where D_0 is the value appropriate to thermal equilibrium. The first two conditions imply by (5a) that $\dot{D}=0$ at $t-t_0$; this in turn implies that $T=t_0$ in (7).

Writing (7) in complex form, substituting in (5b), and integrating, we find:

$$c_{12}=\frac{V_{12}}{2\hbar}\left\{ie^{i\delta t}\left[\frac{\alpha e^{-i\Omega(t-t_0)}}{2(\Omega-\delta)}-\frac{\alpha e^{i\Omega(t-t_0)}}{2(\Omega+\delta)}-\frac{\beta}{\delta}\right]+\gamma\right\}, \tag{9}$$

where γ is an integration constant. Applying the first condition in (8),

$$\gamma=ie^{i\delta t_0}\{(\beta/\delta)-(\delta\alpha\hbar^2/|V_{12}|^2)\}.$$

A final relation on the integration constants is obtained as follows. Substitute (9) on the right of (5a) and (7) on the left. After some algebraic reduction, it will then be found that, if the resulting equation is to hold for all t, γ must be zero. This fact and the last of conditions (8) enable us to evaluate α and β. The final result is

$$D=(D_0/\hbar^2\Omega^2)\{|V_{12}|^2\cos\Omega(t-t_0)+(\hbar\delta)^2\}. \tag{10}$$

SECTION III

We are now in a position to show that the approximation used in obtaining (5) is a consistent one. More specifically, we shall show that (7) and (9) plus small rapidly varying terms form a good approximation to the solution of (4).

Make the *ansatz*:

$$D=D^{(0)}+d; \quad c_{12}=c_{12}{}^{(0)}+c, \tag{11}$$

where $D^{(0)}$ and $c_{12}{}^{(0)}$ are given by (7, 9) and where d and c are rapidly varying functions which are smaller than $D^{(0)}$ and $c_{12}{}^{(0)}$ by a factor of the order of the frequency of variation. Then $\dot{d}$ and $\dot{c}$ will be of the order of $D^{(0)}$ and $c_{12}{}^{(0)}$.

Substitute (11) into (4) and use the fact that $D^{(0)}$ and $c_{12}{}^{(0)}$ are rigorous solutions of (5). Neglecting terms of the order of d and c one obtains the following results, which show that d

and c do indeed have the properties assumed.

$$i\hbar\dot{d}=e^{i(\omega_{12}+\omega)t}V_{12}c_{21}^{(0)}+e^{-i(\omega_{12}+\omega)t}V_{21}c_{12}^{(0)},$$

$$i\hbar\dot{c}=c_{12}^{(0)}(V_{11}-V_{22})\sin\omega t-ie^{i(\omega_{12}+\omega)t}V_{12}D^{(0)}.$$

These could have been used to increase the accuracy of our solution (10).

SECTION IV

The change in the expectation value for the energy of the system since the last collision is given by

$$\Delta E=(\rho_{11}E_1+\rho_{22}E_2)\Big|_{t_0}^{t}.$$

Using (3) and the fact that the diagonal sum of ρ has the constant value unity, we may express ΔE in terms of D. When (10) is used, the final expression is found to be

$$\Delta E=(D_0\omega_{12}|V_{12}|^2/2\hbar\Omega^2)[1-\cos\Omega(t-t_0)].$$

Since the pressure has been assumed to be low, the probability that a given molecule will undergo collision during any short time interval will be proportional to the length of the interval and independent of the history of the molecule. It then follows that the probability that the last collision occurred during the interval $t-\theta$ to $t-\theta-d\theta$ is given by $e^{-\theta/\tau}d\theta/\tau$, where τ is the mean time between collisions. Setting $t_0=t-\theta$ above and integrating the product of these expressions from $\theta=0$ to $\theta=\infty$, we obtain the average change in the expectation value for the energy.

$$\langle\Delta E\rangle=\frac{D_0|V_{12}|^2\omega_{12}\tau^2/2\hbar}{1+\tau^2[\delta^2+(|V_{12}|/\hbar)^2]}. \qquad (12)$$

When a collision next occurs, the expectation value of the energy will return to its Boltzmann value, while the excess will be carried off as thermal motion of the molecules. The mean rate of collisions per unit volume is N/τ where N is the number of molecules per unit volume in the two states considered. (Thus ND_0 is the thermal equilibrium value for ΔN, the population difference of the two levels.) The power absorbed per unit volume is therefore $N\langle\Delta E\rangle/\tau$.

For dipole radiation, V in (2) is equal[4] to the dot product of the dipole moment and the electric (or magnetic) field. Assuming an incident plane wave and allowing for the random spatial orientation of the molecule,

$$|V_{12}|^2=|\mu|^2 8\pi G/3c,$$

where μ is the dipole moment effective in the transition and G is the average incident power per unit area.

Making these substitutions and converting from angular to actual frequency, the power P absorbed by the gas per unit volume is given by

$$P=\frac{4\pi G\Delta N|\mu|^2\nu_0/3hc\tau}{(\Delta\nu)^2+(1/2\pi\tau)^2+(8\pi G|\mu|^2/3h^2c)}. \qquad (13)$$

As mentioned earlier, if more than two levels are active but if no level can make a transition to more than one other level, then the absorptions of the several pairs as given by (13) can be added to give the total absorption.

Note that (13) reduces to the usual formula for low G and gives the correct limiting absorption $\Delta N h\nu_0/2\tau$ for large G.

CONCLUSIONS

The formula (13) definitely predicts an additional broadening of the spectral line as G increases. The functional form checks the experimental results of Pond and Cannon[3] to well within experimental error. (It is easily shown from (13) that, in their notation, $\alpha_0(\Delta\nu)^2$ should be independent of incident power and proportional to the square of the pressure.) Since Pond and Cannon give their results in arbitrary units, a quantitative check cannot be made.

Because the term proportional to G in the denominator of (13) merely adds to the square of the usual line-breadth constant, the power level at which any given saturation effect on line shape occurs will be proportional to the square of the pressure as noted earlier by Townes.[1]

Accordingly, the theory presented here predicts broadening due to saturation and agrees with the experimental results available at this time.

[4] P. I. Richards, Phys. Rev. 73, 254 (1948).

The Spectral Emissivity and Total Emissivity of Beryllium Oxide*

RALPH L. SEIFERT†
Argonne National Laboratory, Chicago, Illinois
(Received February 3, 1948)

A method has been devised for the measurement of spectral and total emissivities of non-metallic surfaces at high temperatures. The maximum temperature for spectral emissivity measurements is about 1700°C. With an extrapolation of spectral emissivity values it is possible to obtain experimental values for total emissivities at even higher temperatures. This method has been applied in the measurement of the emissivities of polished surfaces of three types of commercially prepared beryllia. Ceramic firing of hot-pressed beryllia was found to have very little, if any, effect on the spectral or total emissivity of a surface formed by polishing the final material. The impurity present in dark samples and/or the larger crystal size increases both the spectral and total emissivity by a factor of about two.

I. INTRODUCTION

VARIOUS methods[1] have been used to measure the total emissivity of non-metallic surfaces. These methods are limited either to a relatively low temperature range of measurement or to the use of surfaces prepared in a manner required by the experimental method. The latter limitation is very restricting since the emissivities of substances are influenced greatly by the nature of the surface. The method used in this investigation permits the use of surfaces prepared by any method desired. In this investigation measurements were made up to 1900°C.

Several investigators[2] have developed or suggested methods for the measurement of the spectral emissivity of non-metallic surfaces. Liebmann[3] discussed the various factors involved in obtaining reliable measurements and determined the spectral emissivity of a sintered deposit of powdered beryllia. The method reported in this paper was an adaptation of the methods of Skaupy[2] and of Burgess and Waltenberg.[2] Values thus obtained were checked at the melting point of gold by a procedure similar to that of Wiegand[2] and at the melting point of potassium sulfate by a method dependent upon the discontinuity in the transmissivity of potassium sulfate at its melting point.

II. EXPERIMENTAL METHOD

Beryllia Samples

Sample disks, 1.9 cm diameter×0.3 cm, were cut from blocks of fabricated beryllia. The faces were ground parallel and polished on No. 500 carborundum paper. Measurements were made with three different types of fabricated beryllium oxide. These types were prepared by the Norton Company.

Type 1 was fabricated by hot-pressing high fired beryllia powder in graphite forms. This type was uniformly colored black throughout the entire fabricated piece. The black coloration remained after the sample disks were heated in air. The density was 2.85 g cm^{-3}.

Type 2 was fabricated by hot-pressing Brush S.P. powdered beryllia. This type was white throughout the fabricated piece except for occasional small grey or black regions. There appeared to be a small hole at the center of many of the dark regions. This discoloration also remained after the sample disks were heated in air. The density was 2.844 g cm^{-3}.

Type 3 was fabricated the same as Type 2 except that the fabricated blocks were annealed by ceramic firing after being formed by the hot-pressing method. The specimen used in these measurements had a slight grey color but turned white when heated in air. The density was 2.778 g cm^{-3}.

* This paper is based on work performed under Contract No. W-31-109-eng-38 for the Manhattan Project at the Argonne National Laboratory.
† Present address, Department of Chemistry, Carleton College, Northfield, Minnesota.
[1] C. P. Randolph and M. J. Overholzer, Phys. Rev. **2**, 144 (1913); G. Liebmann, Zeits. f. Physik **71**, 416 (1931); P. F. McDermott, Rev. Sci. Inst. **8**, 185 (1937).
[2] G. K. Burgess and R. G. Waltenberg, Bull. Bur. Stand. **11**, 591 (1915); F. Skaupy, Zeits. f. Physik **12**, 177 (1922); E. Wiegand, Zeits. f. Physik **30**, 40 (1924); W. E. Forsythe, Phys. Rev. **25**, 252 (1925); G. Herrman, Zeits. f. Physik. Chemie **35, Abt B4**, 298 (1937).
[3] G. Liebmann, Zeits. f. Physik **63**, 404 (1930).

Apparatus

The apparatus used to obtain radiation data for the calculation of total emissivities is shown in Fig. 1. A heated beryllia surface was obtained free of temperature gradient by use of the tungsten-tantalum heating block, *B* and *C*, and the beryllia shield and diaphragm, *I* and *J*. The metal block was heated by induction. The tungsten disk, *B*, had to be placed between the tantalum block, *C*, and beryllia sample, *A*, because of the chemical reaction between beryllia and tantalum, forming volatile tantalum oxide and beryllium. The radiation shield, *I*, and diaphragm, *J*, were fabricated from Type 1 beryllia.

In order to eliminate undesirable reflections the inner wall of the quartz tube was coated with Aquadag colloidal graphite from the edge of the optical quartz window, *O*, down to and including the upper surface of the constriction in the quartz wall. The shutter, *P*, protected the quartz window, *O*, from volatilized deposits at all times that measurements were not being made. The transmissivities of the prisms *M* and *T* and windows *N* and *O* remained constant throughout the investigation.

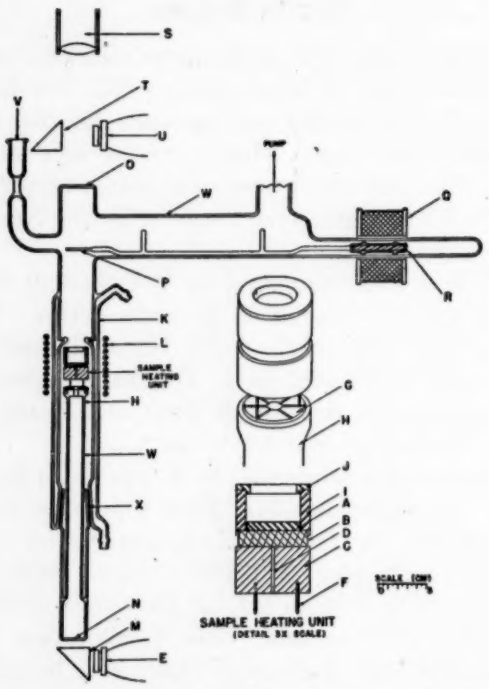

FIG. 1. Apparatus for heating of samples in vacuum. *A*, sample disk; *B*, tungsten heating disk; *C*, tantalum heating block; *D*, "black body" hole; *E* and *U*, calibrated Leeds and Northrup optical pyrometers; *F*, tungsten legs; *G*, grooved beryllia table; *H*, quartz support; *I*, radiation shield; *J*, diaphragm; *K*, water cooled quartz jacket; *L*, induction heating coil; *M* and *T*, silvered prisms; *N*, optical Pyrex window; *O*, optical quartz window; *P*, shutter; *Q*, solenoid; *R*, iron rod sealed in Pyrex; *S*, total radiation pyrometer; *V*, quartz supporting tube; *W*, quartz-Pyrex graded seal; *X*, 34/45 standard taper joint.

The Leeds and Northrup Rayotube total radiation pyrometer, *S*, was equipped with a quartz lens. When the pyrometer was focused on a surface the thermopile in it intercepted radiation from an area 0.6 cm in diameter. The Rayotube was securely mounted in a special holder which permitted adjustment of the vertical distance from specimen to Rayotube but eliminated all lateral motion. The silvered prism *T* was mounted in a special holder which permitted the prism to be moved into place for use with pyrometer *U* and moved out of the way when measurements were made with pyrometer *S*.

Joint *X* was sealed with Apiezon "*W*." To insure reproducibility in the assembly of the apparatus a reference mark was placed on the lower Pyrex tube and a sturdy metal pointer was mounted on the vacuum frame in coincidence with the reference mark.

Mercury vapor pumps with liquid nitrogen traps maintained a pressure of 10^{-6} to 10^{-5} mm of Hg while the heating unit and sample were at the maximum temperature obtainable.

The oscillator used with coil *L* was supplied by two parallel constant voltage transformers. This combination permitted maintaining a very constant temperature of the sample heating unit.

The apparatus used to measure the spectral emissivity of the beryllia surfaces is shown in section in Fig. 2. The beryllia sample disk was placed on a platinum ribbon $1\times6\times0.001$ inches. This ribbon was heated electrically by the output of a filament transformer supplied by a variable transformer. To maintain a constant ribbon temperature the variable transformer was supplied by a constant voltage transformer. A maximum current of 76 amp. was passed through the platinum ribbon.

The beryllia flats shown in Fig. 2 furnished a smooth supporting surface and prevented the platinum ribbon from buckling away from the supporting surface and producing hot spots.

Thus the center of the platinum ribbon could be heated to just slightly below the melting point of platinum without danger of the ribbon melting at any point. The top beryllia flats also served as a guard ring about the sample disk and helped eliminate temperature gradients in the surface of the disk.

Undesirable convection currents were eliminated by use of an insulating firebrick chimney which was shaped as shown in Fig. 2. The inner surface of the chimney was coated with Aquadag colloidal graphite. During a series of measurements the graphite was burned from no more than the lower half inch of the chimney.

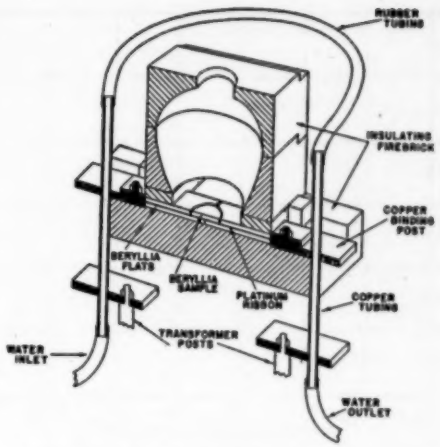

FIG. 2. Apparatus for resistance heating in air (section).

Calibration of Rayotube

The Rayotube was calibrated *in situ* by use of the tungsten disk, B, as a known radiating surface. The top surface of the tungsten was polished with 4/0 emery paper. The tungsten was heated in vacuum to approximately 2200°C for several hours to outgas the tungsten and age its surface. The tungsten disk was then heated to constant temperature at about 900°C. The true temperature of the tungsten disk was measured with the calibrated pyrometer E (Fig. 1) and the brightness temperature of the top surface was measured with the calibrated pyrometer U. The voltage of the Rayotube was measured with a Leeds and Northrup precision potentiometer. This procedure was repeated at approximately 50-degree intervals in the range 900°C to 2000°C. The measurements were reproducible and the equilibrium potentials of the Rayotube remained constant within 0.03 percent over a period several times as long as required to make all the readings at each temperature. After proper corrections were made for the transmissivity of prisms and windows the readings of pyrometers E and U agreed very well with the spectral emissivity data of Worthing.[4]

The total radiant energy (in cal. cm^{-2} $sec.^{-1}$) was calculated at each temperature by the use of Worthing's[4] values for the total emissivity of tungsten. With this data a calibration curve was drawn for the Rayotube under the conditions of the experiment. This procedure did not completely correct for the absorption of radiant energy by the quartz window and lens since the spectral distribution of radiant energy is different for tungsten[5] and beryllia[3] surfaces. Nor does this method allow for possible variation between the two surfaces in the ratio of total hemispherical emissivity and total normal emissivity.

Determination of Total Emissivity

After an initial heating in air to about 1300°C each beryllia sample disk was placed in the apparatus shown in Fig. 1 for preliminary heat treatment in vacuum. It was heated to the maximum temperature obtainable for several hours in order to outgas the sample and volatilize any impurities remaining from the polishing of the upper surface. The Rayotube was adjusted to focus it on the center of the beryllia surface. After the heat treatment the heating unit was brought to a constant temperature; the radiant energy was determined by measurement of the equilibrium potential difference of the Rayotube; and the brightness temperature of the beryllia surface was determined with pyrometer U. These measurements were repeated at different temperatures and the energy radiated from the surface was plotted as a function of the brightness temperature of the beryllia surface. Measurements with the apparatus shown in Fig. 2 later gave the relation between brightness temperature and true temperature for the same beryllia surface. The total emissivity, ϵ_t, was

[4] *International Critical Tables* (McGraw-Hill Book Company, Inc., New York, 1929), Vol. 5, pp. 243 and 245.

[5] L. S. Ornstein, Physica **3**, 561 (1936).

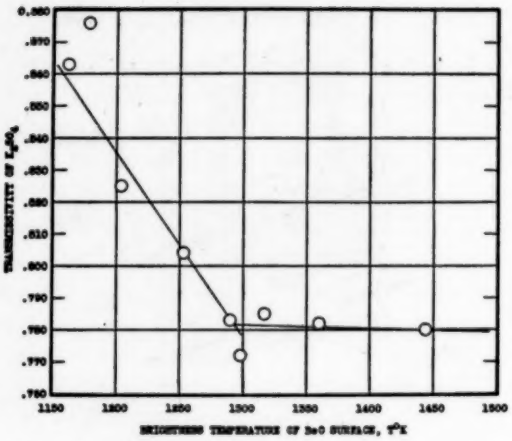

FIG. 3. Transmissivity curve for potassium sulfate layer on beryllia surface.

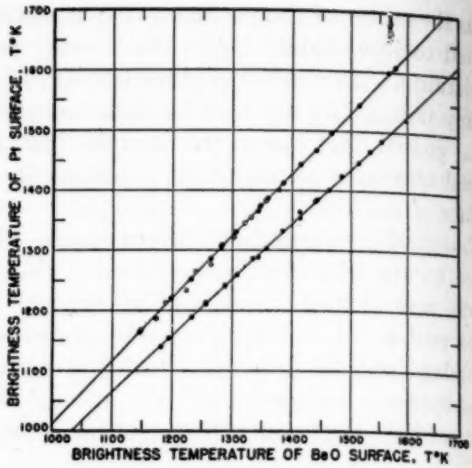

FIG. 4. Brightness temperatures of beryllia surface and adhering platinum surface. Lower line: Type 1 beryllia. Upper line: Type 2 beryllia (dark circles) and Type 3 beryllia (light circles).

calculated at various temperatures by the relation

$$\epsilon_t = W/\sigma T^4 \qquad (1)$$

where W is the total radiant energy in cal. cm^{-2} sec.$^{-1}$ at the true surface temperature T°K, and σ is the Stefan-Boltzmann radiation constant (1.379×10^{-12} cal. cm^{-2} sec.$^{-1}$ deg.$^{-4}$).

Determination of Spectral Emissivity

Platinum was vaporized on one-half of the upper beryllia surface to a thickness of 0.001 to 0.002 cm and polished with 4/0 emery polishing paper. The beryllia disk was then placed on the platinum ribbon of the apparatus shown in Fig. 2. The ribbon was heated to approximately 1600°C for 30 min. During this heating the upper surface was approximately 1400°C. This preliminary heating was necessary in order to obtain reproducible measurements of the relative brightness temperatures of the platinum and beryllia surfaces. With the platinum ribbon at a constant temperature, the brightness temperatures of the beryllia surface and of the adhering platinum surface were measured with the same optical pyrometer. This procedure was repeated at different surface temperatures throughout the available temperature range. The entire temperature range was covered three or four times to check the reproducibility of the measurements. There was no indication of changing emissivities during the time of these measurements.

The brightness temperature of the platinum surface was plotted as a function of the corresponding brightness temperature of the beryllia surface. Stephens[6] determined the brightness temperature of a platinum surface at different absolute temperatures. By interpolation on the above smoothed curve the corresponding brightness temperature of the beryllia surface, T_B, was obtained at each absolute temperature, T. The spectral emissivity, ϵ_λ, at temperature T was then calculated from the relation

$$\log_{10}\epsilon_\lambda = [c/2.303\lambda][(1/T)-(1/T_B)]. \qquad (2)$$

The effective wave-length of light, λ, transmitted by the optical pyrometers used in this investigation was taken as 0.665μ for all temperatures. Wien's radiation constant, c, is 1.432 cm °K. Therefore Eq. (2) reduces to

$$\log_{10}\epsilon_{0.665\mu} = 9352[(1/T)-(1/T_B)]. \qquad (3)$$

The spectral emissivity of each sample was checked at the melting point of gold by an independent method. The spectral emissivity of Type 1 beryllia was also checked at the melting point of potassium sulfate. (These measurements were actually made first, before the platinum was vaporized onto the beryllia surface.)

A circular piece of gold foil (10 mg in.$^{-2}$) was cut to the same diameter as the beryllia sample. A strip about 0.2 cm wide was cut from the center of this disk. The remaining two segments

[6] R. E. Stephens, J. Opt. Soc. Am. 29, 158 (1939).

were rubbed into intimate contact with the beryllia. The segments were placed so as to leave exposed a 0.2-cm strip of clean beryllia surface. The gold foil adhered to the polished beryllia fairly well.

The beryllia surface was heated to the melting point of gold in the apparatus shown in Fig. 2. The brightness temperature of the clean beryllia surface was determined at the first appearance of holes in the gold foil. This procedure was repeated at least twice with each disk. The observed brightness temperatures of the beryllia surface at the melting point of gold seldom differed by as much as 2 deg. for a given sample. (It was found necessary to cool the sample rapidly as soon as melting of the gold was observed, and then to examine the disk under a low power microscope to verify that melting had occurred. If melting had occurred, small globules of gold adhered to the beryllia surface. If the observed holes resulted from volatilization of the gold during a long period of heating, no globules of gold were present.)

The true temperature of the beryllia surface at the instant the melting of the gold foil was observed was assumed to be the melting point of gold, 1336°K. This temperature together with the observed brightness temperature of the beryllia surface permitted the calculation of the spectral emissivity of the beryllia at 1336°K by Eq. (3).

The determination of the spectral emissivity of Type 1 beryllia at the melting point of potassium sulfate was made in the apparatus shown in Fig. 1. A few crystals of anhydrous potassium sulfate were melted so as to cover about half of the upper surface of the beryllia disk. The disk was then heated to constant temperature and the brightness temperature of its surface measured at a point covered with potassium sulfate and at a point free of potassium sulfate. Measurements were made at the same points on the surface at various increasing temperatures. The transmissivity of the potassium sulfate layer, $\tau_{0.665}$, was calculated by the equation

$$\log_{10}\tau_{0.665}=9352[(1/T_B)-(1/T_A)], \quad (4)$$

TABLE I. Brightness temperature (T_B), spectral emissivity ($\epsilon_{0.665}$), and total emissivity (ϵ_t) of three types of fabricated beryllium oxide.

	Type 1			Types 2 and 3		Type 2	Type 3
T°K	T_B°K	$\epsilon_{0.665}$	ϵ_t	T_B°K	$\epsilon_{0.665}$	ϵ_t	ϵ_t
1200	1160.4	0.542	0.665	1104.6	0.212	0.351	0.336
1300	1253.7	0.543	0.706	1187.9	0.209	0.383	0.361
1400	1347.0	0.546	0.746	1271.0	0.210	0.405	0.392
1500	1440.4	0.552	0.785	1354.2	0.213	0.425	0.420
1600	1533.8	0.559	0.819	1437.1	0.217	0.447	0.439
1700	1627.3	0.568	0.843	1519.8	0.222	0.474	0.453
1800	1720.9	0.577	0.867	1602.4	0.228	0.499	0.463
1900	1814.7	0.587	0.894	1684.9	0.235	0.513	0.470
2000	1908.5		0.931	1767.2		0.517	0.474
2100				1849.6		0.514	0.475
2150				1890.7		0.509	0.475
Melting point of gold							
1336	$1288._5$	0.55_2		1216	0.20_4	(Type 2)	
				1217	0.20_7	(Type 3)	
Melting point of potassium sulfate							
1342	1293	0.54_4					

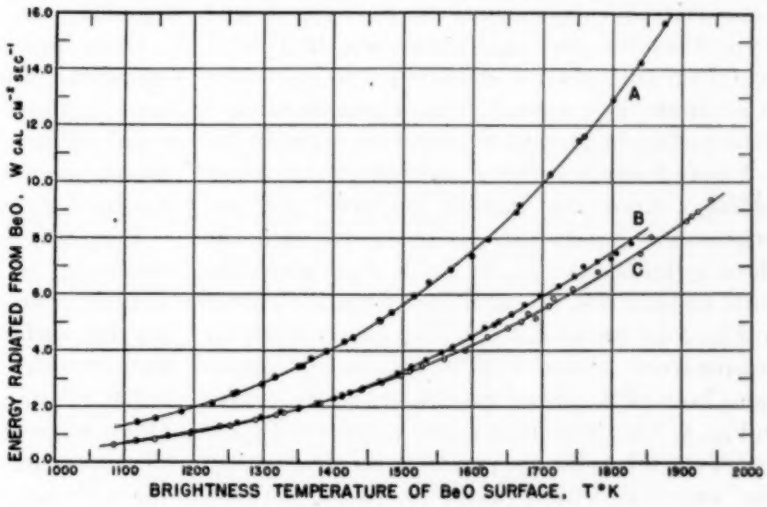

FIG. 5. Curve A: Type 1 beryllia. Curve B: Type 2 beryllia. Curve C: Type 3 beryllia.

TABLE II. Liebmann's values for the spectral emissivity of sintered 0.5μ beryllia.

T°K	1300	1400	1500	1600	1700	1800	1900	2000	2100	2200
$\epsilon_{0.665}$	0.057	0.068	0.080	0.091	0.102	0.113	0.124	0.135	0.146	0.157

where T_B is the measured brightness temperature of the clean beryllia surface and T_A is the apparent brightness temperature of the beryllia surface as viewed through the layer of potassium sulfate. The values of $\tau_{0.665}$ are shown in Fig. 3 as a function of T_B. The layer of potassium sulfate no doubt became thinner during the course of measurements due to evaporation and further creepage over the beryllia surface. This would increase the transmissivity. The observed decrease in transmissivity with increasing temperature resulted from the predominant effect of temperature. Within the experimental error of the measurements the data could be represented by two intersecting straight lines. The point of intersection (Fig. 3) was considered to lie at the melting point of potassium sulfate, 1342°K. The corresponding brightness temperature of the beryllia at the intersection, 1293°K, permitted the calculation of the spectral emissivity of the beryllia surface at 1342°K by Eq. (3).

III. RESULTS

Figure 4 shows the relation between the brightness temperatures of the beryllia surface and of the adhering platinum surface for each of the three types of beryllia used in this investigation. Within experimental error, Type 2 and Type 3 beryllia gave identical results. In Table I are given the spectral emissivities, $\epsilon_{0.665}$, calculated from the curves in Fig. 4 and Stephens'[6] values of the brightness temperature of platinum.

Figure 5 shows the relation between the energy radiated from the beryllia surfaces and the brightness temperatures as measured with the three types of beryllia. In Table I are given the total emissivities, ϵ_t, calculated from the curves in Fig. 5 by use of Eq. (1). The values given for temperatures above 1900°K involve extrapolations both of Stephens' results and of the curves in Fig. 4. The differences in the values for Type 2 and Type 3 beryllia are probably no greater than the variation which might be found between different samples of either one of the types. However, there is considerable difference between the dark Type 1 beryllia and the white Types 2 and 3, both in spectral and total emissivity.

The values of spectral emissivity determined at the melting point of gold and the melting point of potassium sulfate are also given in Table I.

The sample disk of Type 2 beryllia used for the measurements given in Table I had two small grey spots on the surface which was used for the radiation measurements. These spots were about 0.1 cm in diameter and could not be removed by heating the sample in air. The spots were near the edge of the disk and therefore did not affect the measurements of total radiation. Measurements were made of the brightness temperature of the spots each time a corresponding measurement was made on the white surface and the ratio of the spectral emissivities of grey spots and white surface was calculated. The spectral emissivity of the grey spots was approximately twice that of the white surface in the temperature range 1200°K to 2000°K. The higher spectral emissivity of the grey spots and also of the black Type 1 beryllia may be due not only to the impurity present which imparts the color to the fabricated beryllia (carbon, carbide, or suboxide), but also to the crystal size of the beryllia. When viewed with a low power microscope the beryllia crystals present in the grey spots of Type 2 appear to be considerably larger than the crystals present in the white surface adjoining the grey spot.

Other investigators have measured the spectral emissivity of beryllia. Since the beryllia surfaces used in these earlier measurements were fabricated differently than the surfaces used in the measurements reported herein, agreement of results is not to be expected.

Burgess and Waltenberg[2] report a spectral emissivity of 0.37 ($\lambda=0.650\mu$) for beryllia at 1740°K. They do not report the nature of the beryllia surface which was used in making this measurement. The value 0.37 is based on the value of the spectral emissivity of platinum taken to be 0.33 at all temperatures. Based on the more recent and complete measurements of the emissivity of platinum[6] which were used in

calculating the values reported in Table I, the value given by Burgess and Waltenberg for the emissivity of beryllia would be 0.33 at 1755°K.

Liebmann[3] measured the spectral emissivity of a beryllia surface which had been slip-cast on a Nernst glower. The grain size of the beryllia was 0.5μ. His results are given in Table II.

Discussion of Errors

The values given in Table I are reported in accordance with the precision of measurement of the various experimental quantities. However, the accuracy of the values obtained for the spectral and total emissivities is not determined by the precision of measurement of the experimental quantities.

The temperature of all surfaces surrounding the sample during measurement should be so low that the radiant flux from the surrounding surfaces is insignificant compared to that of the hot beryllia surface. In the apparatus shown in Fig. 2 the surfaces which could radiate to the beryllia surface were always colder than necessary to decrease the error in the spectral emissivity from this source to less than 0.1 percent. However, in the measurement of the total emissivity a much greater error resulted from failure to maintain neighboring surfaces at a sufficiently low temperature. There was partial compensation of errors since the Rayotube was calibrated *in situ* and there was a corresponding error in the measurement of the brightness temperature of the beryllia surface. It was estimated that the error in the total emissivity resulting from this source was less than 5 percent.

There is another possible source of error in the measurement of the spectral emissivities and therefore also in the calculated values of total emissivity. While good thermal contact was obtained between the platinum and the beryllia, the temperatures of the two surfaces may not have been identical due to the difference in total emissivity of platinum[7] and beryllia surfaces. The platinum reference surface may therefore have been at a higher temperature than the beryllia surfaces. The magnitude of the error from this source is minimized by the relatively high heat conductivity of beryllia (as compared with other oxides) and by the fact that heat was lost from the platinum and beryllia surfaces by conduction and convection as well as radiation.

The spectral emissivities as measured in this investigation are normal spectral emissivities. This is also true of Stephens'[6] values for platinum. However, there is some uncertainty as to whether the values given by Stephens, determined in vacuum, may be applied to the platinum surfaces used in this investigation, in air. Stephens' results agree well with those obtained by Worthing,[8] who measured the spectral emissivity of platinum in an argon atmosphere. However, there has been a wide variation in the measurements of the spectral emissivity of platinum as made by various investigators.[9] Worthing[9] suggests that these variations may be due in part to the atmosphere used in each case.

The spectral emissivity of the beryllia surfaces was determined by three independent methods which gave values in good agreement. Since it is not probable that the net error inherent in each of the three methods was the same, the total error resulting from the above sources must not have been very great. It is estimated that the values of the spectral emissivity given in Table I are accurate to well within 10 percent and that the values of total emissivity are correct to within 20 percent.

---

[7] C. Davisson and J. R. Weeks, J. Opt. Soc. Am. 8, 581 (1924).

[8] A. G. Worthing, Phys. Rev. 28, 174 (1926).

[9] American Institute of Physics, *Temperature, Its Measurement and Control in Science and Industry* (Reinhold Publishing Corporation, New York, 1941), p. 1164.

On Solutions of He^3 in He^4

F. LONDON,
Duke University, Durham, North Carolina*
AND O. K. RICE
University of North Carolina, Chapel Hill, North Carolina
(Received January 16, 1948)

Elementary thermodynamics has been applied to recent data on the equilibrium concentrations of He^3 in the liquid and vapor phases of He^4. The differences between He^3 and He^4 as regards partial molar heat and entropy have been calculated and briefly discussed. Above the λ-point the energy of He^3 in the liquid is greater than that of He^4 by about 13 cal. $mole^{-1}$, an amount which can be accounted for theoretically by the difference in zero-point energy. But below the λ-point the energy and entropy of He^3 are considerably lower than those of He^4 in the same solution ($\Delta\bar{H}_3-\Delta\bar{H}_4\approx-170$ cal. $mole^{-1}$). The entropy decrease per He^3 atom dissolved is equivalent to the entropy contents of about 50 He^4 atoms in pure liquid helium II. An explanation of this strange result is suggested by Tisza's hypothesis that below the λ-point helium may be considered to be a mixture of a "normal" and a "superfluid" phase. The thermal data obtained lead to the conclusion that the λ-transition of pure He^4 might become a transition of first order in dilute solutions of He^3 in He^4. On this basis, the effect of concentration of He^3 on the λ-point has been considered.

RECENTLY, Fairbank, Lane, Aldrich, and Nier[1] have measured the equilibrium concentrations of He^3 in the liquid and vapor phases of He^4. These measurements provide valuable information which can serve to calculate the energy and entropy of solution of He^3 in He^4. Since the knowledge of energy and entropy is important for an understanding of the structure of these solutions, we thought it worth while to make an elementary analysis of these data.

1. THERMODYNAMICS OF THE LIQUID-VAPOR EQUILIBRIUM

Using the chemical potential μ in the usual way,[2] we apply the equation

$$d\mu_i=-\mathcal{S}_i dT+\mathcal{V}_i dp, \tag{1}$$

to the components in the liquid, under the condition that the composition of the liquid phase is kept constant. $\mathcal{S}_i$ is the partial molar entropy of component i ($i=3$ for He^3 and $i=4$ for He^4), $\mathcal{V}_i$ the partial molar volume, T the absolute temperature, and p the pressure. We assume that in the gas phase the two components form an ideal solution, which is certainly justified below the normal boiling point of helium as the pressure becomes less than one atmosphere. If this assumption is valid we can write, using primes to designate quantities peculiar to the vapor phase,

$$\mu_i'=\mu_i^{0\prime}+RT\ln x_i' \tag{2}$$

where $\mu_i^{0\prime}$ is the chemical potential of the pure component i in the vapor phase, at a pressure equal to the total pressure p of the system, and where x_i is the mole fraction of the component i. Differentiating this, and noting that $\mu_i^{0\prime}$ will obey an equation similar to Eq. (1), we obtain

$$d\mu_i'=-S_i^{0\prime}dT+V_i^{0\prime}dp+R\ln x_i'dT+RTd(\ln x_i'). \tag{3}$$

Since, for an ideal solution $\mathcal{S}_i'=S_i^{0\prime}-R\ln x_i'$ this may be written

$$d\mu_i'=-\mathcal{S}_i'dT+V_i^{0\prime}dp+RTd(\ln x_i'). \tag{4}$$

Applying $d\mu_3=d\mu_3'$ (from $\mu_3=\mu_3'$, one of the conditions for equilibrium between liquid and vapor phases which continue to hold under a change of temperature) we find

$$\Delta\mathcal{S}_3=\mathcal{S}_3-\mathcal{S}_3'=(\mathcal{V}_3-V_3^{0\prime})dp/dT-RTd\ln x_3'/dT. \tag{5}$$

Applying $d\mu_4=d\mu_4'$ we find

$$\Delta\mathcal{S}_4=\mathcal{S}_4-\mathcal{S}_4'=(\mathcal{V}_4-V_4^{0\prime})dp/dT-RTd\ln x_4'/dT. \tag{6}$$

* Work performed under Contract N7onr-455 between the Office of Naval Research and Duke University.

[1] H. A. Fairbank, C. T. Lane, L. T. Aldrich and A. O. Nier, Phys. Rev. **71**, 911 (1947) and **73**, 729 (1948). We wish to thank Dr. Lane for sending us some of these data before publication.

[2] As, e.g., in F. H. MacDougall, *Thermodynamics and Chemistry* (John Wiley and Sons, Inc., New York, 1939), third edition, Chapter X.

We now assume that

$$\bar{V}_3 dp/dT (= p\bar{V}_3 d(\ln p)/dT)$$

and

$$\bar{V}_4 dp/dT (= p\bar{V}_4 d(\ln p)/dT).$$

are small[3] compared to $RTd(\ln x_3)/dT$; we assume also that $V_3^{0\prime} = V_4^{0\prime}$, which seems reasonable for the vapor phase, and which, while not required thermodynamically, is suggested by the assumption that the vapor phase is an ideal solution.[4] We also note that when the solution is very dilute in He^3 the last term in Eq. (6) becomes negligible. We may, therefore, write for the difference of entropy of condensation:

$$\Delta\bar{S}_3 - \Delta\bar{S}_4 = -RTd(\ln x_3')/dT \qquad (7)$$

or, for the difference in enthalpy of condensation:

$$\Delta\bar{H}_3 - \Delta\bar{H}_4 = T(\Delta\bar{S}_3 - \Delta\bar{S}_4) = Rd(\ln x_3')/d(T^{-1}). \quad (8)$$

Since $H = -T^2[\partial(F/T)/\partial T]$ and since the free energy F has to be continuous, it follows from (8) that x_3' has also to be continuous.

In the case where the composition of the liquid phase is not kept constant, we may still make use of Eqs. (7) and (8), provided Henry's law holds for the He^3, which appears reasonable to assume at very low concentrations. We need merely to replace x_3' by C_V/C_L the fraction of the concentrations of He^3 in the vapor and in the liquid phase. Thus if we plot $\log(C_V/C_L)$ against T^{-1}, the slope should give directly $(\Delta\bar{H}_3 - \Delta\bar{H}_4)/2.3R$.

2. DISCUSSION OF THE MEASUREMENTS

Such a plot is shown in Fig. 1. The measured values shown are the results of Fairbank, Lane, Aldrich, and Nier.[1] These values fall quite well along two straight lines which meet at the λ-point ($T_\lambda = 2.19°K$).[5] From their slopes we obtain the following values for the difference of the enthalpies of condensation (compare, e.g., (8)):

$$\Delta\bar{H}_3 - \Delta\bar{H}_4 = 13 \pm 2 \text{ cal. mole}^{-1} \quad \text{for} \quad T > T_\lambda, \quad (9)$$

$$\Delta\bar{H}_3 - \Delta\bar{H}_4 = -168 \pm 20 \text{ cal. mole}^{-1} \quad \text{for} \quad T < T_\lambda. \quad (10)$$

The entropy difference, after subtracting the entropy of mixing, is given by

$$\Delta S_3^0 - \Delta S_4^0 = (\Delta\bar{H}_3 - \Delta\bar{H}_4)/T + 2.3R \log(C_V/C_L). \quad (11)$$

With the above values we obtain

$$\Delta S_3^0 - \Delta S_4^0 = 2.5 \text{ cal. deg}^{-1} \text{ mole}^{-1} \quad \text{for} \quad T > T_\lambda, \quad (12)$$

$$\Delta S_3^0 - \Delta S_4^0 = -80 \text{ cal. deg}^{-1} \text{ mole}^{-1} \quad \text{for} \quad T < T_\lambda. \quad (13)$$

Since we have used straight lines in Fig. 1 it follows that we obtain one constant for each slope.

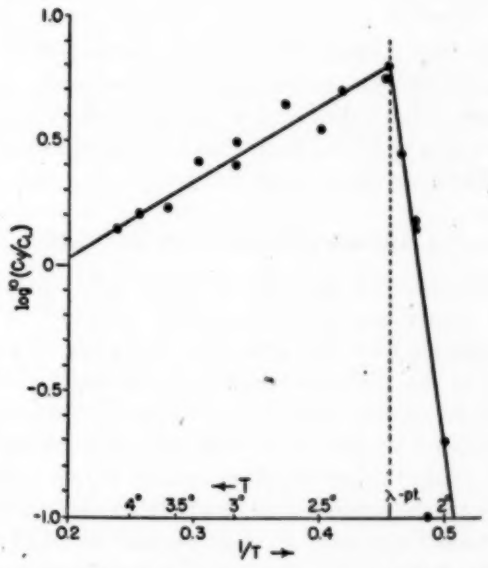

FIG. 1. Equilibrium concentrations of He^3 in He^4 in vapor (C_V) and in liquid (C_L) as function of $1/T$. The dots indicate the measured values of Lane and co-workers (reference 1).

[3] At the normal boiling point of He^4 we have for the liquid phase $pV_4^0 = 32$ cc atmos. mole^{-1}; this is small compared to $RT = 82.1 \cdot 4.2 = 345$ cc atmos. mole^{-1}. Since experiment indicates that $d\ln x_3'/dT$ is of the same order of magnitude as $d\ln p/dT$, or greater, it seems reasonable to neglect the terms $\bar{V}_3 dp/dT$ and $\bar{V}_4 dp/dT$.

[4] See R. H. Fowler and E. A. Guggenheim, *Statistical Thermodynamics* (Cambridge University Press, Cambridge, 1939), pp. 353.

[5] We have assumed that the measurements really dealt with a thermodynamic equilibrium although the question may be raised as to whether evaporation from the superfluid film carrying He^4 only could have falsified the results during the sampling below the λ-point. According to a discussion with Dr. Lane it seems, however, that this effect could at most call for a correction of about 10 percent and could in no way account for the enormous decrease of the He^3 concentration in the vapor phase below the λ-point. In favor of our interpretation we may add the remark that if the measurements were very far from equilibrium conditions it would be a most improbable coincidence that the two curves of C_V/C_L should meet just at the λ-point, the continuity of C_V/C_L being a requirement of thermodynamics, of course only for equilibrium concentrations.

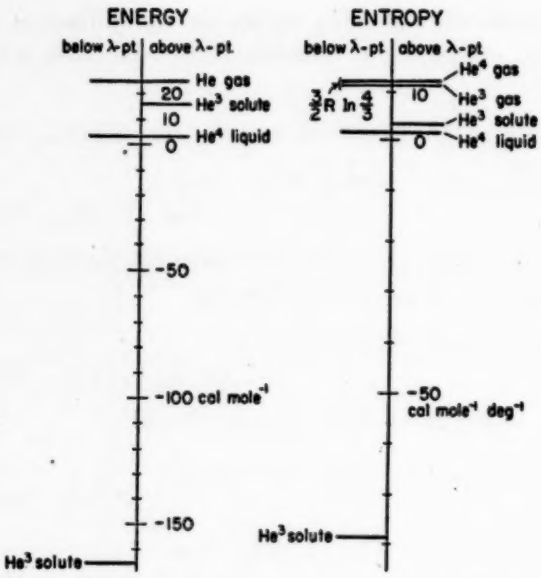

FIG. 2. Partial molar energy and entropy of He^3 and He^4 in close neighborhood to the λ-point. The zeros of the scales are chosen so as to coincide with the values of the entropy and energy of pure liquid He^4 at absolute zero. The energies in the gaseous state of He^3 and He^4 are set equal.

In Fig. 2 these results are represented in the form of energy- and entropy-level schemes taken closely above and below the λ-point. We used the value of 22 cal. $mole^{-1}$ as heat of vaporization of He^4 near the λ-point.

3. INTERPRETATION OF RESULTS

We consider first the value of $\Delta\bar{H}_3-\Delta\bar{H}_4=13$ cal. above the λ-point. It can roughly be accounted for by the different zero-point energies due to the different masses of the two isotopes. The zero-point energy in liquid He^4 has been estimated by one of us to be between 34 and 46 cal. $mole^{-1}$ near absolute zero.[6] If we assume that the zero-point energy of He^3 is given simply by multiplication of that of He^4 by 4/3, the ratio of the masses,[7] we obtain a value between 45 and 61 cal. $mole^{-1}$. If this were the sole effect we would have $\Delta\bar{H}_3-\Delta\bar{H}_4=13\pm2$ cal. $mole^{-1}$. The value derived from Lane's measurements just fits into this interval. However, it is not to be expected that it is the whole effect, since the entropy of He^3 in solution is higher than that of He^4 by about 2.5 entropy units. This corresponds to a free volume of He^3 about 3.5 fold that of He^4 in the same solution. The exact reason for this difference is not clear.

The values of $\Delta\bar{H}_3-\Delta\bar{H}_4$ and $\Delta S_3^0-\Delta S_4^0$ below the λ-point are truly astonishing. If the value of $\Delta S_3^0-\Delta S_4^0=-80$ cal. deg^{-1} were to be interpreted by a change of free volume, it would mean that He^3 has a free volume equal to only 10^{-17} times that of the free volume of He^4 in the same solution. It seems absurd to imagine that such a difference in free volume could occur. We are practically driven to the conclusion that this is an effect of He^3 on the solvent, He^4. The presence of the He^3 must then be able to induce a change involving very many atoms of He^4. Since the entropy per mole He^4 below the λ-point is smaller than 1.6 cal. deg^{-1} while we obtained for $\Delta S_3^0-\Delta S_4^0=-80$, it follows that one single He^3 atom must be able to "disentropize" about 50 He^4 atoms.

We may try to explain this effect by a simple mechanism which is suggested by the model proposed by Tisza[8] and F. London[9] of two inter-penetrating phases, a "normal" and a "superfluid" one in liquid helium below the λ-point. A He^3 atom could presumably move without collision through the superfluid phase of He^4 but not through the normal one. If it found itself in a portion of the superfluid phase it would have an extremely long free path, and its zero-point energy would be low. It might thus be expected to draw around itself a small lake of superfluid He^4. This would mean that the presence of He^3 would cause the appearance of small globules of superfluid He^4 which would have abnormally small entropy (approximately zero, according to Tisza) and abnormally low energy. The question arises as to whether these globules of pure superfluid He^4 can be large enough to account for the large energy and entropy of dissolving of He^3 below the λ-point.

Tisza has pointed out that the thermohydro-

[6] F. London, Proc. Roy. Soc. **A153**, 576 (1936); J. Phys. Chem. **43**, 49 (1939).

[7] We multiply by the ratio of the masses rather than by its square-root as for a harmonic oscillator because there is evidence that the field in which a helium moves, resembles a square-well potential energy more closely than a Hooke's law field. See reference 6 and also M. E. Hobbs, J. Chem. Phys. **7**, 318 (1939).

[8] L. Tisza, Nature **141**, 913 (1938); C. R. Paris, **207**, 1035, 1186 (1938); J. de phys. et rad. **1**, 165, 350 (1940); Phys. Rev. **72**, 838 (1947).

[9] F. London, Phys. Rev. **54**, 947 (1938).

dynamic effects can be explained by his model if one assumes that the normal He atoms in the liquid below the λ-point have a sort of partial pressure, which may be measured by a semipermeable piston which allows the superfluid helium, but not the normal helium, to pass through.

Let us imagine a He^3 atom within a globule of superfluid helium acting much like such a semipermeable piston, holding the normal He^4 atoms beyond a radius r, but allowing the superfluid He^4 to pass into the sphere. The He^3 atom, then, must exert an outward pressure to balance the partial pressure of the normal He^4 atoms outside r. Indeed it exerts such a pressure by virtue of its zero-point energy. Our idea is that the equilibrium of these two pressures determines the size of the globule and thus the number of normal He^4 atoms which are disentropized by one He^3 atom. This is, of course, a very idealized picture.

Since we are interested only in obtaining a rough estimate we shall make the calculation as though the globules were spherical and shall further assume that each one contains only one He^3 atom.

The zero-point energy of an atom of mass m, radius a, which is locked within a spherical cavity of the radius r, is

$$E_0=\frac{h^2}{8m(r-a)^2}. \tag{14}$$

Its zero-point pressure is given by differentiation with respect to the volume $v=(4\pi/3)r^3$

$$p_0=-\frac{\partial E_0}{\partial v}=\frac{h^2}{4m(r-a)^3}\frac{1}{4\pi r^2}. \tag{15}$$

On the other hand, the thermal pressure exerted by liquid helium II on a semipermeable wall, behind which the pure superfluid is contained, is approximately given by [10]

$$p=4.6\cdot 10^3 T^{2.6}\ \text{dyn/cm}^2. \tag{16}$$

Thus, equilibrium is established for the radius r_0 given by equalizing the two pressures:

$$\frac{h^2}{16\pi m r_0^2(r_0-a)^3}=4.6\cdot 10^3 T^{2.6}, \tag{17}$$

or

$$(r_0-a)^3 r_0^2=3.8\cdot 10^{-35}/T^{2.6}.$$

At $T=2.1$°K and for $a=1.4$A (range of the repulsive forces between helium atoms) one obtains the radius $r_0=5.8$A or the volume $(4\pi/3)r_0^3=815$A. The molecular volume of liquid helium is about 45A. Hence, there would be about 815:45=18 He^4 molecules in such a globule. At 2.1°K the entropy of liquid helium is about 1.3 cal. deg^{-1} mole^{-1}. Accordingly, we would be able to account for about 24 cal. deg^{-1} mole^{-1} of the 80 obtained by the evaluation of Lane's experiments.

The significance of this result might still be a matter of opinion, and we do not wish to push this particular picture unduly; it is to be taken merely as a tentative suggestion. In particular, it is still necessary to show why one should consider the zero-point energy of a He^3 atom as determined by the space left free from the normal phase of He^4 alone, whereas we know that the zero-point energy of pure He^4 at 0°K is essentially determined by the space left between *all* He^4 atoms.

4. INFLUENCE OF He^3 ON THE λ-TRANSITION OF He^4

The thermal data (9), (10), (12), (13), which we have derived from the vapor-liquid equilibrium consentration, can be used to calculate the effect on the λ-transition of He^4 caused by the presence of He^3.

While it cannot be said with certainty, it appears to be strongly suggested, if one looks at the data assembled in Fig. 1, that the C_V/C_L-curve has a *discontinuous slope* at the λ-point. This, at any rate, lay at the root of our previous discussion of the measurements. This means that $\bar{H}_3-\bar{H}_4$ has a discontinuity in the liquid phase at the λ-point (9), (10), or rather that the solutions of He^3 in He^4 will have a *first-order transition* instead of a λ-point. The *transition heat* is directly given by (9), (10) to be about 180±20 cal. per mole He^3 dissolved. This is quite similar to the transition of a superconductor in a magnetic field, which also is a first-order transition except for one point on the transition line, namely, for the magnetic field zero, where there is no transition heat, only a discontinuity

[10] F. London, Rev. Mod. Phys. **17**, 310 (1945), Eq. (14).

of specific heat, quite as it is here the case in the (x_3, T) plane for $x_3=0$.

Further, there might be an effect on the *transition temperature*. Our data enable us to calculate the coefficient $(dT/dx_3)_{x_3=0}$, i.e., the *change of the transition temperature* with the concentration x_3 in the limit of very small concentration.

Since we have a phase transition of first order, we may expect an equilibrium in which two solutions of He I and He II co-exist side by side (similar to the "mixed" state of superconductors in a magnetic field). The equilibrium concentrations, x_3^+ and x_3^-, at a given temperature, will not necessarily be the same.

We assume constant pressure. Then, according to (9), (10), (12), (13), the chemical potentials μ^+ and μ^- above and below the λ-point may be written for small concentrations x_3^+ and x_3^-:

$$\begin{aligned}\mu_3^+&=\mu_3^{0\prime}+\Delta\bar{H}_3^+-T\Delta\bar{S}_3^++RT\ln x_3^+\\&=\mu_3^{0\prime}+\Delta\bar{H}_4^+-T\Delta\bar{S}_4^++13\\&\qquad-2.5T+RT\ln x_3^+\\&=\mu_3^{0\prime}+\mu_4^{0+}-\mu_4^{0\prime}+13-2.5T+RT\ln x_3^+;\end{aligned}\tag{18a}$$

$$\begin{aligned}\mu_3^-&=\mu_3^{0\prime}+\Delta\bar{H}_3^--T\Delta\bar{S}_3^-+RT\ln x_3^-\\&=\mu_3^{0\prime}+\Delta\bar{H}_4^--T\Delta\bar{S}_4^--168\\&\qquad+80T+RT\ln x_3^-\\&=\mu_3^{0\prime}+\mu_4^{0-}-\mu_4^{0\prime}-168+80T+RT\ln x_3^-;\\\mu_4^+&=\mu_4^{0+}-RTx_3^+;\\\mu_4^-&=\mu_4^{0-}-RTx_3^-;\end{aligned}\tag{18b}$$

where $\mu_4^{0\pm}$ are the chemical potentials of pure liquid He^4 above and below the λ-point, respectively, and $\mu_3^{0\prime}$ and $\mu_4^{0\prime}$ are the chemical potentials of pure He^3 and He^4 in the vapor phase, respectively. Since there is no discontinuity in the properties of the vapor phase, we do not need to distinguish between the values of $\mu_i^{0\prime}$ above and below the λ-point.

The conditions of equilibrium,

$$\mu_3^+(x_3^+, T)=\mu_3^-(x_3^-, T),\tag{19a}$$

$$\mu_4^+(x_3^+, T)=\mu_4^-(x_3^-, T)\tag{19b}$$

furnish for small concentrations the following two equations:

$$\mu_4^{0+}-\mu_4^{0-}=82.5(T-T_\lambda)-RT\ln(x_3^+/x_3^-),\tag{20a}$$

$$\mu_4^{0+}-\mu_4^{0-}=RT(x_3^+-x_3^-).\tag{20b}$$

We are only interested in the neighborhood of the λ-point and call $T-T_\lambda=\tau$. At the λ-point, μ_4^0 and $\partial\mu_4^0/\partial T=-S_4^0$ are both continuous (no transition heat). Hence, for small τ:

$$\begin{aligned}\mu_4^{0+}-\mu_4^{0-}&\approx\frac{1}{2}\left(\frac{\partial^2\mu_4^{0+}}{\partial T^2}-\frac{\partial^2\mu_4^{0-}}{\partial T^2}\right)\tau^2\\&=\frac{C_p^--C_p^+}{2T_\lambda}\tau^2,\end{aligned}\tag{21}$$

where $C_p^--C_p^+\approx 7.6$ cal. deg^{-1} mole^{-1} is the well-known discontinuity of the specific heat at the λ-point ($T_\lambda=2.19°\text{K}$). Hence,

$$\mu_4^{0+}-\mu_4^{0-}\approx(7.6/2\cdot 2.19)\tau^2=1.73\tau^2.$$

Accordingly, the two Eqs. (20a) and (20b) can be written in the form

$$1.73\tau^2=82.5\tau-RT_\lambda\ln(x_3^+/x_3^-),\tag{22a}$$

$$1.73\tau^2=RT_\lambda(x_3^+-x_3^-).\tag{22b}$$

Eliminating x_3^+ gives the following equation for x_3^-:

$$82.5\tau-1.73\tau^2=RT_\lambda\ln(1+1.73\tau^2/x_3^-RT_\lambda),$$

or for small τ:

$$82.5\tau=1.73\tau^2/x_3^-.$$

This equation has two solutions for τ:

1. $\tau=0$ independent of x_3^-,
2. $\tau\approx x_3^-82.5/1.73=48x_3^-$,

to which belong, according to (22b), the following values of x_3^+

1. $x_3^+=x_3^-$,
2. $x_3^+=x_3^-+(1.73/RT_\lambda)(48x_3^-)^2$.

However, only the first solution, $x_3^+=x_3^-$, $\tau=0$ independent of $x_3^\pm$, can have physical significance; the other one, occurring at a higher temperature, would correspond to a return to He II, evidently the consequence of an illegitimate extrapolation of the free energy branch of He II to higher temperature.

5. CONCENTRATED SOLUTIONS

It is clear that we have to expect marked deviations from Henry's law below the λ-point as soon as the concentration becomes so large that the spheres of influence of the He^3 atoms (Eq. (17))

have a chance to overlap. This will happen when $x_3 \approx 1/100$. Obviously not more entropy than originally contained within the liquid He^4 can be taken away by dissolving He^3. In other words, the difference $\Delta\bar{H}_3 - \Delta\bar{H}_4$, which below the λ-point was found to be negative (Eq. (10)) for very small concentrations x_3, should change sign and should become positive for larger x_3.

Moreover, it is almost certain that pure He^3 cannot exist in a liquid phase at any temperature, at least not for normal pressure.[11] Hence, if He^3 is present in abundance one will have a gaseous phase, which is practically pure He^3 below 1°K, in equilibrium with a liquid phase which is predominantly He^4, and it appears most questionable whether solutions of much more than 1 percent He^3 could exist in the liquid phase.

According to our ideas the Brownian movement of a He^3 globule would essentially be determined by the local state of motion of the normal phase of He^4, which is the one which carries most of the heat content. Hence, in the presence of a heat current in He II, the He^3 atoms will have to follow the direction of the heat transfer which below the λ-point occurs through bodily transfer by motion of the atoms of the normal phase rather than by ordinary heat conduction. This can have a most disturbing effect on the establishment of the vapor-liquid equilibrium. If, for instance, liquid helium is evaporated at constant temperature by pumping off the vapor a heat current is produced towards the surface. In this case the He^3 atoms will be swept towards the surface where the concentration of He^3 will be enriched eventually to the degree that the deviations from Henry's law mentioned above become important and the He^3 can no longer remain dissolved in the liquid phase and will evaporate. Observations which support this view have recently been communicated to us by Lane and will be published by him in the Physical Review in the near future.

[11] That He^3 cannot exist in the liquid state at any temperature and normal pressure appears most probable in view of the estimates of the zero-point energy of liquid He^4 in reference 6. Replacing this zero-point energy by one 4/3 times as large (see reference 7) one obtains a repulsion more than sufficient to compensate entirely the potential energy of the Van der Waals cohesion for any density assumed. The difference in statistics is in this estimate not yet accounted for. Its consideration, of course, would still contribute in the same direction.

SUPPLEMENT TO SECTION 4

Only after concluding the above paper we became aware that the deviations from Henry's law below the λ-point predicted in section 5 for larger concentrations may have an effect of *first* order on the change of the λ-temperature with x_3 calculated in section 4. We may account for this effect by adding to μ_3^- a correction term linear in x_3 which expresses an increasing antipathy of He^3 against being dissolved in liquid He^4 below the λ-point as the concentration x_3 becomes greater.

Thus instead of (18a) we write now:

$$\mu_3^- = \mu_3^{0\prime} + \mu_4^0 - \mu_4^{0\prime} - 168 + 80T + RT \ln x_3^- + a x_3^-. \quad (18a')$$

The term ax_3^- in Eq. (18′) expresses a deviation from Henry's law. One can easily show that a is directly given by:

$$a = (\partial/\partial x_3) \ln(C_V/C_L).$$

If the solubility of He^3 is to decrease *monotonically* starting with the smallest concentrations, then a has to be positive.

Accordingly we now obtain the equation

$$1.73\tau^2 = 82.5\tau - RT \ln(x_3^+/x_3^-) + a x_3^-, \quad (22a')$$

instead of (22a). Equation (22b) is obtained as before.

Elimination of x_3^+ from (22a′) and (22b) yields now the following equation for small τ and small x_3^-:

$$1.73\tau^2/x_3^- - 82.5\tau - a x_3^- = 0$$

with the solutions

$$\tau/x_3^- = 24 \pm (576 + a/1.73)^{\frac{1}{2}}.$$

The solution with the minus sign is the only one which has physical significance. It is the one which corresponds to the solution $\tau = 0$ in section 4. Accordingly we expect $\tau/x_3^- < 0$, i. e., a *decrease* of the λ-temperature with increasing x_3, if indeed our assumption $a > 0$ of a monotonically decreasing solubility is correct.

Breakdown Directions in Lithium Halide Crystals*

J. W. DAVISSON**
Laboratory for Insulation Research, Massachusetts Institute of Technology, Cambridge, Massachusetts

(Received January 22, 1948)

Electrical breakdown paths in the lithium halide crystals form star patterns consisting of 12 paths of the type $[xxy]$ where $x \geqslant y$. The paths lie within the acute sectors of the (110) planes bounded by the directions [110] and [111].

The star assumes the [110] orientation at low temperatures and tends to approach the [111] position as the temperature increases. Under overvoltage conditions, complex $[xxy]$ patterns are obtained; they show abrupt changes in orientation as the paths proceed through the crystal, but follow a definite sequence of directions.

It is shown that, although the breakdown paths seem to mark those directions in which electrons can be accelerated most rapidly to the ionization potential of the lattice, the star paths apparently do not follow simply from an electron wave interaction with the lattice or from a statistical competition between breakdown in the [110] and [111] directions.

I. INTRODUCTION

IT has been shown[1] that lithium halide crystals undergo electric breakdown in the directions $[xxy]$ at elevated temperatures, and that the parameters x and y may be temperature dependent. The present, more detailed investigation of the star patterns and a comparison with the breakdown paths obtained in other crystals give further insight into the mechanism of electrical breakdown.

II. CRYSTALS

The alkali halide crystals used in the following experiments were, in general, grown from the melt. Pure LiF crystals were obtained commercially.*** CsCl and $NaClO_3$ crystals were grown by slow evaporation of the aqueous solution. LiI crystals could not be obtained because the material decomposes readily at its melting temperature.

III. APPARATUS AND PROCEDURE

A crystal section about 1 sq. cm in area and 10 mils in thickness was placed between a metallic point-plane electrode system and immersed in an insulating medium which forced the breakdown to take place through the crystal instead of in the air over its surface. To yield paths that lie close to the surface and to limit the current at breakdown to such small values that fracturing is avoided, a glass microscope slide, which served as a series resistance, was inserted between the crystal and the plane electrode. With liquid insulating media, which were used up to 450°C (the boiling point of sulfur), each crystal section was subjected to numerous breakdowns of (+) and (−) polarity by shifting the point electrode. Above 450°C the crystals were heated in vacuum by radiation from an electric oven (Fig. 1).

In the previous study[1] breakdown was effected by means of a high frequency spark discharge; hence the breakdown voltage was not known in magnitude or sign. For the present investigation a high voltage source was used which produced a pulse of known sign and rise time and a roughly controllable magnitude.† A 4-μf condenser, charged up to 600 volts, was discharged through the primary of an induction coil by means of a thyratron. The high voltage pulse of 50 kv max. and $(10)^{-5}$ sec. front was rectified by means of a kenotron. Direct current breakdown tests were performed with a 50-kv voltage supply consisting of a conventional voltage doubler circuit with accompanying filters.

* This research was made possible through support extended to the Massachusetts Institute of Technology, Laboratory for Insulation Research, jointly by the Navy Department (Office of Naval Research) and the Army Signal Corps under ONR Contract N5-ori-78, T.O.I.

** Present address, Crystal Section, Naval Research Laboratory, Washington, D. C.

[1] J. W. Davisson, Phys. Rev. 70, 685 (1946).

*** The Harshaw Chemical Company, Cleveland, Ohio.

† This unit was designed by D. Young, Laboratory for Insulation Research, Massachusetts Institute of Technology.

IV. GEOMETRICAL CONSIDERATIONS AND OPTICAL MEASUREMENTS

The directions assumed by electrical breakdown paths in the lithium halide crystals may be represented in terms of zonal parameters $[uvw]$ by the indices $[xxy]$ where $x \geqslant y$. (The zonal parameters are the components of the path in the directions of the coordinate axes, that is, in the cube edge directions of Fig. 2.) The double indices xx require that the paths lie within the (110) planes, while the restriction $x \geqslant y$ shows that they are confined to the acute sectors of the (110) planes bounded by the directions [110] and [111]. The indices of the 12 paths, which comprise a complete $[xxy]$ star pattern, are, according to macroscopic symmetry:

$$\begin{array}{cccc} \underline{xxy} & \underline{xx\bar{y}} & \underline{x\bar{x}y} & \underline{\bar{x}xy} \\ \underline{xyx} & \underline{xy\bar{x}} & \underline{x\bar{y}x} & \underline{\bar{x}yx} \\ \underline{yxx} & \underline{yx\bar{x}} & \underline{y\bar{x}x} & \underline{\bar{y}xx} \end{array}$$

where the bar means that the designated index is negative and the underscore signifies that the same path directions represented by indices with negative signs are included.

The pattern may be visualized as follows (Fig. 2): from the midpoint (0) of a (001) cube face four [110] face-diagonal directions are obtained by joining (0) with the midpoints P, Q, R, and S of the vertical cube faces. The two additional [110] directions are given by the surface diagonals U–U' and V–V' which intersect at (0). The four [111] body diagonals result by joining (0) with the midpoints W, X, Y, and Z of the vertical cube edges. The (110) planes, determined by any two intersecting [111] directions, are of two types: two vertical planes $WUU'Y$ and $XVV'F'$ and four oblique planes OWX, OXY, OYZ, and OZW. The direction of a star path, since it lies within a (110) plane, may be specified by its deviation α from a [110] direction. A star pattern of given deviation α, centered at (0), consists of 12 paths directed towards A, A', B, B', C, C', D, D', E, E', F, and F'. The four paths from (0) to E, E', F, and F' make a larger inclination angle with the vertical than the eight remaining paths. In terms of path indices the 4 paths from (0) to E, E', F, and F' are of the type $[xxy]$ and the eight remaining paths are of the types $[xyx]$ and $[yxx]$.

The star patterns, once it has been established that their loci are the (110) planes,†† are completely determined geometrically by the projection of their paths upon the cube face (Fig. 3). For all values of α the four paths from (0) to E, E', F, and F' will always project into the 45° lines and will hereafter be referred to as diagonal paths. The eight remaining paths, the "off-diagonal paths," however, will vary in azimuth ϕ from 0° to 45° as α varies from 0° for [110] to 35.6° for the [111] orientation. (The deviation α and the azimuth ϕ are related by the expression $\sqrt{2}\tan\alpha = \tan\phi$.) It is apparent that the ratio y/x, which completely determines the geometry of the pattern, may be obtained directly from the projection figure by measuring the azimuth of the off-diagonal paths, since $\tan\phi = y/x$.

The breakdown paths obtained experimentally were examined under a stereomicroscope. Only those paths which showed no accompanying crystal fracture at 100× magnification were selected for measurement, unless otherwise stated. The azimuthal angle measurements were made with a petrographic microscope equipped with a translating and rotating stage. Although the azimuth is given relative to the cube edge directions, the diagonal breakdown paths in the 45° positions were actually used as the experimental datum lines. This choice was dictated by the fact that the face diagonals are projection

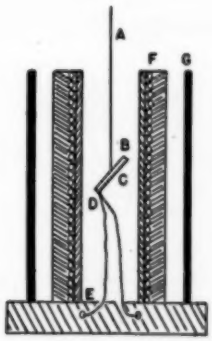

FIG. 1. Breakdown in vacuum. A is the high voltage electrode; B, crystal sample; C, Aquadag coating; D, Chromel-Alumel thermocouple fused to B; E, ceramic base plate; F, ½ in.-×3 in.-cylindrical furnace; G, copper heat shield.

†† Twenty-four path directions would appear if they were not confined to reflection planes. Detailed measurements of typical star patterns are presented in reference 1.

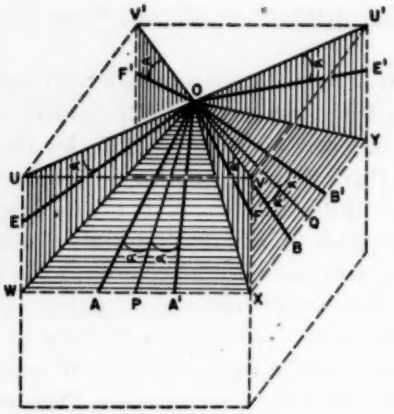

FIG. 2. Geometry of an [xxy] star pattern. The star paths are directed from (0) to A, A', B, B', C, C', D, D', E, E', F, and F'.

paths of the star patterns and are therefore easily identified.

The inclination angles of the paths were measured periodically to verify their [xxy] nature. The horizontal component of the path was obtained by means of a micrometer eyepiece while the vertical component was measured by the fine focus adjustment screw with allowance made for the index of refraction. The experimental error is about $\pm 1°$ for azimuth and $\pm 3°$ for the inclination angle.

V. RESULTS AT MINIMUM VOLTAGE

Lithium Fluoride

The orientation of breakdown paths in LiF as a function of temperature and polarity is shown in the projection diagrams of Fig. 4. The diagrams are to be read as follows: the individual dots and crosses are representative of the orientations observed for negative and positive breakdown paths respectively. The radial lines show the average negative breakdown directions.

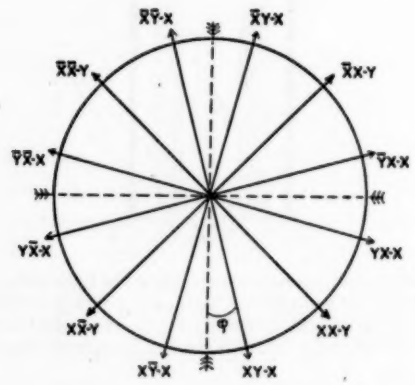

FIG. 3. Projection of an [xxy] star patterns upon the (001) plane.

The diagrams give the following information:

(4A) At $-70°$C and below, only [110] paths are obtained with (−) and (+) d.c. and pulse voltages. The surface diagonals are not represented because [100] and not [110] surface paths were observed.

(4B) At 0°C, (−) pulses yield [110] paths and a star of azimuth 10°; (+) pulses yield only [110] paths.

(4C) At 25°C, d.c. and pulse, (−) a 13° star and rarely [110] paths; (+) only [110] paths.

(4D) At 50°C, pulse, (−) a 13° star; (+) [110] paths.

(4E) At 100°C, pulse, (−) a 15° star; (+) [110] paths dominant with star paths appearing at various azimuths, which, however, are less than 15°.

(4F) At 125°C, pulse, (−) a 15° star; (+) [110] paths are no longer observed; a star of 8° with large individual variations in azimuth is found.

(4G) At 150°C, pulse, (−) a 19° star; (+) a 16° star. Under equilibrium d.c. conditions metallic dendrites are formed. (See below.)

(4H) At 250°C, pulse, for (−) and (+) a 21° star. Equilibrium d.c. yields dendrites, but with overvoltage star paths of 21° azimuth were obtained at 235°C.

(4I) At 300°C, a 23° star (Fig. 5). The crosses in Fig. 4I show the orientation obtained in the vacuum chamber (Fig. 1) and the dots, nearly coinciding, refer to breakdown observed with a liquid embedding medium.

(4J) At 350°C a 25° star for (−) and (+) pulse voltage.

(4K) At 450°C, pulse, (−) and (+) yield a star of azimuth 26°. Individual paths may attain azimuths as great as 30°. Even with a protective resistance [111] paths are frequently obtained especially with positive pulses. Only dendrites were obtained with d.c.

(4L) Above 450°C the breakdown paths behave as follows:

450°C	26° star and [111]
510	[111]
525	[111]
550	[111]
600	[110] and [111]
650	[110]
700	[110]
800	random

No difference in the physical appearance of the (+) and (−) patterns was observed. The paths are generally straight (Fig. 5) but those of the same orientation in a single specimen may not be strictly parallel. At 250°C, for example, the following set of azimuths was obtained: 18.6°, 21.5°, 20.5°, 21°, 21°, 18.5°, 19°, 19°, 21°, 18°, 20°, 19°, 18°, 19°, even though the individual paths were straight and showed no initial bending.

The influence of temperature was also similar for both polarities, but the positive patterns were retarded in azimuth with respect to the negative in the low temperature range. An increase of temperature in the range from 0°C to 450°C tended to shift the patterns towards [111]; a discontinuous jump from an azimuth of about 26° to 45° ([111] paths) seemed to occur near 450°C. The [111] paths appear between 450°C and 600°C, while above 600°C [110] paths were again observed. Complete star patterns most readily form between 200°C and 500°C, while at room temperature usually one or two paths appeared. Above 600°C stunted patterns similar to Fig. 6 were obtained.

Confirming von Hippel's conclusion[2] the same breakdown directions appeared in oblique crystal cuts. In (110) sections, for example, paths at four different angles of inclination were observed. Since a [110] direction is vertical, two paths deviated from the vertical by 13° at room temperature.

Results obtained in thin sections (2 to 3 mils) suggest that a thickness dependence of path orientation may exist. This was particularly noticeable at low temperatures. Under d.c. conditions at −170°C the paths in thick sections tended to start initially with large azimuths and to straighten out almost immediately into the [110] direction. In thin sections, however, the initial change in azimuth took place more slowly with the result that the paths presented a curved aspect tending towards, but usually not attaining, the [110] direction.

[2] A. von Hippel, Zeits. f. Physik **75**, 145 (1932); Zeits. f. Elektrochemie **39**, 506 (1933).

Lithium Chloride

The breakdown behavior of LiCl is shown in Fig. 7:

(7A) At −170°C, d.c. and pulse, (+) and (−), [110] paths dominant.

(7B) At 25°C, with overvoltage (see below), paths appear at all azimuths from 0° to 30°.

(7C) At 25°C, pulse, (−) a 10° star dominant; (+) [110] dominant.

(7D) At 100°C, pulse, (−) a 20° star; (+) a 15° star.

(7E) At 150°C, pulse, (−) and (+), azimuths ranging from 20° to 30°. Direct current yielded white metallic dendrites that lacked orientation.

(7F) At 200°C a star pattern of azimuth 30°.

(7G) At 300°C a path orientation was poor; path development extended only a short distance from the probe with maximum azimuth 30° (Fig. 6).

(7H) At 450°C, same as *G* but orientation is less definite.

The star patterns in LiCl shifted more rapidly

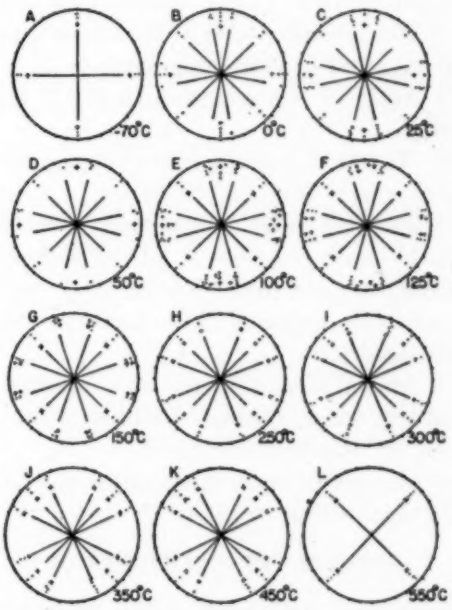

FIG. 4. Orientation of breakdown paths in LiF.

FIG. 5. Negative star in LiF at 300°C.

with increase of temperature than in LiF until they attained an azimuth of about 30° at 200°C. Thereafter the azimuth no longer changed with increase of temperature and hence LiCl did not yield [111] paths at elevated temperatures. The paths in LiCl showed a more pronounced tendency than in LiF to bend near the electrode and to give a wider spread of breakdown directions at constant temperature.

Lithium Bromide

The behavior of breakdown paths in LiBr is shown in Fig. 8:

(8A) At −170°C [110] dominant for d.c. and pulse. Paths appeared also at an azimuth of 15°.

(8B) At −60°C [110] dominant.

(8C) At 25°C average azimuth of 12° for d.c. and pulse.

(8D) At 100°C, pulse, (+) and (−), a 25° star (azimuth varied from 20° to 30°).

(8E) At 150°C a 30° star pattern was formed. The paths began to show a lack of definiteness in orientation and from time to time paths of lower azimuth appeared. Direct current yielded random dendrites.

(8F) At 200°C and above only stunted patterns of Fig. 6 were formed. A maximum azimuth of about 35° has been observed.

The behavior of breakdown paths in LiBr was very similar to that of LiCl.

RESULTS FOR OVERVOLTAGE

The patterns considered above were obtained under voltage conditions just sufficient for breakdown path formation. We know from the work of von Hippel[2] that path directions will change if excessive voltage is applied. Such overvoltage was produced by three methods: (1) as single pulses from the pulse generator described above; (2) as rectified voltage pulses from a leak tester that was drawn rapidly over the crystal surface; (3) as excess d.c. voltage on a probe which was lowered through oil towards the sample until breakdown occurred.

The overvoltage patterns obtained differed in complexity but showed the same sequence of path transitions. The most complex patterns were obtained in LiCl and LiBr by method (2). The (100) projection of a typical one is shown in Fig. 9, the thermal dependence of the patterns in Table I. The transformations involved only the off-diagonal paths. An initial star was formed whose azimuth increased with decrease of temperature. This star transformed abruptly into the [110], or nearly [110], directions and these in turn transformed into a 30° star. The 30° paths usually transformed by means of a smooth curve in LiBr (Fig. 10) or by discontinuous jumps yielding a spider leg-like pattern in LiCl into the orientation of normal breakdown.

When methods (1) and (3) were used, the overvoltage pattern always began at a later stage of development than in the above. A star with an azimuth in excess of that of normal breakdown, but not exceeding 30°, usually reduced azimuth smoothly in LiBr and discontinuously in LiCl until the normal breakdown direction was attained. In LiF overvoltage frequently yielded [111] paths at room temperature

FIG. 6. Typical heat degeneration of 30° patterns in LiCl and LiBr.

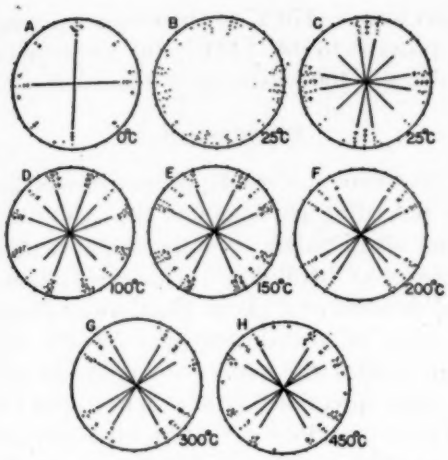

FIG. 7. Orientation of breakdown paths in LiCl.

and above; whereas in LiCl and LiBr [111] paths were never observed under normal conditions and with excess voltage only at −170°C in conformity with the orientation of the initial star with temperature. LiF does, however, exhibit a discontinuous reduction in azimuth from 30° to normal breakdown as shown in Table I.

METALLIC DENDRITES

Dendrites were first observed by von Hippel[3] in the alkali halide crystals. They constitute a metallic (Na metal in NaCl, etc.) extension of the cathode within the crystal. The metallic growths, which form when moderate d.c. fields are impressed at elevated temperatures, frequently assume a definite crystallographic orientation; thus [111] dendrites appear in NaF, [100] and [110] in NaCl, etc.

In the lithium halide crystals the dendrites seemed to form at lower temperatures than in the other alkali halide crystals. In LiF they appeared (Fig. 11) as delicate pink growths resembling sea weed. Their intricate structure, which distinguishes them from the dendrites in the other alkali halides, may be due to a tendency to grow along star path directions. In general, it was not possible to assign lattice directions to the structure because it grows by the formation of a series of blobs, but, at times, a definite [110] orientation was noticed. All the dendrites grew (slowly compared with breakdown paths) from the cathode even when the point electrode was rendered positive. Frequently the dendrites which were formed under excess d.c. voltage conditions terminated in breakdown paths as they approached the anode surface.[3]

Von Hippel has concluded[4] that the dendrites are probably electronic and not electrolytic in origin. It is thus possible that the dendrites and breakdown paths were formed by similar processes. It is of interest to note that the orientation of dendrites and breakdown paths was not necessarily the same at a given temperature.

SUPPLEMENTARY OBSERVATIONS ON RELATED CRYSTALS

Sodium Chlorate

It was shown previously[1] that sodium chlorate also yields star patterns. This crystal belongs to a different symmetry class and possesses a more complex structure than the lithium halides. The following results were obtained: at 200°C in 3 samples for (+) and (−) voltage precise star patterns of azimuth 18°; at 100°C and at 25°C a star of azimuth 22.5°; at −60°C and at −170°C [111] paths at an azimuth of 45°, also paths at azimuths 12°, 18°, and 22.5°. Inclination angle measurements show that the paths observed were again of the type $[xxy]$ with $x \geqslant y$ to an accuracy of 3°.

Sodium Fluoride

The path orientation in LiF with increasing temperature is represented by the scheme:

$$[110] \rightarrow [xxy] \rightarrow [111].$$

This behavior is at variance with the results obtained in NaF[1] which showed the [111] paths

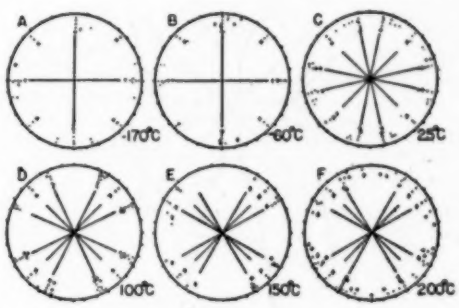

FIG. 8. Orientation of breakdown paths in LiBr.

[3] A. von Hippel, Zeits. f. Physik **98**, 580 (1936).

[4] A. von Hippel, J. App. Phys. **8**, 829 (1937).

TABLE I. Overvoltage patterns.

I. LiBr (+) and (−)	
(−170°C)	45°[111] paths
(25°C)	23°→0°→30°→12°
(100°C)	20°→0°→30°→22°
(150°C)	13°→0°→32°→28°
(300°C)	0°→30°
II. LiCl (+) and (−)	
(25°C)	10°——→30°→17°→10°→18°
(25°C)	18°→0°→30°→0°
(100°C)	14°→0°→30°→12°→17°
III. LiF (−)	
(25°C)	30°→15°→0°→9°→12°

Azimuth 0°=[110]

at low and the [110] paths at high temperature. The orientation of the paths in NaF as a function of temperature was therefore rechecked and confirmed.

For both polarities the tendency of breakdown path orientation in NaF changed from [111] at −170°C to [110] at 200°C. The [110] paths were still observed at 700°C. In spite of numerous tests in the intermediate temperature range, no indication of star paths was noticed; in every case both [111] and [110] paths were observed. With overvoltage, especially of negative sign, [100] paths accompanied by incipient (100) cleavage fractures were obtained at all temperatures investigated.

Cesium Chloride

Below 450°C cesium chloride has a body-centered cubic lattice. The dominant breakdown direction from −170°C to the transition temperature proved to be [111]; in addition, with overvoltage, [100] paths were observed.

DISCUSSION

The experimental results presented in this and in the preceding paper[1] show that all the face-centered alkali halide crystals exhibit a thermal dependence of breakdown path orientation. All the halide salts of a given alkali atom show the same type of transformation. Except in the lithium halides the paths are confined to the three basic directions [100], [110], and [111]. In addition, random paths are observed at low temperatures in salts with low lattice energies.

The general behavior of breakdown paths may conform to the following mechanism.[5] Assuming that the paths result from local melting of the crystal by electronic avalanches, they mark those directions for which the conduction electrons can most readily be accelerated by the applied field to ionizing velocities. These directions will depend upon the interaction of the electronic wave-length and charge with the lattice. In a given direction the periodic lattice alternately transmits and reflects an electron as its velocity increases. Conversely, for a given wave-length the lattice is transparent in some directions and reflecting in others. During acceleration, since the wave-length is changing, first one and then another direction will become transparent, and the direction finally observed is the one in which the electron moved the greatest distance

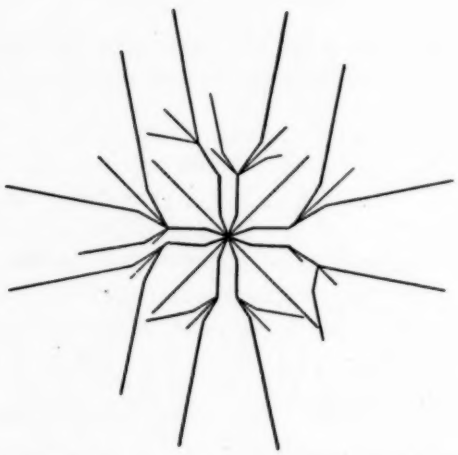

FIG. 9. (001) projection of the overvoltage pattern in LiCl at 25°C.

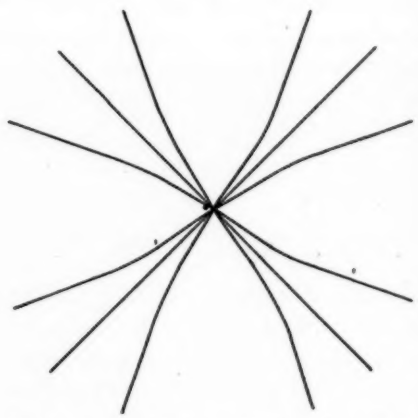

FIG. 10. Reduction of 30° star LiBr 25°C.

[5] A. von Hippel, Trans. Faraday Soc. **42A**, 78 (1946).

between the ionization acts. Under normal breakdown we may expect to observe only one direction at each temperature, but with excess voltage a sequence of directions would be expected. The results obtained with overvoltage suggest that the patterns correspond to a deceleration of fast electrons near the probe into the crystal, since the final orientation corresponds to that of normal breakdown. In a sense the path directions mark the converse of Brillouin zones, because the zones represent regions of total reflection.

If the above mechanism is correct, it would seem that the star paths do not correspond to directions which may be derived by a simple wave interaction picture. One notices that the three basic breakdown directions [100], [110], and [111] correspond to the three largest interplanar spacings or the three shortest interatomic distances in the lattice. If higher order paths are observed, the types [102], [112], and [123], etc. would be next in line in the sequence of interplanar spacings. However, only paths of the type $[xxy]$ where $x \geqslant y$ were observed and none of the above fall into this category.

It is possible to account for the geometrical locus of the patterns in the lithium halide crystals by assuming, as von Hippel has suggested,††† that the star paths may result from a competition in breakdown between the [110] and [111] directions. Because the distance between ionizing impacts may be very short, a statistical average direction would be observed macroscopically.

According to such a mechanism of competition the path orientation should follow a simple statistical distribution law. A careful examination of the (+) breakdown paths in LiF at 25°C, however, did not show this. A count of paths in six crystal sections placed less than 1 path in 100 of those not falling in [110] directions at azimuths between 1° and 9°. Most of the paths lay between 10° and 13° and a few appeared at greater azimuths, while on a statistical basis one would expect paths at all angles from 0° to 13°. The orientations observed in the overvoltage patterns, which are reproducible and which follow the same sequence in each of 8 branches, are also difficult to explain in terms of a statistical breakdown mechanism, but seem to reflect an underlying order.

FIG. 11. Metallic dendrites in LiF at 200°C.

It is hoped that further work may definitely establish the role of the star pattern in the breakdown process.

ACKNOWLEDGMENT

The author wishes to express his gratitude to Professor Arthur von Hippel for his interest and advice throughout the course of this work.

††† In discussion with the writer.

Letters to the Editor

PUBLICATION of brief reports of important discoveries in physics may be secured by addressing them to this department. The closing date for this department is five weeks prior to the date of issue. No proof will be sent to the authors. The Board of Editors does not hold itself responsible for the opinions expressed by the correspondents. Communications should not exceed 600 words in length.

Neutron Deficient Isotopes of Rhodium and Palladium

M. LINDNER AND I. PERLMAN
Radiation Laboratory and Department of Chemistry, University of California, Berkeley, California
April 5, 1948

AS a part of an investigation being carried out on the nuclear reactions resulting from the irradiation of antimony with high energy particles (200-Mev deuterons), it became of interest to examine the products some 20 mass units below the target nucleus, that is, around mass number 100. This region covers heavy isotopes of Mo and Tc, stable isotopes of Ru, and light isotopes of Rh and Pd. It was not possible to isolate chemically the rhodium fraction from the complex mixture of reaction products, but the palladium fraction could be purified in good yield. The decay curve was too complex to resolve accurately as it was proved to consist of at least six different palladium activities and a similar number of daughter activities growing in with a considerable spread of half-lives. By periodically isolating from the palladium the silver and rhodium daughters, a considerably better picture of the species present could be obtained. For example, silver fractions removed at intervals proved the presence of palladium β^--emitters as part of the following isobar pairs: 13-hr. Pd^{109}–40-sec. Ag^{109*}, 26-min. Pd^{111}–7.5-d. Ag^{111}, 21-hr. Pd^{112}–3.2-hr. Ag^{112}. In similar manner the presence of two new neutron deficient isotopes of palladium was deduced by removing rhodium daughters periodically. The rhodium so obtained could be resolved into half-life periods suggestive of two activities reported by Sullivan, Sleight, and Gladrow[1] as 21-hr. Rh^{100} and 5.9-day Rh^{101}. These activities were formed from palladium at rates corresponding to half-lives of ~4 days for the parent of Rh^{100} and ~10 hr. for the parent of Rh^{101}.

In order to better characterize these isotopes tentatively assigned to Pd^{101} and Pd^{100}, they were prepared in another manner. It was estimated that 50-Mev deuterons on rhodium (Rh^{103}) should promote $(d,4n)$ and $(d,5n)$ reactions in good yield and minimize the yield of Pd^{103} $(d,2n$ reaction). Furthermore Pd^{99} would probably have a half-life too short to interfere with the measurements and Pd^{98} could probably not be reached at this energy. The palladium β^--emitters could, of course, not be made by irradiating rhodium.

A thin rhodium metal foil was bombarded with 50-Mev deuterons in the 184-inch cyclotron, the rhodium was dissolved by $KHSO_4$ fusion, and the palladium fraction was removed by precipitating palladium dimethylglyoxime from slightly acid solution.

The palladium fraction proved to contain the activities that were sought, and the resolution into the components was accomplished by methods described below. The palladium contained three activities, of half-lives 9 hr., 4.0 days, and 17 days. Rhodium which was removed from the palladium showed a 4.3-day period which is the daughter of 9-hr. Pd and a 19.4-hr. Rh daughter of the 4.0-day Pd. The 57-min. Rh^{103*} daughter of 17-day Pd^{103} was not observed because of the low yield of Pd^{103} and the unfavorable conditions for detection. Since the rhodium isotopes are probably the same as those reported by Sullivan, Sleight, and Gladrow[1] from deuterons on ruthenium, and since the present measurements are not in disagreement with the isotopic assignments made by them, the decay chains may be summarized:

$$Pd^{101} \xrightarrow{9\text{ hr.}} Rh^{101} \xrightarrow{4.3\text{ day}} Ru^{101}$$

$$Pd^{100} \xrightarrow{4.0\text{ day}} Rh^{100} \xrightarrow{19.4\text{ hr.}} Ru^{100}.$$

9-hr. Pd^{101}.—From the ratio of x-rays to positrons it was estimated that this isotope decays ~90 percent by orbital electron capture and ~10 percent by positron emission. The positron energy was measured as 2.3 ± 0.2 Mev with a low resolution beta-ray spectrometer. No electrons or γ-rays were seen. The half-life as determined in three different ways gave values from 8 to 10 hours. The positron decay was measured directly using the spectrometer; the decay was determined indirectly by the rate of decrease in amount of 4.3-day Rh^{101} which grew into the palladium fraction, and the x-ray decay curve showed this component when corrected for the growth of 19.4-hr. Rh^{100}.

4.0-day Pd^{100}.—After the decay of 9-hr. Pd^{101}, the half-life for Pd^{100} was determined by removing the rhodium isotopes which had grown and, following the decay after the 19.4-hr. Rh^{100}, again came to equilibrium. Absorption data taken soon after rhodium removal showed no appreciable amount of electrons. In the electromagnetic radiation were found x-rays characteristic of the region, a hard gamma-ray of about 1.8 Mev (lead absorbers), and a soft gamma-ray of 90 kev (lead, aluminum, and silver absorbers). This isotope apparently decays entirely by orbital electron capture.

4.3-day Rh^{101}.—Rhodium removed from palladium contained only the 4.3-day Rh^{101} after the 19.4-hr. Rh^{100} had decayed. Using lead absorbers, a 0.35-Mev gamma-ray was detected, as were K x-rays characteristic of the rhodium region. Measurement with the spectrometer showed no positrons, but a line of electrons was observed which could have arisen from K-shell conversion of the 0.35-Mev gamma-ray. If so, the measured abundance of electrons indicated ~10 percent conversion.

19.4-hr. Rh^{100}.—This rhodium isotope could be removed from the palladium fraction which had been purified fol-

lowing the decay of 9-hr. Pd^{101}. Positrons of 3.0 Mev and conversion electrons of 0.6 Mev were determined with the spectrometer. Lead absorption curves taken on samples in which the electrons and positrons were taken out with beryllium showed characteristic x-rays and a 1.2-Mev γ-ray. In comparing the yield of positrons and x-rays, it was estimated that the decay proceeds $\sim$5 percent by positron branching and $\sim$95 percent by orbital electron capture. Gamma-rays corresponding to the 0.6-Mev electron as well as annihilation radiation were apparently in too low abundance to be seen readily.

Cross sections for the formation of the palladium isotopes from rhodium with 50-Mev deuterons could only be approximated principally because of uncertainties in the deuteron beam strength and in the target geometry with undeflected beam. Values are based on yields of x-rays and relative to each other are probably considerably more reliable than the absolute values.

Product	Reaction	$\sigma(cm^2 \times 10^{24})$
Pd^{103} (17 day)	$d,2n$	0.0024
Pd^{101} (9 hr.)	$d,4n$	0.24
Pd^{100} (4.0 day)	$d,5n$	0.28

The cooperation of Dr. Duane Sewell, Mr. J. T. Vale, and the 184-inch-cyclotron group is gratefully acknowledged.

This paper is based on work performed under Contract No. W-7405-eng-48 with the Atomic Energy Commission in connection with the Radiation Laboratory of the University of California, Berkeley, California.

[1] W. H. Sullivan, N. R. Sleight, and E. M. Gladrow, *Rhodium Radioisotopes Induced in Deuteron-Bombarded Ruthenium*, Declassified Plutonium Project Report No. MDDC-918.

Telluric Bands of Methane in the Fraunhofer Spectrum

ROBERT R. MCMATH, ORREN C. MOHLER, AND LEO GOLDBERG
McMath-Hulbert Observatory of the University of Michigan, Lake Angelus, Pontiac, Michigan
April 2, 1948

IN an earlier communication,[1] the writers described preliminary results obtained from a high resolution recording of the solar spectrum between 1 and 2μ. This initial investigation was carried out with a spectrometer consisting of a Cashman PbS cell employed in conjunction with a 15,000-line plane grating and 25-foot focal length lens arranged in Littrow fashion. Sunlight was imaged on the spectrometer slit by a 12-inch by 50-foot achromat mounted in the 70-foot McGregor tower of the McMath-Hulbert Observator.

Beginning in October, 1947, the lens optics were eliminated by the installation of a four-mirror Pfund-type spectrometer, employing a 15,000-line plane reflection grating loaned by the Mt. Wilson Observatory. The grating was specially ruled to produce a high concentration of energy in the green fourth-order spectrum. The over-all focal length of the spectrometer is 23½ feet. Also, the objective lens in the solar tower was replaced by a Cassegrain reflecting telescope of 10½-inch aperture and approximately 45-foot focal length. With this arrangement, the solar spectrum has been mapped with greatly improved resolution from 1 to 2.5μ. The spectrum was registered in the form of direct-intensity tracings by a Speedomax recorder, giving a dispersion of about 1.25 wave numbers per centimeter on the tracings. The slit width employed varied from 0.04 cm^{-1} at 1.6μ to 0.07 cm^{-1} at 2.2μ.

The new solar map contains not only a wealth of solar atomic lines but also numerous well resolved band structures originating in the earth's atmosphere. Of particular interest is a band system centered at 6003 cm^{-1}, or 1.6660μ, which appears to be due to absorption by atmospheric CH_4 molecules. This feature is clearly shown on many tracings, the first of which was obtained in August, 1947. The band consists of a zero branch in which 10 components are clearly shown, a positive branch made up of 11 components, and a negative branch showing 8 members. A tracing of the central Q-branch, together with the first two members of the P- and R-branches, is shown at the bottom of Fig. 1.

The 1.66μ band of methane has been investigated in the laboratory by Moorhead[2] and by Norris and Unger,[3] with relatively low resolution. On the laboratory tracings the zero branch is unresolved and, according to Norris and Unger, appears sharp and intense, with a slight broadening on the low frequency side. The observed broadening suggests that the line spacings in the Q-branch increase toward the low frequency end of the band, which is confirmed by the Lake Angelus tracings. The line spacing in the P- and

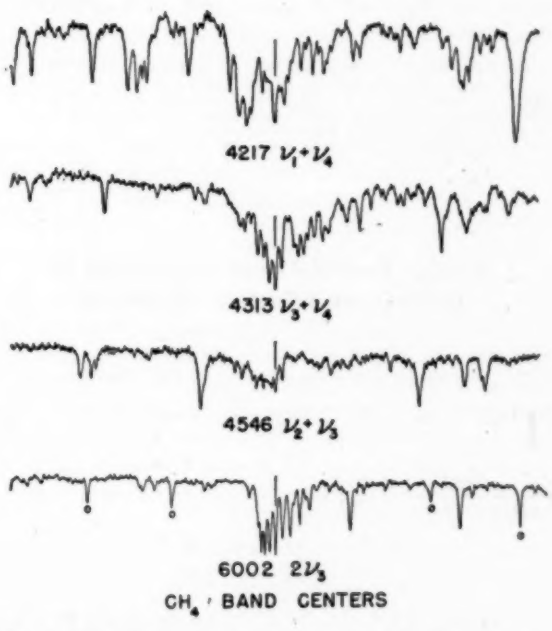

FIG. 1. Band centers of the CH_4 molecule in the absorption spectrum of the earth's atmosphere. The central vertical lines correspond to the listed wave numbers. The small circles in the lower tracing mark the 0–1, 1–2, 2–1, and 3–2 lines of the $2\nu_3$ band.

R-branches increases regularly with decreasing frequency, the extreme limits being 9.6 and 11.8 cm^{-1}; but the average value, 10.6 cm^{-1}, agrees exactly with that found in the laboratory. Of further interest is the absence of the first member of the P-branch, which is also missing from the laboratory spectrum.

The only important source of disagreement between the laboratory and solar observations lies in the wave numbers of the band components, which are systematically 3 cm^{-1} lower than those given by the laboratory measurements. In view of the much higher resolution obtained with the solar spectrometer, the discrepancy is perhaps to be expected. Infra-red wave-lengths at Lake Angelus are determined, by use of overlapping orders, with respect to visual Fraunhofer lines whose wave-lengths are known with high precision. In this way, the wave-lengths of infra-red lines can be determined with an error appreciably less than 0.1 cm^{-1}.

As a check on the identification of the 1.66μ band, a search was made for additional zero branches of the methane spectrum observed in the laboratory[4] at 4216, 4313, and 4546 cm^{-1}. Three prominent features were found close to the expected positions, as shown in Fig. 1.

Very recently, Migeotte[5] has observed 14 regularly spaced and intense lines in the 3.4μ region, which he ascribes to atmospheric methane. The spectroscopic evidence for the existence of methane in the earth's atmosphere therefore seems conclusive.

A preliminary analysis of the 1.66μ band indicates a high order of agreement with the theory of the CH_4 molecule as developed by D. M. Dennison and others.[6] The details of the analysis will be published in the Astrophysical Journal. We wish to acknowledge the helpful advice of Professors E. F. Barker and D. M. Dennison of the University of Michigan.

[1] McMath, Adel, Goldberg, Mohler, Phys. Rev. **72**, 644 (1947).
[2] J. G. Moorhead, Phys. Rev. **39**, 83 (1932).
[3] W. V. Norris and H. J. Unger, Phys. Rev. **43**, 467 (1933).
[4] Cf. Herzberg, *Infrared and Raman Spectra*, p. 308.
[5] M. V. Migeotte, Phys. Rev. **73**, 519 (1948).
[6] D. M. Dennison, Rev. Mod. Phys. **12**, 175 (1940).

Errata: Second-Order Corrections to Quadrupole Effects in Molecules

[Phys. Rev. **73**, 627 (1948)]

J. BARDEEN AND C. H. TOWNES
Bell Telephone Laboratories, Murray Hill, New Jersey

THE right-hand side of Eq. (1) should read:

$$\left(\frac{3eqQK}{8I(2I-1)J(J+2)}\right)^2\left(1-\frac{K^2}{(J+1)^2}\right)$$
$$\times\frac{(F(F+1)-I(I+1)-J(J+2))^2}{(2J+1)(2J+3)}$$
$$\times(I+J+F+2)(J+F-I+1)(I+F-J)(J+I-F+1).$$

The second line on the right of Eq. (2) should read:

$$[1-(K^2/(J+2)^2)][1/(2J+1)(2J+5)].$$

A Possible Influence of the Moon on Recurrent Geomagnetic Activity

OLIVER R. WULF AND SETH B. NICHOLSON
U. S. Weather Bureau and Mount Wilson Observatory, California
March 24, 1948

THE tendency for magnetic activity to recur at 27-day intervals has suggested the rotation of the sun as the cause and has led to extensive studies to discover what solar features may be associated with the terrestrial magnetic activity. Recently we have given evidence[1] for a connection between the appearance of patches of bright flocculi at the east limb of the sun and the relatively abrupt recurrent onsets of terrestrial magnetic activity in 1943–44. We now wish to call attention to a correspondence between certain recurrent magnetic activity and the moon's declination.

Such 27-day recurrent magnetic activity is not always conspicuous. It can be readily seen in several series from 1930 to 1933, which are portrayed in Fig. 5 of reference 1.[2] The first series shown there began with the abrupt onset of February 12, 1930. The ten onsets in this series (designated by +'s) came within two days after the dates of maximum northerly declination of the moon.

In the second series, which began on April 19, 1930, the eight onsets (designated by ●'s) came within one day of maximum southerly declination of the moon.

In the third series, beginning on November 24, 1930, the eight onsets (designated by diamonds in Fig. 5—1) came within one day of maximum southerly declination.

In the fourth series (designated by X's), beginning on June 26, 1931, the onsets came three and then four days before the moon's maximum southerly declination. Directly following, there is a series, not designated in Fig. 5—1 but readily seen, with onsets on November 13 and December 10, 1931, January 7, February 3, March 2, March 28, April 22, and May 21, 1932, all of which occurred within two days of the dates of maximum southerly declination of the moon. Early in the long fifth series, designated by triangles and beginning with November 4, 1931, the onsets came four days after maximum northerly declination of the moon, but the lag decreased as the series progressed until at the end it was only one day.

The onsets of the three conspicuous mounds of activity in 1933 designated by squares in Fig. 5—1 occurred on the dates of maximum southerly declination of the moon.

In 1943–44 the onsets of the main series of mounds of activity, shown in Fig. 1 of reference 1, generally came near maximum northerly declination of the moon while those of the other series came near maximum southerly declination. The onsets in the main series lagged behind maximum northerly declination in the middle of the series by four or five days, but later by as little as one day.

In a well defined series which began about January 29, 1923, seven consecutive onsets all came two days or less before the dates of the moon's maximum northerly declination.

Other series can be found throughout the years in which the onsets do not come near the dates of maximum declination of the moon but they appear to be less prominent

than those that do. There are also years in which the whole tendency toward a few well marked series is not pronounced. In the years 1930-33, when 27-day recurrent series were conspicuous, the moon's maxima in declination were near 28°, the maximum in the 19-year cycle.

The intervals in the above series approximate 27 days more closely than they do the intervals between the maxima of lunar declination.

The above correspondences do not suggest that solar effects are unimportant in magnetic activity but only that the moon may be a factor in determining when such conspicuous 27-day series occur.

If this latter be true, the mechanism may be related to the fact that the tidal air mounds, which are constantly being raised under the moon as the earth rotates on its axis and as the atmosphere circulates over the earth's surface,[3] have their greatest asymmetry with respect to the equator when the declination of the moon is a maximum.

[1] O. R. Wulf and S. B. Nicholson, Pub. A.S.P. **60**, 37 (1948).
[2] Hereafter referred to as Fig. 5–1.
[3] O. R. Wulf, J. Terr. Mag. **50**, 185 (1945); O. R. Wulf and S. B. Nicholson, *ibid* **52**, 175 (1947).

Decay of Negative Mesons in Light Elements

A. MARCH
Institute for Theoretical Physics, University of Innsbruck, Innsbruck, Austria
April 2, 1948

ACCORDING to investigations of Conversi, Pancini, and Piccioni,[1] decay electrons are observed when negative mesons are stopped in carbon. This is in sharp contradiction to all expectations. For according to the theory one should think that when a meson, after having been sufficiently slowed down, is captured by an atom, it would be absorbed by a nucleus in a time of the order of magnitude 10^{-13} sec. after it has reached the K-orbit, whereas the decay requires about 10^{-6} sec. Thus theory and experiment differ by a factor 10^{-12}. Sigurgeirsson and Yamakawa[2] obtained the same result for other light elements; they found that the probability of capture increases gradually with increasing atomic number and reaches the value for the probability of radioactive decay in the neighborhood of $Z_0 \sim 10$.

A discrepancy between theory and experiment by a factor 10^{12} creates for the current nuclear theories a very serious situation. Unless we are prepared to admit that all we believe we know about mesons and nuclear processes is thoroughly wrong, the only possible explanation of the discrepancy we can think of is that the conventional theories neglect a fundamental constant by which the use of the quantum-mechanical concepts is limited. And indeed there is a very simple explanation of the effect if one adopts the idea of a fundamental length, l_0, of the order of magnitude 10^{-13} cm, the introduction of which into the theory I recently suggested.[3] The idea of l_0 is founded on the thesis that it is in principle impossible to distinguish in space by any experiment two particles at rest the separation of which is $<l_0$. The particles are then "coincident." According to this assumption the most accurate localization that can be made for an elementary particle consists in referring it to a particle with which it it in coincidence. This limitation of accuracy makes it necessary to interpret the wave function $\varphi(xyz)$ of a particle in a way that corresponds to the possibilities of observation: $\varphi(xyz)$ defines no longer the probability of finding the particle at the point xyz—that would be meaningless—but that for finding it in coincidence with a reference particle to which the position xyz is attributed (so that the coordinate x may have any value between $x-l_0$ and $x+l_0$). Accordingly, the interpretation of all interaction terms that occur in the theory has to be altered The problem we are dealing with here depends on the interaction of a meson (wave function φ) with a proton (wave function ψ) For a pseudoscalar meson this interaction is given (apart from an irrelevant factor) by $\int(\psi^*\sigma\psi)\,\mathrm{grad}\varphi$. We will denote the proton of the nucleus which represents the center of the K-orbit with P_0; we do not know its exact position but this is of no consequence because we use P_0 only as a reference particle; therefore we may attribute to P_0 the position $r=0$. Let us now consider what it means if we put $(\psi^*\sigma\psi)=\sigma\cdot\delta(\nu)$($\delta(\nu)$=Dirac's function). The ordinary theory would interpret the equation as description of the proton P_0. According to our theory, however, the equation does not mean P_0 but any proton which coincides with P_0. This follows immediately from our interpretation of the wave function ψ. Now with $(\psi^*\sigma\psi)=\delta(\nu)$ the interaction becomes $\int(\psi^*\sigma\psi)\,\mathrm{grad}\varphi=\sigma(\mathrm{grad}\varphi)_0$, the index 0 meaning that grad φ is to be taken on the point $r=0$. In the former theory the expression would determine the probability for the absorption of the meson by the proton P_0. In the theory, however, which takes regard of the length l_0 the expression means the probability that the meson is absorbed by any proton which is in coincidence with P_0.

Now the φ-function of the K-orbit depends only on r so that on the point $r=0$ the vector grad φ has the same strength in all directions; therefore $\sigma(\mathrm{grad}\varphi)_0=0$. This means that a nucleus consisting only of protons which are all in coincidence with one another is not able to absorb a pseudoscalar meson. An absorption $\neq 0$ can only take place if the protons of the nucleus do not build up a spatially indissoluble unit. The protons which coincide with P_0 lie within a sphere of the radius l_0. Because of their own extension the radius R of the nucleus which is unfit to absorb a meson becomes so $3l_0/2$. R is in dependence on the atomic weight A approximately given by $R=(l_0/2)^3(A)^{\frac{1}{3}}$. $R=3l_0/2$ corresponds, therefore, to $A=27$, $Z_0\sim 13$. But it is to be expected that the critical value of Z_0 will be somewhat smaller as the nuclei must not be supposed to be exactly spherical.

It should be noted, however, that for a longitudinal vector meson the interaction is not determined by $(\mathrm{grad}\,\varphi)_0$ but by $(\mathrm{div}\,\pi)_0$, which is $\neq 0$. For vector mesons a restriction of their absorption should therefore not exist.

[1] M. Conversi, E. Pancini, and O. Piccioni, Phys. Rev. **71**, 209 (1947).
[2] T. Sigurgeirsson and A. Yamakawa, Phys. Rev. **71**, 319 (1947).
[3] A. March, Acta Phys. Austr. **1**, 19, 137 (1947).

The Relative Abundances of the Zinc and Cadmium Isotopes

WALLACE T. LELAND AND ALFRED O. NIER
Department of Physics, University of Minnesota, Minneapolis, Minnesota
April 2, 1948

TWELVE years ago one of us[1] reported values for the relative abundances of the zinc and cadmium isotopes. Since that time numerous improvements have been made in mass spectrometry. Thus, in view of the present-day interest in more accurate nuclear constants it appeared worth while to repeat some of the early work. In the new work we employed a 60° mass spectrometer similar to one already described.[2] Compounds having a negligible vapor pressure at ordinary temperatures could be volatilized by a small oven built into the ion source.

In the investigation of zinc, ZnI_2 was employed and measurements were made for the ZnI_2^+, ZnI^+, and Zn^+ ions. Although the fractional spread in masses varied from approximately 2 percent for ZnI_2^+ ions to 10 percent for Zn^+ ions, no systematic differences in the abundance ratios in the three positions could be observed, so it could be concluded that any discriminatory effects in the instrument were negligible. Table I shows the results obtained.

TABLE I. Isotopes of zinc.

	Mass number				
% Abundance	64	66	67	68	70
Present work	48.89	27.81	4.07	18.61	0.620
Earlier work*	50.9	27.3	3.9	17.4	0.5

* See reference 1.

The numbers given are the averages for the ZnI_2^+, ZnI^+, and Zn^+ spectra, each weighted equally. The calibrations and consistency of the results lead us to believe that the abundance ratio of any pair of isotopes is accurate to within one percent. With a packing fraction of -7.0 and a conversion factor of 1.000275 in going from the atomic to the chemical scale a chemical atomic weight of 65.40 is computed. This is to be compared with the chemical value 65.38.

In cadmium, ions CdI_2^+, CdI^+, and Cd^+ were investigated. Table II gives the results. As in zinc the numbers

TABLE II. Isotopes of cadmium.

	Mass number							
% Abundance	106	108	110	111	112	113	114	116
Present work	1.215	0.875	12.39	12.75	24.07	12.26	28.86	7.58
Earlier work*	1.4	1.0	12.8	13.0	24.2	12.3	28.0	7.3

* See reference 1.

given are the averages found for the three types of ions. Here, too, we believe any discriminatory effects to be sufficiently small to state that the abundance ratio of any pair of isotopes is accurate within one percent. A packing fraction of -6.0 yields a chemical atomic weight of 112.42, which is to be compared with the chemically determined value 112.41.

These data indicate that the mass spectrometer as employed in the early work must have discriminated against ions of different mass sufficiently to give an error as large as 20 percent in the abundance ratio of the most widely separated isotopes of zinc and cadmium. That an error should have existed is perhaps not surprising since the primary purpose in the earlier work was to obtain very high resolution so that rare isotopes could be detected. Thus extremely narrow slits were employed. As we now know, these conditions can lead to abnormal discrimination.

The instrument used in this work was built with a grant from the Graduate School. This research was supported by Navy Contract N5ori-147, T. O. III, between the Office of Naval Research and the University of Minnesota. Material assistance was also given by the University of Minnesota Technical Research Fund.

[1] A. O. Nier, Phys. Rev. **50**, 1041 (1936).
[2] A. O. Nier, Rev. Sci. Inst. **18**, 398 (1947).

The Isotopic Composition of Xenon

A. H. W. ATEN, JR.
Institute for Nuclear Research, Amsterdam, Holland
April 6, 1948

WEFELMEIER, in a paper on the exceptional relations between the nuclei of samarium,[1] pointed out that the proportion in which the isotopes of xenon occur is abnormal, too. He suggested that this irregularity should be explained by a transition of four xenon isotopes to tellurium either during or shortly after the formation of our present atomic nuclei. However, we are now in a position to understand that the peculiar situation in xenon has a much more trivial cause.

It is a well-known fact that nuclei with even atomic weight are found in nature in larger concentrations than nuclei with odd atomic weight, because of the difference in binding energy between these two types of nuclei. Thus, if in one element three isotopes occur with consecutive mass numbers—two even ones and one odd one—the concentration of the odd one is always less than the sum of the concentrations of the even ones. The only exception—and a very striking one—is xenon, where Xe^{129} is more than four times as frequent as its two neighboring isotopes together. In this element the percentages of the isotopes have been observed as follows:[2] Xe^{124}:0.094 percent; Xe^{126}:0.088 percent; Xe^{128}:1.90 percent; Xe^{129}: 26.23 percent; Xe^{130}:4.07 percent; Xe^{131}:21.17 percent; Xe^{132}:26.96 percent; Xe^{134}:10.54 percent; Xe^{136}:8.95 percent. It is evident from these figures that everything would be normal if the concentration of Xe^{129} were about ten times smaller.

It has repeatedly been pointed out that by far the larger part of the noble gases, which originally accompanied the material of the earth, have been lost from our atmosphere, probably during the earliest part of its history.[3] This theory explains the insignificant quantities of the other noble gases compared with argon. At present this element consists almost entirely of A^{40}, the isotope which was formed by K-capture in K^{40} after most of the original noble gases had disappeared.[4]

Recently Katcoff[5] has shown that I^{129} has an exceedingly long half-life, at least of the order of 10^7 years, unless its beta-rays should be too weak to be detected. Originally, according to a general rule[6] it must have been about as frequent as the stable isotope I^{127}. If the half-life of I^{129} is as long as about 2.10^8 years, demonstrable traces of this isotope must still exist. Indications, though no definite proof, of this fact were indeed obtained by Katcoff.

After the concentration of the original xenon in our atmosphere had fallen to its present low value, the Xe^{129} formed by beta-emission from the I^{129}—which at that time had a much higher concentration—in the iodine of the earth's outer crust and of the ocean, mixed with the small rest of the original xenon. This was sufficient to give to this single isotope its abnormally high concentration.

[1] W. Wefelmeier, Ann. d. Physik **36**, 373 (1939).
[2] A. O. Nier, Phys. Rev. **52**, 933 (1937); M. Lounsbury, S. Epstein, and H. G. Thode, Can. J. Research (in press).
[3] H. N. Russel and D. M. Menzel, Proc. Nat. Acad. Sci. **19**, 997 (1933); V. M. Goldschmidt, Geochem. Verteilungsgesetze 9. Skr. Norsk Vid. Ak. Oslo. Mat-Nat. No. 4, 18 (1937).
[4] C. F. Weizsäcker, Physik. Zeits. **38**, 623 (1937); A. Bramley, Science **86**, 424 (1937).
[5] S. Katcoff, Phys. Rev. **71**, 826 (1947).
[6] J. Mattauch and S. Flügge, *Nuclear Science Tables* (Interscience Publishers, Inc., New York), p. 104.

On the Use of the Kurie Plot

F. N. D. KURIE
Department of Physics, Washington University, St. Louis, Missouri*
March 29, 1948

THERE have been a number of examples in recent literature where, in the mind of this author, the Kurie plot has been somewhat overzealously applied. The method was originally suggested by Kurie, Richardson, and Paxton[1] as a method of examining experimental data for their compliance with either the Fermi or the Konopinski-Uhlenbeck theory of β-decay. In applying the method to data, which we now know to be poor, they found a number of cases (Cl^{38}, K^{42}) in which deviations between theory and experiment were very wide. They showed that, by assuming that these substances emitted two groups of β-particles, a closer consonance between theory and data was obtained.

Because of the continuous distribution of the energy of β-particles there is no straightforward experimental method of ascertaining whether a β-spectrum represents a single β-transition or several. Because of this the Kurie plot has been widely used to aid in this examination. If it were clearly established that a simple spectrum was represented in detail by the Fermi theory, this method of plotting would be a very powerful tool, because, in principle, it is capable of disentangling a complex spectrum to give the upper limits and intensities of all its components. However, at the present stage, the application of the Kurie plot for this purpose is always suspect, since there is no case where the plot is linear down to low energies. Konopinski[2] has given a good summary of the existing data and has pointed out that in the particularly careful work of Lawson and Cork on In^{114} and of Tyler on Cu^{64} there are deviations from the linear Kurie plot below energies corresponding to between $\frac{1}{3}$ and $\frac{1}{2}$ of the maximum energy. Thus, even in the most painstaking work and for allowed transitions, agreement between theory and experiment seems to be good only near the upper limit of the β-spectrum. There appears to be no case in which even so optimistic a statement can be made for forbidden spectra.

It is not proposed that the Kurie plot method be abandoned, for there is no other method available for examining a spectrum for complexity. Rather, it is proposed that an argument based on such plots *alone* is not sufficient to establish complexity, and that upper limit values of the lower energy β-particles, derived from such an analysis, should be accepted with some scepticism.

On the other hand, if the Kurie plot gives evidence of complexity, and if there is demonstrated the existence of gamma-rays of energies nearly equaling the differences of these upper limits, and if coincidence counting gives data consistent with the implied complexity, then there is strong evidence in favor of the disintegration scheme proposed.

* Under Contract N6ori-117, T.O.1.
[1] F. N. D. Kurie, J. R. Richardson, and H. C. Paxton, Phys. Rev. **49**, 368 (1936).
[2] E. J. Konopinski, Rev. Mod. Phys. **15**, 209 (1943).

Achromatization of Debye-Scherrer Lines*

H. EKSTEIN AND S. SIEGEL
Armour Research Foundation, Chicago, Illinois
April 2, 1948

THE ultimate limit of precision in lattice parameter measurements by the Debye-Scherrer method is given by the spectral width of the primary characteristic radiation, which causes an irreducible width of the line even with an infinitely narrow collimator.** The line could be sharpened by monochromatization of the primary beam, but the elimination of all but a small fraction of the spectral band of a characteristic line would result in a prohibitive loss of intensity.

One can sharpen the diffraction line by achromatizing the characteristic radiation, i.e., by causing all rays of wave-lengths belonging to a spectral line to converge to a focus after diffraction. In Fig. 1 a point source of x-rays, A, radiates a polychromatic beam toward the crystal $QTUR$ so that the central ray AC satisfies the Bragg condition for diffraction by the lattice plane dd' and for the most intense wave-length λ of the spectral band. After diffraction the rays diverge from an apparent source A' so that every ray has only one definite wave-length. A polycrystalline sample P is mounted normal to the central ray $A'E$. All rays diffracted by P will come to a focus N. The distance $CE=V$ is given by

$$V=F\left(1+2\frac{\tan\theta}{\tan\theta_m}\right)\left(-\frac{1}{\cos 2\theta}\right)+l\frac{\cos(\theta_m+\alpha)}{\cos(\theta_m-\alpha)},$$

where $F=NE$, $l=AC$, $\theta_m=\measuredangle ACd$, θ is the Bragg angle

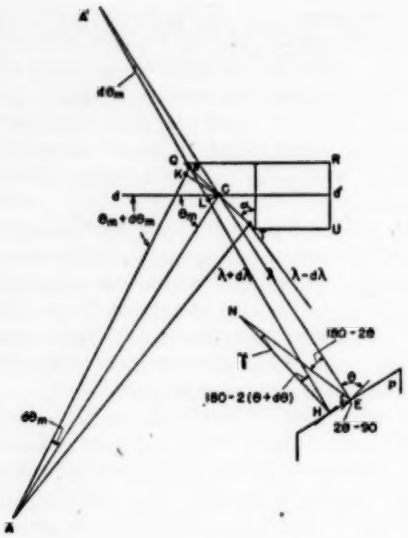

FIG. 1. Principle of the achromatization method.

of the sample P for the wave-length λ, and α is the angle between the normal to the lattice plane and the ground surface QT of the crystal. If an x-ray source of finite width S is substituted for the point source A, then the width of the achromatized image near N is

$$S' = S\cos 2\theta \frac{\cos(\theta_m+\alpha)}{\cos(\theta_m-\alpha)}.$$

By proper choice of θ_m and α, the image can be made much narrower than the source.

FIG. 2. Photograph of achromatized CoK_{α}- doublet. Annealed steel, 310 reflection. $\alpha = 90$, $\theta_m = 72.°2$, $F = 7.92$ cm.

The relative difference $|\Delta d/d|_R$ of two lattice parameters of the sample giving rise to two lines which are just resolved in the Rayleigh sense is

$$\left|\frac{\Delta d}{d}\right|_R = \frac{1.22S}{2F}\cot\theta\frac{\cos(\theta_m+\alpha)}{\cos(\theta_m-\alpha)},$$

whereas for the Debye-Scherrer method with an infinitely narrow collimator

$$\left|\frac{\Delta d}{d}\right|_R = \frac{1.22w}{\lambda} \approx 5\times 10^{-4},$$

where w is the spectral width of the characteristic line. Thus, it should be possible to increase the resolution by an order of magnitude beyond the ultimate limit inherent in the conventional method.

Figure 2 illustrates the achromatization principle for a case where the two components of a $K\alpha$-doublet are brought to an approximate focus at N. Our ultimate aim, however, is to achromatize a single α_1 line, using a fine focus tube now under construction.

The authors wish to thank Dr. A. Guinier for an inspiring discussion.

* Supported by the National Advisory Committee for Aeronautics, Washington, D. C.

** H. Ekstein and S. Siegel, National Advisory Committee for Aeronautics, Tech. Note No. 1375 (October 1947).

A New Isomer of Element 43 (Tc) of Very Small Excitation Energy

O. HUBER, P. MARMIER, H. MEDICUS, P. PREISWERK, AND R. STEFFEN
Swiss Federal Institute of Technology, Zurich, Switzerland
March 29, 1948

AMONG the numerous isotopes of element 43 (technetium) which can be produced by (p,n) reactions from those of Mo, there is one with a half-life of 53 minutes. It decays by positron emission [$E_{max} = (2.45\pm0.03)$ Mev] and by orbital electron capture,[1] and emits nuclear γ-rays of (0.380 ± 0.004) Mev, (0.873 ± 0.004) Mev, (1.48 ± 0.01) Mev, (1.85 ± 0.01) Mev, and (2.74 ± 0.01) Mev. It has presumably a mass number of 92 or 94. We have observed electron lines of (13.0 ± 0.8) kev, (31.5 ± 0.5) kev, and (33.0 ± 0.4) kev in a magnetic semicircular spectrometer, the intensities of which decrease with same half-life as the positron intensity. The differences between the energies of these electron lines indicate that they arise from K, L, and M conversions in Tc. Hence the excitation energy amounts to (33.4 ± 0.4) kev. In order to check that these electron lines are not due to transitions of the excited residual Mo nucleus but arise from an isomeric state of Tc, we have investigated the x-rays associated with the conversion. Photographs taken with a crystal spectrograph of the Cauchois type showed the $K\alpha_1$, $K\alpha_2$, and $K\beta_1$ lines of both Tc and Mo, those caused by Mo being weaker. The x-ray decay period was likewise about one hour. The Mo lines obviously originate from K-capture. Since besides the above-mentioned low energy conversion

lines no intense converted radiation is observed, the presence of the Tc x-radiation proves that the 33.4-kev transition is an isomeric one of the Tc nucleus. The half-life (53 minutes) is in good agreement with the value derived from a semi-empirical energy-lifetime relation[2] for 33.4 kev and an angular momentum change $\Delta L = 4$.

We hope to succeed in determining, by means of an isomer separation, the shorter lifetime, caused by the ground state of Tc, from which the positron emission and electron capture result.

A more extensive report on these measurements will appear in Helv. Phys. Acta.

[1] P. C. Gugelot, O. Huber, H. Medicus, P. Preiswerk, and R. Steffen, Helv. Phys. Acta 20, 240 (1947).
[2] M. L. Wiedenbeck, Phys. Rev. 69, 567 (1946).

On the Radioactivity of K^{40}

HANS E. SUESS
Institute of Physical Chemistry, University of Hamburg, Hamburg, Germany
February 25, 1948

SEVERAL recent papers in this journal[1-3] have dealt with the decay of K^{40} by following Bleuler and Gabriel[4] in assuming $(7\pm1)\times10^8$ years for the beta-decay period, $(2.4\pm0.5)\times10^8$ years for the total period, and a branching ratio corresponding to 1.9 capture processes per beta-decay. It should be pointed out that the interpretation Bleuler and Gabriel gave of their experimental observations does not agree with the following:

A branching ratio of 1.9 would mean a yield of argon sufficiently large to make it easily detectable in old rocks and gaseous exhalations.[5,6] No excessive abundance of argon, however, has yet been reported in such cases. A careful investigation of two samples of sylvine and one of carnallite has been carried out recently[7] in order to reach a final conclusion on this question. From the data of Bleuler and Gabriel a content of at least 1.5×10^{-2} cm³ argon per gram sylvine, was to be anticipated, as the sylvine's age exceeded 2×10^8 years. Analysis of the gases collected from the samples, however, gave an upper limit of 0.02×10^{-2} cm³ argon. The carnallite analysis gave a similar result. These results indicate that only a few percent of the decaying K^{40} can yield A^{40}. This, as well as geochemical evidence as a whole, makes it seem most unlikely that more than 10 percent of the decaying K^{40} is converted into argon.

From the general systematics of the abundance of nuclei in the universe[8] it is possible to estimate the concentration of K^{40} at the time of its formation. It can in that way be estimated that the K^{40} content of potassium hardly exceeds the Lu^{176} content of lutetium, which is 2.5 percent. The age of the elements is certainly greater than 33×10^8 years, the figure given by Holmes[9,10] for the age of the earth. A total period of 2.4×10^8 years leads to an improbable value of more than 60 percent K^{40} in potassium at the time specified. A total period of 7×10^8 years, however, leads to 1 percent K^{40} in potassium 45×10^8 years ago; both these values do not seem far wrong for the original concentration of K^{40} and the age of the elements, respectively.

By considering the fact that the large concentration of A^{40} in the atmosphere has undoubtedly originated from K^{40}, we find from the present amount of atmospheric argon[11] and the present amount of K^{40} in the earth[12] and assuming a total period of 7×10^8 years, that approximately 0.5 percent of the total amount of the decay products produced during the last 33×10^8 years is now present in the atmosphere in the form of argon. The major part of A^{40} is probably left occluded in the earth's interior; yet the proportion of atmospheric to occluded argon is not necessarily as small as assumed previously[6,13] because a large part of the earth's surface was probably in a molten liquid state during the long period extending from 33×10^8 until 20×10^8 years ago. We can thus take 0.5 percent as a lower limit for the branching ratio for the decay of K^{40}.

The conclusion from geochemical evidence, that more than 0.5 percent and less than 10 percent of the decaying K^{40} is converted into A^{40}, seems to make it most probable that, as in the case of Lu^{176},[15] the full number of capture processes is accompanied by the emission of hard gamma-quanta known to be emitted by excited A^{40} nuclei[1,14]. The hard quanta are emitted at a rate of 3 quanta according to Gray and Tarrant,[16] or at a rate of 7 ± 1.5 quanta according to Gleditsch and Gráf,[3] per 100 beta-rays. Geochemical evidence seems to make the lower value appear slightly more probable. A value of 5 ± 2 percent for the branching ratio might be considered to be within the limits of error if all the data concerned.

The suggested scheme (Fig. 1) makes it necessary to regard the soft radiation with an approximate intensity

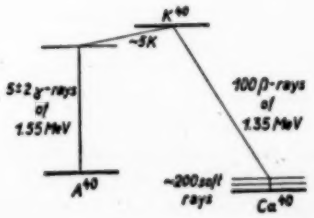

FIG. 1. Disintegration scheme of K^{40}. Total half-life period 7×10^8 year.

of 2 quanta per beta-ray[4,5] as connected with the beta-process. Haxel and Houtermans[17] have recently observed a soft radiation of similar quality from Rb^{87} coinciding with the beta-emission. It seems reasonable to assume a similar process to occur in the beta-process of K^{40}.

[1] H. A. Meyer, G. Schwachheim, and M. D. de Souza Santos, Phys. Rev. 71, 908 (1947).
[2] E. Gleditsch and T. Gráf, Phys. Rev. 72, 640 (1947).
[3] E. Gleditsch and T. Gráf, Phys. Rev. 72, 641 (1947).
[4] E. Bleuler and M. Gabriel, Helv. Phys. Acta 20, 67 (1947).
[5] F. C. Thompson and S. Rowlands, Nature 152, 103 (1943).
[6] F. G. Houtermans and P. Jordan, Zeits. Naturforsch. 1, 125 (1946).
[7] P. Harteck and H. Suess, Naturwiss. 34 (1947).
[8] H. E. Suess, Zeits. Naturforsch. 2a, 322 (1947).
[9] A. Holmes, Nature 157, 680 (1946).
[10] F. G. Houtermans, Zeits. Naturforsch. 2a, 322 (1947).
[11] F. Paneth, Nature 139, 180 (1937).
[12] V. M. Goldschmidt, Videnskapsakad. Oslo (1938).
[13] C. v. Weizsäcker, Physik. Zeits. 38, 623 (1937).
[14] H. Wäffler and O. Hirzel, Helv. Phys. Acta 19, 216 (1946).
[15] A. Flammersfeld, Zeits. Naturforsch. 2a, 86 (1947).
[16] L. H. Gray and G. T. P. Tarrant, Proc. Roy. Soc. A143, 681 (1934).
[17] O. Haxel and F. G. Houtermans, lecture held at the meeting of the German Physical Society at Göttingen, September, 1947.

Inorganic Crystals for the Detection of High Energy Particles and Quanta

ROBERT J. MOON
Institute of Radiobiology and Biophysics, The University of Chicago, Chicago, Illinois
March 29, 1948

THIS investigation was suggested by the interesting experiments reported by H. Kallmann[1] on the counting of high energy particles and quanta by the photoelectric detection of individual light flashes. Selected 1P28 and 1P21 photo-multiplier tubes were employed for the detection of the scintillations, and a variety of crystals were employed for the scintillating material. A 10,000-ohm resistor was used in the anode circuit of the photo-multiplier tube in which pulse voltages up to 50 millivolts were developed and were further amplified and fed into a scale of 128. Pulses from the photo-multiplier which were less than 1 millivolt were not counted by the scaler. This level corresponded to approximately 10 photoelectrons, or with an estimated geometry of 10 percent and a photocathode yield of one photoelectron per fifty quanta it would correspond to approximately five thousand quanta liberated in the crystal. The pulses reached their maximum value in about one-half microsecond, and the duration of the pulse was approximately one microsecond although the capacity of the cable from output of the photo-multiplier to input of the amplifier contributed to the lengthening of the pulse.

As is usually done, spurious pulses which originate in the photo-multiplier tube were practically eliminated by tube selection and by cooling the tube with solid CO_2. In addition, other spurious pulses originated in the crystals. For example: CaF_2 (clear crystals both artificial and natural) produced scintillations in the absence of radiation. After exposing these crystals to ultraviolet light they showed visible phosphorescence and the next day were producing some two hundred pulses per second. Upon cooling with solid CO_2 this was reduced to less than twenty pulses per second. Similarly, such exposed crystals showed thermal luminescence upon heating to 100°C, which died away upon prolonged heating. After cooling to room temperature in the dark, these crystals were no longer sources of spurious pulses. After all precautions had been taken to reduce background effects, the counting rate became one count per second, mainly because of cosmic rays.

TABLE I.

I. Excellent response	II. Fair response
$CaWO_4$ (Scheelite)	$PbCO_3$ (cerusite)
CaF_2 (synthetic and natural fluorite)	Phenatite
$LiAlSi_2O_6$ (Spodumene)	Apatite (pale yellow)
Al_2O_3 (synthetic sapphire)	$CaB_2Si_2O_8$ (danburite)
LiF (synthetic)	
III. Medium response	IV. Weak response
$MgSO_4KCl3H_2O$ (Kainite)	$SrSO_4$ (celestite)
Topaz	Tourmaline (pink)
$Be_3Al_2Si_6O_{18}$ (beryl)	$CaSo_42H_2O$ (gypsum)
$CaCO_3$ (calcite)	$CaBSiO_4(OH)$ (datolite)
Sulfur	Maple syrup sugar crystal
	Halite (NaCl)
	NaCl (artificial)
V. No response	
SiO_2 (clear quartz)	$KAlSi_2O_8$ (orthoclase)
$CoCO_3$ (aragonite)	$KMg_3Al_2Si_3O_{10}(OH)_2$ (phologopite)
Al_2O_3+Cr (artificial ruby)	$KAl_3Si_3O_{10}(OH)_2$ (muscovite)
	KCl (artificial)

Many inorganic crystals were tried. Calcium tungstate (Scheelite) was by far the best. Its high density of six grams per cubic centimeter, high atomic weight components, and excellent fluorescent properties with minor phosphorescence make it well suited for the detection of beta- and gamma-radiation. Table I lists the various materials investigated.

It may be noted that the variety of elements as well as the nature of the crystal affords many possibilities for radiation detectors. For example, Al_2O_3 (synthetic sapphire), with a hardness next to diamond, could serve both as a durable window to a photo-multiplier tube and as the scintillating material. Such a tube would probably be most useful in a linear form. Crystals which contain boron would be useful detectors for neutrons.

Naphthalene and $CaWO_4$ were compared. A clear naphthalene crystal, 9 g in weight, 4.5 cm long, and having a polished face 11 mm×16 mm yielded less than one-third the number of pulses per second as a 9.3-g $CaWO_4$ crystal with a 7-mm×10-mm polished face, whereas an 8-mm naphthalene crystal of 4.0 g with a 20-mm×20-mm face yielded less than one-sixth the number of pulses per second due to gamma-rays of radium, and yet the tungstate and the naphthalene were equally sensitive to electrons from a radium $D+E$ source. The geometry attained with electrons was nearly 40 percent in both cases. Pulse height and shape were indistinguishable for the two compounds, and the maximum pulses corresponded to some 200,000 quanta per gamma-ray.

An 11.3-g $CaWO_4$ crystal with a 2.16-cm² polished face was compared with a standard thin walled glass Geiger-Müller counter 18 mm in diameter×60 mm in length, and the crystal yielded 25 times as many counts per second as the G-M tube with the source at 54 cm; if the ratio of areas is taken into account, the crystal is 125 times more sensitive.

A 100-microgram radium standard at a distance of 54 cm produced 470 counts per second through the 2.16 cm² of the calcium tungstate crystal which corresponds to 2.18 gamma-photons per disintegration of radium in equilibrium with its daughter products. These results indicate nearly a 100 percent counting efficiency.

The results with calcium tungstate are contrary to those of H. Kallmann, who found no trace of pulses with calcium tungstate of any thickness of the phosphor layer and a saturated response to gamma-rays with a tungstate thickness of 0.2 mm. This discrepancy between the results may be accounted for if Kallmann used powdered tungstate instead of large clear crystalline lumps, or perhaps his tungstate contained some impurity which damped or absorbed the fluorescence, such as in the case of synthetic ruby where a small amount of chromium is added to aluminum oxide.

[1] H. Kallmann, Nature and Technik (July 1947).

Artificial Alpha-Active Bismuth Isotopes

D. H. TEMPLETON AND I. PERLMAN
Radiation Laboratory and Department of Chemistry, University of California, Berkeley, California
March 29, 1948

WHEN lead was bombarded with approximately 200-Mev deuterons in the 184-inch cyclotron, a great variety of nuclear reactions were noted. Fission has been demonstrated by the identification of radioactive fission products,[1] and a mixture of isotopes from Bi (element 83) to Au (element 79) has been partially identified. These were produced by reactions analogous to those reported from other irradiations with high energy particles.[2]

This report has to do with some new short-lived emitters of alpha-particles produced from high energy deuterons on lead. The alpha-activity was in very low abundance compared with the Geiger counter activity and was first observed in the unseparated target material. The decay curves could be resolved into 2-min., 9-min., 27-min., and 1–2-hr. components. The longest period was too weak for accurate half-life determination. The three longest periods were chemically identified with the bismuth fraction, but the chemical separation was too slow to permit observation of the 2-min. period. Lead which was bombarded with 100-Mev deuterons showed the 1–2-hr. and 27-min. periods, but the shorter periods could not be detected. Therefore, the 2-min. and 9-min. activities are probably of lower mass number than the longer-lived ones. All of these isotopes of bismuth are believed to be of lower mass number than 203 since lead, enriched in Pb^{204}, did not show any alpha-activity when bombarded with 20-Mev deuterons.[3]

The alpha-particle energies of the three longer periods were all in the range of 5.5 ± 0.3 Mev, as measured by an alpha-particle pulse analyzer.[4] The lack of precision was caused by the high background of electrons and by the inability to prepare extremely thin samples. Because these energies seem to low for alpha-particle half-lives of the order of minutes and since the bismuth fraction showed a great preponderance of electrons over alpha-particles, it is concluded that the alpha-emission represents but a small branching in the predominantly orbital electron capture decay. For example, a 30-min. period and a 100-min. period could be resolved out of the Geiger counter decay curve and, under the assumption that these are the same as the 27-min. and 1–2-hr. alpha-periods, alpha-particle to electron ratios of 7×10^{-4} and 6×10^{-5}, respectively, were calculated. The half-lives for alpha-decay for the 27-min. and 1–2-hr. activities then become about 1 month and 3 years if it is assumed that there is almost one electron emitted per orbital electron capture disintegration.

These data show that alpha-instability as reflected by the alpha-particle half-lives follows the same trend in the case of bismuth isotopes as that noted for the isotopes of polonium. In the case of polonium it has long been noted that there is a minimum half-life at ThC′ (Po^{212}) and that the half-lives increase both toward lower and higher mass numbers. This curve has been extended[5] to show that the half-life for Po^{208} is even longer than for Po^{210} but that the partial alpha-half-life then decreases again at lower mass numbers as exemplified by Po^{206}. In the case of bismuth, the earlier noted half-lives showed a decrease from heavier masses toward AcC (Bi^{211}) which has a 3-min. half-life. Recently Broda and Feather[6] reported that RaE (Bi^{210}) undergoes rare alpha-branching corresponding to a partial alpha-half-life of about 10^4–10^5 yr. Below RaE the half-life increases still further, as shown by the failure to detect alpha-activity in Bi^{209}. However, the present studies show that very light isotopes of bismuth ($Bi^{<208}$) again have measurable alpha-half-lives.

We wish to acknowledge the assistance and cooperation of Dr. John Woodyard, Dr. D. C. Sewell, and all those whose operation of the 184-inch cyclotron made these irradiations possible.

This paper is based on work performed under Contract Number W-7405-eng-48 with the Atomic Energy Commission in connection with the Radiation Laboratory of the University of California, Berkeley, California.

[1] Perlman, Goeckermann, Templeton, and Howland, Phys. Rev. **72**, 352 (1947).
[2] Cunningham, Hopkins, Lindner, Miller, O'Connor, Perlman, Seaborg, and Thompson, Phys. Rev. **72**, 739 (1947).
[3] D. H. Templeton, J. J. Howland, and I. Perlman, Phys. Rev. **72**, 766 (1947).
[4] Ghiorso, Jaffey, Robinson, and Weissbourd, *An Alpha-Pulse Analyzer Apparatus*, Plutonium Project Record, **1413**, 17.3 (1946) (to be issued).
[5] D. H. Templeton, J. J. Howland, and I. Perlman, Phys. Rev. **72**, 758 (1947).
[6] E. Broda and N. Feather, Proc. Roy. Soc. London **A190**, 20 (1947).

Decay Scheme of 62-Day Isotope of Element 43 (Tc)

O. HUBER, H. MEDICUS, P. PREISWERK, AND R. STEFFEN
Swiss Federal Institute of Technology, Zurich, Switzerland
March 29, 1948

THE disintegration of the 62-day isotope of element 43 (technetium), which is believed to have the mass number 95,[1] has been investigated. In addition to the known γ-lines at (0.201 ± 0.002) Mev[2] and (0.810 ± 0.005) Mev,[1] we found by measurements in a magnetic lens spectrometer[3] conversion, photo-, and Compton recoil electrons arising from two new γ-lines of (0.570 ± 0.002) Mev and (1.017 ± 0.010) Mev. Absorption measurements of the electrons and γ-rays showed that the 201-kev γ-line has a conversion coefficient of 0.044 ± 0.008. The relative intensities of the γ-lines were determined by analyzing the absorption curve in lead; the sensitivity of the counter[4] has been accounted for. The absorption coefficients for the experimental arrangement were determined empirically by means of standard γ-ray emitters. The strengths of the γ-lines were found to have the following ratios: $N_{201}:N_{570}:N_{810}:N_{1017}=0.7:0.4:0.3:0.03$. From the $\gamma-\gamma$-coincidence counting rate it follows that the 570-kev and 810-kev radiations are in coincidence with the 201-kev line. Up to now the disintegration had been assumed to take place only by orbital electron capture.[5] Cloud-chamber photographs also showed, however, positrons with energies up to 0.4 Mev. Comparing the number of positron tracks

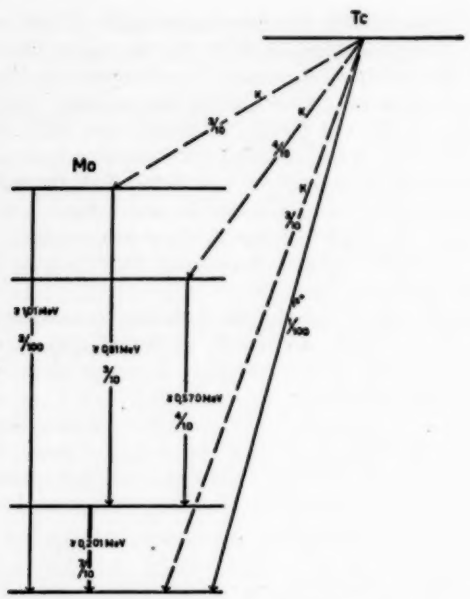

FIG. 1. Decay scheme of the 62-day Tc.

with the number of conversion electrons arising from the 201-kev radiation, as well as from the annihilation coincidence counting rate, we estimate that about 0.8 percent of the transitions take place by positron emission. The intensity ratios of x-rays and γ-rays show that one third of the electron capture transitions lead directly to the ground level. Summarizing these measurements, we propose a term scheme according to Fig. 1.

A detailed report will appear in Helv. Phys. Acta. We take pleasure in thanking Professor P. Scherrer for his stimulating interest in this work.

[1] J. E. Edwards and M. L. Pool, Phys. Rev. **72**, 384 (1947).
[2] D. C. Kalbfell, Phys. Rev. **55**, 422 (1939).
[3] The magnetic lens spectrometer used was designed by Dr. W. Zünti, and its description will appear in Helv. Phys. Acta.
[4] H. Bradt, P. C. Gugelot, O. Huber, H. Medicus, P. Preiswerk, and P. Scherrer, Helv. Phys. Acta **19**, 77 (1946).
[5] A. C. Helmholz, Phys. Rev. **60**, 415 (1941).

Use of Photo-Conductive Semiconductors as Amplifiers

EDMUND S. RITTNER
Philips Laboratories Inc., Irvington-on-Hudson, New York
March 29, 1948

RECENT studies[1] at the Bell Telephone Laboratories have revealed that diamond may be employed as an electron amplifier by virtue of its internal secondary emission. Current amplification factors as high as 500 have been observed by exposure to electrons of 15,000-ev energy. Because of deleterious space charge effects produced by the impingement of electrons on the insulator and by electrons trapped at imperfections in the crystal, the experiments were performed with a pulsed beam technique and with an alternating field across the sample.

There are several extremely important advantages to be derived from the employment of a photo-conductive semiconductor rather than an insulator in this application:

(1) the above-mentioned space charge effects which oppose the flow of current through the specimen in the case of insulators will be absent in the case of semiconductors;

(2) the number of internal secondary electrons released per incident primary electron will be proportional to the quotient (energy of primary electrons/energy gap between filled band and conduction band); this quotient will be greater in the case of semiconductors by a factor of the order of 5 to 10;

(3) in analogy with the secondary photo-effect, the total number of electrons flowing through the semiconductor circuit will, in most cases, far exceed the number of electrons internally released by the bombarding electrons;[2]

(4) the loss of electrons via external secondary emission will be less in the case of semiconductors;[3]

(5) the impedance of the semiconductor device will be of a more suitable magnitude for use in conjunction with usual electronic circuits, the "dark" current being entirely analogous to the no-signal plate current in a vacuum tube amplifier.

Optimum results will probably be achieved with thin specimens of the same order of thickness as the penetration depth of the primary electron beam. Single crystals, in general, present the advantage of extremely high charge carrier mobility relative to polycrystalline samples, although even the latter can be employed to great advantage.

The amplification factor will be proportional not only to the charge carrier mobility and the energy of the incident electrons but also to the field strength applied to the sample, limitations being imposed by the total power input, which will cause heating of the specimen. Care should be exercised to prevent the deflection of the incident beam to an electrode of the sample. For low primary beam intensities the increase in current through the semiconductor on bombardment will be a linear function of the beam intensity.

The main disadvantage of this type of amplifier is the fact that highest amplification factors can be obtained only at a sacrifice in frequency response.[4] The frequency response can be improved with an attendant reduction in amplification factor by exposure of the sample to steady background illumination, by raising the temperature of the sample, or by incorporation of the proper impurities into the photo-conductive layer.

Preliminary experiments have been carried out with a thin polycrystalline layer of selenium deposited on a glass base furnished with two tungsten wire electrodes 5 mm apart. Selenium was chosen because of the ease with which it can be fashioned into a photo-conductive cell. The data are shown in Table I.

These results are subject to improvement by factors of one or more orders of magnitude by changes in the geometry of the electrode configuration and in the tech-

TABLE I. Increased conductivity in selenium induced by electron bombardment.

D.c. voltage across photo-conductor	Electron accelerating voltage	Beam current, μa	Increase in current through photo-conductor, μa	Amplification factor
225	1000	0.015	0.95	63
225	2000	0.015	1.85	123

Notes
Sample resistance = $1.12 \times 10^9 \Omega$.
Cross-sectional diameter of primary beam ≅1 mm.

nique of preparing the photosensitive layer. Still further improvement of similar magnitude is possible by reverting to thin single crystals.

Further work on selenium as well as on other photoconductive semiconductors such as silicon, germanium, and lead sulfide is in progress.

The author wishes gratefully to acknowledge his indebtedness to various members of the staff of Philips Laboratories, Inc., particularly to G. A. Espersen for making available the equipment employed in making the measurements, to M. J. Lun for assistance in the measurements, and to R. H. Ahlert for aid in preparing the photoconductive layer.

[1] K. G. McKay, Tele-Tech. 7, 72 (1948).
[2] A. von Hippel and E. S. Rittner, J. Chem. Phys. 14, 372, 373, 375 (1946).
[3] H. Bruining, *Die Sekundär—Elektron—Emission fester Körper*, (Verlag, Julius Springer, Berlin, 1942), p. 82.
[4] See reference 2, pages 375 and 376.

Ultrasonic Observation of Twinning in Tin

W. P. MASON, H. J. MCSKIMIN, AND W. SHOCKLEY
Bell Telephone Laboratories, Murray Hill, New Jersey
March 25, 1948

AT the suggestion of the last named writer some experiments have been performed with a view to observing the effects of individual moving dislocations. If a dislocation moves across a test specimen with a speed approaching that of sound, a displacement of the order of the lattice constant d should occur in a time of order of diameter of specimen divided by the speed of sound. This requires instruments capable of measuring displacements of about 10^{-8} cm occurring in times of 10^{-6} sec., values which lie in ranges already exploited in connection with ultrasonic delay lines.

The method of experimentation consists of pressing the metal specimen directly against a quartz crystal with a liquid seal, applying stresses which deform the metal, and observing the resulting motion imparted to the quartz. The mechanical arrangement giving the most satisfactory results is shown in Fig. 1. The tin specimen is prepared from 99.9 percent pure tin. The crystal grain size is about $\frac{1}{16}$ in. The specimen (a cone tapering from $\frac{1}{8}$-in. to $\frac{1}{16}$-in. diameter) presses against the quartz crystal on the right, and on the left is soldered to a silver paste baked on the tip of a long tapered glass rod. The quartz

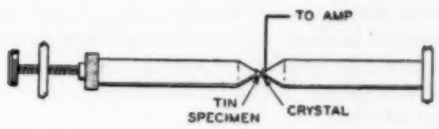

FIG. 1.

crystal (0.5 mm thick and $\frac{1}{4}$-in. diameter) is similarly attached to the other glass rod. The two glass rods are lined up in a V block and pressure is applied by a screw through a rubber pad. During the time of observation (described below) the ultrasonic disturbance does not have time to reach the ends of the glass rods; furthermore, the transient pressure wave developed on the quartz is less than 1 percent of the applied load. As a consequence of these facts, the deformation takes place essentially at constant load. Increasing the applied load by turning the screw provokes additional transient yielding. The tapering of the rods tends to eliminate transverse reflections.

The voltage generated by the quartz crystal is amplified and split into two parts; one part actuates the trigger of a sweep circuit while the other is delayed 15 microseconds by a fused quartz delay line and then applied to vertical plates of the oscilloscope. Various electrical and mechanical tests indicate that crystal plus electrical circuits have an adequate band width for the effects studied. The sensitivity is such that a force of 1000 dynes gives $\frac{1}{8}$-in. deflection on the oscilloscope. Because of the nature of the mechanical impedances on either side of the specimen, voltages are proportional to velocity of yield with 1000 dynes corresponding to a rate of yield of 1.6×10^{-3} cm/sec. over the $\frac{1}{16}$-in. face of the tin specimen.

Observation of the voltage output on fast and slow sweeps shows that the noise generated consists of pulses lasting about 30 microseconds. Pantograph tracings of the photographs of two such pulses are shown in Fig. 2, together with a calibrating timing wave. Out of 15 photographs taken, 11 were similar to (a) and 4 to (b). The fine structure is not the same on any two traces, which suggests that it is characteristic of the twinning process rather than of some mechanical resonance in the specimen. The distance moved in one cycle of the fine structure is about 2A for (a) and about $\frac{1}{2}$A for (b). The period of the fine structure corresponds to 3 microseconds for (a) and 1 microsecond for (b), and the time for a compression sound wave to cross the specimen is 1 microsecond.

These results are in general agreement with passage at the speed of sound of twinning dislocations from side

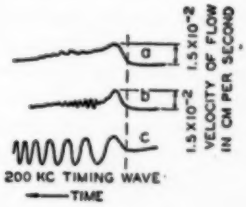

FIG. 2.

to side in the specimen. However, the magnitude of the displacement is about ten times larger than would be expected from the twinning of one pair of planes. The net volume contraction of the tin as viewed from the quartz is about 10^{-8} cm³.

Somewhat similar experiments carried out with large aluminum crystals failed to give detectable signals.

On the Mechanism of Electron Emission at the Cathode Spot of an Arc

JEROME ROTHSTEIN
Signal Corps Engineering Laboratories, Fort Monmouth, New Jersey
April 5, 1948

THE experiments of Smith[1] on the thickness of the mercury arc cathode dark space show that the hypothesis of field emission fails to account for the high current densities (10^4 amp./cm²) observed at the cathode spot.

The fact that the arc can be extinguished by a current interruption of less than 10^{-8} second,[2] together with evidence indicating a low cathode temperature even at the arc spot itself, shows that thermionic emission is also inadequate.

Smith's[3] theory ascribing the high current density to thermal excitation of the conduction electrons runs into the following difficulty, which applies to thermionic emission as well. Taking the diameter of an arc spot as 10^{-2} cm, the velocity of the spot in a magnetic field as 10^4 cm/sec.[3,4] the arc current as 1 ampere, and the cathode fall as 10 volts, we see that the cathode spot must be excited to full emission in 10^{-6} second by an energy of only 10^{-5} watt second. Furthermore, it is hard to conceive of any plausible mechanism for preventing the "hot" electrons in the cathode spot from losing their energy by interacting with other conduction electrons and even with the atoms of the cathode.

The hypothesis that the entire current is carried by positive ions[5] runs into difficulties such as communicating too much momentum to the cathode, accounting for the high temperature, and inability to explain why an interruption of less than 10^{-8} second should extinguish the arc.

A new theory is proposed that is applicable to the class of arcs characterized by relatively low spot temperature and relatively high spot mobility, e.g., liquid cathodes, Cu, Ag, Au, Fe, Ni. The mechanism may play a partial role in other cases as well. It is assumed that a region possibly 10^{-5} cm thick of very dense metallic vapor exists immediately adjacent the cathode spot. The high density perturbs the atomic fields so that the normally sharp energy levels are spread into bands, including conduction bands. Metallic conduction is then possible from the cathode to this region, which is at a sufficiently high temperature to emit thermionically into the plasma. The ions bombarding the cathode serve to maintain the high local density.

From the work of Birch[6] on the conductivity of Hg in the supercritical region, it appears that a particle density N equal to 10^{22} atoms per cc gives essentially metallic conduction. Consider the arc spot. If n atoms leave it per cm² per sec. with a velocity distribution $f(c)$, the particle density in a layer of thickness d outside it is given by

$$p=(1/d)n\int_0^\infty f(c)(\alpha/c)dc=n\int_0^\infty f(c)(dc/c)=N=10^{22}, \text{ say.}$$

To estimate n, we recall a current density of 10^4 amp./cm², about 10 percent of which is carried by ions, giving 6×10^{22} ions/cm²/sec. bombarding the Hg arc spot. This is about ten times the net "evaporative" loss, so somewhat more than this number of atoms leave the cathode. The coefficient of accommodation is probably small, so many of them leave with large velocities giving small contributions to the integral. For want of a better choice at this time, we describe the low velocity fraction by a Maxwellian distribution corresponding to an effective temperature T. We have

$$p=\left[4n\Big/\left(\frac{\pi 2kT}{m}\right)^{\frac{1}{2}}\right]\int_0^\infty xe^{-x^2}dx=N,$$

whence

$$n/(T)^{\frac{1}{2}}\simeq 10^{-4}\ N.$$

Taking $N=10^{22}$, $n=10^{19}$ gives $T=100°K$, $n=10^{20}$ gives $T=10^4$. In view of experimental uncertainties, this can be considered satisfactory.

Additional evidence in favor of the conduction theory is afforded by Smith's[1] observation that a continuous spectrum originates within 10^{-3} cm from the cathode surface. As is well known, continuous spectra can be obtained from high pressure Hg lamps.

Mierdel's[2] work gives an independent estimate of the thickness of the dense region. If the arc conduction atoms are leaving with velocities of 10^4 or 10^5 cm per Mc and the source is cut off for 10^{-8} or 10^{-9} second, they can move 10^{-4} or 10^{-5} cm in this time. The fact that this extinguishes the arc indicates that the dense region is somewhere near this thickness or less.

A more detailed paper working out various refinements and consequences of the theory is in preparation.

[1] C. G. Smith, Phys. Rev. **69**, 96 (1946).
[2] G. Mierdel, Zeits. f. Tech. Physik **17**, 452 (1936).
[3] C. G. Smith, Phys. Rev. **62**, 48 (1942).
[4] A. Dufour, J. de phys. et rad. [5] 1, 109 (1911).
[5] J. Slepian, Phys. Rev. **26**, 407 (1926).
[6] F. Birch, Phys. Rev. **40**, 1054 (1932); **41**, 641 (1932).

Hyperfine Structure in the Spectrum of Np^{237}

F. S. TOMKINS
Argonne National Laboratory, Chicago, Illinois
April 5, 1948

IN the course of numerous routine spectrographic analyses of very small samples of Np^{237} it was observed that many of the neptunium lines appeared very broad, even under moderate dispersion (5A/mm), suggesting the presence of wide hyperfine structure.[1] The widest neptunium line in the region investigated, at 3829.15A, was then photographed by use of the third order of a Baird

three-meter grating spectrograph (dispersion = 1.7A/mm), with the result that this line was shown to be a flag-pattern type hypermultiplet in which the first three components were resolved.

Larger samples of the isotope have become available and the spectrum has been investigated in some detail using a Fabry-Perot interferometer. The source used was a water-cooled Schuler type hollow cathode tube, and the spectrograph a Bausch and Lomb large littrow type with glass optics.

Under high resolving power all lines exhibiting hyperfine structure appear as flag patterns, some degraded in spacing and intensities toward the red and the others toward the violet. Approximately fifty of these lines have been completely resolved— —in each case into six components. This is strong evidence that we are here concerned with a case analogous to that found in praseodymium, where every line showing hyperfine structure which can be resolved is shown to consist of six components.[2]

For neptunium, as in the case of praseodymium, this can be interpreted only to mean that for each of the widely split spectral terms involved, J is greater than I and, consequently, the number of hyperfine levels into which the term is split is equal to $2I+1$. Thus it appears that for Np^{237}, $I=5/2$.

This work will be published in detail in the near future.

* This document is based on work performed under Contract Number W-31-109-eng-38 for the Atomic Energy Project at the Argonne National Laboratory.

[1] F. S. Tomkins and M. Fred, Argonne National Laboratory, Project Report ANL-4018, August 13, 1947.

[2] H. E. White, Phys. Rev. 34, 1391 (1929).

Characteristics of the Parallel-Plate Counter

L. Madansky and R. W. Pidd
Randall Laboratory of Physics, University of Michigan, Ann Arbor, Michigan

March 29, 1948

THE measurement, by means of particle counters, of very short time intervals is important in the study of successive nuclear transitions and in the measurement of the lifetime of the meson. Lifetimes as short as 10^{-7} second have been measured.[1,2] One of the fundamental limitations in such measurements is the inherent delay time of the counter. In a Geiger counter this delay has its origin in the drift time of the secondary electrons from the point of production to the small avalanche region surrounding the central wire, and consequently varies from one count to another. When the paths of the primary electrons are restricted, by means of slits, to a very small region about the central wire, the delay time can be limited to about 10^{-7} second. The lower limit in lifetimes that can be measured is about 0.3 the average delay time of the counters, provided the distribution of inherent counter delays is accurately known. Hence, the Geiger counter is not applicable to the measurement of lifetimes less than 3×10^{-8} second even with extreme collimation.

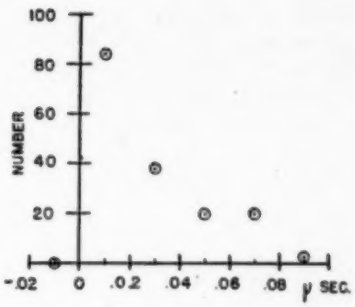

FIG. 1. Time delay distribution.

Since the delay time is inherent in the cylindrical geometry, it has been proposed[3] that parallel-plate electrodes be substituted for the cylindrical electrodes in the Geiger counter. In the case of the parallel geometry the whole counter volume should be uniformly avalanche sensitive; thus, the beginning of the avalanche should follow the formation of the initiating ion without delay.

For the experiment to be described a counter was constructed using 3-mil copper foil as the parallel surfaces. The foils were stretched as "drum heads" in 2-inch diameter circular frames, and were placed 1 mm apart. The counter was filled to a pressure of 2 atmospheres with a mixture of 90 percent argon, 10 percent N-butane. It was necessary to quench the discharge with a Neher-Pickering circuit having a time constant of 10^{-3} second. Under these conditions the counting threshold was 3000 volts with a 900-volt plateau. The pulses produced (without amplification) in a 70-ohm transmission line were about 600 volts in amplitude and had a rise time of less than 10^{-8} second, which agrees with the breakdown time given by Loeb.[4] The efficiency of the counter for electrons was 10 percent.

The delay was measured by causing beta-rays to traverse a thin walled cylindrical Geiger counter and the parallel-plate counter in tandem. To reduce as far as possible the delay in the Geiger counter the beam was restricted by slits which limited it to a 1-mm region surrounding the central wire.

The parallel-plate pulse initiated a $\frac{1}{2}$-microsecond sweep on an oscilloscope (5RP11 tube operated at 10 kv) and the Geiger pulse was displayed as a vertical deflection. A point on the sweep which represented "zero" delay for both counters was found in an auxiliary experiment by connecting the parallel-plate counter simultaneously to the horizontal and vertical circuits. To place the zero in the best part of the screen, a small fixed delay was introduced into the vertical deflection circuit. A deviation to the right of zero on a sweep going from left to right indicated an excess of Geiger delay over parallel-plate delay, whereas a deviation to the left of zero indicated a larger delay for the parallel-plate counter. Results of photographs of the dispersion of the Geiger pulses are shown in Fig. 1. It is seen that, within the accuracy of measurement, there are no pulses to the left of zero, while the distribution to the right shows an average delay for the cylindrical

counter of 2×10^{-8} second. The delay error of the parallel-plate counter appears to be less than the accuracy of measurement which is 10^{-8} second.

The advantage of the short delay time, large solid angle, and large output pulse of the parallel-plate counter should make possible measurements of lifetimes of the order of 10^{-9} second. However, the present indications are that the efficiency is low (~10 percent) and that the recovery time is comparatively long (~0.01 sec.). A coincidence set of parallel-plate counters has been constructed to measure short-lived metastable states of nuclei.

The authors are indebted to Professor H. R. Crane for many valuable suggestions. The work was supported by the U. S. Navy, Bureau of Ordnance, under Contract NOrd 7924.

[1] L. Madansky and M. L. Wiedenbeck, Phys. Rev. **72**, 185 (1947).
[2] S. De Benedetti and F. K. McGowan, Phys. Rev. **71**, 380 (1947).
[3] J. W. Keuffel, Phys. Rev. **73**, 531 (1948).
[4] L. B. Loeb, *Fundamental Processes of Electrical Discharges in Gases* (John Wiley and Sons, Inc., New York, 1939), p. 426.

Proceedings of the American Physical Society

MINUTES OF THE MEETING AT CHICAGO, ILLINOIS

DECEMBER 29–31, 1947

THE 282nd meeting of the American Physical Society was held in Chicago at the University of Chicago on Monday, Tuesday, and Wednesday, December 29, 30, and 31, 1947. For the first time since 1940, and possibly for the last time altogether, we thus met in conjunction with the American Association for the Advancement of Science. Two symposia of our meeting—that pertaining to "High Altitude Research by Rockets," arranged by a group headed by F. L. Whipple, and that pertaining to "Physics of Polymers of Biological Interest," arranged by our Division of High-Polymer Physics (J. W. Oiska being the programme officer)—were designated as joint symposia with Section B of the Association. We also had the privilege of staging the address of L. A. DuBridge in his capacity as retiring vice president of the Association. The American Association of Physics Teachers held concurrent meetings, and allowed us to figure as co-sponsors of their symposium "Microwaves and their Uses." Several invited papers on nuclear physics and solid-state physics appeared on the general programme, and the Division of High-Polymer Physics presented three sessions of invited and contributed papers in addition to the symposium before mentioned. Contributed papers in the general programme numbered sixty-seven. Registration at our desk totaled 463; others must have registered at the desk of the American Association of Physics Teachers, still others must have attended from other sections of the American Association for the Advancement of Science. It is painful to record that one of our sessions was missed by at least one-third of the people who wanted to attend it because the would-be audience exceeded by the corresponding fraction the utmost capacity of the hall. This is a symptom of the growth of our Society; but happily we need not yet omit the University of Chicago from the list of our meeting places, since timelier reservation would have made a larger hall available.

The dinner, under the auspices of the American Association of Physics Teachers, was held on Tuesday evening in International House with an attendance of about 240, completely filling this dining room. Paul Klopsteg gave an after-dinner demonstration lecture on the art and science of archery under the title "Bows and Arrows."

The Council met on Tuesday afternoon. W. V. Houston was nominated to the Governing Board of the American Institute of Physics for a three-year term as one of our representatives. The Council accepted the gracious invitation of the University of Wisconsin to hold the 1948 Summer Meeting in the East in its buildings at Madison. Eight candidates were elected to Fellowship, and one hundred and thirty-eight to Membership: their names are appended.

Word has reached the Society of the death of four of its members: F. L. Bishop (University of Pittsburgh), C. A. Briggs (Washington, D. C.), C. R. Fountain (Washington, D. C.), D. F. Windenburg (David Taylor Model Basin).

Elected to Fellowship;

Marius Bohun-Greene, W. W. Havens, Jr., H. W. Fulbright, F. W. Preston, L. J. Rainwater, H. K. Schilling, Lennart Simons, W. A. Wildhack.

Elected to Membership;

A. A. Aardal, Raymond V. Adams, Jr., Richard Akerib, Fernando Alba, Neal S. Anderson, Nicholas G. Anton, Arthur Ashkin, Fred Ashworth, David Breed Beard, Harold W. Bell, Lawrence H. Bennett, Rene H. Bernas, Warren Berning, Andre Berthelot, Earl C. Biffle, Lamont V. Blake, Jean P. Blaser, Frederick Kenneth Bloom, Merle H. Bragdon, Arthur A. Broyles, Lester Elkin Burkhart, Robert L. Butenhoff, Morton Camac, B. H. Cherner, C. L. Christ, Giuseppe Cocconi, Ernest Cohen, George I. Cohn, Marcello Conversi, Walter E. Crandall, William G. Cross, Thomas McLellan Davis, James W. Davisson, Leo Diesendruck, Thomas R. Dolezal, John S. Dooling, Edward A. Dunlap, David L. Dye, C. A. Dyer, William V. Eakins, Herbert Elion, John E. Euller, Myron L. Feistman, Robert O. Fleming, Jr., Richard C. Fowler, Abraham S. Friedman, J. Bruce French, Owen Gailor, Eugene H. Berber, Roy J. Glauber, Philip A. Goldberg,

Sidney Golden, Virginia Griffing, R. C. Guthrie, J. Halter, Howard G. Hanson, William H. Hartley, Roger F. Hibbs, Egon A. Hiedemann, J. J. Hopfield, Malcolm M. Hubbard, Res Jost, Werner Kaenzig, Morton F. Kaplon, Isabella Karle, Robert Karplus, Lee Kean, Thomas A. Keenan, Leason K. Kington, Paul P. Kisliuk, Edward Andrew Kmetko, Louis J. Koester, Jr., Edwin F. Kulikowski, Lester Lees, Howard O. Lorenzen, Clarence F. Luck, Daniel Maeder, Anna I. McPherson, A. T. McPherson, Harold Mendlowitz, Melvin L. Merritt, Raymond B. Meyer, H. R. Milley, R. C. Mobley, William Lind Morris, George Newell, Jr., William Everett Nickell, Eugene Ray Nixon, Albert H. Oshiver, Eli Ossofsky, Anderson Pace, Jr., Irving H. Page, James Thomas Palladino, Benjamin J. Patton, Richard J. Phelps, John Philosophos, Harold J. Plass, Henry H. Plotkin, John H. G. Poole, Fernando E. Prieto; John F. Pudvin, Robert V. Pyle, Israel Reff, A. E. Remund, R. B. Rice, John E. Robinson, Antonio Romero-Juarez, Alma Rosenbaum, Richard F. Rutz, Matthew H. Schrenk, Franklyn K. Schwaneflugel, John R. Sewell, Anatole M. Shapiro, Denman Shaw, Jesse William Smith, Teddy Lynn Smith, Arnold Sommerfeld, Edwin A. Speakman, Joseph Sperrazza, Martin Stearns, Richard S. Stein, Christos G. Stergiopoulos, Malvin D. Stern, Lloyd Russell Stevens, Alan H. Stillman, Harold E. Swanson, Gwynne B. Sartz, David H. Templeton, Richard N. Thayer, Charles E. Treanor, Donald Tuomi, Robert J. Urick, Andre G. Voisin, Agnes C. Wales, Pei Hsin Wei, J. Wyart, Leo C. Young, Lotfi A. Zaden.

KARL K. DARROW, *Secretary*
American Physical Society
Columbia University
New York 27, New York

Invited Papers on the General Programme

The Physics of Radar. L. A. DUBRIDGE, *California Institute of Technology.* (Retiring address of the vice-president of Section B of the AAAS.)

Interactions between Elementary Particles. ENRICO FERMI, *University of Chicago.*

Mass-Spectrographic Identification of Radioactive Isotopes. A. J. DEMPSTER, *Argonne National Laboratory.*

Neutron Polarization and Ferromagnetism. D. J. HUGHES, *Argonne National Laboratory.*

Low Temperature Transformations in Lithium and Some of Its Alloys. C. S. BARRETT, *University of Chicago.*

Joint Symposium of the American Physical Society and Section B of the AAAS

High Altitude Research by Rockets

Introduction: Research by Rockets. J. A. VAN ALLEN, *Johns Hopkins University.* Motion Pictures.

Sky Brightness. H. A. MILEY, *Air Materiel Command.*

The Measurement of Atmospheric Pressure between the Altitudes of 65 and 110 Km. W. G. DOW, *University of Michigan.*

Theoretical Considerations of Ambient Temperature Measurements of the Upper Atmosphere. ERIC BETH, *Air Materiel Command.*

Pressure and Temperature of the Upper Atmosphere. R. J. HAVENS, *Naval Research Laboratory.*

Ionosphere Experiments Utilizing Rockets. T. R. BURNIGHT, *Naval Research Laboratory.*

The Use of a Beacon to Measure Ion Density in the *E*-Layer. MARCUS O'DAY, *Air Materiel Command.*

Characteristics of the Sun's Spectrum Obtained from V-2 Rockets. J. J. HOPFIELD, *Johns Hopkins University.*

Some Aspects of the Solar Spectrum between 3000A and 2300A. H. E. CLEARMAN, *Johns Hopkins University.*

Solar Ultraviolet Spectroscopy from V-2 Rockets. R. TOUSEY, *Naval Research Laboratory.*

Cosmic-Ray Studies from V-2's. G. J. PERLOW, *Naval Research Laboratory.*

Cosmic-Ray Bursts in the Upper Atmosphere. H. E. TATEL, *Johns Hopkins University.*

Direct Measurement of the Flux of Charged Cosmic-Ray Primaries. J. A. VAN ALLEN, *Johns Hopkins University.*

Joint Symposium of the Division of High-Polymer Physics and Section B of the AAAS

Physics of Polymers of Biological Interest

The Hydrolysis of Proteins, H. B. BULL, *Notre Dame University.*

Proteins as Polycondensations of Amino Acids. DOROTHY WRINCH, *Smith College* (abstract follows).

Studies of the Melting Points, Rigidities, and Optical Activities of Gelatin Gels. J. D. FERRY AND J. E. ELDRIDGE, *University of Wisconsin* (abstract follows).

Viscosity and Streaming Birefringence of Nucleic Acid. J. P. GREENSTEIN, *National Institute of Health* (abstract follows).

The Study of Macromolecular Reactions of Biological Interest. PAUL DOTY, *Northwestern University.*

Contributed Papers

A1. Total Cross Sections of Fe, Ni, and Bi for Fast Neutrons. C. K. BOCKELMAN, L. W. SEAGONDOLLAR, AND H. H. BARSCHALL, *University of Wisconsin.*—A continuation of previous work on the scattering of fast neutrons as a function of neutron energy[1] has been undertaken. Neutrons of continuously variable energy were obtained by bombarding a thin Li target with protons. The total cross sections of Fe, Ni, and Bi have been measured over the 10-kev to 500-kev energy range with a resolving power of 20 kev, and over the 200-kev to 1500-kev range with a resolving power of 150 kev. With the higher resolution,

definite maxima and minima were found for Fe and Ni, but not for Bi. These data are in good agreement with previous measurements obtained by use of photo-neutron sources.[2] With the lower resolution, the total cross section for each of the three elements was found to decrease monotonically as the neutron energy increased. A comparison of the experimental results with predicted values[3] will be made.

[1] Seagondollar and Barschall, Phys. Rev. **72**, 439 (1947).
[2] Fields, Russell, Sachs, and Wattenberg, Phys. Rev. **71**, 508 (1947).
[3] Feshbach, Peaslee, and Weisskopf, Phys. Rev. **71**, 145 (1947).

A2. Beta-Spectra of Cu^{64} as a Test of the Fermi Theory. C. SHARP COOK AND LAWRENCE M. LANGER, *Indiana University.*—A detailed investigation of the energy distributions of the negatrons and positrons emitted by Cu^{64} has been made under optimum conditions, using a large, scatter-free, magnetic spectrometer of high resolution. The spectrometer uses a radius of curvature of 40 cm and employs a radially inhomogeneous magnetic field to obtain second-order focusing in 180° with a resolution of 0.5 percent. Chemically separated, cyclotron sources of high specific activity about 0.2 mg/cm² thick were mounted on a backing support of 0.02 mg/cm². The particles were detected by a counter whose window has a range of 2.5 kev. It is found that for *both* positrons and negatrons, there are more particles at low energy than are predicted by the Fermi theory. The positron distribution begins to deviate from the Fermi straight line at a higher energy than do the negatrons and the deviation is much greater. In addition, the ratio of the number of positrons to the number of electrons is larger than that predicted by the theory for all energies below 0.2 Mev. Whereas the experimental data of Backus covering the region below 50 kev agree with our data over this region, the interpretation of Backus' results by Lewis and Bohm is not consistent with our measurements for the entire energy distribution.

A3. Momentum Conservation in the Beta Decay of P 32 and the Angular Correlation of Neutrinos with Electrons. CHALMERS W. SHERWIN, *University of Illinois.*—It is possible, by evaporation of carrier free P 32, to produce what appear to be mono-layer beta-active sources. These sources maintain their characteristics for several hours of pressures of about 10^{-7} mm of Hg. The momentum of the recoil ion is measured by timing its flight in a field free space. Recoil momentum spectra are observed at 180°, 135°, 90°, and 45° with respect to the electrons. It is shown that (a) momentum is not conserved between the electron and the recoil nucleus; (b) the experimental data are in disagreement with any hypothesis in which the neutrino and the electron are most probably emitted in the same hemisphere; (c) for recoil ions above about 25-ev energy, the observed recoil momentum spectra agree rather well with those spectra calculated on the assumption of a $(1-\beta\cos\theta)$ neutrino-electron angular correlation function; and (d) below 25 ev, too many recoils are observed compared to any neutrino theory which gives agreement for high momentum recoils. Since the reason for the disagreement below 25 ev is not understood, the selection of the $(1-\beta\cos\theta)$ function must be regarded as tentative.

A4. H^3 and the Mass of the Neutrino. JOHN R. PRUETT, *Indiana University.*—Tritium appears to have an anomalously short life (10–20 years) for its energy release (11–15 kev). Konopinski* has shown that this could be explained on the basis that an unobserved part of the energy is released in the form of a (anti) neutrino of very small but finite rest mass. He confined himself largely to purely statistical considerations in obtaining an estimate of the (anti) neutrino mass (μ m) needed (1/45 to 1/30 of the electron's rest mass m). At least two fairly important factors were ignored by him: the influence of the Coulomb field on the electron and a relativistic correction factor which arises from the summation over spins of the emitted particles, $1-(\mu/WK)$. Here W, K are the total energies of each particle in units of mc^2. When these factors are taken into account, one finds that considerably larger values of μ are needed than those estimated by Konopinski. Taking 20 years for the half-life and making the comparison to He^3 as done by Konopinski, one finds $\mu=0.277$ if the energy release is 11 kev, $\mu=0.054$ if 15 kev. No neutrino mass would need to be assumed if the energy released were found to be as high as 20 kev. The influence of the neutrino mass on the shapes of the H^3, C^{14}, and other spectra will also be discussed.

* E. J. Konopinski, Phys. Rev. **72**, 518 (1947).

A5. Short Lived Metastable State in an "Even-Even" Nucleus: Ge^{72}. J. C. BOWE, M. GOLDHABER, R. D. HILL, W. E. MEYERHOF, AND O. SALA,* *University of Illinois.*—Among the radiations of Ga^{72} (14.1 hr), which decays to Ge^{72}, internal conversion electrons corresponding to a transition of 0.7 Mev have been noticed by M. Deutsch and K. Siegbahn (private communication). Using delayed coincidences, we find that internal conversion electrons with a range in Al of ~240 mg/cm² are emitted from an excited state of Ge^{72} with a half-life period of $(5\pm0.5)\times10^{-7}$ sec. These electrons follow a weak beta-branch of Ga^{72} with an intensity of the order of 1 percent. We have been unable to detect delayed gamma-rays and we conclude that at least 50 percent of the delayed transitions are internally converted. These facts are compatible with the assumption that we are dealing here with a $0\rightarrow0$ transition with no change of parity, similar to the classical case in RaC′ first investigated by C. D. Ellis and R. H. Fowler. For such a transition no gamma-ray emission is possible and the excitation energy is transferred by direct interaction from the nucleus to an electron of the K, L or higher shells. No good agreement between experiment and theory can be obtained if other types of isomeric transitions are assumed (e.g. $\Delta l=2$, 3 or 4).

* Rockefeller Fellow of the University of São Paulo, São Paulo, Brazil.

A6. Multiple Nuclear Isomerism. E. DER MATEOSIAN, M. GOLDHABER, C. O. MUEHLHAUSE, AND M. MCKEOWN, *Argonne National Laboratory.*—In the course of an investigation of the activity induced in Sb by slow neutrons we noticed three previously unobserved short periods with the following half-lifetimes: 1.3 min., 3.5 min., and 21 min.

Their saturation intensities are of the order of a few tenths of one percent of those of the known activities, Sb^{122} (2.8 d.) and Sb^{124} (60 d.). Using a sample of Sb enriched in Sb^{122} (96.3 percent Sb^{122}) we found that the 1.3- and 21-min. periods are both due to isomers of Sb^{124} (60 d.) and that the 3.5-min. period is due to an isomer of Sb^{122} (2.8d.). Characteristic $K\alpha$ radiation of Sb was found to be associated with the 3.5-min. period, but not with the 1.3- and 21-min. periods. The 3.5- and 21-min. periods both show intense soft electrons with half-value thicknesses in Al of 1.7 mg/cm² and 0.2 mg/cm², respectively, indicating internal conversion electrons with approximate energies of 110 kev and 14 kev, respectively. The isomeric transition of Sb^{124} (21 min.) appears to be of lower energy than the K work function of Sb (31 kev). The 1.3-min. isomer decays with the emission of negative beta-rays of 3.2 ± 0.2 Mev maximum energy.

A7. Coincidence Experiments on Sc^{46} and Au^{198}.* E. T. JURNEY AND MARGARET R. KECK, *Indiana University.*—Coincidence measurements of the type described by Mitchell, Langer, and McDaniel[1] have been made on the isotopes Sc^{46} (85 d.) and Au^{198} (2.8 d.). For Sc^{46} both gamma-gamma and beta-gamma coincidences were found. The ratio of the number of gamma-gamma coincidences per gamma-ray counted was $(0.720\pm0.08)\times10^{-3}$. This indicates cascaded gamma-rays in the decay scheme. The ratio of the number of beta-gamma coincidences counted to the number of beta-rays counted was constant for absorber thicknesses up to 0.068 g/cm². Our results are in agreement with the disintegration scheme proposed by Feister and Curtiss; our coincidence techniques are not selective enough to obtain beta-gamma coincidences involving the high energy, low intensity beta-ray group reported by Peacock and Wilkinson. Earlier measurements on Au^{198} by Clark definitely indicate gamma-gamma coincidences. We repeated this experiment using gold which had been chemically separated and obtained no evidence of gamma-gamma coincidences. The ratio of beta-gamma coincidences to counted beta-rays was found to be constant for absorber thicknesses up to 0.270 g/cm², which is in agreement with Clark and with Norling, indicating that the beta-ray spectrum is simple, and leads to an excited state of Hg^{198} from which a gamma-ray of 0.41 mv follows.

* This research was supported by a grant from the Office of Naval Research.

[1] A. C. G. Mitchell, L. M. Langer, and P. W. McDaniel, Phys. Rev. 57, 1107 (1940).

A8. Beta-and Gamma-Rays of Ga^{72}. A. C. G. MITCHELL, B. D. KERN, AND D. J. ZAFFARANO, *Indiana University.*—The spectrum of Ga^{72} (14.1 hr.) is being investigated using a magnetic lens spectrometer. The spectrum is quite complicated and to date only the lines of higher intensity are known. Photoelectric lines, using a lead radiator, have been found for which the gamma-ray energy is 0.64, 0.84, 2.15 and one of higher energy. The distribution of the Compton electrons from a copper radiator was studied and gave lines corresponding to gamma-rays at 0.64, 0.71, 0.84 and the high energy lines. In addition there is some evidence for a weak line at 1.48 mv. The beta-ray spectrum shows an internally converted line, gamma-ray energy 0.71 mv. The beta-ray spectrum is complex. There are at least three groups with end points at 3.09, 2.2, and 0.79 mv.

A9. Gamma-Radiation from Scandium, Cerium, and Terbium. J. M. CORK, R. G. SHREFFLER, AND C. M. FOWLER, *University of Michigan.*—Spectrometric studies have been made of the radiations from specimens of scandium, cerium and terbium, irradiated in the Oak Ridge pile by the (n,γ) reaction. The isotopes formed should be Sc^{46} (85 d.), Ce^{141} (28 d.), and Tb^{160} (72 d.). Scandium shows no converted gamma-ray but by absorption in copper and lead a gamma-line is observed at 1.15-Mev. Cerium has converted gamma-rays of 137.1 and 145.0 kev. Terbium shows many lines due to internal conversion. K–L–M differences are observed characteristic of the next heavier element, dysprosium, showing the gamma-radiation follows beta-emission. The lines as identified show gamma-rays of 85.6, 194.7, 213.2, and 298.0 kev, and by absorption a gamma-ray at 1.10 Mev. In one case conversion due to N electrons is identified.

A10. On the Emission of Continuous γ-Radiation during β-Decay. C. S. WANG AND D. L. FALKOFF,* *University of Michigan.*—The continuous γ-ray spectrum due to the sudden change in nuclear charge during β-decay has been treated by Knipp and Uhlenbeck[1] and F. Bloch,[2] who calculated the bremstrahlung by second-order perturbation theory in which the perturbing potentials were the Fermi electron-neutrino interaction for the allowed β-decay, and the electromagnetic interaction for the γ-emission. Knipp and Uhlenbeck also calculated the γ-spectrum by first-order perturbation theory assuming the Fermi energy distribution for the outgoing β-particles and using only the electromagnetic coupling to the radiation field. We have extended these calculations to the different types of β-interactions and to various orders of forbiddenness and find, contrary to a remark of Morrison and Schiff,[3] that the two methods give essentially the same result: The γ-spectrum has practically the same shape, and the ratio of the total γ-intensity to β-energy is the same for forbidden as allowed transitions. We are able to account for this by consideration of a simple classical analog for the bremstrahlung.

* National Research Council Pre-doctoral Fellow.

[1] J. K. Knipp and G. E. Uhlenbeck, Physica III, 425 (1936).

[2] F. Bloch, Phys. Rev. 50, 272 (1936).

[3] P. Morrison and L. I. Schiff, Phys. Rev. 58, 24 (1940).

A11. Introduction of Two Neutrons into Atomic Nuclei under H^3 Bombardment. D. N. KUNDU AND M. L. POOL, *Ohio State University.*—H^3 particles have been used for the introduction of two neutrons into atomic nuclei. The H^3 was produced by bombarding Be with 10-Mev deuterons as previously reported. The target was metallic Rh and Co placed immediately behind the Be foil. After chemistry, the Rh fraction of the first foil showed the 35-hour Rh^{106} activity. The activated layer of the bombarded Co block

was etched out with nitric acid and the Co fraction showed the 1.75-hour Co^{61} activity. Beta-energy measurements by absorption in aluminum gave as the maximum values 0.6 Mev for the 35-hour Rh and 1.1 Mev for the 1.75-hour Co. No gamma is emitted by Co in the 1.75-hour period. The possibility that the activities are produced by ordinary neutrons from the Be has been excluded. Since Rh^{103} and Co^{59} are the only stable isotopes of Rh and Co with 100 percent abundance, two neutrons have been introduced into each of the Rh^{103} and Co^{59} nuclei according to the reactions $Rh^{103}(H^3,p)Rh^{105}$ and $Co^{59}(H^3,p)Co^{61}$, respectively. The mechanism appears to be mostly an Oppenheimer-Phillips process with H^3. The results indicate a probable evidence of the di-neutron ($_0n^2$).

W1. Depolarization of Light Scattered by Macromolecular Solutions. PAUL DOTY* AND S. J. STEIN, *The Royal Institution, London, and the Polytechnic Institute of Brooklyn.*—The light scattered transversely from a solution through which a parallel beam of monochromatic, polarized light passes, can be readily resolved into vertically and horizontally polarized components. When the incident light is vertically polarized these components in the scattered light are designated as V_v and H_v; when it is horizontally polarized the components are denoted by V_h and H_h, respectively. A qualitative theory is presented which predicts the variation of these four components with such variables as molecular weight, concentration, molecular size, solvent-solute interaction, and ionic charge. These details are discussed separately for flexible and rigid molecules. The results for the different components can be combined to predict the behavior of the conventionally measured depolarization ratios: ρ_v $(=H_v/V_v)$ and ρ_h $(=V_h/H_h)$. It is clear that less ambiguous interpretations of data are possible if the absolute values of the individual components are measured rather than the ratios as heretofore. The calculation of macromolecular dimensions by measuring depolarization ratios is discussed and several important errors in the literature are corrected. Some measurements on polymer solutions and tobacco mosaic virus solutions under different conditions are presented and interpreted in terms of the theory. In particular, a correlation of orientation in the contacts of polymer segments is noted and a precise test of the calculation of dimensions of rod-like molecules from depolarization measurements indicates the essentially qualitative nature of this relation.

* Present address: Chemistry Hall, University of Notre Dame, South Bend, Indiana.

W2. Absorption Analysis of High Molecular Substances. INGRID CLAESSON AND STIG CLAESSON,* *University of Uppsala, Sweden.*—Some preliminary experiments have been carried out in order to investigate the possibilities of using adsorption analysis in the study of high polymeric substances. The experimental arrangements for adsorption analysis developed by Tiselius and one of the present authors will be described. So far the so-called *frontal analysis* has been used. This means that the solution is forced through a column with adsorbent and the concentration of the effluent is followed continuously with a micro-interference-refractometer. Activated charcoal has been used as adsorbent. It has been possible to show the occurrence of different discrete fractions in nitrocelluloses, polyvinylacetates, and synthetic rubbers. The fractions are similar in molecular weight only as they fail to show up as separate boundaries when the original rather polydisperse solution is ultracentrifugated. The fractions from the adsorption analysis are less polydisperse than the original solution. From a separate study it has been found that the amount adsorbed decreases with increasing molecular weight of the high polymeric substances and the same is true for the rate of adsorption (diffusion effect) which is rather slow. Both these effects will cause the higher molecular species to occur in the first fractions, making it possible to fractionate high polymeric substances according to molecular weight. The separation factor is however not large enough to account for the occurrence of the discrete fractions mentioned earlier. Thus it appears that adsorption analysis makes it possible to fractionate high polymeric substances both according to molecular weight and to other variables.

* Visiting Professor, University of California.

W3. Elasto-Viscous Properties of Polyisobutylene I: Relaxation of Stress in Whole Polymer of Different Molecular Weights at Elevated Temperatures. R. D. ANDREWS,[1] N. HOFMAN-BANG,[2] AND A. V. TOBOLSKY.[1]—Stress relaxation in polyisobutylene whole polymers of different average molecular weights has been investigated over the temperature range 30°–100°C at different elongations. The relaxation curve for a given molecular weight, when plotted as "reduced stress" *vs.* logarithmic time, has the same shape at different temperatures, differing only in position along the time scale. Activation energies for relaxation, calculated by use of the Arrhenius equation, are found to be experimentally identical for the different molecular weights, having the average value 15.4 kcal. The shape of the relaxation curve is independent of elongation up to approximately 70 percent elongation; beyond this value the relative decrease in stress between any two arbitrary time values increases with increasing elongation. The relaxation curve does not correspond to exponential, hyperbolic tangent, or exponential integral functions; the experimental points are fit best by a hyperbola. Reciprocal viscosity average molecular weight plotted against the logarithm of the time at which the reduced stress has a certain arbitrary value, at a fixed temperature and elongation, yields straight lines. Relaxation rate depends on molecular weight with sufficient sensitivity so that stress relaxation may be a practical method of measuring the molecular weights of raw polymers directly in the solid state.

[1] Frick Chemical Laboratory, Princeton University, Princeton, New Jersey.
[2] Present address: The Technical University of Denmark, Copenhagen, Denmark.

W4. The Viscosity of Glass. HOWARD A. ROBINSON AND EDWARD M. MAN, JR., *Armstrong Cork Company.*—A careful study has been made of empirical formulae which have been proposed connecting the viscosity of glasses with temperature. It is shown that the Waterton equation

$$\eta = A \exp\left[\frac{b_0}{T} e^{B/T}\right],$$

and the Fulcher equation,

$$\eta = A \exp[B/(T-T_0)],$$

are essentially identical and that both can be made to fit experimental results well within the experimental error from $\log\eta = 16$ down to $\log\eta = 1.5$. Beyond these extremes the formulae diverge. It will be shown that A, B, and T_0, the constants of the Fulcher equation, are linear functions of glass composition. Factors will be presented for the two component Na_2O-SiO_2 glasses: Successful applications of these ideas have been made to glasses containing as many as eight components. It is, therefore, possible to calculate the viscosity of glasses of quite wide compositional ranges by means of these empirical factors with an average accuracy of less than five degrees Centigrade for each viscosity point calculated.

W5. Use of the Electron Microscope in Exploring the Smoothness of Surfaces. ROBLEY C. WILLIAMS, *University of Michigan.*—The application of the electron microscope in the study of surface detail has been greatly extended in recent months by the improvement of techniques which allow extremely small irregularities to be photographed. It is now possible to discern sharp surface discontinuities of magnitude less than 5 angstrom units. The methods have been used to explore the detail in the surfaces of polymers such as collodion, polyvinyl formal (Formvar), and polythene, and in the surfaces of nonorganic materials such as crystals, thin evaporated films, and glass.

B1. Interpretation of the Triton Moment. R. G. SACHS, *University of Wisconsin.*—The present status of the interpretation of the triton moment will be summarized. Two distinctly different approaches to the problem have been taken: (1) Villars has estimated the contribution to the moment of the exchange current produced by a pseudoscalar meson field and has found it to be adequate. Presumably other types of meson field would also produce the required exchange current. (2) The character of the wave function required to explain the moment in the absence of exchange currents has been determined. It was found in this case that the wave function must contain a large admixture of ^3P, ^4P, and ^4D states. A measurement of the He^3 moment would lead to a clearcut decision between the interpretations (1) and (2), since (1) leads to a He^3 moment ten percent greater in magnitude than the neutron moment while (2) leads to a He^3 moment no more than six percent greater. A decision in favor of (2) would appear to indicate the existence of strong three body spin-orbit interactions in nuclei since a binding energy calculation has indicated that the tensor interaction would not lead to a wave function containing the required admixture of states. A decision in favor of (1) would seem to be strong evidence for the existence of meson exchange currents in nuclei.

B2. The Hyperfine Structure of K^{40}.* LUTHER DAVIS, JR. AND JERROLD R. ZACHARIAS. *Massachusetts Institute of Technology.*—The atomic beam magnetic resonance method has been used to determine the hyperfine structure $\Delta\nu$ of K^{40} and to make a positive assignment of the results to the nucleus of mass 40. The apparatus used in these measurements was similar to that described by Zacharias, but with the addition of a mass spectrometer in place of the usual surface ionization detector, which in this case serves as the source of ions for the mass spectrometer. The mass spectrometer reduces the general background due to other alkali atoms in the apparatus and other isotopes of potassium in the beam. The entire apparatus has been designed for measurements with artifically radioactive nuclei, such as Na^{22}, and a special oven with a long exit canal was used to conserve material. At mass number 40 transitions were observed at weak field and low frequencies (2 to 8 Mgc) which correspond to an alkali atom with a nuclear spin of 4. A resonance at 1285.745 Mgc in a field of 2.58 gauss and another at 1285.774 Mgc in a field of 3.37 gauss when weighted yield a value of the $\Delta\nu$ for K^{40} of $1285.73 \pm .05$ Mgc. This confirms previous results.

* This work has been supported in part by the Signal Corps, the Air Materiel Command, and the Office of Naval Research.

B3. An Ion Source for Isotopic Mass Comparisons. A. E. SHAW, *Argonne National Laboratory.*—Experiments have been continued with the source of positive ions described in a previous paper[1] in which solid samples were heated in a tungsten crucible to a high temperature by electron bombardment. It was found that a fraction of the bombarding electrons may be used to ionize neutral atoms as they leave the crucible. Ionized atoms with all charges up to six have been observed with 500-volt electrons. This source is suitable for comparing the masses of the isotopes of heavy elements with those of the light elements for which more accurate masses are known. Preliminary observations have been made with a double-focusing mass spectrograph on the doublet, $Cu^{+1}-Pt^{+6}$, at mass 65. Uranium ions with four charges appear at the equivalent mass 59.5 and have been compared with the nickel masses. Platinum with six charges can be compared with the oxygen molecule at mass 32; and platinum with five charges with potassium 39.

[1] Phys. Rev. 71, 277 (1947).

B4. The Packing Fraction of Zirconium. WILFRID RALL,* *Metallurgical Laboratory.*—The packing fraction of the zirconium isotopes, relative to uranium, has been determined directly. Mass spectra permitting comparison of doubly charged zirconium ions with quintuply charged uranium ions were obtained with a double-focusing mass spectrograph of the type used by Dempster[1] with a spark as source of ions. Since quintuply charged uranium-238

occurs at 47.6, only the zirconium isotopes at 46, 47, and 48 were measured. The zirconium-uranium packing fraction difference was calculated from measurements of eighteen mass spectra, on the assumption that it was the same for the three zirconium isotopes. The value obtained was $-(12.1\pm0.9)\times10^{-4}$. This agrees, within the experimental error, with the curve given by Dempster,[1] since his value of 5.6×10^{-4} for uranium gives $-(6.5\pm0.9)\times10^{-4}$ for zirconium. However, more precise measurements are necessary fully to check the smoothness of the packing fraction curve in this region. Evidence for a source of error inherent in the method of obtaining these mass spectra was indicated by the variation in relative position of lines which was greater than the error of measurement.

* Now a Fellow of the Institute of Radiobiology and Biophysics, University of Chicago.
[1] A. J. Dempster, Phys. Rev. 53, 64 and 869 (1938).

B5. Radioactive Selenium 73 and 75. WILLIAM S. COWART AND M. L. POOL, *Ohio State University.*—Germanium was bombarded with 20-Mev α-particles and the arsenic and selenium fractions were removed by chemical separations. A new activity of 7.0-hours half-life was found in the selenium fraction. The emission was found to consist of 1.29-Mev positrons (0.59 g/cm² Al) and a small amount of x-rays which had a wave-length of about 1.2A. K-electron capture is thus evident in this short positron period. Gamma-rays if present were very weak compared to the annihilation radiation. Since the activity is not produced by deuteron bombardment of As or Se, the assignment is made to Se^{73}. The decay is into a long period, presumably the 90-day period of As^{73}. No evidence of decay into the 2.08-day period of As^{73} was found. Alpha-particle bombardment of Ge and deuteron bombardment of As give a long period activity in Se^{75}. Based upon nearly three years of decay a value of 127 ± 2 days was found. Decay is by K-electron capture.

B6. Threshold for Proton-Neutron Reaction in Copper. W. E. SHOUPP, B. JENNINGS, AND W. JONES, *Westinghouse Research Laboratories.*—The threshold energy for the production of neutrons from the bombardment of copper with protons has been measured with a BF_3 chamber, surrounded with paraffin, as a neutron detector. The proton energy was calibrated against the $Li^7(p,n)$ reaction previously reported. The (p,n) threshold occurs at $E_t=2.164$ Mev giving $Q=-2.131\pm.01$ Mev, and is evidently associated with the copper isotope Cu^{65}. This gives for the mass difference, $(Zn^{65}-Cu^{65})=1.376$ Mev. Using 64.955 mμ for the mass of Cu^{65}, the mass of Zn^{65} is 64.956 mμ. Since the Zn^{65} decays by positron emission, the maximum energy of the positron spectrum may be computed to be 0.355 Mev.

B7. The Electro-disintegration of Cu^{63}, Ag^{107}, and Ag^{109}. J. S. LAUGHLIN, L. S. SKAGGS, A. O. HANSON, AND J. J. ORLIN, *Urbana, Illinois.*—The external electron beam from the University of Illinois betatron has been used to study the electro-disintegration of Cu^{63}, Ag^{107}, and Ag^{109} with electrons of energies 13 Mev, 16 Mev, and 17½ Mev. Sets of thin, uniform foils were inserted in the electron beam and the activities induced by the concommittant electro- and photo-disintegration reactions measured. The intercept in the first foil of the linear increase of activity as a function of foil position represents the electro-disintegration effect plus a small, known background x-ray effect. The electron current was measured by placing an open air ionization chamber just behind the foils which collected the ionization produced by the electrons which passed through the foils. The cross sections for the $(e;n,e')$ reaction at 16 Mev were determined to be 17, 49, and 77×10^{-29} cm² for Cu^{63}, Ag^{107}, and Ag^{109}, respectively. The slope of the activity curves together with the theoretical value of the radiation cross section and the x-ray spectrum were used to estimate the photo-disintegration cross sections. These were consistently 400 times greater than those for electro-disintegration.

B8. Technique of Producing an External Beam of Electrons from the Betatron. L. S. SKAGGS, J. S. LAUGHLIN, AND L. H. LANZL, *Urbana, Illinois.*—The beam is removed from the University of Illinois betatron, using a magnetic shunt of laminated iron mounted inside a specially designed donut.[1] The mounting allows considerable motion of the shunt with respect to the donut. The electron orbit is sensitive to the position, size, and shape of the magnetic shunt; too close proximity to the equilibrium orbit or too great a height causes automatic expansion of the orbit before the electrons have reached their maximum energy. A standard injector is used with its entire structure at a greater radius than that of the entrance end of the magnetic shunt. The perturbation of the magnetic field due to the shunt is removed at the time of injection by firing a 12-microsecond saw tooth pulse through a degaussing coil which surrounds the shunt. The beam emerges from the donut through a 1.5-mil Duralumin window and has a width of about 0.7 cm and a height of 0.2 cm. The duration of the pulse of mono-energetic electrons is less than one microsecond and the energy can be continuously varied. The current is of the order of 10^{-8} amperes.

[1] L. S. Skaggs, G. M. Almy, D. W. Kerst and L. H. Lanzl, Phys. Rev. 70, 95 (1946).

B9. Search for Weak Natural Radioactivities by the Method of Active Daughter Extraction. TRUMAN P. KOHMAN, *University of Chicago.*—It has been suggested[1] that some of the apparently stable nuclides of even mass number which lie near the stability limits may actually be beta-labile with very long lifetimes. The immediate decay products would be relatively short-lived radionuclides, which by chemical extraction would be extremely sensitive indicators for the activity of the parents. Ca^{48} appears to be well outside the zone of stability.[2] A test for the presence of 44-hour Sc^{48} in 3-kg calcium gave negative results, indicating a minimum half-life for Ca^{48} of 5×10^{18} years. Sn^{115} seems definitely outside the stability zone for odd

mass numbers. In^{115} has a 4.5-hour metastable state, to which Sn^{115} should decay if the $Sn^{115}-In^{115}$ mass difference exceeds the In^{115*} excitation energy, 0.338 Mev. A search for In^{115*} in 1.2-kg tin showed no activity, indicating a minimum half-life for this mode of decay of Sn^{115} of 5×10^{14} years. Since Sn^{115} and In^{115*} have the same spin, this sets an upper limit to the $Sn^{115}-In^{115}$ mass difference at 0.34 Mev.

[1] T. P. Kohman, "The limits of beta-stability," Phys. Rev. 73, 16 (1948).
[2] See also I. Joliot-Curie, J. de phys. et rad. [8] 6, 209 (1945), and Saha and Saha, Nature 158, 6 (1946).

B10. Performance of an Electron Multiplier Tube Counting Alpha-Particles. S. K. ALLISON AND L. DEL ROSARIO, *University of Chicago.*—Alpha-particles from polonium were slowed down in air and admitted to an electrostatic deflector which selected energies (homogeneous to ~1 percent) in the range between 0.4 and 1.6 Mev. The particles were then detected by an electron multiplier tube of the type developed by J. S. Allen, having 12 beryllium copper electrodes. The pulses put out by the tube were electronically amplified in voltage by factors of 273, 546, and 1082 in various trials, and scaled and counted on conventional equipment. The combination of the tube and the relatively low external amplification constitutes a very reliable and stable detector of the presence of alpha-particles; for instance, when counting 1150 particles per minute the background, with the polonium screened off, would be 20 per minute. The distribution of pulse heights is fully developed at 500 volts per stage in the tube. At a pressure of 4×10^{-5} mm, half the alpha-pulses put out by the tube were less than 0.03 volts in height and half above this value. A corresponding point in pulses from electrons whose energies were not accurately known but must have been less than 34 kev occurred at 0.005 volts, and if pulses less than 0.04 volts were discriminated against, the equipment responded only to alphas in the presence of betas. It is possible that at lower pressures than ours, the alpha-pulse height distribution might be different.

X1. A Theory of Commercial Yarn Testing. CHARLES J. GEYER, JR.,* C. H. REICHARDT,** AND GEORGE HALSEY,** *Textile Foundation.*—A method has been devised for the application of the theory of the three-element shear model of Eyring and co-workers to textiles which does not necessitate the location of the "basic spring line" and thus is readily applicable to both yarn and fiber tests and to the commercial inclined-plane and pendulum-type testers. It is also applicable as a first approximation to those textiles which do not possess a "basic spring line" as such. The method employs the conventional spring constants or elastic moduli but determination of the viscous constant involves the magnitude of the relaxation in constant rate of elongation experiments (or the magnitude of the creep in constant rate of loading experiments) from the upper envelope per interval of time. The relationship has been employed to establish the correlation between the visco-elastic properties of "slashed" and "unslashed" viscose tire cord rayon yarns and also to show the identity of single filament stress-strain relationships with those of yarns of normal twist of the same textile. The simplicity of technique which enables this method to be used as a routine laboratory test for the determination of the visco-elastic properties of textiles affords it a distinct advantage over previous methods, which were often unsatisfactory from both a theoretical and an experimental viewpoint.

* American Viscose Corporation, Front Royal, Virginia.
** Fellows, The Textile Foundation.

X2. Creep, Recovery, and Permanent Set for GR-S and Hevea. S. D. GEHMAN, *Goodyear Tire and Rubber Company.*—In all of the tests with Hevea and GR-S, a considerable part of the creep was due to permanent set. The proportion increases with the elongation and duration of the test. At low elongations, GR-S shows much more creep than Hevea but a smaller portion of it is due to permanent set. At the start of the creep test, the flow appears to be due largely to the reversible yielding of relatively weak bonds which can reform under the action of the elastic network when the load is removed. For longer periods of time or for higher elongations, the flow involves more deep-seated changes in structure. Larger units of structure are displaced or stronger bonds broken with resultant permanent molecular displacements upon removal of the load. For Hevea at high elongations it is probable that flow occurs in the amorphous material between the crystallites with whole crystallites being displaced with reference to each other. Under such circumstances, the original relative molecular configurations cannot be reassumed upon removal of the load. Correction of the creep curves for permanent set gives nearly straight lines on a plot against logarithmic time.

X3. The Thermodynamics of a Strained Elastomer. I. General Analysis. M. MOONEY, *United States Rubber Company.*—The thermodynamic functions of principal interest in a strained elastomer are the entropy and energy of deformation. The volume is of secondary importance, and it can be assumed, with sufficient accuracy for most purposes, that the volume is linear in the temperature and the mean pressure. The basic partial differential equations of thermodynamics can then be integrated, yielding expressions for the energy and entropy of deformation in terms of observable quantities. In the present analysis the volume effects due to changes in mean pressure and crystallinity are taken into account; the effects associated with change in shape are sharply separated from those associated with change in volume. It is shown that the superelastic functions of deformation previously published* have a very general validity.

* M. Mooney, J. App. Phys. 11, 582 (1940).

X4. The Thermodynamics of a Strained Elastomer. III. The Thermal Coefficient of Modulus and the Statistical Theory of Elasticity. L. E. COPELAND AND M. MOONEY, *United States Rubber Company.*—Published thermoelasticity data are critically analyzed by means of thermodynamic equations developed in the first paper of this

series. Equations known to be of the proper form are fitted by least squares to the experimental data, which were first corrected to allow for the changes in shape when tested under variable temperature and constant volume. If the measurements are accepted as truly reversible, the data show that several different elastomers depart considerably in some respects from the predictions of the statistical theory of elasticity. Some thermoelasticity measurements in torsion are reported which seem to give the most reliable evidence that stress is proportional to absolute temperature.

X5. The Effects of Pile Bombardment on Uncured Elastomers.* W. L. DAVIDSON, *Clinton National Laboratory and B. F. Goodrich Company*, AND I. G. GEIB, *B. F. Goodrich Company*.—Previous work on the effects of ionizing radiations on hydrocarbons has established that four competitive processes are usually operative: (1) Dehydrogenation, (2) condensation or polymerization, (3) hydrogenation (action of nascent hydrogen on any unsaturated matter present), (4) decomposition (C—C cleavage). The chain reacting nuclear pile offers an ideal means for subjecting relatively thick samples of matter (such as rubber) to uniformly high concentrations of radiation. Such studies on natural rubber, butyl rubber, and polyisobutylene allow one to draw the following conclusions: (1) Uncured natural rubber undergoes a slight curing action when exposed to pile radiations. (2) Polyisobutylene samples are appreciably degraded by pile radiations. (3) The same effects as noted in (1) and (2) are greatly enhanced by secondary alpha-particles, produced by an (n, α) reaction on boron^{10} (milled into the elastomer). However even a 2-hour bombardment of natural rubber yields a product greatly inferior to sulfur vulcanizates. (4) Pile bombardment does not introduce measurable unsaturation in polyisobutylene and decreases the unsaturation in natural rubber but slightly. (5) A typical butyl rubber stock is permanently degraded by pile irradiation showing upon cure reduced tensile strength compared to that of a control sample. (6) Natural rubber shows a weak but measurable radioactivity days after bombardment, probably because of its mineral content. polyisobutylene is not appreciably active.

* Part of the experimental work for this report was performed for the Atomic Energy Commission while Dr. W. L. Davidson was a member of the Clinton Laboratories Training School on leave from the B. F. Goodrich Company.

Y1. The Hydrolysis of Proteins. H. B. BULL, *Northwestern University*.

Y2. Proteins as Polycondensations of Amino Acids. DOROTHY WRINCH, *Smith College*.—The native proteins are polycondensations of α-amino acids, $NH_2-CHR-COOH$, in *levo* form, about 21 different species and 2 cyclic amino acids being recorded to date. The proteins are of unknown structure and the question then arises as to the light, if any, which polycondensations of known structure can throw upon this problem. The similarities and dissimilarities of proteins in particular and high molecular weight substances in general are discussed. The latter, several of which belong to the domain of crystal physics, are far more striking. They include the perfection of regularity of atomic arrangement attained by protein crystals and the high prevalence of twinning. The implications of the facts include the following. (1) While high molecular weight substances in general are "open" structures, whether they be chains (with or without branches or cross bonds) or 2- or 3-dimensional networks, the molecules of protein are "closed." (2) Some or all of the monomers in proteins have functionality higher than 2. Possibilities regarding this higher functionality are investigated. The further implications for the structure of proteins of the facts assembled are discussed, particularly the existence of protein twins, which leads to a new theory of twinning.

Y3. Studies of the Melting Points, Rigidities, and Optical Activities of Gelatin Gels. JOHN D. FERRY AND JOHN E. ELDRIDGE, *University of Wisconsin*.—Four ossein gelatin samples, previously degraded to varying extents to give number-average molecular weights ranging from 17,000 to 45,000, have been studied in solution in 0.15 M NaCl at *p*H 7. Gels were formed by chilling solutions at 0° for 24 hours and then subjected to the following measurements: (1) melting point as a function of gelatin concentration and degree of degradation, (2) rigidity as a function of temperature and degree of degradation, (3) optical activity as a function of temperature and degree of degradation. The melting point data gave a series of straight lines, one for each sample, when the logarithm of the concentration was plotted against the reciprocal of the absolute temperature of melting; the slopes were identical. With increasing temperature, the gel rigidity approached zero while the optical activity decreased to a constant value which was independent of molecular weight. In every case, the rigidity disappeared at a lower temperature than that at which the optical activity attained its minimum value. At a given temperature below the melting point, both rigidity and optical activity increased with increasing molecular weight. The gelation process is regarded as the formation of a three-dimensional network due to the gradual cross-linking of gelatin molecules at rather widely separated points. The optical activity curves indicate that some of these cross-links exist above the melting point but disappear above 40°C.

Y4. Viscosity and Streaming Birefringence of Nucleic Acid. JESSE P. GREENSTEIN, *National Institute of Health*.—Aqueous solutions of the tetrasodium salt of thymus nucleic acid show anomolous viscosity and intense birefringence of flow. The compound behaves monodisperse in the ultracentrifuge and an S=11 has been calculated for a highly polymerized sample tested. When such solutions are irradiated by ultraviolet light (2537A) or by x-rays, these properties are considerably diminished at a rate which is roughly proportional to the amount of radiation administered. On cessation of ultraviolet irradi-

ation, the reduced value for the viscosity remains constant. On cessation of x-irradiation, the reduced value for the viscosity diminishes further with time of standing. There are thus two consecutive phenomena as a result of x-irradiation, that which occurs during irradiation and which has no apparent temperature coefficient, and that which occurs after irradiation has ceased, and which is dependent upon the temperature. The average S for the particles of nucleic acid after x-irradiation is about 5. Such particles do not pass through cellophane. No ammonia or phosphate is released. A similar reduction in viscosity and birefringence occurs in nucleic acid solutions treated with various salts, and with proteins.

Y5. The Study of Macromolecular Reactions of Biological Interest. PAUL DOTY, *Notre Dame University.*

C1. On the Neutral Meson. R. E. MARSHAK, *University of Rochester.*—It is proposed to accept the hypothesis of Anderson *et al.*[1] that the light meson decays into an electron and a neutral meson of mass 70 Mev, and to identify this neutral meson with the unobserved particle accompanying the light meson in the disintegration of the heavy meson. This identification has the following three consequences: the mass of the heavy meson is 180 Mev (which is within the experimental error of the British measurements), the spin of the heavy meson is $1/2\hbar$ (independent of the spins of the light and neutral mesons), and the capture of light negative mesons by heavy nuclei can still be explained in terms of the virtual creation of negative heavy mesons directly coupled to nucleons. If, further, the neutral meson is assumed to be directly coupled to the nucleon, and to possess a spin of zero, the capture of a negative light meson by a nucleus and the decay of light mesons should be accompanied by the emission of two light quanta. If the neutral meson is coupled to the nucleon, together with the heavy meson (so that its spin is $\frac{1}{2}\hbar$), it will not emit gamma-rays.

[1] Anderson, Adams, Lloyd, and Race, Phys. Rev. 72, 724 (1947).

C2. Sea Level Latitude Effect of Cosmic Radiation.* PETER A. MORRIS, W. F. G. SWANN, AND H. C. TAYLOR, *Bartol Research Foundation.*—On a recent voyage from Rio de Janeiro to Boston the vertical intensity of the total and hard components of the cosmic radiation were measured with a Geiger-counter telescope apparatus, with the following results:

Percentage diminution in the vertical intensity.

Telescope	Total radiation no lead	Hard component 8 cm	Hard component 16 cm	Soft component 8-cm diff.	Soft component 16-cm diff.
1 and 2	5.05±0.55	5.26±1.27	5.36±1.33	4.3±4.6	4.5±4.3
1	5.34±0.77	4.96±0.92	6.20±0.97	6.0±2.8	3.7±2.9
2	4.76±0.75	5.56±0.88	4.51±0.91	2.6±3.7	5.3±3.2
Combined		5.32±0.46		4.46±0.61	

Careful consideration has been given to the probable errors as derived from statistical analysis, and the results are interesting as indicating, more reliably than heretofore, a latitude effect for the soft component comparable with that for the hard component.

* Supported by funds from the Navy and from the National Geographic Society; also by airplane services from the U. S. Army Air Force.

C3. High Energy Atmospheric Showers.* HENRY L. KRAYBILL, *University of Chicago.* (*Introduced by Marcel Schein.*)—The altitude dependence of high energy atmospheric showers in the cosmic radiation was measured between 30,000 and 40,000 feet pressure altitude in a B-29 airplane. The counting rate of counters in threefold coincidence was determined for horizontal counter separations of 9 feet, 13.5 feet, and 42 feet. The counting rate of the counters separated by 13.5 feet was found to be equal to the rate of counters separated by 9 feet. The counting rate of counters with separation of 42 feet was 0.6 of the rate of counters with spread of 9 feet. The counting rate of both the large and the small separations decreased with altitude above 30,000 feet. Near 40,000 feet the combined counting rate of the counters with separation of 9 feet and 13.5 feet was approximately two-thirds of their rate at 30,000. These results, together with previously reported measurements[1] between 15,000 feet and 33,000 feet, show the existence of a maximum in the frequency *versus* altitude curve of high energy atmospheric showers at an elevation near 30,000 feet.

* The research described in this abstract was supported in part by U. S. Navy.
[1] Henry L. Kraybill and Paul J. Ovrebo, Phys. Rev. 72, 351 (1947).

C4. The Mean Life of Negative Mesotrons.* HAROLD K. TICHO, *University of Chicago.*—The fact that negative mesotrons stopped in materials of low atomic number do disintegrate has been explained as resulting from comparable probabilities for disintegration and capture by the nuclei of the absorber. If this explanation is valid, a change of the mean life of negative mesotrons should occur.[1] To establish this effect experimentally, and to determine whether it has any bearing on the recent result for the mean life obtained at Climax,[2] a magnetic lens and a special timing circuit were used such that the mean lives of positive and negative mesotrons could be determined separately. The precision of this device will be discussed.

* The research described in this abstract was supported in part by U. S. Navy.
[1] Harold K. Ticho and Marcel Schein, Phys. Rev. 72, 248 (1947).
[2] Harold K. Ticho, Phys. Rev. 72, 255 (1947).

C5. The East-West Asymmetry of the Mesotron Component at 35,000 Feet.* VICTOR H. YNGVE, MARCEL SCHEIN, AND HENRY L. KRAYBILL, *University of Chicago.*—The East-West asymmetry of mesotrons passing through 22 cm of lead was measured in a B-29 airplane at altitudes between 30,000 feet and 40,000 feet. At 27° north magnetic latitude and at an elevation of 35,000 feet the asymmetry at a 45° zenith angle was found to be 45 percent. This

very large asymmetry is close to the predicted theoretical value, assuming that the primaries in the energy range covered by the experiment are all positively charged. The predicted value is obtained from the observed latitude effect and the theory of Lemaitre and Vallarta. Since a large fraction of the primaries are included within the energy range covered by this experiment, it is obvious that the mesotron-producing component of the cosmic radiation predominantly consists of primary protons.

* The research described in this abstract was supported in part by U. S. Navy.

C6. Burst Production at an Altitude of 11,200 Feet.* E. F. FAHY AND MARCEL SCHEIN, *University of Chicago.*—The frequency of large cosmic-ray bursts were detected in coincidence with extensive atmospheric showers registered by four independent counter coincidence sets spread over the chamber in a horizontal plane. The chamber, which was filled with 50 atmospheres of pure argon, was first surrounded by 7.7 cm of lead and later by 12 cm of lead. Only a few percent of the large bursts under the lead were accompanied by extensive atmospheric showers at an altitude of 11,200 feet (Climax, Colorado). Since these bursts are very absorbable in the atmosphere between 11,200 feet and sea level, it is suggested that they should originate from the disintegration of mesotrons with a lifetime shorter than 10^{-3} second.

* The research described by this abstract was supported in part by U. S. Navy.

C7. Calculations on the Mesotron Distribution at the Geomagnetic Equator.* J. STEINBERGER AND MARCEL SCHEIN, *University of Chicago.*—The energy spectrum at sea level and the intensity *versus* altitude curve were calculated for mesotrons at the geomagnetic equator. The assumptions were similar to those made in a previous calculation by the authors.[1] The energy spectrum at sea level is in rough agreement with the experimental data; however, the maximum occurs at energies higher than the one measured by J. G. Wilson.[2] This could actually be due to a production of low energy mesotrons in the lower part of the atmosphere.

* The research described in this abstract was supported in part by U. S. Navy.
[1] Marcel Schein and J. Steinberger, Phys. Rev. **72**, 734 (1947).
[2] J. G. Wilson, Nature **158**, 414 (1946).

C8. The Absorption Curve of Mesotrons On Mount McKinley, Alaska.* MARCEL SCHEIN AND THOMAS H. CARR, *University of Chicago.*—The penetration of mesotrons was measured through thicknesses of 10, 20, 30, 40, and 50 cm of lead at an elevation of 18,200 feet above sea level. Special precautions were applied to minimize the effect of scattering in the lead. The data show that a large number of mesotrons is present between energies of 1.5×10^8 ev and 7×10^8 ev at this altitude. Using the measured energy spectrum on Mount McKinley, the diffusion of mesotrons was calculated between the elevations of 18,200 feet and 14,250 feet (Mt. Evans, Colorado). The results show that at 14,250 feet the theoretical number of mesotrons between 10^8 ev and 4×10^8 ev is considerably smaller than that actually found by experiment.[1] This fact strongly indicates that a secondary production of slow mesotrons exists in the lower part of our atmosphere.

* The research described in this abstract was supported in part by U. S. Navy.
[1] David B. Hall, Phys. Rev. **66**, 321 (1944).

C9. Mesotrons in the Stratosphere.* MARCEL SCHEIN, *University of Chicago.*—A discussion will be given of recent results on the intensity and on the production of mesotrons. These results were obtained in the high atmosphere in airplanes and balloons. In particular, the problem will be considered whether mesotrons of energies lower than 4×10^8 ev are produced in the primary act of mesotron creation.

*The research described in this abstract was supported in part by U. S. Navy.

C10. Periodic Variation of Ground Level Count of Cosmic-Ray Air Showers. PAUL J. OVREBO, *Aircraft Radiation Laboratory.*—Observations, with triple coincidence counters, of high energy atmospheric showers in the cosmic radiation have been made at ground level for a six month period between April 16 and October 16, 1947. The daily counting rate is found to undergo variation in a periodic fashion. A Cree analysis of the data suggests a period of 22 days. Assuming sine type of variation, different periods were fitted to the data by method of least squares. A maximum amplitude of 9.7 percent of the daily average count was found for a period of 21.5 days. The daily average count for the six months is 17.08. Comparison with the daily Zurich sun spot number showed no obvious correlation. No study of the relation with meteorological phenomena has as yet been made.

C11. On the Insensitive and Recovery Times of Self-Quenching Counters. S. S. FRIEDLAND, *Memorial Hospital and New York University* AND A. D. KRUMBEIN, *New York University.*—An investigation of the insensitive times and recovery times of self-quenching Geiger-Müller counters, using the method described by Stever, has been undertaken. Various quenching mixtures have been studied. The percentage of the quenching molecule present as well as the total pressure was varied to study their effects on the values obtained. Attempts will be made to correlate these data with existing theories.

C12. Pulse Shape of Self-Quenching Counters. C. D. THOMAS, *West Virginia University.*—An investigation of the shape of the pulse decay from a self-quenching counter has been carried out under the condition that the time constant of the circuit, including capacity in addition to that of the tube, is not negligible in comparison to the transit time in the tube. The resulting mathematical expression yields the voltage on the wire as a function of time and of physical constants of the counter and the circuit. In addition to the exponential decay, this formula contains product terms of it with an exponential integral and a term varying inversely with time. By varying conditions it is possible to approximate either pure self-quench-

ing or external quenching. Some data obtained by photographing pulses from counters using different circuit constants has been studied and compared to the predicted form.

D1. A Two-Dimensional Potential Problem with Application to Soil Drainage. DON KIRKHAM, *Iowa State College.*—A thin sheet of conducting material, surface conductivity γ, infinitely long, and of width H, rests coplanarly on rectilinear legs of the same material of width a, ($a \ll 2H$), height h, ($h \gtrsim a/2$), and equal spacing, A. On the longitudinal center line and at a distance $h-d$ from the base of each leg is located a circular electrode of radius r, ($r \lesssim a/4$). Utilizing former results,[1] the potential and flow are calculated when the uppermost surface is at potential V, the electrode zero. If $A > 2H$, the current per electrode I is approximately (an upper limit)

$$I = 2\pi\gamma V / \ln \cot^2 \frac{\pi a}{8H} \cdot \frac{\sinh \pi(2d-r)/a}{\sinh \pi r/a} \cdot \frac{\sinh^2 2\pi h/a - \sinh^2 \pi r/a}{\sinh^2 2\pi h/a - \sinh^2 \pi(2d-r)/a},$$

a result independent of A, also valid when the electrodes rest on the bases of the legs. This problem arises in the analogous groundwater case, that of seepage from waterlogged soil into long drainage tubes installed in trenches cut into an impervious substratum underlying a pervious upper layer, the trenches being back-filled with the pervious soil.

[1] D. Kirkham, Proc. Soil Sci. Soc. Am. (1947).

D2. The Cesium Rectifier. A. W. HULL, E. E. BURGER, AND R. E. TURRENTINE, *General Electric Research Laboratory.*—This is a new type of hot-cathode vapor rectifier, in which cesium vapor functions both as conducting gas and thermionic coating material. The cathode is of the familiar type used in thyratrons, namely, a multivane structure of nickel vanes, surrounded by a heat-shield. However, the vanes are uncoated except by the monatomic film of cesium which is reformed continually by condensation. The tube must be heated to approximately 150°C during operation, to maintain the desired vapor pressure of 0.01 mm. Cesium is unique in having the lowest ionization potential and the lowest thermionic work function of any known substance. Hence one would expect optimum efficiency from this dual use of cesium. This expectation appears to be realized, the over-all efficiency at 250 volts being better than 98 percent for the experimental tubes tested. Typical values are: cathode heating power, 200 watts; peak electron emission, 2000 amperes; voltage drop at 600 amperes, 3 volts.

D3. Response of a Linear System to an Input with Uniformly Increasing Frequency.* H. EKSTEIN, *Armour Research Foundation.*—This problem, or rather its mechanical analog, was previously solved exactly for the case of an L–C–R circuit by F. M. Lewis.** His method is too cumbersome for more general systems. An approximate solution, for slow frequency modulation, expressible in terms of elementary functions, is given. The problem reduces to the evaluation of the integral

$$I = \int_{-\infty}^{\infty} Y(p) \exp\left[-\frac{i(p-\omega)^2}{2\beta}\right] dp,$$

where Y is the admittance of the system, $\beta = \Delta\omega/\Delta T$ the rate of increase of the angular frequency, and ω the instantaneous angular frequency. The method of evaluation used is the saddle-point method (method of steepest descent). Features of the calculated response curve are:

1. The maxima of the response curve lag behind those of the quasi-stationary curve.
2. The maxima are lowered with respect to the quasi-stationary case.
3. At certain frequencies a damped oscillation appears (ringing).

The lag, the depression of the maximum, and the frequency at which "ringing" appears can be calculated in a simple manner although only approximately.

* Sponsored by Squier Signal Laboratories, Fort Monmouth, New Jersey.
** F. M. Lewis, Trans. A.S.M.E. **54**, 253 (1932).

D4. Transit Time of Electrons between Electrodes of Simple Geometry. DELBERT N. EGGENBERGER AND PAUL L. COPELAND, *Illinois Institute of Technology.*—In simple cases the transit of an electron starting from rest is proportional to the length of path and inversely proportional to the square root of the potential difference through which the electron falls. The dependence of the proportionality factor on the geometry and on the current density has been treated mathematically in those cases for which a simple symmetry exists. In the absence of space charge the transit time is computed directly by the aid of the known potential distribution and the energy equation. Where space charge exists, the definition for current density, Poisson's equation, and the energy equation are combined to give an expression for the transit time of electrons. This expression has been evaluated for complete space charge by the use of the solutions for current as a function of potential difference which have been developed by Langmuir and Blodgett[1] and by Page and Adams.[2] Approximations have been made to give the transit time as a function of current density.

[1] Langmuir and Blodgett, Phys. Rev. **24**, 49 (1924).
[2] Page and Adams, Phys. Rev. **68**, 126 (1945).

D5. Further Study on Direct Coupled Pentode Pair and Decade Rings. LEO SEREN AND LAWRENCE JONES, *General Electric Research Laboratory.*—Pentode pairs, in which the plate of one pentode is tied to the screen grid of another, and vice versa, have been studied further.[1,2] Such a pair has two distinct states of equilibrium and is used in scalers, electronic switches, etc.[3] Topics that will be discussed include: (1) stability of the pair for different plate resistors, plate supply voltages, and grid bias voltages; (2) triggering adjacent pentode pairs by means of triodes; (3) shape and size of pulse for triode triggering; (4) resolution of the triggering action for closely spaced input pulses; (5) power requirements. One result of this study has been a decade ring which has a resolution better

by a factor of two than that reported in the past for direct coupled pentode pairs.[2] Using 6AK6 pentode pairs with 21,000-ohm plate resistors a decade ring has been built which resolves any two pulses as close as 0.9 microsecond and three pulses as close as 2.0 microseconds.

[1] V. H. Regener, Rev. Sci. Inst. 17, 180 (1946).
[2] Leo Seren, Rev. Sci. Inst. 18, 654 (1947).
[3] V. H. Regener, Rev. Sci. Inst. 17, 185, 375 (1946); also see reference 2.

D6. An Electronic Analogy Computer for Studying Servomechanism Response. M. SHEPHERD, JR.,[1] J. H. BALDWIN,[2] AND G. H. FETT, *University of Illinois.*—A servomechanism analogy computer has been developed which utilizes electronic circuits to represent the actual components. All system elements have been reduced to equivalent resistors and capacitors together with appropriate mixing and feed-back circuits. The computer has all constants of the system referred to a new time base so that the transients developed in the system can be observed visually on a cathode-ray oscilloscope. A force function of either step displacement or step velocity is impressed at a frequency of 20 cycles per second, the transient is viewed for about 0.01 second, and the remainder of the time is utilized to restore the system to equilibrium. A detailed example of a servomechanism is given, in which an amplifier controls the field current of a d-c generator which supplies power to a separately excited d-c motor. The counter e.m.f. of the motor is arranged for by an appropriate feed-back and mixing link between the motor load analogy and the armature input circuit analogy. Both stable and unstable servomechanism arrangements can be examined with this computer. The effect of changing circuit parameters is easily noted by the change in oscillograph pattern.

[1] At present with Farnsworth Radio and Television Corporation.
[2] Westinghouse Educational Fellow, University of Illinois, 1947; at present with Electronic Laboratories of Canada, Ltd., Vancouver, B.C.

D7. Shaped Field for 180° Spectrograph. F. M. BEIDUK AND E. J. KONOPINSKI, *Indiana University.*—A 180° spectrograph built recently by L. M. Langer employs the magnetic field between two annular ring pole faces. This construction permits a shaping of the radial dependence which causes perfect focusing of the electrons diverging from a point source on the main circle and moving in the median plane between the poles. The condition for this may be expressed by

$$\int_0^{\delta_0} \frac{(f+\gamma)d\delta}{(1+\delta)[(1+\delta)^2-(f+\gamma)^2]^{\frac{1}{2}}}=\frac{\pi}{2}. \qquad (1)$$

δ is the radial distance from the main circle in units of its radius; γ is the direction cosine of the emerging electron; δ_0 is the root of the radical in the integrand; f is the vector potential multiplied with the distance from the center in proper units. A solution in power series gives the result for the magnetic field:

$$H=H_0\left[1-\frac{3}{4}\delta^2+\frac{7}{8}\delta^3-\frac{9}{16}\delta^4+\frac{51}{320}\delta^5\cdots\right]. \qquad (2)$$

This disagrees with Boch's* earlier calculation, beyond the first two terms. Boch starts with an approximation formulated by Hartree, in place of (1), which makes his higher order terms meaningless. The discrepancy was discovered by Langer in a graphical plot of the orbits. The shaped field also supplies some focusing of electrons deviating from the median plane but only outside the main circle.

* Rev. Sci. Inst. 4, 575 (1933).

D8. Force between Magnets in a Medium. JOHN A. ELDRIDGE, *State University of Iowa.*—The force between magnetic poles in a medium is usually given as $F=m_1m_2/\mu r^2$. This follows from the relations $\mathbf{B}=\mathbf{r}_0m/r^2$ (where $\mathbf{r}_0$ is a unit vector) and $\mathbf{F}=m\mathbf{H}$. Several writers (Wilberforce, Page, Adams, Murdock) have remarked that these relations are incorrect. To obtain a correct relation *magnetic pole* must be exactly defined: Pole density $(\alpha)=-\text{div.}\mathbf{P}$, where $\mathbf{P}$ is the intensity of magnetization (magnetic polarization). It then follows that $\mathbf{H}=\int\mathbf{r}_0\alpha d\tau/r^2$, or for large r (where we can consider poles as points) $\mathbf{H}=\mathbf{r}_0m/r^2$. It can also be shown that the force on a pole is given by $\mathbf{F}=\int\mathbf{B}\alpha d\tau$ or for a point pole $\mathbf{F}=\mathbf{B}m$. Since $\mathbf{B}=\mu\mathbf{H}$ the force between point poles becomes $F=m_1m_2\mu/r^2$, where m_1, m_2 are the poles actually existing, including the poles in the medium. The results show that the force between two ideal permanent magnetic shells is increased (not decreased) by the presence of a paramagnetic medium, exactly as for the force between currents. (Similar relations hold for ideal electrets.) More aptly the force between magnets can be regarded as a force between "apparent currents" I_1, I_2, where the apparent current density σ is defined by $\sigma=\text{curl.}\mathbf{P}$. Here $\mathbf{B}$ (not $\mathbf{H}$) is obtained from $\mathbf{I}$ by the Biot-Savart law and $\mathbf{F}=\mathbf{I}\times\mathbf{H}dl$ (not $\mathbf{I}\times\mathbf{B}dl$).

D9. The Magnetic Susceptibility of Uranium Oxalate. C. A. HUTCHISON AND N. ELLIOTT, *University of Chicago.*—Magnetic susceptibilities of tetravalent uranium compounds published in the literature may be interpreted as showing the U^{4+} ion to be in a $^3F_2$ state. We have prepared the compound $U(C_2O_4)_2\cdot 3H_2O$ and measured its susceptibility over the temperature range 78°–328°K. The Weiss-Curie law is obeyed in the range 240°–328°K, but deviation is found at the liquid nitrogen temperature. At the higher temperatures the Weiss constant has the value $\theta=+165$°K. The magnetic moment of the U^{4+} ion is 3.66 Bohr magnetons, in good agreement with the value 3.62 calculated for a $^3H_4$ state, and provides evidence that the heavy elements are like the rare earths in electronic structure. The magnetic susceptibility of uranium oxalate as a function of temperature is similar in behavior to that of praesodimium sulphate octahydrate, and deviation from the Weiss-Curie law can be explained as due to the crystalline field around the U^{4+} ion.

D10. On the Width of r-f Absorption Lines in Solids. J. H. VAN VLECK, *Harvard University.*—In crystals, the breadth of the absorption lines arising from nuclear magnetic moments is caused mainly by the "dipolar" or

"magnetic" interaction between the different nuclear spins. The resultant line width is computed by calculating, by quantum mechanics, the mean-square deviation from the central Larmor frequency and assuming that the shape of the line is approximately Gaussian. The resulting line width agrees surprisingly well with measurements by Purcell and Bloembergen on CaF_2, including prediction on how the width depends on the angle between the applied constant field and the principal cubic axes. On the other hand, the absorption lines of many paramagnetic salts in the microwave region, arising from electronic spin, are often considerably narrower than the dipolar mechanism would predict. It is shown that this discrepancy is probably caused by exchange coupling between the spins. The exchange forces do not influence the mean square, but can greatly increase the mean fourth power of the frequency deviation. As a result the line is peaked more sharply in the center, and has a smaller half-breadth than otherwise. Since exchange integrals diminish rapidly with distance, this mechanism explains why the narrowing is found mainly in materials with a high concentration of paramagnetic ions.

D11. Comparison of Detection Methods for Microwave Spectra.* JOHN ROGERS, RICHARD J. WATTS, AND DUDLEY WILLIAMS, *Ohio State University*.—A report will be given on experimental results obtained with several methods for observing microwave absorption in the 1.25-cm region. The methods employed include: (1) single-crystal detection with a broad band audio-amplifier, (2) single-crystal detection with differentiation and with rejection filters for low frequencies, (3) single-crystal detection with double modulation of the Klystron reflector, and (4) single-crystal detection with several forms of Stark-effect modulation tubes. The relative advantages and limitations of these methods will be discussed in connection with results on ammonia, methanol, cyanogen bromide, and other gases.

* The work was done with aid from Watson Laboratories of the Army Air Forces Air Materiel Command and the Ohio State University Research Foundation.

E1. Fluctuations in Properties of Liquids and the Effect of Radiations on Them.* GEORGE ANTONOFF, ALEXIS YAKIMAC, AND DUNCAN RANDALL, *Fordham University*.—In a paper given before this society on November 10, 1945, it was mentioned that two phases in equilibrium contain an equal number of molecules per unit volume. This means that a liquid must be associated to be in equilibrium with its vapor. X-ray analysis corroborates this view indicating the presence of loose aggregates. They assume a series of temporary positions so that one particle may get into an aggregate and get out and so on. The conditions of mobile equilibrium is attained when a large aggregate leaves the liquid, disintegrates into molecules thereby increasing pressure which compels molecules to go back into the liquid and join the aggregates. This theory was criticized in a private letter by Bridgman because such systems can have real existence only if they exhibit fluctuations which can be detected experimentally. I thus made experiments with alcohol, water, and aqueous solutions. Densities measured in a thermostat regulated within 0.002°C showed distinct fluctuation beginning with the 4th decimal. In some organic liquids there are fluctuations within 3 decimals which are affected by radiations. They ultimately stop. Water exhibits no fluctuations within three decimals, but in the fourth and following a zig-zag curve obtained is somewhat distorted by radiations, but fluctuations show no tendency to stop.

* This paper, mailed on September 30 and intended for the Houston meeting, was unluckily mislaid by the Secretary.

E2. The Damping Capacity of Anodized Aluminum. A. HAMMOND, J. MICHENER, J. KOEHLER, AND E. SALKOVITZ, *Carnegie Institute of Technology*.*—The logarithmic decrements of single crystals and of polycrystals of aluminum were measured before and after the deposit of an oxide film. It was found that the damping increases by a factor of two if a film 10^{-4} cm thick is deposited. Since the specimens weigh two grams or more and the weight of the oxide is only five milligrams, it does not seem possible that this effect arises simply from a loading of the specimen. The measurements were made by gluing the rod-shaped specimens to piezoelectric quartz crystals. The damping was then determined by investigating the electrical behavior of this composite oscillator near its fundamental frequency using an a.c. bridge of the type described by T. A. Read.[1] All measurements were made at a frequency of 38.5 kilocycles and at a strain amplitude of 10^{-4}. Two single crystals and two polycrystals were used and the specimens were anodized and then stripped of oxide twice. The decrements encountered ranged from 1 to 10×10^{-4}. The decrement measurements are good to ±10 percent.

* This work was done under a contract with the Office of Naval Research.

[1] T. A. Read, Phys. Rev. 58, 371 (1940).

E3. Piezoelectric Effect in Polycrystalline Barium Titanate. WALTER L. CHERRY, JR., AND ROBERT ADLER, *Zenith Radio Corporation*.—Polycrystalline barium titanate is rendered piezoelectric by application of an electric field. After removal of the field the effect decreases, rapidly at first, then gradually, and stabilizes at about 0.85 of the initial level. The degree to which this material is made piezoelectric and its stability depend on the time of exposure and field intensity. Highly piezoelectric pieces of good stability are produced in a few minutes with field strengths of 20 kv/centimeter. Several hours are required at lower fields. The piezoelectric axis has the direction of the electric field used in forming. Subsequent application of an alternating field in this direction causes elongation and contraction. An alternating field, perpendicular to the direction of polarization, causes shear in the plane of the polarizing and alternating fields. The electromechanical coupling coefficient is about 0.40 for shear and 0.35 for longitudinal vibrations.

E4. Rupture of Metal Foils under Constant Load. WALLER GEORGE AND GEORGE IRWIN, *Naval Research Laboratory*.—The process of rupture of notched metal

foils loaded in tension has been studied using microscope and high speed camera techniques with the object of extending Griffith's[1] concept of critical crack length to fracturing of ductile metals. The majority of the measurements made used six-inch widths of commercial aluminum, lead, tin, zinc, and copper foils. The notch was a short, narrow cut in the center of the loaded section of the test sheet. The typical fracturing process consists of a slow elongation of the notch normal to the direction of the applied tensile load until a critical length is reached. The velocity of extension of the crack then increases rapidly and the rupture process is completed with a velocity as much as eight orders of magnitude larger than that at the beginning. A comparison of lengths for onset of rapid fracturing with theory is given. The general usefulness of this simple experiment for studies of fracturing of metals is discussed.

[1] A. A. Griffith, Trans. Roy. Soc. **A221**, 163 (1920).

E5. Stress-Induced Interstitial Diffusion of Carbon and Oxygen Atoms in Tantalum.* T'ING-SUI KÊ, *University of Chicago.*—Relaxation phenomena have been observed in tantalum specimens containing small amounts of carbon or oxygen. The internal friction peaks occur respectively around 150°C and 170°C for carbon and oxygen when the frequency of vibration is about one cycle per second. The activation energies associated with these relaxations were found to be 25,000 calories per mole for carbon and 29,000 calories per mole for oxygen. An analysis of the internal friction-temperature curves and a study of the thermal variation of the relaxation strength were made. These indicate that the observed relaxations are associated with the anelasticity caused by the stress induced preferential distributions of carbon or oxygen atoms among the three possible types of tetragonal interstitial positions in tantalum which has a body-centered cubic structure. The establishment of such preferential distributions can only be accomplished by the diffusion of carbon or oxygen atoms among these interstitial positions. Such a picture had been proposed by Snoek in interpreting the relaxation phenomena observed in alpha-iron (body-centered cubic) containing small amounts of carbon or nitrogen. The observations in tantalum thus indicate that such relaxations are characteristic of all interstitial solid solutions of body-centered cubic metals.

* This research has been supported by ONR.

E6. Calculation of the Dielectric Constant of Tellurium.* V. A. JOHNSON, *Purdue University.*—Scanlon and Lark-Horovitz[1] have recently investigated the electrical properties of tellurium. In order to compare their results with semiconductor theory, it is necessary to know the dielectric constant of tellurium. The value is estimated from optical constants by two different methods. The first method, developed by Mullaney,[2] uses the classical dispersion formula to obtain the dielectric constant from the index of refraction and coefficient of extinction. Since tellurium is non-isotropic, there are two sets of such data depending upon whether the single-crystal axis is parallel or perpendicular to the plane of incidence. For these two cases, the dielectric constant is found to be 5.0±0.5 and 2.2±0.5, respectively. For a tellurium sample composed of many randomly oriented crystals, the dielectric constant may be taken as an average. The second method uses reflectivity data and is based upon the electromagnetic theory of light in a conducting medium. This method yields a dielectric constant of 3.9 for tellurium. The second method, applied to reflectivity data for selenium, yields a dielectric constant in agreement with the observed values.

* This work was supported by Signal Corps contract.
[1] W. Scanlon and K. Lark-Horovitz, Physical Review **72**, 530 (1947).
[2] J. F. Mullaney, Physical Review **66**, 326 (1944).

E7. Effect of Atmosphere on the Outgassing and Evaporation Rates of Antimony. R. L. LONGINI, *Westinghouse Research Laboratories.*—A practical limitation for the rate of outgassing metals such as antimony is set by the evaporation of the metal. When an inert gas is introduced during the outgassing process, the rate of both processes is determined by diffusion through the gas. On the basis of kinetic theory considerations it seemed plausible, however, that the evaporation would be slowed much more than the outgassing rate as one proceeds from straight evaporation to the diffusion mechanism. Consequently, it would be possible to speed the outgassing rate, for instance by raising the temperature, and still keep within the limit set by evaporation, if an inert gas were used. This was verified by direct weighings, on a microbalance, of a heated sample of antimony in a helium atmosphere. Results obtained checked well with theoretical expectations. The rate of evaporation was reduced to about two percent when introducing 0.01 atmosphere of helium, whereas the outgassing rate remained practically unaffected by helium at this pressure. A pressure of 0.10 atmosphere of helium was needed before the outgassing rate changed sufficiently to measure the decrease.

E8. Bridge Values of β for Non-Ohmic Disks. S. BLOOMENTHAL, *Automatic Electric Company, Chicago.*—If the non-Ohmic character of contacts between silicon carbide crystals originates in a thin layer of silica on each, then the ferrous oxide-silica reaction ought to affect the electrical characteristics. The bridge method of Baker* was used to obtain β in the relation $E=CI^{\beta}$ applying to non-Ohmic disks 0.75″×0.05″, consisting mainly of silicon carbide. β has the average bridge values 0.26, 0.28, 0.31, 0.32, and 0.34 for heat treated disks pressed from mixtures containing 0, 2½, 5, 7½, and 10 percent powdered iron, respectively. The direct current at 53 volts was about one m.a. Values of β from d.c. measurements were lower than those observed with the bridge. In view of the approximation used, some difference in results by the two methods is expected. An increased disparity was noted between β-values obtained by the two methods for disks from the batches containing appreciable additions of powdered iron. This is believed due to the enhanced temperature sensitivity of the current-voltage relation.

* Baker, Phil. Mag. **37**, 498 (1946).

E9. Half-Dislocations. W. SHOCKLEY, *Bell Telephone Laboratories.*—The stress fields of screw dislocations of the form $u=v=0$, $w=(b/2\pi)\tan^{-1}y/x$ have energies of interaction in an isotropic medium closely analogous to the field energy of two current-carrying wires. Two such dislocations, R apart, have potential energy $(b_1b_2\mu/2\pi)\ln R$. Any dislocation can be resolved into two components for which the net displacement on a circuit about the dislocation is (1) perpendicular (Taylor-type) and (2) parallel (Burgers-screw type) to the dislocation axis. The force between two parallel dislocations does not involve cross terms of type (1), (2). These results are employed in analyzing the stability of a dislocation in the face-centered cubic lattice with a slip of $(a/2)(01-1)$ in the (111) plane compared to two "half-dislocations" of $(a/6)(11-2)$ and $(a/6)(-12-1)$ which together produce the same net displacement across the (111) plane. It is found that the repulsive forces due to the Taylor-like component of these dislocations overcomes the attraction due to the screw components so that the half-dislocations tend to separate. A consideration of the nature of the "half-slipped" plane shows that it will be greatly hardened for slip on planes cutting through it and that this effect may play a major role in the hardening of unused slip planes.

E10. Studies of the Glow Discharge in Mercury Vapor Contained in Cylindrical Tubes with Glass Walls. B. PEARSON DELANY AND PAUL L. COPELAND, *Illinois Institute of Technology.*—The breakdown potential in the vapor between a mercury cathode and a nickel anode, and also in mercury vapor between nickel electrodes in cylindrical glass tubes of various dimensions, has been studied as a function of the vapor pressure. The results are analyzed with the aid of Pachen's law. Significant variations in the breakdown potential which depend upon the history of the tube preceding the breakdown are observed. The behavior of the discharge as an electrical circuit element has also been studied.

E11. Ionization Potentials of Some Hydrocarbon Series. RICHARD E. HONIG, *Socony-Vacuum Laboratories.*—A new method is described which permits ionization and appearance potentials to be determined reproducibly, within ± 0.02 volt, by electron impact in a conventional 180° mass spectrometer. The energy spread of the ionizing electrons, while not eliminated, is accounted for in an analytical expression that describes the ionization efficiency curve of argon near the initial upward break. It is shown that an ionization or appearance potential can be determined graphically by drawing a tangent or critical slope to the efficiency curve which has been plotted on a semi-log scale. Absolute values are obtained by referring the unknown to the ionization potential of a calibrating gas (usually krypton). For the monatomic gases studied, electron impact and spectroscopic values agree within the experimental uncertainty. For some known polyatomic molecules, the "vertical" impact values exceed the "adiabatic" spectroscopic potentials by 0.02 to 0.2 volt, depending on molecular complexity. Paraffins, 1-olefins, and 2-olefins show a systematic reduction in potential with chain length. A similar decrease is observed when the monoolefins are arranged according to the number and size of substitutions on the basic ethylene structure.

Z1. Dynamic Mechanical Properties of Rubber-Like Materials. A. W. NOLLE, *Massachusetts Institute of Technology.*—The differential dynamic Young's modulus for representative rubber-like materials has been measured over a frequency-temperature range which at its widest limits extends from 10^{-1} to 10^{5} cycles per second and from -50 to 100°C. This dynamic modulus, measured for the case of small sinusoidal strain variations, is a complex number so that for each experiment both a real modulus and a loss-angle tangent are reported. Described are five methods of measurement which have been used to obtain natural frequency, resonant frequency, band width, decrement, etc. Methods include mechanical and magnetostrictive excitation. In addition, the bulk wave modulus and its loss-angle tangent, at 10^{7} c.p.s., are measured by an ultrasonic-pulse method. The results show the existence of dispersion over at least six decades of frequency. The loss factor and complex compliance, as functions of frequency and temperature, are analyzed and discussed. The dynamic-modulus results, in the limiting case of very low frequency, below the range of appreciable relaxation effects, are shown to be in agreement with the kinetic theory of rubber-like elasticity. Compounds of Buna-N, Butyl, GR-S, Neoprene, and natural rubbers are considered, and characteristic differences are described. This work was supported in part under Contract NObs-25391, Task No. 1, with the Bureau of Ships.

Z2. Method for the Absolute Measurement of Dynamic Properties of Linear Structures at Sonic Frequencies. W. JAMES LYONS AND IRVEN B. PRETTYMAN, *Firestone Tire and Rubber Company.*—A full account, including the theoretical basis, is given of a method whereby the dynamic stretch modulus, coefficient of internal friction, and hysteretic energy loss of textile yarns and cords, composed of either continuous filaments or staple fibers, can be accurately determined at longitudinal-vibration frequencies above 100 cycles/sec. The method, which employs electromagnetic excitation, is applicable also to glass cords, and metallic wires and cables. Results have been obtained at frequencies extending to above 300 cycles/sec. A concise description is given of the improved stretch-vibrometer. Results on a typical cotton cord show that energy absorption by this instrument is negligible, permitting the calculation of an accurate internal friction coefficient, and absolute hysteretic loss. Measurements on eight natural and synthetic textile fibers reveal that the dynamic moduli range from 6.4×10^{10} dynes/cm² for Velon monofil to 32×10^{10} dynes/cm² for a ramie cord. The dynamic moduli of Fiberglas and steel cords were found to be 54 and 106 $\times10^{10}$ dynes/cm², respectively. The internal friction coefficients are found to vary hyperbolically with frequency: in a 11/4/2 cotton cord, for example, from 15 to 3×10^{9} poises between frequencies of 60 and 320 cycles/sec.

Z3. Transducer Measurements of the Mechanical Properties of Polymer Solutions. THOR L. SMITH, JOHN D. FERRY, AND FREDERIC W. SCHREMP, *University of Wisconsin.*—Apparatus has been designed for studying the mechanical properties of concentrated polymer solutions in small oscillating deformations, at audiofrequencies. A rod, driven by a coil in a magnetic field, oscillates vertically along its axis in a cylindrical tube of solution. The gap between rod and tube is 1 mm and the amplitude of vibration about 0.002 mm, so the maximum shear is very small and the maximum rate of shear moderately small even at 1000 cycles. By measuring the electrical resistance and reactance of the coil when in motion and when rigidly clamped, or when in motion with different masses attached to vary the inertia, the mechanical resistance and reactance of the system can be obtained from well-known transducer relationships. The former yields the real part of the dynamic viscosity of the solution, η'; the latter, under favorable conditions, yields the real part of the dynamic rigidity, G'. For polymer solutions, the viscosity η' is found always to be very much smaller than the ordinary viscosity measured in steady flow. Examples of experimental data will be given.

Z4. Geometric Disorder in Linear Polymers. S. T. GROSS, *General Aniline and Film Corporation.*—Appearance of x-ray fiber diagrams is qualitatively related to single chains and groups of chains in the fiber sample. Several types of disorder can be localized in this manner. Some of the various types of geometric isomerism in polymers are considered, and in the general type of fiber diagram to be expected for each is noted. A number of polymers are discussed in relation to the above factors, and an explanation (based on the recently postulated restricted orientation of side groups)[1] is proposed for the non-crystalline structure of polyvinyl acetate and its hydrolysis to crystalline polyvinyl alcohol. Reasons for not obtaining a non-crystalline form of cellulose triacetate from this cause are considered.

[1] S. T. Gross, C. A. Schildknecht, and A. O. Zoss, Am. Chem. Soc. meeting in New York, October 1947.

F1. On the Exact Solution to the Problem of Light Scattering by a Plane-Parallel Atmosphere in Accordance with Rayleigh's Laws. S. CHANDRASEKHAR, *University of Chicago.*—The equations of radiative transfer allowing properly for the polarization characteristics of the radiation field and in accordance with Rayleigh's laws are formulated and solved exactly for the case of an incident parallel beam of radiation. The method consists in starting with certain functional equations governing the laws of diffuse reflection and transmission by a plane-parallel atmosphere, reducing them to pairs of functional equations of the standard form

$$X(\mu)=1+\mu\int_0^1\frac{\Psi(\mu')}{\mu+\mu'}[X(\mu)X(\mu')-Y(\mu)Y(\mu')]d\mu', \quad \text{(i)}$$

and

$$Y(\mu)=e^{-\tau_1/\mu}+\mu\int_0^1\frac{\Psi(\mu')}{\mu-\mu'}[Y(\mu)X(\mu')-X(\mu)Y(\mu')]d\mu', \quad \text{(ii)}$$

where $\Psi(\mu)$ is an even polynomial in μ, and τ_1 is the optical thickness of the atmosphere, and finally, relating in a unique manner the various constants occurring in the solutions with the moments of the X and Y functions appropriate for the problem. Rational approximations to the solutions of Eqs. (i) and (ii) can be obtained and starting with these approximate solutions the exact equations can be solved by iteration.

F2. Theoretical Analysis of the Effect of Imperfections in Diffraction Gratings. U. FANO AND R. D. HUNTOON, *National Bureau of Standards.*—It is of interest for the construction of diffraction gratings to estimate in advance the effect of imperfections in the spacing or shape of the grooves. Partial results in this direction can be obtained by an elementary theory in which each groove is considered as infinitely thin source of light. However, an extension of Rayleigh's dynamical theory of gratings makes it possible to develop a more general theory in which the nature of the approximations involved and their quantitative import are kept in sight. A complete account of this investigation will probably be published in the National Bureau of Standards Journal of Research.

F3. An Electronic Eyepiece for Spectroscopy of Near Infra-Red. ZABOJ V. HARVALIK, *School of Mines and Metallurgy, Rolla, Missouri.*—An electronic eyepiece for the observation of near infra-red of the spectrum is described. It can be attached to any spectroscope, and consists of an image tube of the type 1-P-25 which converts infra-red into visible images. The spectrum is projected by the telescope system of the spectroscope upon the mosaic face of the image tube. The infra-red radiation releases photoelectrons from the mosaic face of the image tube, which are focused by an electronic lens system upon a fluorescent screen. This fluorescent screen consists of a phosphor which, when activated by electrons, shows luminous characteristics similar to the sensitivity of the human eye. The visible range of a spectroscope, equipped with an electronic eyepiece, is extended to approximately $\lambda=1130$ mμ (11,300A) although very high intensity infra-red radiations can be observed to $\lambda=1145$ mμ (11,450A).

F4. Fine Structure of He II λ4686.* J. E. MACK AND N. AUSTERN, *University of Wisconsin.*—The $3s^3S_1-4p^3P_1$ and $3p^3P_1-4s^3S_1$ components of the hydrogen-like spectrum of helium have been separated.

* Supported by the Office of Naval Research.

F5. On the Structure of the Mercury Band λ2540. S. MROZOWSKI, *Great Lakes Carbon Corporation.*—The well-known molecular band of mercury at λ2540 was studied with high dispersion (second order of the 30-foot University of Chicago grating). In absorption, only the long wave-length edge, two sharp maxima of absorption reported some time ago by Wood and Voss,* and a new short wave-length edge are observed. The band, however, could be obtained in emission using an exceptionally well water-cooled mercury arc in end-on observation. The whole band

appears much sharper than in absorption. The long wave-length maximum is resolved into two very sharp components and a series of additional very sharp lines (or edges) converging toward the long wave-length edge are observed. The great sharpness of the emission lines (or edges) is hard to reconcile with the currently adopted classification of this band as a $^3O_u^+ \rightarrow {}^1\Sigma_g^+$ transition in the Hg_2 molecule. The λ2482 band of the ionized mercury molecule Hg_2^+ was also studied and a complex structure of a number of maxima (edges) was detected.]

* R. W. Wood and V. Voss, Proc. Roy. Soc. 119, 689 (1928).

F6. Force Constants and Assignments of the Raman Frequencies of Methylbromoacetylene and Methyliodoacetylene. ARNOLD G. MEISTER, *Illinois Institute of Technology.*—Using the Wilson FG matrix method and a modified valence force potential energy expression, force constants for methylbromoacetylene and methyliodoacetylene were determined. The C−Br stretching force constant was found to be 4.352×10^5 dyne/cm while the C−I stretching force constant was determined as 3.571×10^5 dyne/cm. These values compare with 3.129×10^5 and 2.648×10^5 dyne/cm, respectively, for similar bonds in CH_3Br and CH_3I as given by Crawford and Brinkley.[1] As a result of the calculations it seems necessary to change some of the assignments of Cleveland and Murray[2] for the Raman frequencies of methylbromoacetylene and methyliodoacetylene. For both molecules the line near 690 cm^{-1} does not appear to be a type A_1 fundamental frequency but more likely is the first overtone of the 343 cm^{-1} type E fundamental. Also, the C−C stretching frequency probably was not observed since its calculated value was found to lie in the 1014–1036 cm^{-1} region and Cleveland and Murray reported no line in this region for either molecule.

[1] B. L. Crawford, Jr. and S. R. Brinkley, Jr., J. Chem. Phys. 9, 71 (1941).
[2] F. F. Cleveland and M. J. Murray, J. Chem. Phys. 11, 452 (1943).

F7. The Use of Photo-Tubes in the Ultraviolet Region by Fluorescence. ROBERT D. COWAN,* *University of Chicago*—RCA multiplier photo-tubes types 931A and 1P28, sensitive down to about 3000A and 2000A, respectively,[1] have been used in conjunction with fluorescent materials for detecting light of wave-lengths as short as 1942A. From intensity measurements in the region 2300 to 3000A, first made directly with a 1P28, and then using the 1P28 in combination with the fluorescent material supplied by Eastman Kodak Company for sensitizing photographic plates, the efficiency of the fluorescence method has been estimated as about one forty-fifth. Of this, a factor of about twelve is geometrical in origin, and the remaining factor of three or four indicates a quantum efficiency of fluorescence of roughly thirty percent. The 931A's in the writer's possession are five to ten times as sensitive as the 1P28's to the fluorescent radiation. They can thus be used as substitutes for 1P28's with the loss of a factor of only five or ten in sensitivity down to 2300A, and a considerable gain in sensitivity below 2100A. Use in the vacuum ultraviolet region has not yet been successful due to lack of sufficiently intense light sources.

* National Research Fellow.
[1] R. W. Engstrom, J. Opt. Soc. Am. 37, 420 (1947).

F8. Experimental Determination of Lorentz-Lorenz Correction in Ultraviolet Absorption. LOIS E. JACOBS AND J. R. PLATT, *University of Chicago.*—Absolute absorption intensities were determined in the region 1750–2350A for isoprene, both in the vapor and in *n*-heptane solutions, using a small vacuum fluorite spectrograph. The apparent *f*-values computed from areas under the curves were 0.38 and 0.47 for the isoprene vapor and solution, respectively. Average deviation of individual intensity measurements were 6 percent for the vapor and 12 percent for the solution, with the integrated areas having an estimated error of less than 5 percent. These experimental *f*-values lead to a Lorentz-Lorenz correction of 1.23, which can be compared with the value of 1.32 calculated from Chako's theoretical formula. The difference of 8 percent is probably not significant. This discrepancy is much less than that obtained by Pickett and co-workers for the cyclic dienes. These studies are being continued on the *cis*- and *trans*-piperylenes.

F9. Molecular Orbital Treatment of the Ultraviolet Spectra of Benzene and Borazole. C. C. J. ROOTHAAN AND R. S. MULLIKEN, *University of Chicago.*—The ground state and the first excited states of benzene and borazole are treated according to the semi-empirical molecular orbital method. Comparing the observed spectra with the computed energies, a spectroscopic value of −2.6 ev for the bond integral β is obtained in the case of benzene. In the case of borazole this procedure includes one more parameter, which takes care of the difference in electronegativity of boron and nitrogen. Taking a reasonable value for this parameter, a value of −2.3 ev for the bond integral between boron and nitrogen, β^*, is obtained in fair agreement with theoretical expectations.

F10. X-Ray Optical Images. PAUL KIRKPATRICK AND A. V. BAEZ, *Stanford University.*—When x-rays from a point source undergo total (not Bragg) reflection at a concave surface a real line image may be formed. If after one such reflection the rays impinge upon a second suitably oriented concave reflector a real point image may result. Real optical images of extended objects may thus be produced with x-rays. The method is analogous to the production of optical images by crossed cylindrical lenses. Spherical glass surfaces coated with gold or platinum, and having radii of curvature between 20 and 100 meters, have been successfully used, though the spherical form has been adopted for reasons of convenience rather than of theoretical superiority. Near grazing incidence a spherical mirror has practically the properties of a cylindrical mirror with focal length $Ri:2$, where i is the grazing angle and R the radius of curvature. The theoretical minimum distance between object points resolvable with x-ray mirrors, as the problem is now conceived, is of the order of 100A,

though this resolution at present appears to be incompatible with high magnification. Theoretical resolving power is not strongly dependent upon wave-length. Optical systems with more than two mirrors have been used to attain desired magnifications and to improve image characteristics.

F11. A Microphotometer for X-Ray Diffraction Diagrams.* R. PEPINSKY AND H. I. WEST, JR., *Alabama Polytechnic Institute.*—A photometer is described for measurement of the integrated intensity of reflections on x-ray diffraction photographs. The film is placed against the face of a cathode-ray tube, e.g., a 5UP11 or 5FP5, and a finely-focused scanning electron beam on the fluorescent screen serves as light source. The beam sweeps linearly at 30 c.p.s. across the tube, and a 2-megacycle modulation is applied perpendicular to the slow sweep to produce a scanning ribbon, both the width and length of which can be controlled as desired. The transmitted light is received by a 931A photo-multiplier, the output of which is amplified and fed to the vertical plates of a second cathode-ray oscillograph. The horizontal sweep of the second c-r tube is linear and synchronized to the slow sweep of the first tube. Thus photometer traces of the x-ray reflections appear on the presentation tube. These can be recorded by tracing directly from the tube face. A procedure for electronic integration of these photometer traces is also described, the proper section of the trace being visually selected by two movable pips on the presentation tube; the voltage signals between these pips is fed to an integrating amplifier, the output of which appears as a meter reading. Measurements of the linearity of the photometer are presented.

* This development supported by Signal Corps Engineering Laboratories, Bradley Beach, New Jersey.

SUPPLEMENTARY PROGRAMME

SP1. Viscous Slip along Grain Boundaries and Diffusion of Zinc in Alpha-Brass.* T'ING-SUI KÊ, *University of Chicago.*—The viscous behavior of the grain boundaries in 70–30 alpha-brass was demonstrated by measurements of anelastic effects similar to those previously reported in the case for aluminum.[1] It was shown that the grain boundaries cannot sustain a shear stress and that they have a coefficient of viscosity decreasing with an increase of temperature. Using the same specimen, the activation energy associated with stress induced preferential orientation of pairs of zinc atoms in alpha-brass (which is a diffusion process), first observed by Zener,[2] was determined. It has a value of 40,000 calories per mole which is identical, within experimental error, to the activation energy of 41,000 calories per mole associated with the grain boundary slip in alpha-brass. This would indicate that the mechanism of the grain boundary slip in alpha-brass as manifested in the anelastic measurements is similar to the volume diffusion of zinc in alpha-brass.[3]

* This research has been supported by ONR.
[1] T. S. Kê, Phys. Rev. **71**, 533 (1947); **72**, 41 (1947).
[2] C. Zener, Trans. A.I.M.E. **152**, 122 (1943); Phys. Rev. **71**, 34 (1947).
[3] To be called for after Session G if time permits.

Author Index to Abstracts of Papers Presented at the Chicago Meeting

Allison, S. K., and L. del Rosario—No. B10
Andrews, R. D., N. Hofman-Bang, and A. V. Tobolsky—No. W3
Antonoff, George, Alexis Yakimac, and Duncan Randall—No. E1
Beiduk, F. M. and E. J. Konopinski—No. D7
Bloomenthal, S.—No. E8
Bockelman, C. K., L. W. Seagondollar, and H. H. Barschall—No. A1
Bowe, J. C., M. Goldhaber, R. D. Hill, W. E. Meyerhof, and O. Sala—No. A5
Bull, H. B.—No. Y1
Chandrasekhar, S.—No. F1
Cherry, Walter L., Jr. and Robert Adler—No. E3
Claesson, Ingrid and Stig Claessen—No. W2
Cook, C. Sharp and Lawrence M. Langer—No. A2
Copeland, L. E. and M. Mooney—X4
Cork, J. M., R. G. Shreffler and C. M. Fowler—No. A9
Cowan, Robert D.—No. F7
Cowart, William S. and M. L. Pool—No. B5
Davidson, W. L. and I. G. Geib—No. X5
Davis, Luther, Jr. and Jerrold R. Zacharias—No. B2
DeLany, B. Pearson and Paul L. Copeland—No. E10
Der Mateosian, E., M. Goldhaber, C. O. Muehlhause, and M. McKeown—No. A6
Doty, Paul—No. Y5
—— and S. J. Stein—No. W1
Eggenberger, Delbert N. and Paul L. Copeland—No. D4
Ekstein, H.—No. D3
Eldridge, John A.—No. D8

Fahy, E. F. and Marcel Schein—No. C6
Fano, U. and R. D. Huntoon—No. F2
Ferry, John D. and John E. Eldridge—No. Y3
Friedland, S. S. and A. D. Krumbein—No. C11
Gehman, S. D.—No. X2
George, Waller and George Irwin—No. E4
Geyer, Charles J., Jr., C. H. Reichardt, and George Halsey—No. X1
Greenstein, Jesse P.—No. Y4
Gross, S. T.—No. Z4
Hammond, A., J. Michener, J. Koehler, and E. Salkovitz—No. E2
Harvalik, Zaboj V.—No. F3
Honig, Richard E.—No. E11
Hull, A. W., E. E. Burger, and R. E. Turrentine—No. D2
Hutchison, C. A. and N. Elliott—No. D9
Jacobs, Lois E. and J. R. Platt—No. F8
Johnson, V. A.—No. E6
Jurney, E. T. and Margaret R. Keck—No. A7
Kê, T'ing-Sui—Nos. E5, SP1
Kohman, Truman P.—No. B9
Kundu, D. N. and M. L. Pool—No. A11
Kirkham, Don—No. D1
Kirkpatrick, Paul and A. V. Baez—No. F10
Kraybill, Henry L.—No. C3
Laughlin, J. S., L. S. Skaggs, A. O. Hanson, and J. J. Orlin—No. B7
Longini, R. L.—No. E7
Lyons, W. James and Irven B. Prettyman—No. Z2
Mack, J. E. and N. Austern—No. F4
Marshak, R. E.—No. C1
Meister, Arnold G.—No. F6
Mitchell, A. C. G., B. D. Kern, and D. J. Zaffarano—No. A8
Mooney, M.—No. X3
Morris, Peter A., W. F. G. Swann, and H. C. Taylor—No. C2
Mrozowski, S.—No. F5
Nolle, A. W.—No. Z1
Ovrebo, Paul J.—No. C10
Pepinsky, R. and H. I. West, Jr.—No. F11
Pruett, John R.—No. A4
Rall, Wilfrid—No. B4
Robinson, Howard A. and Edward M. Man, Jr.—No. W4
Rogers, John, Richard J. Watts, and Dudley Williams—No. D11
Roothaan, C. C. J. and R. S. Mulliken—No. F9
Sachs, R. G.—No. B1
Schein, Marcel—No. C9
—— **and Thomas H. Carr**—No. C8
Seren, Leo and Lawrence Jones—No. D5
Shaw, A. E.—No. B3
Shepherd, M., Jr., J. H. Baldwin, and G. H. Fett—No. D6
Sherwin, Chalmers W.—No. A3
Shockley, W.—No. E9
Shoupp, W. E., B. Jennings, and W. Jones—No. B6
Skaggs, L. S., J. S. Laughlin, and L. H. Lanzl—No. B8
Smith, Thor L., John D. Ferry, and Frederic W. Schremp—No. Z3
Steinberger, J. and Marcel Schein—No. C7
Thomas, C. D.—No. C12
Ticho, Harold K.—No. C4
Van Vleck, J. H.—No. D10
Wang, C. S. and D. L. Falkoff—No. A10
Williams, Robley C.—No. W5
Wrinch, Dorothy—No. Y2
Yngve, Victor H., Marcel Schein, and Henry L. Kraybill—No. C5

Proceedings of the American Physical Society

Minutes of the 1947 Annual Meeting at New York

January 29–31, 1948

THE 1947 Annual meeting of the American Physical Society was held, like all of the Annual meetings preceding it since that of 1942, at Columbia University in New York City. The dates were Thursday, Friday, and Saturday, January 29, 30, and 31, 1948. Thus, for the sixth consecutive year the burden of receiving our meeting fell upon the physics staff of Columbia University, with minor assistance from other institutions of the New York area (Bell Telephone Laboratories, College of the City of New York, New York University) who provided the lantern operators. Special commendation must be lavished upon W. W. Havens and W. A. Nierenberg, the general managers of the meeting. This was the largest task that ever was imposed by our Society upon any host institution, since upwards of 1650 people registered for the meeting. Three of our Divisions (Electron Physics, Solid-State Physics, Fluid Dynamics) held concurrent sessions; they all provided groups of invited papers, and a considerable number of contributed papers which appeared on the general programme. The American Association of Physics Teachers, having met with us at Chicago, did not join in the New York meeting: it is difficult to imagine how we could have found space for it if it had. We had also the Retiring Presidential Address of President L. A. DuBridge, and invited papers on a variety of topics by C. D. Anderson, R. F. Bacher, James Franck, P. M. Morse, H. C. Pollock (with F. R. Elder and R. V. Langmuir) and Julian Schwinger: the last was repeated by popular request. There were 188 contributed papers, including three read by title.

At the Business Session of the Society, the Tellers (a group at the Brookhaven National Laboratory headed by P. M. Morse) reported the outcome of their long and tedious labors of examining about 2900 ballots. J. R. Oppenheimer is President of the Society, F. W. Loomis its Vice-President, G. B. Pegram its Treasurer and K. K. Darrow its Secretary for the year 1948 (and until the end of the Annual Meeting to be held in January 1949); Frederick Seitz and L. A. Turner are members of the Council for the next four years; S. A. Goudsmit, E. M. Purcell, and V. F. Weisskopf are members of the Board of Editors for the next three years; J. T. Tate continues as Editor of the Physical Review and Reviews of Modern Physics. Two Amendments to the By-Laws of the Society were proposed by the Council and adopted by the members: the texts are printed hereinafter.

The Council met on Thursday evening, and elected to Fellowship P. H. Abelson, Henry Eyring, J. W. Liska, and R. B. T. Roberts; to Membership it elected 113 candidates, a smaller number than usual at this time because it had acted at the Chicago meeting on nominations received during December. As the 1948 Nominating Committee it appointed L. A. DuBridge (Chairman), H. L. Dryden, J. R. Dunning, F. G. Dunnington, G. F. Hull Jr., H. M. James, W. Shockley, J. T. Tate, and J. H. Van Vleck. A memorial notice of the late Willard Severinghaus, long the Secretary of this Society, written by H. W. Farwell, was ordered sent to the Physical Review for publication. The By-Laws of the Division of Fluid Dynamics were approved, as also were amendments by the By-Laws of the Division of High-Polymer Physics. The Council voted to donate wartime and postwar (up to 30 June 1948) issues of *Physical Review* and *Reviews of Modern Physics* to selected universities in Germany and Japan. From the reports of the Treasurer and of the Editor it transpired that the "lush period," during which the Society made a net profit on *Physical Review* owing to lessened size and relatively low unit printing costs of this journal, has ended: we must anticipate a drain on the surplus of the Society henceforth.

The dinner of the Society was held on Firday evening in the Grand Ballroom of the Hotel New Yorker, with an attendance of 346; and

R. F. Bacher delivered an after-dinner address entitled "The physicist and the future development of atomic energy."

The Society has lost through death V. Karapetoff and Ernest Blaker.

The membership of the Society stood at 6839 just before this meeting, and will have been augmented to 6952 by the elections which occurred at the Council meeting if all of those who were elected accept membership.

Elected to Fellowship: P. H. Abelson, Henry Eyring, J. W. Liska, R. B. T. Roberts.

Elected to Membership: Richard David Albert, Kenneth Dillion Allen, Frank Andrews, Romuald Anthony, Edward V. Ashburn, Gordon L. Baker, Roland S. Barker, Charles E. Barnett, Paul A. Beck, Arthur H. Benade, Jack Benveniste, Robert Berman, Rolf Bjornerstedt, Franklin C. Brooks, Paul Rice Camp, Lars Carlbom, Richard O. Carlson, Cheng Shu Wang Chang, Robert Lee Chaplin, Jr., Philippe J. P. Chastagner, Jr., Richard H. Chow, Kuang-ya Chu, John H. Clements, James Curtis, William Osborne Davis, T. G. de Zoeten, E. W. Emery, William Noel English, Lawrence H. Ginsberg, Joseph R. Goberna, Gerson Goldhaber, J. Mayo Greenberg, Pierre Grivet, Jack Ingval Hagen, Gordon E. Hansen, Richard J. Hayden, Henry Hemmendinger, Eugene B. Hensley, Roger H. Hildebrand, Terrell L. Hill, Freddy Ba Hli, Norman Hornstein, Ralph W. Hubbard, Arthur J. Hudgins, Bernard David Hyams, James M. Hyatt, Erling Jensen, Claude Kitchener Jones, Charles M. Judson, J. F. Kane, Herbert Karsh, Graham M. Keyser, Paul B. Klevin, Robert J. Kraushaar, Charles V. Larrick, Hans Larsson, K. Lehovec, Murray L. Lesser, George LeSuer, Michael Albert Lewis, Robert B. MacDonnell, Victor Mayper, Jr., E. H. McLaren, Robert R. McMath, Darwin J. Mead, Arnold Merlin, F. J. Milford, Richard L. Moore, James H. Morrissey, Emil Motchok, Charles B. Officer, Ernest Okonski, John R. Pellam, Robert W. Pidd, Giovanni Polvani, T. C. Randle, Robert A. Rapuano, Herbert David Rix, Thomas R. Roberts, Franklin Alanson Rodgers, J. Donald Roll, S.J., Barnett Rosenberg, Allan M. Sachs, Richard Whiley Safford, Abraham Irving Sawelson, DeForest F. Smith, Ralph G. Steinhardt, Jr., W. G. Stone, Emory J. Stovall, Jr., Alice Fensterwald Strouse, Albert I. Talkin, T. I. Taylor, Adolph H. Toepfer, Sol Triebwasser, Charles W. Tucker, Maurice H. Van Horn, Frank Wagner, Jr., James D. Wallace, Stanley Wallack, Paul Wang, Tien-Chuan Wang, Raymond M. Warner, Jr., Ernest T. Watterud, Joseph W. Weinberg, Donald B. Wheeler, Jr., Jack E. Whitener, John A. Wieland, Leo Wiesner, C. S. Wilkinson, Jr., Robert E. Wisnieff, Herman Yagoda, Peter E. Yankwich, Donald Robert Yennie.

Amendments to the By-Laws. Article I Section 2 of the By-Laws is rewritten as follows: "A newly-elected Member or Fellow, upon completion of membership by payment of his first annual dues, shall have the option of having his membership commence either on the first of January of the year in which he was elected or on the first of January of the following year. Should he fail to indicate his choice clearly, his membership shall commence on the first of January of the year of his election if his annual dues are received before July first of that year, and shall commence on the first of January of the year following his election if his annual dues are received after June thirtieth of the year of his election. (This amendment goes into force at the 1948 Washington meeting.)" To Article V Section 1 of the By-Laws the following words are added: "and that the Council shall have the power to waive this rule for a limited number of papers to be added to the supplementary programme."

KARL K. DARROW, *Secretary*
American Physical Society
Columbia University
New York 27, New York

Retiring Presidential Address

Electron Emission from Metal Surfaces: A Review. L. A. DUBRIDGE, *California Institute of Technology.*

Invited Papers on the General Programme

Cosmic-Ray Effects at Thirty Thousand Feet. C. D. ANDERSON, *California Institute of Technology.*

Plans for the Brookhaven National Laboratory. P. M. MORSE, *Brookhaven National Laboratory.*

Memorial Address in Honor of Max Planck. JAMES FRANCK, University of Chicago.

The Physicist and the Future Development of Atomic Energy. R. F. BACHER, *U. S. Atomic Energy Commission.*

Recent Developments in Quantum Electrodynamics. JULIAN SCHWINGER, *Harvard University.*

Visible Radiation from Accelerated Electrons in 70-Mev Synchrotrons. H. C. POLLOCK, F. R. ELDER, AND R. V. LANGMUIR, *General Electric Company.*

Invited Papers of the Division of Electron Physics

Some Considerations Concerning Theories of the Oxide Cathode. CONYERS HERRING, *Bell Telephone Laboratories.*

The M.I.T. Electron-Physics Programme: Past, Present, and Near Future. W. B. NOTTINGHAM, *Massachusetts Institute of Technology.*

Spectral Distribution of the External Photoelectric Yield from Semiconductors. L. APKER, *General Electric Company.*

Secondary Electron Emission from Insulators. J. B. JOHNSON, *Bell Telephone Laboratories.*

The Separation of Isotopes in Quantity by Electromagnetic Means. LLOYD P. SMITH, *Cornell University.*

Conductivity Induced in Insulators by Electron Bombardment. K. G. MCKAY, *Bell Telephone Laboratories.*

General Characteristics of Phosphors. H. W. LEVERENZ, *RCA Laboratories.*

Some Physical Properties of Infra-Red Phosphors. W. L. PARKER, *Polytechnic Institute of Brooklyn.*

Electrical Phenomena in Gases at Microwave Frequencies. W. P. ALLIS, *Massachusetts Institute of Technology.*

Some Discharge Phenomena in Fluorescent Lamps. E. G. F. ARNOTT, *Westinghouse Electric Corporation.*

Cathode Phenomena in the Electric Arc. J. D. COBINE AND C. GALLAGHER, *General Electric Company.*

Resolution in Electron Microscopes. JAMES HILLIER, *RCA Laboratories.*

Symposium of the Division of Solid-State Physics

Crystallographic Factors in Lattice Imperfections. R. SMOLUCHOWSKI, *Carnegie Institute of Technology.*

Basic Principles of Operation of Crystal Counters. FREDERICK SEITZ, *Carnegie Institute of Technology.*

Ferromagnetic Domains. H. J. WILLIAMS, *Bell Telephone Laboratories.*

Ferromagnetic Resonance. J. L. SNOEK, *Philips Research Laboratories, Eindhoven, Holland.*

Joint Symposia of the Fluid Dynamics Committee and the Institute of Aeronautical Sciences

Upper-Atmosphere Research

Upper-Atmosphere Temperatures from Remote Sound Measurements. E. F. COX, *Naval Ordnance Laboratory.*

Heat Transfer to Bodies Traveling at High Speed in the Upper Atmosphere. J. R. STALDER AND DAVID JUKOFF, *Ames Aeronautical Laboratory.*

Wind Tunnel Testing Problem in Super-Aerodynamics. HSUE-SHIEN TSIEN, *Massachusetts Institute of Technology.*

Physics of Rarefied Gases

Physics of Rarefied Gases. I. ESTERMANN, *Carnegie Institute of Technology.*

The Temperature of a Highly Rarefied Gas. LYMAN SPITZER, JR., *Princeton University.*

The Propagation of Sound in Air at Low Pressures. R. B. LINDSAY, *Brown University.*

Friction and Heat Conduction in Rarefied Gases. K. F. HERZFELD, *Catholic University of America.*

On the Theory of the Transport Phenomena in Rarefied Gases. G. E. UHLENBECK, *University of Michigan.*

Contributed Papers

C1. New Experiments Concerning the Surplus Gamma-Radiation from Rocks. VICTOR FRANCIS HESS AND J. DONALD ROLL, S.J., *Fordham University.*—Two experiments were performed to determine if the surplus gamma-radiation from granite, observed by one of the authors (V.F.H.), could be due to cosmic rays inducing fission of uranium or thorium or artificial radioactivity within the granite. *A.* A large sample of dunite, an ultrabasic rock which is practically free of radioactive elements, was placed in an iron house surrounding an ionization meter. The ionization observed with the dunite was practically zero. *B.* The iron house was then filled with crushed granite, first at Fordham, then in an underground station where the cosmic-ray intensity was reduced to a few percent of the surface value. No difference in ionization due to the granite was observed at the two levels. Thus the surplus gamma-radiation cannot be ascribed to the effect of cosmic radiation on the granite. Since E. Gleditsch and T. Gráf have recently published a new determination of the intensity of gamma-radiation from potassium which is considerably higher than other values found in the literature, further experiments are necessary before it can be decided whether the surplus radiation is due to a previously underestimated intensity of gamma-rays from potassium or to some unknown source.

C2. The Nature of the Primary Cosmic Radiation.* MARCEL SCHEIN, *University of Chicago.*—The penetration and shower production of cosmic-ray particles was investigated close to the top of the atmosphere at a geomagnetic latitude of 52° North. It was found that most of the particles from the vertical are capable of traversing very large thicknesses of lead and, hence, they cannot consist of electrons. A very large East-West asymmetry of the hard component was recently observed by the author in collaboration with V. H. Yngve and H. L. Kraybill in a B-29 plane at an altitude of 35,000 feet. This can only be explained if we assume that a considerable fraction of the primaries is positively charged. Most of the primary particles should carry a single charge since there has been no marked latitude effect observed on cosmic-ray phenomena corresponding to an energy range around 10^{11} ev. All the above-mentioned facts strongly indicate that the large majority of the primary cosmic rays must consist of protons.

* This research was supported in part by the U. S. Navy.

C3. Specific Primary Ionization in Hydrogen by a Coincidence-Counter Method.* FRANK L. HEREFORD, *Bartol Research Foundation.*—Considerable discrepancies exist in the comparison of the experimentally and theoretically determined variation of the primary ionization with energy of incident particles. Bethe's theory predicts a logarithmic increase in ionization above a certain minimum point in the curve, which hitherto has not been confirmed.[1] With a coincidence train containing three high pressure counters and one low pressure counter this minimum was recently observed[2] in a helium-butane mixture. The experiment has been repeated using a low pressure hydrogen counter, results again confirming the predicted minimum and subsequent increase of ionization with energy. More elaborate path-length calculations[3] have made possible a more precise determination of ionization by sea-level cosmic radiation than was previously possible.[2] The counter method avoids the uncertainty inherent in cloud-chamber measurements

in distinguishing between the primary and total ionization. The only assumption involved is that creation of a single ion pair will discharge the counter with unit probability.

* Supported by the Office of Naval Research.
[1] M. G. E. Cosyns, Nature 139, 802 (1937); W. E. Hazen, Phys. Rev. 63, 107 (1943).
[2] F. L. Hereford, Phys. Rev. 72, 982 (1947).
[3] See abstract RT2, E. E. Witmer and M. A. Pomerantz.

C4. Detection of Ionizing Radiation by Ultra High Frequency Gas-Discharge Counters.* SANBORN C. BROWN, *Massachusetts Institute of Technology.*—Characteristics of a coaxial mode cavity resonator as a gamma-ray counter making use of a 3000-mc gas discharge will be described. The breakdown of a discharge in gases at these frequencies does not depend upon secondary effects, and since the breakdown field is not controlled by positive ions, shorter breakdown times and shorter resolving times than of a Geiger-Müller counter are realized. The u.h.f. discharges show ambipolar diffusion as the controlling factor in loss of electrons, and a d.c. clearing field is superimposed on the a.c. field to eliminate electrons most rapidly. A quenching agent is present to suppress electron emission from positive-ion bombardment of the walls. The discharge is quenched by pulsing the magnetron power source down by suitable electronic circuits. The plateau characteristics are similar to those found with a Geiger-Müller counter. The sensitivity can be made the same as that of a Geiger-Müller counter of similar geometry. The minimum resolving time achieved is 5 microseconds. Pulse rise times measured by delay-line clipping methods show the pulse rising from 0.05 volt to 3 volts in 6×10^{-9} second.

* This work was supported in part by the Signal Corps, the Air Materiel Command, and O.N.R.

C5. A Pulse Transformer Technique for Application to Coincidence Counting. B. G. FARLEY, *Yale University.*—For amplitude-type coincidence discrimination, differentiating transformer coupling networks offer certain advantages in pulse amplification and shaping, particularly because they allow the application of positive pulses to all grids with little d.c. level change if grid current is drawn. By designing transformers with low mutual and leakage inductances and resistance, pulses of the order of 100-volt height and 0.1-microsecond width at the base are easily obtained with power video tubes. One method of discrimination is to connect the outputs of the final transformers in each channel in parallel. The discrimination time of such a circuit with proportional counters is in the vicinity of 10^{-7} sec. to 10^{-8} sec., the exact time depending on the conditions of variability of the pulses and amount of noise. With identically recurring, artificial pulses the discrimination is, of course, considerably better.

* Assisted by the Office of Naval Research.

C6. High Efficiency, High Speed Scintillation Counters for Beta- and Gamma-Rays. MARTIN DEUTSCH. *Massachusetts Institute of Technology.*—Counters that, according to Kallman,[1] use naphthalene screens and photo-multiplier detection have been investigated with the following results: Substantially every electron is counted if it spends sufficient energy in the screen, namely about 0.15 Mev at room temperature or 0.05 Mev at dry-ice temperature. Screens several cm thick have been used giving an efficiency of 20 percent for counting 1.2-Mev gamma-rays and even higher for softer gamma-rays. Energies of beta- and gamma-rays can be determined from bias curves with accuracy comparable to ordinary absorption measurements. Coincidence resolving times at least as short as 0.1 microsecond can be used without measurable losses. No marked difference in performance is found between ordinary "moth flakes" and so-called chemically pure naphthalene. Large clear lumps can be obtained easily by cooling from the melt. Solid benzene performs as well as naphthalene. Solid bromobenzene gives smaller pulses but may be useful because of its higher density. α- and β-bromonaphthalene and 1,4-dibromobenzene gave no useful pulses. This work was supported in part by the Office of Naval Research.

[1] H. Kallman, Natur und Technik (July 1947).

C7. Characteristics of Geiger Counters Filled with Lead Tetramethyl Vapor. C. L. MEAKER, C. S. WU, AND L. J. RAINWATER, *Columbia University.*—Geiger Counters filled with tetramethyl lead vapor have been thoroughly investigated. This is a self-quenching gas which exhibits a satisfactory plateau over wide voltage ranges irrespective of the material of the cathode cylinder. The useful life of the counter under constant high counting rate was found to be more than 10^9 counts in all counters tested. The efficiency for detecting electrons *vs.* vapor pressure has been studied. At a pressure as low as 14 mm of Hg, an ordinary standard thin-wall silvered counter counts approximately 100 percent of the composite beta-particles from phosphorus P^{32}. Because of this low gas pressure, the dead time of counters filled with lead tetramethyl vapor is much less than counters filled with the mixture of argon and alcohol. Typical values for the counter dead time are near 5×10^{-5} sec. Counters filled with this vapor are particularly useful for measurements involving very high counting rates. The effect of the time constants of the amplifier circuit on the determination of dead time of a counter will be discussed.

C8. High Pressure Cloud Chamber with Intense Magnetic Field. T. H. JOHNSON AND R. P. SHUTT, *Brookhaven National Laboratory.*—The paper describes the design of a high pressure cloud chamber suitable for photographing a considerable number of mesons decaying in the gas. The probability of photographing a meson at the end of its range is proportional to the stopping power of the gas, to the sensitive time, to the window area, and to the average range. The sensitive time, determined by diffusion, is proportional to the pressure, p. Thus the probability factor for the chamber is proportional to p^2. The magnetic field required to offset multiple scattering in the determination of meson momentum must be increased approximately at p^1. In 300 atmospheres of argon the momentum of a particle with 10-cm residual range can be determined in a field of 30,000 gauss with 10 percent accuracy.

The chamber design incorporates coils external to a non-magnetic pressure cylinder which will produce a field of this intensity when excited by four Navy mine sweep generators delivering 2160 kw intermittently. A massive rectangular yoke of iron holds the pole pieces together against the high internal pressure. Stereo photographs are made through small windows of thick glass and a column of water inside the pressure volume. The cloud chamber is hydrostatically supported by oil contained within the pressure cylinder.

C9. Probability of Meson Track Endings in a High Pressure Cloud Chamber. RICHARD W. SAFFORD, *Brookhaven National Laboratory.*—Calculations have been made of the probability of obtaining meson track endings in a proposed high pressure cloud chamber with 200-atmosphere pressure of argon and a magnetic field of 30,000 gauss, relative to a cloud chamber at atmospheric pressure and no magnetic field. The paths of mesons in the magnetic field were calculated taking into account Bethe-Bloch energy losses in the various absorbing materials (iron, oil, lead, and argon at 200 atmospheres) for a range of incidence angles and energies. Scattering was not considered. Results for cloud chambers of the same dimensions, normalizing for the probability in a cloud chamber at atmospheric pressure with no magnetic field, were as follows: cloud chamber at atmospheric pressure, $P=1$; high pressure cloud chamber with no magnetic field, $P=200$; high pressure cloud chamber with magnetic field, $P=450$; high pressure cloud chamber with magnetic field surrounded by 20 cm of lead, $P=350$. The cloud chambers were considered biased to the same energy range by lead. Probabilities are given for the same sensitivity time.

D1. Gamma-Rays from Alpha-Particle Reactions. DAVID E. ALBURGER, *Yale University.**—Energies of gamma-rays from sodium, magnesium, aluminum, silicon, phosphorus, and sulfur targets under cyclotron bombardment by 7-Mev alpha-particles have been measured by observing the maximum range of Compton-recoil electrons in aluminum. Two beta-ray counters were arranged on a line with the target so that electrons in the forward direction produced in the end wall of the first counter could pass through both counters giving coincidences. The thickness of aluminum absorber placed between the counters at which the counts were reduced to the random coincidence rate gave the maximum range of the electrons. Using the modified Feather relation to compute the recoil-electron energy and adding the energy of the back-scattered gamma-ray the following gamma-rays were found: sodium, 2.75 ± 0.25 Mev; magnesium, 1.81 ± 0.18 Mev and 4.3 ± 0.3 Mev with an intensity ratio of 3 to 1; aluminum, 3.5 ± 0.3 Mev; silicon, 2.3 ± 0.2 Mev; phosphorus, 2.55 ± 0.25 Mev and 4.1 ± 0.4 Mev with an intensity ratio of 8 to 1; sulfur, 2.4 ± 0.3 Mev. Comparison of these with the Q-values of proton groups in the corresponding αp reactions shows that in cases where correlation can be made the transition from the second excited state to ground in the product nucleus is favored.

* Assisted by the Office of Naval Research.

D2. Proton Groups from Deuteron Bombardment of Sulfur. PERRY W. DAVISON, *Yale University.**—Bombardment of H_2S gas with 3.3-Mev deuterons yields eight groups of protons. The possibility that the two shortest-range groups are due to air (N_2 and O_2) contamination has been ruled out on the basis of yield and variation of yield with deuteron energy. On the same basis the longest range group is believed due to nitrogen. All except this longest-range group are assigned to the reaction $S^{32}(dp)S^{33}$, S^{32} being the predominant isotope. The Q-values calculated are given in the following table.

Q in Mev	Level in Mev	Relative yield	Spacing in Mev
Q_0 6.50	0.00	1	0.98
Q_1 5.52	0.98	1/2	0.99
Q_2 4.61	1.89	3	1.05
Q_3 3.56	2.94	35	0.90
Q_4 2.66	3.84	43	0.92
Q_5 1.74	4.76	120	0.92
Q_6 0.82	5.68	350	

* Assisted by the Office of Naval Research.

D3. Energy Levels of A^{41}. ERNEST POLLARD AND PERRY W. DAVISON,* *Yale University.*—Argon gas has been bombarded by 3.4-Mev deuterons, and the protons emitted in the $A^{40}(dp)A^{41}$ reaction by absorption in aluminum were observed by use of a double coincidence method. Eight groups of protons are observed of which two are probably due to slight contamination by air and a third is possibly so explained. The remaining groups can be assigned to levels in the A^{41} nucleus. The Q-values in Mev, relative yields, and spacings are listed.

Q in Mev	Level spacing (Mev)	Intensity
Q_0 3.82		1
Q_1 3.19	0.63	0.7
Q_2 2.65	0.54	4
Q_3 1.97	0.68	1
Q_4 1.66	0.31	1 (? O_2)
Q_5 0.95	0.71	8

* Assisted by the Office of Naval Research.

D4. Proton-Proton Scattering at 2.4 and 3.0 Mev.* WILLIAM SLEATOR, JR., J. M. BLAIR, E. E. LAMPI, AND J. H. WILLIAMS, *University of Minnesota.*—The differential proton-proton scattering cross section has been measured at 2.4 and 3.0 Mev at angles from 8° to 45° by a method similar to that of Herb, Kerst, Parkinson, and Plain.[1] Protons from the Minnesota Van de Graaff generator reached the scattering chamber (inside diameter 43 cm) through a collimator of half-angular spread 0.5° and entered a Faraday cage. Scattered protons were observed with two proportional counters, one fixed for monitoring, and the other movable in angle. The slit system defining the scattering volume had a half-angular aperture of 0.66° for measurements below 15° and 1.23° for those above 15°. At 15° both analyzers were used to check geometrical factors. The observed scattering cross sections, uncorrected for finite geometry, are given in the table. The over-all probable error is approximately 2 percent. The values at 2.4 Mev

(above 15°) are on the average larger than those of HKPP by about 2.9 percent. Measurements at higher energies are in progress.

Proton-proton cross section per unit solid angle (in barns)

Angle	8°	10°	12.5°	15°	17.5°	20°	25°	30°	35°	40°	45°
2.4 Mev	8.16	3.23	1.41	0.820	.635	.575	.540	.536	.522	.483	.459
3.0 Mev	5.22	2.10	1.00	0.657	.560	.512	.499	.484	.462	.441	.413

* Assisted by the U. S. Navy.
[1] Herb, Kerst, Parkinson, and Plain, Phys. Rev. 55, 998 (1939).

D5. The Charge Distribution in Nuclei and the Scattering of High Energy Electrons. M. E. ROSE, *Clinton National Laboratory.*—The possibility of determining the shape of the charge distribution in nuclei as well as nuclear radii by the scattering of high energy electrons has been investigated. Assuming a Coulomb interaction between protonic charge elements and electron, the nuclear form factor can be directly related to the ratio of observed to point charge (Mott) scattering. While total cross sections are essentially unchanged, the cross section for large momentum losses, such as would occur for about 50-Mev electrons elastically scattered through angles of order $\pi/2$, is reduced from the Mott value by readily observable amounts. The case of scattering in deuterium has been considered in view of the possibility of a direct determination of the deuteron wave function apart from quadripole moment effects. Competition from scattering with nuclear excitation and disintegration, atomic ionization, and bremsstrahlung are not serious provided that the electron energy is in the neighborhood of 50 Mev, the scattering angles of order $\pi/2$ and the electrons observed in the scattering experiment are scattered with small energy loss.

D6. Sensitivity of Proton-Proton Scattering to Potentials at Different Distances. G. BREIT, A. A. BROYLES, AND M. H. HULL, *Yale University.**—The small changes in potential energy δV are taken to be in small intervals ΔR at distance R. Estimates are made for the combined effect of $q=(\delta V)\Delta R$ for $R\ mc^2/e^2=3$, 5 and simultaneous change in depth δD of short-range (e^2/mc^2) well. Similarly the combined effect of q, δD and change in range is studied. For an assumed $R\ mc^2/e^2=5$, measurement of scattering with an accuracy of 1 percent determines q with an accuracy approaching 1 kev through a distance e^2/mc^2. The energy region 200–600 kev is found to have special merits for the determination of the shape of the potential energy curve.

* Assisted by the U. S. Navy.

D7. Inelastic Scattering of Protons by Light Nuclei. KENNETH E. DAVIS AND EVERETT M. HAFNER, *University of Rochester.*—Energy states of light nuclei can be found by studying inelastically scattered protons by use of incident beams of several Mev. The method was introduced by Wilkins[1] and developed by others. We have attempted to improve further the sensitivity and resolution of the experiment. An incident beam of 7.0 Mev is defined to 2 percent by a slit system in the cyclotron fringing field. The thin solid target is oriented at an angle that is favorable from the standpoint of homogeneity of scattered proton groups. A fixed scattering angle of 35 degrees is used as a compromise between excessive Coulomb scattering at lower angles and loss of resolution, due to uneven targets, at high angles. Energies are resolved by 180-degree focusing in a magnetic field, and protons are detected in Eastman NTA photographic plates. Energy intervals of several Mev in the nuclear spectra are covered in each measurement. An interesting result obtained with this equipment is a level that has been tentatively assigned to Be^9, appearing at 2.42 Mev above the ground state (0.79 Mev above the dissociation energy) and having a width less than 0.15 Mev. Other results for several light nuclei will be discussed.

[1] T. R. Wilkins, Phys. Rev. 60, 365 (1941).

D8. The Reaction $He^3(n, p)H^3$ and the Neutrino Mass. D. J. HUGHES AND C. EGGLER, *Argonne National Laboratory.*—The mass of the neutrino can be measured by a careful determination of the Q-value for an (n, p) reaction if the resulting β-emitter has an accurately known end point. We have determined the Q-values for the reactions $N^{14}(n, p)C^{14}$ and $He^3(n, p)H^3$ from the proton ranges in a cloud chamber. The hitherto unobserved helium reaction was found by use of pile neutrons and helium containing about 10^{-3} percent He^3. From the measured mean ranges and the stopping power of the chamber, the range in air of the N^{14} proton is 0.991 cm, and that of the He^3 proton is 0.980 cm. The range results, together with the range energy curve given by Livingston and Bethe, give the following values for the proton energy and the neutrino mass:

$$He^3;\quad E_p=552\text{ kev};\quad \mu c^2=4\pm25\text{ kev},$$
$$N^{14};\quad E_p=557\text{ kev};\quad \mu c^2=1\pm25\text{ kev}.$$

By far the largest part of the error results from the uncertainty in the range energy curve. However, the relative mass of the neutrino in the two cases is known much better; actually the experiment shows that the mass of the neutrino for H^3 and C^{14} is the same within about 5 kev.

D9. A New Table of Absolute Nuclear Abundances. HARRISON BROWN, *University of Chicago.*—The only table of absolute nuclear abundances heretofore available has been that compiled by V. M. Goldschmidt,[1] in 1937. Since that time developments have warranted a re-evaluation of existing information. Following the method of Goldschmidt, the two main sources of data utilized in compiling the new table were stellar spectra and meteorites. Stellar spectra data were used in order to evaluate the abundances of very light elements together with elements which clearly would have been fractionated from less volatile constituents during the process of planet formation. Meteoritic abundances have been used in all other cases. The new table possesses the same general characteristics as Goldschmidt's table, but significant changes have resulted from the following developments: (1) more extensive stellar data; (2) more precise linking of stellar abundances to meteoritic abundances; (3) more accurate evaluation of the ratio of metal to silicate phase in meteorites and in the minor

planets; (4) statistical evaluation of standard deviations of elemental abundances in meteorites; (5) development of a general theoretical background guiding the use of meteoritic data in the compilation of such a table.

[1] V. M. Goldschmidt, *Geochemische Verteilungsgesetze der Elemente* (Oslo, 1938), Chapter IX, "Die Mengenverhältnisse der Elemente und der Atom-Arten."

D10. Nuclear Magnetic Moments as Integral Multiples of a Natural Unit. ENOS E. WITMER, *University of Pennsylvania*.—A study of the most accurately measured magnetic moments of nuclei appears to support the conclusion that they are either exactly or very nearly *integral multiples of* $\mu_N/672$, where μ_N is a nuclear magneton. This conclusion is based on the accurate g-values or ratios of g-values for H^1, H^2, H^3, Li^6, Tl^{205}, and the difference of the g-values for Ba^{135} and Ba^{137}. For H^1 the magnetic moment is taken to be $1876\ \mu_N/672$. This is in general accord with a previous statement by the writer,[1] but the natural unit here is only one-fourth as large as in that statement. It is in accord with and helps to explain the fact that for the experimental nuclear g-values, $84g$ is frequently, but not always, very close to an integer.

[1] Enos E. Witmer, Proc. Nat. Acad. Sci. **32**, 283 (1946).

D11. The Hyperfine Structure of Hydrogen and Deuterium. JOHN E. NAFE AND EDWARD B. NELSON, *Columbia University*.—The atomic-beam magnetic resonance method has been applied to measure the h.f.s. separation of the ground state of H and D by observing frequencies of the r-f field required to induce transitions among certain of the magnetic levels of the h.f.s. multiplets in magnetic fields of the order of 1 gauss. The resonance minima were of the theoretical width for transitions which are field independent in the first order. For hydrogen we find $\nu_H = 1420.410 \pm 0.006$ Mc and for deuterium $\nu_D = 327.384 \pm 0.003$ Mc. The ratio $\nu_H/\nu_D = 4.33867 \pm 0.00004$. The h.f.s. separations ν_H and ν_D, and their ratio ν_H/ν_D may be calculated from known values of the magnetic moment of the proton, μ_p, the magnetic moment of the deuteron, μ_d, and the ratio μ_p/μ_d. The measured ν_H and ν_D are larger than the calculated values by 0.25 percent and 0.26 percent, respectively. The ratio of the measured h.f.s. separations is 0.017 percent lower than the calculated ratio. The latter discrepency is 18 times the probable error in our measurement.

D12. Effect of Large Quadrupole Interactions on Nuclear Radiofrequency Spectra at Twice Larmor Frequency. NORMAN F. RAMSEY, *Harvard University*.*—The work of Feld and Lamb[1] on the effect of a nuclear electrical quadrupole moment on the radiofrequency spectrum of a diatomic molecule in a magnetic field is extended to a special case not considered by them. This is a case in which the electrical quadrupole interaction energy is so large that even in magnetic fields of several thousand gauss the magnetic interaction energies are small compared to the electrical quadrupole interaction energy. In this case it is shown theoretically that for a spin of $\frac{3}{2}$ there are certain circumstances under which the maximum of absorption will occur at double the Larmor frequency instead of at the Larmor frequency, and will have a field and molecule dependence similar in many ways to a resonance at the Larmor frequency. This result has the important implication that special care must be used in identifying the radiofrequency resonance absorption spectra or an error of a factor of two in the value of a nuclear magnetic moment can easily be made. The approximate shape and intensity of the radiofrequency absorption spectrum under these circumstances is calculated in order that a comparison of the theoretical shapes and intensities with the experimental ones can be used as a means of recognizing if an absorption is a double Larmor frequency one. This theory may be applied for example to identify the radiofrequency spectra of diatomic molecules containing Br and Cl.

* Part of this work was done at Columbia University.

D13. The Application of $Li^6(n, \alpha)$ and $B^{10}(n, \alpha)$ to Slow-Neutron Monitoring. MAURICE M. SHAPIRO AND JOHN R. BARNES, *Clinton National Laboratories*.—When slow neutrons impinge on a photographic emulsion impregnated with lithium or boron, the yield of disintegration tracks from the $Li^6(n, \alpha)$ and $B^{10}(n, \alpha)$ reactions, respectively, is very high. Moreover, when a suitable emulsion is employed, the tracks are dense and easily observable under high power magnification. These observations suggested the applicability of the Li and B reactions to slow-neutron health monitoring. Further investigation showed that this method of monitoring is more sensitive by several orders of magnitude than the $N^{14}(n, p)$ reaction currently employed in some laboratories. For example, in the Li-loaded plates the yield of tracks from a given slow-neutron flux is about 150 times the yield of the $N^{14}(n, p)$ tracks. Furthermore, each track (produced by a triton and an alpha-particle recoiling in opposite directions) is ten times as long as, and considerably denser than, the proton track from nitrogen. Therefore, it is easier to recognize and count. With boron-loaded emulsions, the alpha-particle tracks are even more numerous although shorter than the tracks from Li. Either of these proposed techniques of slow-neutron health monitoring permits higher accuracy, while reducing enormously the time and labor consumed in microscopic counting of tracks.

E1. Conversion of a D.C. Motor-Generator into a Low Noise Power Amplifier. H. S. SOMMERS, JR., P. R. WEISS, AND W. HALPERN, *Rutgers University*.—Because of the need for a noise-free d.c. power source for various servo applications, such as precision control of an electromagnet or furnace, a commercial motor-generator set has been converted into a low noise power amplifier. The generator serves as the low frequency output of a wide-band negative feed-back amplifier. The high frequency output consists of a hard tube bank, in parallel with the generator, feeding directly into the load; an inductance inserted between the generator and the load keeps the armature from shorting the hard tube output. The band width to 3-db point of a model amplifier with 100-watt d.c. output, and voltage gain of 100, extends from d.c. to 3 kc/sec. The undistorted swing is 0–100 v at d.c., drops to 1-v r.m.s. at 30 c.p.s., and then rises to 2.5-v r.m.s. at 200 c.p.s. The noise output of the

generator is reduced by a factor of 5000 at d.c., 300 at 30 c.p.s., 800 at 120 c.p.s., and finally unity at 8 kc/sec. This amplifier, which has been used in a magnet current servo that reduced peak-to-peak field fluctuations at all frequencies to less than 10^{-8} times the d.c. field, is being directly scaled to excite a 40-kw magnet.

E2. Electron Optical "Schlieren" Effect. L. MARTON, *National Bureau of Standards.*—In close analogy to the light optical "Schlieren" effect (sometimes called Töppler's shadow method) there exists an electron optical effect of similar nature. For its observation an image of a point electron source was produced, by means of a magnetic lens, on a center stop. At about half the distance between source and lens a magnetized recording wire was placed. In a conjugate plane with proper focusing a "Schlieren" image of the magnetic field surrounding the recording wire was observed. Experiments are being carried out for practical application of this effect to a quantitative measurement of the field distribution on recording wires, to studies of field distribution from ferromagnetic domains, to studies of space charge distribution, and to investigations of electromagnetic field distribution of standing waves, of cavity resonators, of wave guides, et cetera. Results of measurements on magnetized wires will be shown.

E3. Application of the Electron Optical "Schlieren" Effect. D. L. REVERDIN, L. MARTON, AND S. H. LACHENBRUCH, *National Bureau of Standards.*—As an application of "Schlieren" optics, the radial change of index of refraction of a thin electron beam can be made visible by observing the "Schlieren" pattern. This is done by placing the beam perpendicular to the path of another electron beam. By this means information regarding either the radial potential distribution or the radial space charge distribution of the thin beam can be obtained. The potential distribution of a homogeneously distributed electron beam of circular cross section which acts as a cylindrical lens has been obtained, and the focal length for paraxial rays has been calculated. For such a space charge "lens" beam of 300 microamperes and 5000-volt accelerating potential, the calculations give, as a first approximation, a deflection sufficient for the "Schlieren" observation. The same experiment can also be studied for a more general space charge distribution, such as an electron cloud produced by a heated filament. Another application is the dispersion of an electron beam by a standing microwave field inside a wave guide. The deflection of 5000-volt electrons in a microwave field of 100 volt/cm is adequate for "Schlieren" observation.

E4. Electron Motion in Deflecting Field of Magnetic Dipole. S. H. LACHENBRUCH, *National Bureau of Standards* (Introduced by Dr. L. Marton).—After a brief outline of their derivation, the equations and graphs of the trajectories of electrons moving in the equatorial plane of a magnetic dipole field under various conditions are shown, their properties discussed, and the results interpreted. Application of the equations of motion to the inverse-cube field distribution of a short dipole yields a differential equation whose exact solution is given in terms of elliptic integrals. When the distance unit is normalized, this trajectory equation involves a single parameter, B, into which are lumped all given conditions (dipole moment, permeability, electron energy, and initial direction of motion). For attracting fields a critical value of B is found, at which the form of the trajectory is radically altered. As the dipole strength approaches the critical value, the deflection angle increases rapidly and the trajectory approaches a spiral having as asymptote a circle about the dipole. Beyond this critical condition the electrons execute a small loop near the dipole and are thereafter repelled. The critical value is described numerically in terms of actual conditions, and the property is interpreted both as a practical limitation and as one to be utilized.

E5. A Study of Cathode Behavior in the Inert Gases as Applied to Minimum Sparking Potentials.* HAROLD JACOBS AND ARMAND P. LAROCQUE, *Sylvania.*—The minimum sparking potentials, V_m, are determined for barium magnesium, and aluminum in the five inert gases and are found to be as follows.

	Helium	Neon	Argon	Krypton	Xenon
Barium	157	129	94	104	83
Magnesium	160	150	123	115	120
Aluminum	189	160	154	135	150

It is shown that, in general, the V_m tends to decrease with decreasing work function, ϕ, of the surface. The second Townsend coefficient, γ, is shown to decrease with increasing F/P in the region studied, with the exception of helium. At a constant F/P, γ tends to decrease with increasing ϕ in all cases studied.

* This work was undertaken in joint cooperation of the Applied Physics Laboratory of Johns Hopkins University and by the United States Navy.

E6. Thermionic Emission of Oxide-Coated Filaments.* HAROLD JACOBS, GEORGE HEES, AND WALTER CROSSLEY, *Sylvania.*—The emission of oxide-coated filaments on different alloys (Ni, B-Ni, Ba-Ni, Co-Ni, Pt-Ni, V-Ni, tensite) was measured over a period of 500 hours. An empirical emission equation was used instead of Richardson's equation and was found to be as accurate and more simple to use.

$$I_0 = A' \exp(-e\psi/kT).$$

It was found that A' and ψ varied over life such that, $\log A' = K\psi + B$, K and B being constants. The total emission at 800°K was determined and found to be affected by the solute element or elements.

* This work was undertaken in cooperation with the United States Army Signal Corps Engineering Laboratories.

E7. Decay of Thermionic Emission of Barium-Strontium Oxide Cathodes during Space-Charge-Limited Operation. W. E. DANFORTH AND W. E. RAMSEY, *Bartol Research Foundation.*—By means of a "feeler pulse," applied at a known and variable time after the application of anode voltage (of a value where the operation is space charge limited), the variation of a cathode's intrinsic capacity to emit has been briefly studied. The circuit for accomplishing

this will be described. It is found, as would be expected, that a relatively small space-charge-limited current can result in reduction of intrinsic emitting capacity, even though, by virtue of the space-charge limitation, this current remains constant in time. Results will be described of studies of decay of emission-limited current, showing that the decay pattern is not constant in a given tube, but may in certain cases be absent initially and develop during operation. In agreement with others, it is found that, in general, a decay curve cannot, over the whole range, be described by a constant plus one exponential. At least two exponentials are required and involve time constants, to quote a typical example at 900°C of 1.5×10^{-3} second and 5×10^{-4} second. This work was done under OSRD and is now in the province of Bureau of Ships.

E8. Anomalies in the Initiation of Cold-Cathode Discharges. JEROME ROTHSTEIN, *Evans Signal Laboratory.*—Life testing several hundred cold-cathode, triggered modulator tubes, constructed in this laboratory, disclosed several interesting anomalies in the initiation of the discharge. In accordance with their effect on output current pulse on a synchroscope screen, they were classified as amplitude jitter, time jitter, and pulse distortion. The first is tube drop fluctuation, the second fluctuation in time of onset of the main discharge relative to the trigger pulse. This fluctuation, usually a few tenths of a microsecond, was superimposed on a secular delay of several microseconds. Distortion was mainly of three kinds, the first a gradual increase followed by a sudden jump to near normal current. The second consisted in a rise to about half-value for about half the pulse, normal value thereafter. The third was pronounced broadening and flattening of the entire pulse. Distortion, jitter, and growth in secular delay were usually associated, became more pronounced with age, were exaggerated at lower operating voltages, and seem to be intimately connected with the state of the cathode and the glow-arc transition mechanism.

E9. Results and Semitheoretical Calculations in Microwave Breakdown.[1] D. Q. POSIN, *Massachusetts Institute of Technology and North Dakota State College.**—A considerable number of experimental results were obtained revealing the dependence of electrical breakdown at microwave frequencies on a number of parameters such as pressure of gas and width of breakdown gap; also a semitheoretical formulation was established for sparking field strength, by using certain known ionization functions and certain assumed ones. In addition, the effect of an external magnetic field in facilitating breakdown within a wave guide was studied for the case of 3-cm waves and explanations of the effect have been considered which tend to indicate the change in the power-carrying capacity of a given wave guide when placed in an external magnetic field. Calculations have been made of the equivalent rectangular pulse width for actual trapezoidal pulse of the same height, by using the ionization theory mentioned above.

[1] The experimental work is based on research done for the Office of Scientific Research and Development under Contract with the Massachusetts Institute of Technology. A number of the calculations have been performed at North Dakota State College.

* Now at the Department of Physics, North Dakota State College.

E10. Measurements of Breakdown in Low Pressure Helium at Microwave Frequencies.* MELVIN A. HERLIN AND SANBORN C. BROWN, *Massachusetts Institute of Technology.*—An electric field of sufficiently high frequency applied to electrons in a gas may deliver energy to the electrons without imparting to them any continuous drift motion in the field direction. The criterion for breakdown of a low pressure noble gas at microwave frequencies is therefore that ionization by collision of electrons with neutral gas molecules replace loss by diffusion to the walls of the discharge tube. This condition is mathematically expressed as the solution of a simple boundary value problem which has been checked experimentally. This breakdown principle is applied to converting microwave breakdown measurements into measurements of ionization rates as a function of the electric field strength and frequency. Experimental results will be presented and their relationship to the usual d.c. first Townsend coefficient will be explained.

* This work has been supported in part by the Signal Corps, the Air Materiel Command, and O.N.R.

E11. Electric Fields in the Cathode Dark Space of an Abnormal Hydrogen Discharge. S. V. GALGINAITIS,* *University of Wisconsin.*—By measuring the magnitude of the Stark effect of the H gamma-line emitted from the cathode dark space of a hydrogen discharge, the course of the electric field as a function of distance from the cathode was obtained. A water-cooled aluminum cathode was used, and the current densities were as high as 1.50 amp./cm². For a given current, the field strength was greatest at the surface of the cathode, and decreased uniformly with distance to a zero value near the boundary of the negative glow. However, the length of the region of the cathode fall did not coincide with the visual length of the cathode dark space, since while the visual dark space seems to shrink with increasing current density, the spectrograms showed that the length of the region of the cathode fall increases with increasing current density. In the range of currents used, the field at the surface of the cathode increased with increasing current density.

* Now at the University of Louisville.

E12. Imprisonment of Resonance Radiation in Gas Discharges. T. HOLSTEIN, *Westinghouse Research Laboratories.*—When an excited gas atom makes an optical transition to the ground state, the emitted resonance line is highly absorbable by normal atoms of the gas. Under suitable conditions, as is shown in a previous paper,[1] the resultant imprisonment of radiation may cut down the radiative loss of atomic excitation by an order of magnitude. In gas discharges at low or intermediate pressures ($\gtrsim$1 mm), the additional processes which affect the concentration of excited atoms, n_r, are, primarily, excitation and de-excitation collisions of electrons with normal and excited atoms, respectively. Amplifying the treatment of the above quoted paper to include these collision processes, we obtain, in the stationary case, an integral equation for n_r. This equation may be solved approximately by a variational method in which the maximum value of a

characteristic functional gives directly the fraction, Δ, of excitation energy returned to the electrons by de-excitation encounters. Calculations of n_r and Δ have been carried out for the case of Doppler broadened radiation.

[1] T. Holstein, Phys. Rev. 72, 1212 (1947).

E13. Types of Sparking in High Vacuum Diodes. W. E. RAMSEY AND W. E. DANFORTH, *Bartol Research Foundation.*—Studies of sparking phenomena in high vacuum diodes with barium-strontium oxide cathodes show a multiplicity of phenomena which has led us to speak of four types of sparking. The classification is based upon the nature of the triggering mechanism; the appearance of the sparks bear no relation to the type. It is found that disruptive breakdown occurs when any one of the following conditions obtain: (a) The current density from any point on the cathode exceeds a certain critical value. (b) The field at any point of the cathode exceeds a certain critical value. (c) The electrons striking the anode exceed a critical energy. (d) Points on the anode reach a critical temperature. Types (a) and (b) are referred to as "cathode initiated sparking." Highly active cathodes will exhibit type (a) in the space-charge-limited state, whereas type (b) will predominate with a poor emitter, operating in the emission-limited state with high anode potentials. Types (c) and (d) are anode initiated with the latter being the most frequent cause of breakdown under operation with long pulses (10 microseconds and greater). The experimental basis for this classification will be described. The work was done under OSRD and is now in the province of Bureau of Ships.

E14. Thermal Emittance of Various Materials Used as Anodes in Radio Receiving Tubes. A. D. POWER, *Radio Corporation of America.*—Thermal emittance measurements have been made at several temperatures up to 400°C on various old and new materials used as anodes in radio receiving tubes. The values obtained at 200°C range from 0.07 for uncoated nickel, to 0.98 for a new nickel-coated steel base with a mixed carbon and graphite coating. Basic equations are presented, followed by a brief description of the apparatus and procedure together with results obtained and a discussion of their accuracy.

E15. Ballistic Treatment of the Traveling Wave Amplifier.* D. L. BENEDICT, *Harvard University.*—A first-order theory for the traveling wave interaction of beams and slow electromagnetic waves to attain significant amplification in the microwave region has been developed. Newton's laws are applied to describe the balance of energy in the exchange between wave and beam and the resulting growth of stored electromagnetic energy in a reference system moving with the velocity of the wave. The results are translated back to the stationary system showing the dependence of gain on electron and wave velocity, beam current, and other measurable quantities. Two restrictions are imposed; namely, (a) $(v_e-v_p)\tau 2\pi/\lambda_g \ll 1$, (b) the energy extracted from the beam shall not be large compared with $mv_p(v_e-v_p)$. The manner in which these restrictions may be removed in application of the theory will be indicated.

* Work supported by Office of Naval Research.

F1. Measurement of Longitudinal Magnetostriction with Automatic Recording. E. A. NESBITT AND H. J. WILLIAMS, *Bell Telephone Laboratories.*—A new method of measuring magnetostriction is described which permits one to record automatically the change in length of a magnetic specimen, resulting from a change in magnetic field strength. One portion of a ring specimen is rigidly clamped and the diametrically opposite point is connected to a cylindrical coil (L-coil) which is suspended in a radial magnetic field so that the axial motion of the coil produces a change in its flux linkages. The specimen is toroidally wound (H-coil), and the terminals of the H-coil and L-coil are connected to a Cioffi recording fluxmeter.[1] A change of current through the H-coil actuates the mechanism and change in length is plotted automatically against magnetizing field on a $7\frac{1}{2}''\times 10''$ sheet. Use of this instrument is illustrated for a "soft" magnetic material, vanadium Permendur (49 percent iron, 49 percent cobalt, 2 percent vanadium) having a magnetostriction of 51×10^{-6} for an H of 830 oersteds, and for a "hard" magnetic material, Alnico V, having a magnetostriction of 30×10^{-6} for an H of 1600 oersteds. This and other materials for permanent magnets are found to have high magnetostriction in accordance with theory.

[1] Phys. Rev. 67, 200 (1945).

F2. Energy Calculations for Domains. W. SHOCKLEY, *Bell Telephone Laboratories.*—The origin, shape, and size of the tree patterns described by Williams and Bozorth can be understood in terms of the energies involved and the orientation of the surface. The underlying domain structure which is polarized in the (0 ± 10) easy direction produces a surface charge $\pm I\sin\theta$ where the normal to the surface is $(0, \sin\theta, \cos\theta)$, leading to a magnetostatic energy of $1.70\, I^2 \sin^2\theta W/(1+\mu^*)$ per unit area, where W is the width of the domain structure and μ^* is the permeability of the domains in fields perpendicular to the (010) direction. Domains of closure which eliminate all the magnetostatic energy can be constructed by using (± 100) domains joining the (0 ± 10) domains across walls whose normals are parallel to $(\pm\sin\theta, \sin\theta, \cos\theta)$. For $\theta > 4°$ and $W > 0.01$ cm the wall energy required for closure is less than the magnetostatic energy. Complete elimination of magnetostatic energy does not occur because a more stable state can be produced by leaving some free poles and eliminating some wall energy. At smaller slopes this results in the tree patterns. Numerical calculations, including the effect of magnetostrictive energy, show semiquantitative agreement with all observed features, including predictions of the direction of spin precession in domain walls.

F3. New Magnetic Powder Patterns and their Interpretation. H. J. WILLIAMS AND R. M. BOZORTH, *Bell Telephone Laboratories.*—New types of powder patterns, and explanations of types previously reported,[1] have been obtained by deposition of colloidal magnetite on electrolytically polished surfaces of single crystals of iron containing 3.8 percent silicon. A specimen, having its long dimension almost parallel to a (110) direction, has domains of sheet or slab form set transverse to the long dimension, as postulated by Néel.[2] Lack of exact parallelism of the surface

with a (001) plane causes the formation of domains of closure having a form suitable for carrying transverse flux. A surface parallel to a $(0\bar{1}1)$ plane has a complicated structure, the main features of which are understood. When a field is applied normally to a specimen cut almost parallel to a (100) plane and having a "dagger-blade" pattern,[3] some of the lines are intensified and some obliterated; from this the variation of magnetization across the Bloch wall can be determined.

[1] H. J. Williams, Phys. Rev. 72, 529 (1947).
[2] Néel, J. de phys. et rad. 5, 241 (1944).
[3] H. J. Williams, Phys. Rev. 70, 106 (1946).

F4. Anomalous Magnetic Susceptibilities of Zinc Single Crystals at 4.2°K. S. G. SYDORIAK, *Yale University.**—The de Haas-van Alphen effect was discovered in zinc by J. A. Marcus and was studied by him at temperatures down to 14°K by measuring the body force on a single crystal. Although the magnetic susceptibility perpendicular to the hexagonal axis, $\chi_\perp$, was -0.150×10^{-6} for all fields and for all temperatures from 100°K to 14°K, $\chi_\parallel$ alternated with field at 14°K. Using a torsion method to measure $(\chi_\parallel-\chi_\perp)$ and a cryostat suitable for work at liquid helium temperatures, it is found that at 4.2°K the effect is much more pronounced than at 14°K. In the range 1.3 to 3 kilogauss, $(\chi_\parallel-\chi_\perp)$ changed sign 18 times. At fields >2 kilogauss the peak-to-peak variation is 0.340×10^{-6}, so, if we can assume $\chi_\perp=-0.150\times10^{-6}$, $\chi_\parallel$ actually swings between diamagnetic and paramagnetic values. Spacing of the peaks is such that $1/H$ of adjacent peaks differs by 0.046 ± 0.001 per kilogauss, in qualitative agreement with Blackman's theory. Above 3 kilogauss, however, the spacing is greater. At constant field the effect of ϕ, the angle between field and hexagonal axis is striking. Between $-90°$ and 0° there were 12 minima and 11 maxima in $(\chi_\parallel-\chi_\perp)$. The amplitude of the swings is greatest at $\phi=0$ and symmetrical about $\phi=0°$. At room temperature $(\chi_\parallel-\chi_\perp)$ is -0.048×10^{-6}.

* Assisted by the Office of Naval Research.

F5. Ferromagnetic Resonance Absorption in a Single Fe Crystal.* ARTHUR F. KIP AND ROBERT D. ARNOLD, *Massachusetts Institute of Technology.*—Ferromagnetic resonance in a single iron crystal† at microwave frequencies has been observed by methods similar to those of Griffiths.[1] For a given frequency, the value of applied magnetic field, H_s, necessary for maximum absorption has been measured as a function of the angle θ between H_s and the crystal axis. For $\nu=23{,}670$ mc/sec., H_s for resonance is 2480 gauss in the (100) direction and 3280 gauss in the (110) direction. Values at 9250 mc/sec. are 210 gauss and 930 gauss, respectively. Results are consistent with Kittel's theory.[2] Results at the higher frequency (requiring relatively large H_s) are consistent with the assumption that M_s, the magnetic moment/unit volume, aligns with H_s. Results at the lower H_s required at 9250 mc/sec. are consistent with the known fact that at the values of H_s used M does not always align with H_s. A consequence of this is that for θ near 45° a second resonance is found at a lower value of H_s.

* This work has been supported in part by the Air Materiel Command, the Signal Corps, and the O.N.R.
† Kindly loaned by Bell Telephone Laboratories.
[1] J. H. E. Griffiths, Nature 158, 670 (1946).
[2] Charles Kittel, scheduled to appear in Phys. Rev. 73, 155 (1948).

F6. Paramagnetic Resonance Absorption in Copper Sulfate.* ROBERT D. ARNOLD AND ARTHUR F. KIP, *Massachusetts Institute of Technology.*—The method for studying paramagnetic resonances in a magnetic field at microwave frequencies used by Zavoisky,[1] Cummerow and Halliday,[2] and others has been applied to a single crystal and to a powder of $CuSO_4\cdot H_2O$. The frequency used was 9047 mc/sec. The magnetic field necessary for maximum absorption in the single crystal was studied as a function of the angle between the magnetic axis of the crystal and the direction of the magnetic field. Anisotropy in the crystal was found to cause a variation in the magnetic field for resonance of from 3080 gauss for the magnetic axis parallel to the field to 2860 gauss for the magnetic axis perpendicular to the magnetic field. Results in the powder are in at least qualitative agreement with single-crystal results. Theoretical considerations referring to these results are given in paper G8 by Van Vleck.

* This work has been supported in part by the Air Materiel Command, the Signal Corps, and the O.N.R.
[1] E. Zavoisky, J. Phys. U.S.S.R. 10, 197 (1946).
[2] R. L. Cummerow and D. Halliday, Phys. Rev. 70, 433 (1946).

F7. Ferromagnetic Resonance Absorption at Microwave Frequencies. W. A. YAGER, *Bell Telephone Laboratories.*—After having observed[1] the sharp resonance absorption at a wave-length of 1.25 cm in annealed Supermalloy, further experiments have been carried out in several materials subjected to various superposed field strengths. New measurements on an annealed sample of Supermalloy over the range from 15 to 7500 oersteds indicate that the apparent r-f permeability μ_R, for 1.25-cm waves, has a minimum value of around 0.09 at about 200 oersteds, and at lower fields increases rapidly to unity as the applied magnetic field decreases toward zero. This behavior is compared with theory. In the unannealed condition, after severe cold rolling, the resonance maximum is broader than in the annealed state but its position and, therefore, the "g" value remain unchanged. Measurements on a hydrogen-treated sample of pure iron and an annealed sample of nickel are in general agreement with the results reported in the original paper of Griffiths.[2]

[1] W. A. Yager and R. M. Bozorth, Phys. Rev. 72, 80 (1947).
[2] J. H. E. Griffiths, Nature 158, 670 (1946).

F8. Effects of Nuclear Electric Quadrupole Moments in Nuclear Paramagnetic Resonance Absorption. R. V. POUND, *Harvard University.*—In liquids $\partial^2V/\partial z^2$ fluctuates very rapidly as a consequence of thermal agitation and averages nearly to zero in one r-f period. Thus a nuclear electric quadrupole moment affects the absorption line due to the nuclear magnetic moment only through a shortening of the "spin-lattice" relaxation time, T_1. This effect has been found to be large for aqueous solutions of Br^{79} and Br^{81}, providing identification of the two lines through their different widths. In crystals having lower than cubic symmetry the magnetic moment lines of nuclei possessing quadrupole moments should be split by the interaction with $\partial^2V/\partial z^2$, z being along the field direction. The Li^7 lines in powdered Li_2CO_3 and $Li_2SO_4\cdot H_2O$ have been found to

spread over 80 and 50 kc/sec. and to have shapes in agreement with a quadrupole interaction. In single crystals of $Li_2SO_4 \cdot H_2O$, the Li^7 line has been found to break up into three components for certain orientations of the crystal in the magnetic field. Experiments are under way to determine the dependence of the splitting on orientation to see if it is in agreement with estimates, based on the crystal structure, of $\partial^2 V/\partial z^2$, to which the H_2O molecule may be a large contributant.

F9. Fine Structure of the Proton Paramagnetic Resonance Line in Crystalline Hydrates. G. E. PAKE, *Harvard University.*—Fine structure has been observed in the nuclear resonance absorption line for protons in crystalline hydrates. The stability of a permanent magnet, which provided the field of 6820 gauss, facilitated line shape studies. Measurements on a single crystal of $CaSO_4 \cdot 2H_2O$ reveal four component lines with pattern width varying from zero to 22 gauss, depending upon the magnetic field direction in the crystal. The number of component lines and the dependence of their spacing on field direction are calculated by treating the magnetic dipole-dipole interaction as a perturbation of the two-proton system in the water molecule; the more distant proton moments, neglected in this calculation, provide finite width for the component lines. Variation of the splitting with field direction determines the orientation in the lattice of the line connecting protons of the water molecule. The length of this line in $CaSO_4 \cdot 2H_2O$ is measured by the splitting to be 1.58A; for an assumed H—O—H bond angle of 108°, the O—H distance is 0.98A. The isotropically oriented microcrystals of powdered hydrates lead to a characteristic fine structure which determines the proton-proton distance somewhat less accurately.

F10. Orientation of Domains in Polycrystalline $BaTiO_3$. G. C. DANIELSON, *Bell Telephone Laboratories.*—The orientation of domains in $BaTiO_3$ polycrystalline ceramic disks has been determined from back reflection x-ray diffraction photographs as well as from their piezoelectric effects.[1-3] The observed changes in the relative intensity of the (510) and (015) planes, using copper radiation, and the (311) and (113) planes, using chromium radiation, upon application of an electric field can be interpreted in terms of orientation of the ferroelectric domains. A method of quantitatively measuring the angular distribution of domains is indicated. Just above the Curie temperature the application of an electric field changes the symmetry of many $BaTiO_3$ crystals as shown by an increase in the number of non-cubic crystals.

[1] S. Roberts, Phys. Rev. 71, 890 (1947).
[2] W. P. Mason, Phys. Rev. 72, 869 (1947).
[3] W. L. Cherry and R. Adler, Phys. Rev. 72, 981 (1947).

F11. The Existence of Relations Among the Thermomagnetic and Galvanomagnetic Coefficients.* H. B. CALLEN, *Massachusetts Institute of Technology.*—The application of Onsager's reciprocal relations** to the thermomagnetic and galvanomagnetic effects in isotropic systems allows one to express the coefficients of all the effects in terms of six independent "kinetic coefficients." There are, thus, two independent relations among the eight commonly defined*** coefficients in a magnetic field. One of these relations, connecting the Ettinghausen and Nernst coefficients and the isothermal heat conductivity, has been previously obtained by Bridgman, but there has hitherto been some doubt and speculation as to the existence of relations other than this. The second relation is a rather complicated one, but may be shown to degenerate in weak magnetic fields into the equalities between the adiabatic and isothermal values of the electric and heat conductivities.

* This work was supported by O.N.R. and the U. S. Signal Corps.
** L. Onsager, Phys. Rev. 37, 405 (1931); 38, 2265 (1931).
*** A. Sommerfeld and N. H. Frank, Rev. Mod. Phys. 3, 1 (1931).

G1. Antenna Current Distributions.[1] RICHARD C. RAYMOND AND WAYNE WEBB, *Pennsylvania State College.*—An apparatus has been built and used to measure the current amplitude distributions on some types of high frequency antennas. Comparison of the measured distributions with several assumed distributions shows that none fit very precisely. Calculation of radiation resistances from the current distributions by the Poynting vector method gives fair agreement with measured resistances as determined by the standing-wave method. The differences between the measured and commonly assumed distributions are such that their effects on the radiation resistance are relatively small.

[1] This work was supported in part by the Army Air Forces.

G2. Nuclear and Molecular Magnetic Moments in Microwave Zeeman Spectra.* C. K. JEN, *Harvard University.*—The Zeeman effect of a number of microwave spectral lines has been studied by applying a magnetic field in a resonant cavity which acts as the absorption cell. In a detailed investigation of ordinary ammonia gas, the doublet separation in a weak magnetic field was found to be approximately 0.72 mc per 1000 gauss. The Zeeman separation proves to be very nearly independent of the quantum numbers for various spectral lines, in agreement with the results of Coles and Good.[1] Almost the same constant separation applies to the satellites due to nuclear quadrupole moments. The observed effects can be explained theoretically only when we assume that the g-factor due to N^{14} nuclear spin and that due to molecular rotation are of the same order of magnitude, and that for a weak field the two g-factors combine through the spin-rotation coupling. The analysis yields a g-factor 0.48 ± 0.03 for the molecular moment, when one uses the known value of 0.403 for the N^{14} nuclear moment, both expressed in nuclear magnetons. Thus, measurements of the Zeeman effect for microwave spectra should provide a new source of information about the nuclear and molecular magnetic moments and the way they are coupled.

* The research presented in this abstract was carried out under contract with the Office of Naval Research and the Signal Corps.
[1] D. K. Coles and W. E. Good, Phys. Rev. 70, 979 (1946).

G3. Pure Rotational Spectrum of ICl. C. H. TOWNES* B. D. WRIGHT,** AND F. R. MERRITT, *Bell Telephone Laboratories.*—About thirty lines due to the $J=3->4$ rotational transition of ICl have been found at wave-lengths near 1.1 cm. From these lines the nuclear quadrupole coupling, $eqQ=eQ(\partial^2V/\partial z^2)$, may be determined for I as minus 2930 mc, and for Cl^{35} as minus 82.5 mc. The iodine coupling is so large that effects[1] of the order $(eqQ)^2/B$ must be taken into account in order to fit the experimental results adequately. A line due to molecules in the first excited vibration state was detected so that the rotational constants B_e and α_e can be determined as 0.114164 cm^{-1} and 0.000536 cm^{-1}, respectively, for ICl^{35}. These are in agreement with previous, less accurate determinations.[2] The frequency interval between ICl^{37} and ICl^{35} lines gives a mass difference between Cl^{37} and Cl^{35} about one part in 2000 less than mass-spectroscopic measurements.[3]

* Now at Columbia University.
** Now at University of Chicago.
[1] Bardeen and Townes, Phys. Rev. to be published.
[2] Curtis and Patkowski, Phil. Trans. Roy. Soc. 232, 395 (1934).
[3] Mattauch, *Nuclear Physics Tables* (Interscience Publishers, Inc., 1946), p. 130.

G4. Stark Effect in High Frequency Fields. F. R. MERRITT AND C. H. TOWNES,* *Bell Telephone Laboratories.*—Stark effect on molecular lines falling in the microwave region has been obtained by a number of workers. Because of the relatively long time required for radiation absorption to take place at microwave frequencies, the Stark field may be varied appreciably during one absorption process. A solution of the time-dependent wave equation can be obtained by perturbation methods which is good for any frequency of variation of the Stark field small compared to other molecular frequencies. At low frequencies this solution reduces to the normal static-field solution. At frequencies of the order of the line width 1 megacycle, the Stark components do not change frequency synchronously with the Stark field, but new lines appear in the absorption spectrum separated by integral multiples of the frequency of the applied field. At still higher frequencies the spectrum is again reduced to the normal number of Stark components, but their frequencies represent an average of the Stark field. These effects have been observed experimentally with the $J=1->2$ line of OCS. Relative intensities of lines under different conditions have been calculated and agree well with experimental results. A similar behavior should be produced by other time-dependent perturbations.

* Now at Columbia University.

G5. Microwave Absorption Spectrum of COSe.* M. W. P. STRANDBERG AND T. WENTINK, JR., *Massachusetts Institute of Technology.*—The $J=2$ to 3 transition in the pure rotation spectrum of COSe, which is a linear molecule, was investigated using a Stark modulation microwave spectroscope.[1] The spectrum which lies between 23,500 and 24,500 Mc/sec. contains lines due to all the known stable isotopes of selenium in conjunction with the C^{12} and O^{16} isotopes. No quadrupole effects were observed. Rough measurements of intensity ratios are in agreement with the reported abundances. Weaker lines were observed for $C^{12}O^{16}Se^{8}$ and $C^{12}O^{16}Se^{78}$ and for excited vibration states of the $C^{12}O^{16}Se$ molecule with several selenium isotopes. The symmetrical stretching $v_1=1$ and the bending vibration $v_2=1$ were excited in sufficient amounts to be observed. From the intensity compared to the ground state lines the fundamental infra-red vibration frequency ω_2 has been estimated to be 440 cm^{-1}. Further work is in progress to obtain accurate mass ratios and interatomic distances.

* This work has been supported in part by the Signal Corps, the Air Materiel Command, and O.N.R.
[1] R. H. Hughes and E. B. Wilson, Jr., Phys. Rev. 71, 562 (1947).

G6. Stark Effect in the COSe Molecule.* T. WENTINK, Jr., M. W. P. STRANDBERG, AND R. HILLGER, *Massachusetts Institute of Technology.*—The Stark splitting has been measured for many of the lines in the COSe spectrum near 24,000 Mc/sec. A square-wave Stark voltage was used with the Stark electrode essentially grounded for half the cycle so that the Stark components and the undeviated line are both sharp. Field strengths of 7.5 kv/cm are obtainable. The Stark field is parallel to the microwave electric field and only the π components of the spectrum are observed. For the $J=2$ to 3 transition in COSe, components are observed for $m=0$, ±1, and ±2 which are well resolved from the undeviated line. In the ground vibration state they show a quadratic Stark effect, which corresponds to a dipole moment of 0.752 ± 0.007 Debye units. Values for the several selenium isotopes are the same within experimental error. The quadratic Stark splitting has also been measured for molecules in the $v_1=1$ stretching vibration mode. The dipole moment measured for this state is 0.728 ± 0.007 Debye units. The lines for the excited bending vibration show a linear Stark effect except for Stark splittings that are small compared to the *l*-type doubling.

* This work has been supported in part by the Signal Corps, the Air Materiel Command, and O.N.R.

G7. Minimum Detectable Absorption in Microwave Spectroscopy and an Analysis of the Stark Modulation Method. W. D. HERSHBERGER, *Radio Corporation of America.*—It is shown that the minimum detectable absorption coefficient for an isolated spectral line, as measured in a matched wave guide of optimum length, is $[(4kTN\Delta f)/(Po/e)]\alpha_e$, where N is the noise factor and Δf the band width of the receiver, α_e is the attenuation constant for the wave guide, and Po/e is the average microwave power available at the receiver. The equivalence between cavity and wave guide methods is developed. The Stark modulation method of Hughes and Wilson is analyzed, assuming a quadratic Stark effect, and expressions are developed for the modulation factor of a microwave at twice and four times the frequency of the Stark field. For a matched guide the modulation factor is $\alpha_e l/4$. Also the shift in line position is calculated, and finally, the directions in which improvement in sensitivity may be expected are indicated.

G8. Theory of the Width of Microwave Lines in Cupric Salts. J. H. VAN VLECK, *Harvard University.*—In a magnetic field of the order 10^3 gauss, cupric salts have a resonance absorption in the microwave region caused by the

magnetic dipole moment of the electron spin. Since a crystalline field cannot split the twofold degeneracy of the ground level, the absorption lines for a single crystal are broadened only by dipolar coupling. The phenomenon of "exchange narrowing"[1] makes this broadening less than one would calculate from the mean square under the Gaussian hypothesis. As the result of the action of the crystalline field, the g-factor is anisotropic. Hence, the position of the lines in single crystals depends on the orientation of the principal axes relative to the magnetic field. This anisotropy broadens the lines for a powder even without the dipolar effect. A calculation is made of the resulting line structure on the basis of the model of the crystalline field for $CuSO_4 \cdot 5H_2O$ developed by Krishnan and Mookherji[2] and by Polder.[3] Comparison with experiment is made in abstract F6 by Arnold and Kip.

[1] C. J. Gorter and J. H. Van Vleck, Phys. Rev. **72**, 1128 (1947).
[2] K. S. Krishnan and A. Mookherji, Phys. Rev. **54**, 533, 841 (1938).
[3] D. Polder, Physica **9**, 709 (1942).

G9. Anomalies in the Infra-Red Spectra of Phosphine and Arsine. VIRGINIA M. MCCONAGHIE AND HARALD H. NIELSEN, *Ohio State University.*—The infra-red spectrum of phosphine has been measured by Fung and Barker[1] who interpreted it on the basis that the molecule is an accidentally spherical rotator. The spacing between rotation lines in the fundamental bands ω_1 and ω_3, however, leads to rather different values of the moment of inertia of the molecule. It is found in measurements made here that much the same condition exists for the AsH_3 and AsD_3 molecules. It may be demonstrated that the spacing between rotation lines in the two fundamental bands ω_3 and ω_4, which overlap each other in the spectra of all these molecules, may be expected to be anomalous. The frequency ω_3, which is along the z axis (symmetry axis) of the molecule and the twofold degenerate frequency, ω_4, which is in the xy plane of the molecule, are nearly alike. This resonance gives rise to a first-order Coriolis interaction between a nearly isotropic three-dimensional oscillator and an accidentally spherical rotator. In the P and R branches of the frequencies ω_3 and ω_4 ($\omega_3 < \omega_4$) a value for the rotational spacing between rotation lines $\Delta\nu = (1+\zeta')(h/4\pi^2 Ic)$ is predicted; in the R and P branches of these same bands a rotational line spacing of $\Delta\nu = (1-\zeta')(h/4\pi^2 Ic)$ is expected as J assumes large values. ζ' may be regarded as the Coriolis coupling coefficient.

[1] Lai Wing Fung and E. F. Barker, Phys. Rev. **45**, 238 (1934).

G10. Interaction of Nuclear Quadrupole Moments with Molecular Rotation in Asymmetric Rotor Molecules. J. K. BRAGG, *Harvard University.*—A theoretical treatment is given of the splitting of the rotational levels of an asymmetric top molecule due to interaction of electric quadrupole moments of one or two nuclei with the electric field of the molecule. The matrix elements of the coupling operator $3(I\cdot J)^2 \cdot \frac{3}{2} I\cdot J - I^2 J^2$ are the same as for linear molecules and symmetric tops, but the parameter $\langle(3\cos^2\theta - 1)/r^3\rangle_{Av}$ depends on the transformation which diagonalizes the energy of the asymmetric top in question, and involves two constants of the molecule for a given vibrational and electronic state, $\partial^2 V/\partial z^2$ and $\partial^2 V/\partial x^2 - \partial^2 V/\partial y^2$, where x, y, z refer to the directions of the principal axes and V is the electrostatic potential at the nucleus in question. The possibility of use of these facts in identification of asymmetric rotor spectra is mentioned, and experimental work in progress on two molecules, CHF_2Cl and CH_2Cl_2, is described.

G11. Absorption by N_2 and O_2 of Solar Wave-Lengths in the Extreme Ultraviolet. K. C. CLARK, *Harvard University.*—The presence of ionized layers in the upper atmosphere is known to depend in part on the incident solar radiation, which undoubtedly contains prominent emission lines of H and He at wave-lengths sufficiently short to ionize the atmospheric gases. Absorption coefficients of N_2 and O_2 were measured with a vacuum spectrograph with an electrodeless discharge to produce with constant intensity the H Lyman series through the seventh member (λ926) and the principal line λ584 of the HeI series. From the absorption coefficients measured for H Lyman 2, 3···7 and HeI λ584, the height of maximum absorption by the atmosphere is computed for each wave-length with standard estimates of the composition and temperature. The F layer may plausibly be assigned to ionization of N_2 and O by HeI λ584. Because of their strong absorption by N_2 far above the dissociation height of O_2, the lines of H and HeI measured cannot ionize atmospheric O_2. Similarly, none of the lines measured can penetrate to the height of the D layer. The E layer may still be attributed to possible ionization of O_2 by higher members of the Lyman series or by continuous blackbody solar radiation in the range $\lambda\lambda$1010–910.

G12. Experimental Check on Intensity Distribution in Small-Angle X-Ray Scattering. JOHN TURKEVICH AND HARRY H. HUBBELL, JR.,* *Princeton University.*—The Guinier formula for the intensity of x-rays scattered at small angles by finely divided materials has been checked experimentally in several respects. With a sample of carbon black, seven crystal-monochromated wave-lengths gave scattered intensity *versus* angle curves which superposed within experimental error over a 10,000 to 1 intensity range when the angles were divided by the appropriate wave-lengths. The wave-lengths used ranged from 0.71 to 2.28A. Three filtered $K\alpha$ wave-lengths gave similar results on this sample and also on three gold colloids and several other samples. A gold colloid prepared by precipitation with sodium citrate from gold chloride solution gave a scattering curve agreeing with that predicted over a fifteenfold intensity range for three wave-lengths. Electron microscope pictures show this colloid consists of spherical particles of 200±24A diameter, with about 57 percent of the particles falling in this range. The scattered intensity curve shows unmistakably the first secondary maximum in intensity predicted by the theory and in nearly the right position. Intensities were measured by a Geiger counter whose linearity was repeatedly checked. Photographs also show the secondary maximum shifting with wave-length as predicted.

* Now at Middlebury College.

G13. The Effect of Apparatus Geometry on Small-Angle X-Ray Scattering Curves. HARRY H. HUBBELL, JR., *Princeton University.*—It was calculated that the frequently used Gaussian-error type approximation to the intensity as a function of angle for x-rays scattered by finely divided materials was not valid for intensities less than one-tenth that scattered at zero angle. Calculations showed that the secondary maxima and minima predicted by Guinier's[1] exact scattering theory for homogeneous spherical particles will be smeared out by the use of slits instead of pinholes to define the x-ray beam. The first secondary maximum will move toward smaller angles as the slits are made longer. Increasing the length of the slit rapidly fills the minimum of the intensity curve, but raises the intensity of the secondary maximum much less. Methods suggested by other workers for correcting scattering curves observed with slit geometry to corresponding pinhole curves destroy any secondary peaks which might appear. These peaks have been observed (see previous paper). The effect of a distribution in particle sizes was shown to be a further smearing out of the secondary maximum until as narrow a spread as one having a mean deviation of 12 percent in particle diameter gives a scattering curve without any secondary peak.

[1] A. Guinier, Ann. de physique **12**, 161 (1939).

G14. A High Temperature X-Ray Diffraction Camera.* JAMES W. EDWARDS, RUDOLPH SPEISER, AND HERRICK L. JOHNSTON, *The Ohio State University.*—In this Laboratory, we have developed an x-ray powder diffraction camera that is designed for use up to 3000°K. The sample in form of a wire, compacted rod, or contained (wherever suitable) in a thin-walled quartz or ceramic tube is heated indirectly by conduction and radiation in a thin-walled graphite, tantalum, molybdenum, or tungsten furnace. The furnace is heated by high frequency (0.5 megacycle) eddy currents induced by a small induction coil. The cylindrically shaped furnace and the sample are held coaxially in the induction coil and slowly revolved. The specimen temperature is maintained constant to ±0.2 percent by an especially designed temperature regulator. A copper water-cooled jacket, with slots fitted with metal foil to filter the diffracted x-radiation, completely surrounds the furnace and is used to protect the x-ray film from the heat and light. The Straumanis film arrangement is used. The temperature of the furnace is measured with a disappearing filament optical pyrometer. The entire camera is evacuated and operated at pressures less than 1×10^{-4} mm Hg. X-ray diffraction patterns of molybdenum at 2500°K have been made. Copper $K-\alpha$ radiation has been used and exposure times of 2 hours. Very satisfactory patterns of molybdenum were obtained.

* Supported by the Office of Naval Research.

G15. On the Diffraction of X-Rays from Coarse Powders. ZIGMOND W. WILCHINSKY, *Standard Oil Company of New Jersey, Louisiana Division.*—In developing the integrated intensity equation for diffraction of x-rays from coarse powders, it is necessary to consider the contribution of diffracted energy from each particle. For any particle below the surface of the sample, the incident and diffracted rays are of course attenuated. In a previous development[1] the required absorption factor was computed in the same manner as for a fine powder, whereas in the present treatment the absorption factor is obtained by considering the statistical distribution of coarse particles. The predictions of these two theories differ conspicuously for the case of a coarse powder consisting of a single crystalline phase. According to the older theory, the integrated intensity should not be affected by particle size; however, the proposed theory predicts that under certain conditions the integrated intensity could be considerably lower than for an ideal fine powder. Experimental results indicate that the integrated intensity decreases with increasing particle size and decreases with decreasing degree of compaction of the powder, in accord with the new theory.

[1] G. W. Brindley, Phil. Mag. **36**, 347 (1945).

H1. Test of the Hypothesis that the Sea-Level Cosmic-Ray Meson Disintegrates into a Photon and an Electron.* R. D. SARD AND E. J. ALTHAUS, *Washington University.*—The hypothesis has been tested by searching for delayed coincidences between the 50-Mev photon, detected by its materialization in a Pb sheet and the arrival of the meson that gets stopped. From top down: Geiger-Mueller tubes, A; 12.5-cm Pb filter; G-M tubes, B; 21.6 g/cm² brass absorber; anti-coincidence G-M tubes, C; 9.74 g/cm² Pb photon converter (calculated chance of at least one electron emerging, 50 to 60 percent); G-M tubes, D; G-M tubes, E. The circuit[1] records simultaneous and delayed coincidences ($AB:DE$) between coincidences of D and E and of A and B For detecting the photon, an anti-coincidence circuit permits registration only when C is not triggered within 10 μsec. Without C and the Pb sheet, ($AB:DE$) delayed 1.16 to 7.93 μsec. (due to decay electrons from brass) occur at 0.42±0.07/hr. With C and the Pb sheet, ($AB-C:DE$) delayed 1.16 to 7.93 μsec. (decay photons from brass) should occur at about 0.24/hr. if the hypothesis is correct. There have been only 4 in 314 hrs., and these can be accounted for by the measured inefficiency of C.

* Work supported in part by the U. S. Navy.
[1] We are indebted to B. Rossi, M. Sands, and M. H. Hubbard of M.I.T. for provision of the coincidence circuit. It was designed by Sands (B. Rossi, M. Sands, and R. D. Sard, Phys. Rev. **72**, 120 (1947)).

H2. The Decay of Slow Mesons.* G. E. VALLEY, *Massachusetts Institute of Technology.*—The mean life for decay of slow positive and negative mesons has been examined for mesons stopped in beryllium. Within the experimental error, the mean lives of mesons of both signs is equal to the accepted value of about 2.2 μsec. It is found that approximately equal numbers of mesons of each sign decay in beryllium. There is no evidence that more than one charged particle is emitted during the decay of either a positive or a negative meson in beryllium. The experiment is now being repeated to find out the behavior of mesons stopped in magnesium.

* The research described in this letter was supported partially by the Office of Naval Research.

H3. The Production of Mesotrons in Cosmic-Ray Stars in the Stratosphere.* J. J. LORD AND MARCEL SCHEIN, *University of Chicago.*—Two Ilford, type C2 plates sent along with a free-balloon experiment in the stratosphere were exposed to cosmic radiation at an altitude greater than 60,000 feet for a period of eight hours. In the two square centimeters of the plate examined so far, the rate of star production corresponded to approximately 6000 stars of more than 4 long-range particles per cubic centimeter of emulsion per day. In some of the stars, nuclei heavier than α-particles were emitted which then disintegrated at the end of their range into two particles ("hammer track"). One of the stars consisted of ten well separated particles emitted from a common center. Two of the tracks in this star were identified as protons by their total number of grains *versus* range.[1] Two very long-range tracks (917 and 1512 microns), one of which originated in the center of a star and both stopping in the emulsion, were identified as mesotrons. Since, in these events of mesotron production, the total energy in the stars appears to be only a few hundred Mev, it does not seem to be impossible that mesotrons can be created artificially by the recently developed high energy machines.

* This research was supported in part by the U. S. Navy.
[1] Lattes, Occhialini, and Powell, Nature **160**, 453 (1947).

H4. On the Interpretation of Data on Large Air Showers.* JOHN M. BLATT, *Massachusetts Institute of Technology.*—Two ionization chambers of area A, a distance $2a$ apart, record a count only if more than N particles traverse *each* chamber. Assuming all showers to hit vertically, let $S(N_0)$ be the number of showers per unit area per second in which *more* than N_0 particles cross the plane of observation. We assume the *same lateral structure function $f(r)$ for all showers*, i.e., the particle density a distance r from the shower axis is $p(r)=N_0f(r)$. If we neglect the finite size of the chambers, the counting rate $W(N, a)$ is an integral involving $S[N/Af(r)]$. The integral equation can be inverted, giving $S[N/Af(r)]$ as an integral involving $\partial^2W/\partial a^2$. The implications of this solution will be discussed. We then assume $S(N_0)$ proportional to $N_0^{-\gamma}$, and $f(r)=$ Molière's expression.[1] $W(N, a)$ was computed for $\gamma=1.65, 1.70, 1.75$. The curves show extremely sharp drops between $a=0$ and $a=0.005$ characteristic units (about 1-meter separation). The correction for the finite chamber size was found explicitly. It decreases the drop somewhat but does not eliminate it. The experimental results of Williams will be compared with this theory in the following paper.

* The research described in this abstract was supported partially by the Office of Naval Research.
[1] Heisenberg *et. al.*, *Cosmic Radiation* (Dover Publications, New York, 1946), p. 36.

H5. The Lateral Distribution Function of Cosmic-Ray Air Showers.* ROBERT W. WILLIAMS, *Massachusetts Institute of Technology.*—An arrangement of four ionization chambers with electronic coincidence and photographic recording of pulse height was used to investigate the lateral distribution of particles in large cosmic-ray air showers (Auger showers). The ionization chambers are thin-walled cylinders filled with five atmospheres of argon, purified to permit quantitative electron collection. At an altitude of 10,000 feet the number of two-chamber coincidences caused by showers was measured as a function of the separation between the two chambers, the other two chambers being used to help distinguish showers from nuclear disintegrations. The minimum particle density selected was 300 particles/m^2, and at all distances the number of coincidences varied approximately as (particle density)$^{-1.7}$. Between 12.2 meters and 0.36 meter the number of coincidences increased by a factor of two, somewhat less than expected from Blatt's calculations using Molière's lateral distribution function for the density of shower particles. This discrepancy, if real, would suggest that the actual distribution function is less concentrated at the core than the Molière function.

* The research described in this abstract was supported partially by the Office of Naval Research.

H6. Ionization Chamber Bursts at High Altitudes.* T. COOR AND G. A. SNOW, *Princeton University.*—A thin-wall, low pressure ionization chamber has been sent aloft by means of balloons to a pressure of 1.5 cm Hg. Sizes of pulses (0.8 to 20$\times$ionization of $Po-\alpha$) were telemetered to ground where they were recorded along with pressure. The frequency of bursts of all sizes increased rapidly up to the highest altitude reached. For bursts $>2Po-\alpha$ the rate *vs.* pressure curve corresponds to an exponential absorption in the atmosphere with a mean free path of 160 g/cm^2. In the range $0.8-2Po-\alpha$ the increase is much slower with altitude and a leveling off occurs at *ca.* 2 cm Hg. The ionization produced by all bursts $>0.8Po-\alpha$ was computed to be about 12 percent of the total ionization at 1.5 cm Hg. The absolute rate of those events is in fair agreement with the rate of star production found in photographic plates sent with the flights. The most reasonable assumption is that these bursts are stars and that they are closely associated with the primary process.

* Supported by the Office of Naval Research.

H8. Meson Induced Fission. J. A. WHEELER, *Princeton University.*—Experimental and theoretical evidence suggests that the non-electric interaction between ordinary mesons and nuclei is very weak in comparison to the electric forces. On this assumption it is possible to calculate for a relativistic particle of mass 200 and spin 0 the energy levels in the extended field of the nucleus. In the case of uranium the calculated energy release in the transition from the 2-s. to the 1-s. level is 6.7 Mev. The process in which this energy is transferred to the nucleus to cause fission is calculated to compete favorably with radiation, Auger transitions, and pair production. The energy required to produce fission of a nucleus with a meson in the 1-s. state is calculated to exceed by about 0.6 Mev the normal fission energy. That slow ordinary negative mesons will produce fission appears possible in the case of uranium and reasonably probable in the case of heavier nuclei where the energy available exceeds with greater certainty the threshold for fission.

H9. The Altitude Variation of Large Pulses in Ionization Chambers.* ROBERT I. HULSIZER, *Massachusetts Institute of Technology.*—Ionization pulses occurring in unshielded

cylindrical ionization chambers, borne by balloons to altitudes up to 87,000 feet (20 g/cm²), were recorded by means of a radio link to the ground. The chambers were constructed of $\frac{1}{32}$-inch brass, two inches in diameter by $5\frac{1}{2}$ inches long, and were filled with six atmospheres of argon. The number of pulses, corresponding to an energy loss in the chamber of 6.3 Mev, increases by approximately a factor of four between 30,000 feet (306 g/cm²) and 70,000 feet (45 g/cm²).

* The research described in this abstract was supported partially by the Office of Naval Research.

H10. The Absorption in Carbon and Lead of Cosmic-Ray Particles at Very High Altitudes.* MARTIN A. POMERANTZ, *Bartol Research Foundation.*—Curves concerning the absorption in lead of cosmic-ray particles at very high altitudes have been obtained. These reveal the nature of the variation with altitude of the intensity of the so-called "soft" component (here construed to consist of electrons and slow mesons). A progressive increase in the relative intensity of particles having a range in lead of less than approximately 25 g/cm² occurs at atmospheric depths between 250 mm of Hg and about 80 mm, followed by a rapid decrease apparently to zero at the top of the atmosphere. The absorption coefficient of particles having ranges exceeding the aforementioned value does not vary appreciably with altitude. A comparison of the relative stopping powers of carbon and lead indicates that the absorption in 17 g/cm² of C is equal to that in 8.8 g/cm² of Pb at an atmospheric depth of 250 mm. The Pb-equivalent decreases to 6.1 g/cm² at 100 mm, and thereafter increases with altitude, the value at 50 mm being 13.9 g/cm². A flight with standard apparatus utilizing an out-of-line counter has demonstrated that the effect of showers in the present experiments amounts to less than 5 percent of the measured intensities.

* Supported by Office of Naval Research.

J1. A Generalization of a Theorem by Larmor in Hydrodynamics. I. OPATOWSKI, *University of Michigan.*—If $S(x_1, x_2, x_3)=$const. is the equation of a surface to which a steady motion of a fluid is constrained, then the streamlines of the flow are determined on that surface by the equation $\int M(q_2dx_1-q_1dx_2)/(\partial S/\partial x_3)=$const., where the q_i's are the contravariant components of the velocity of the fluid, M is any function satisfying the equation $\Sigma_{i=1}^{i=3}\partial(Mq_i)/\partial x_i=0$ and x_3 is intended as eliminated in the integrand of the above formula by means of $S(x_1, x_2, x_3)=$const. If the x_i's are orthogonal cartesian coordinates, then $M=\rho=$the density of the fluid.[1] If the x_i's are general curvilinear coordinates, $M=\rho(a)^{\frac{1}{2}}$, where a is the value of the determinant of the coefficients a_{ij} in the expression for the length of arc: $ds^2=\Sigma_{i,j}a_{ij}dx_idx_j$. The result facilitates the study of streamlines of helical, spiral and general conical flows. In the latter, the streamlines are intersections of skew cones with surfaces of revolution. The result is valid for non-viscous fluids in absence of mass forces. No restrictions on compressibility and rotationality are necessary.

[1] J. Larmor. Rep. Brit. Assoc., 562–563 (1897).

J2. Response Time in Vacuum Gages. S. A. SCHAAF AND R. R. CYR.—A typical system for measuring pressures in a rarefied gas consists of a vacuum gage connected to the gas by a length of tubing, usually with an orifice of diameter smaller than that of the tubing at the end. The interior surface of this system will outgas at a fairly constant rate for a long period of time so that an equilibrium state will be reached with a definite non-constant pressure distribution along the tubing. The response time constant for the system to come to equilibrium and the difference in pressure between gas and gage are functions of the outgassing rate and the geometry of the system. An analysis is made assuming molecular flow and formulas are obtained for the response time and the pressure difference. It is shown that there is an optimum value of the tubing diameter for a given orifice diameter, gage volume and length of tubing. This optimum is rather critical; if the diameter is too small, response time constants of the order of hours may result. Experimental work has been done and the results compared with theory. This work was done under Office of Naval Research Contract.

J3. Selection of Adiabatic Parameters in the Theory of Oscillation of Gas Globes from Underwater Explosions. A. B. ARONS, *Stevens Institute of Technology.*—Three important parameters appearing in the theory of gas globe oscillation[1] are γ, the adiabatic exponent, k, the adiabatic energy constant, and E, the bubble energy per unit mass of the original explosive. These parameters cannot be calculated with sufficient accuracy from *a priori* considerations, but it is shown that if they are selected to fit three independent pieces of experimental evidence, the theory then fits the remaining experimental results and can thus be used to predict bubble pulse properties such as maximum radius, peak pressure, positive impulse, period, etc. over wide ranges of the independent variables. In this theory γ and E are fitted to period data, and k to bubble pulse peak pressure data. The resulting values for TNT are found to be: $\gamma=1.25$; $E=490$ cal/gm; $k=0.0552Z_0^{\gamma-1}$, where Z_0 is the absolute hydrostatic depth in feet.

[1] B. Friedman, "Theory of underwater explosion bubbles." Institute for Mathematics and Mechanics, New York University. Report No. IMM-NYU 166.

J4. Energy Partition in Underwater Explosion Phenomena.* D. R. YENNIE AND A. B. ARONS, *Stevens Institute of Technology.*—A survey is made of existing knowledge with respect to the distribution of energy in underwater explosions. It is shown that approximately 40 percent of the initial energy is radiated in a series of pressure waves which, from the point of view of energy flux, can be treated as approximately acoustical in the range subject to experimental measurement. Approximately 20 percent of the initial energy is dissipated through irreversible processes associated with the propagation of the shock front. The acoustical energy measured in the bubble pulse pressure waves is found to be very much less than the total energy lost by the bubble during the same interval, as determined from period measurements. Finally, after the oscillations have effectively died down, it is found that approximately

10 percent of the energy has been expended in displacing the water to form a gas bubble. About 30 percent of the energy is unaccounted for, and no direct evidence as to the mechanism of the loss appears to be available. The values quoted apply specifically to TNT as the explosive.

* The study upon which these results are based was made at the Underwater Explosives Research Laboratory, Woods Hole Oceanographic Institution under contract with the Navy Department Bureau of Ordnance.

J5. Relation between the Limiting Line Phenomenon and the Kármán Transonic Similarity Theory. W. PERL, *Columbia University.*—Kármán has recently given a small-perturbation treatment of compressible potential flows in the transonic speed range.[1] A verification of this theory in the lower transonic range (subsonic free stream), analogous to Kármán's verification[1] in the upper transonic range (supersonic free stream), is offered by the theoretical pressure distribution calculations of references 2 and 3. In references 2 and 3 the highest subsonic free stream Mach number M_1 at which a continuous potential flow exists for a Kaplan profile of thickness ratio τ is found, for variable τ, to satisfy the relation $(1-M_1)/\tau^{\frac{1}{3}}=K$, where K approaches, for small τ, a constant limiting value of the order of magnitude one. The pressure coefficient at a fixed point on the profile is expressible as $c_p=\tau^{\frac{1}{3}}f(K)$. These relations agree with the Kármán theory. The potential limit Mach number M_1 is identified in reference 3 as the lowest Mach number for the appearance of the limiting line phenomenon. The calculations of references 2 and 3 also offer a similar verification of the Kármán theory under the condition of local Mach number unity at a fixed location on the profile. Finally, the small perturbation form of the method of reference 3 agrees in general with the Kármán similarity theory.

[1] Th. von Kármán, "Similarity law of transonic flow," J. Math. and Phys. 26, 3 (1947).
[2] Carl Kaplan, "The flow of a compressible fluid past a curved surface," NACA ARR 3K02 (1943).
[3] W. Perl, "Calculation of compressible flows past aerodynamic shapes by use of the streamline curvature," NACA TN 1328 (1947).

J6. The Solitary Wave and Periodic Waves in Shallow Water. JOSEPH B. KELLER, *New York University.*—The equations for irrotational motion of an incompressible inviscid liquid with a free surface, over a rigid bottom and under the influence of gravity, are expressed in dimensionless form. The solution is expanded in powers of the ratio of the average depth to a typical horizontal dimension. It is found that the zero order terms in the expansions satisfy the equations of the non-linear shallow water theory, which were first obtained in this way by K. O. Friedrichs. For two dimensional motion over a horizontal bottom the only steady state solutions of these equations are the constant or piecewise constant, bore-like solutions. If the constant velocity is (g. depth)$^{\frac{1}{2}}$, the first order terms yield a two parameter family of periodic steady solutions similar to those of Korteweg and DeVries. When the wave-length in these solutions is infinite, they reduce to a one parameter family of solitary waves, similar to those of Rayleigh and Boussinesq. The present solutions yield more information and are physically more reasonable than the former ones, and have the added advantage of being obtained systematically. The method of obtaining higher approximations is perfectly definite, and the equations for the determination of the next approximation are given.

J7. Reflection and Transmission of Sound by a Spherical Shell. HERBERT B. KELLER AND JOSEPH B. KELLER, *New York University.*—A periodic point source in medium 1 is at the center of a spherical shell of medium 2 which is surrounded by medium 3. The densities, sound speeds and shell radii are arbitrary. For this case an exact, explicit expression for the sound pressure is obtained. If the shell radii become infinite but the thickness remains constant, and if media 1 and 3 are the same, the solution reduces to that of Rayleigh for plane waves normally incident on a flat plate. If the shell radii become infinite and if media 2 and 3 are the same, the solution yields the acoustic Fresnel formulae for normal incidence of a plane wave on a plane interface between two half-infinite media. For finite radii, with media 1 and 3 identical and the shell thickness small compared to a wave-length, a simpler form for the solution is obtained. This solution is found to agree with the approximate solution of H. Primakoff and J. B. Keller[1] for the sound fields reflected and transmitted by a thin shell of any shape, when their result is specialized to the present case.

[1] H. Primakoff and J. B. Keller, J. Acous. Soc. Am. 19, 820 (1947).

J8. On the Resistance to Motion through Highly Rarefied Gases. M. HEINEMAN,* *Harvard University.* (Introduced by R. Courant.)—A general formula is derived, valid at all Mach numbers M in the region of free molecule flow (infinite mean free path L), for the momentum per second due to impinging molecules on a convex body of any shape. In order to obtain the total force, the momentum per second of the reflected molecules must also be computed. This is done for the cases of specular reflection and of diffuse reflection with accommodation. Numerical tables of the drag coefficient C_D as a function of M have been worked out for both types of reflection for the following cases: an inclined plate, a sphere, a cylinder moving perpendicularly to its axis, a cone moving parallel to its axis, and an ellipsoid, to its major axis. It is indicated how the force might be calculated when the collisions between the reflected molecules and the rest of the gas are no longer negligible as in the case of free molecule flow. The method consists essentially in finding an expansion in terms of powers of $1/L$, for the velocity distribution function of the non-uniform gas.

* Now at New York University.

J9. On Supersonic Flow Patterns. M. M. MUNK, *Naval Ordnance Laboratory.*—In plans, supersonic, two-dimensional potential flows of a barotropic fluid reducibility of the equation for the reciprocal Legendre potential in the hodograph to the simple wave equation is associated with the absence of curvature of the Mach lines in the physical plane, and with tangency of the hodograph characteristics and the lines of constant direction of the conjugate charac-

teristics. For perfect gases, this condition prevails at a Mach number given by $M^2=4/3-\gamma$; equal to 2.5 for air. In the neighborhood of that Mach number, drawing of the Mach line net is particularly simple. The criterion for straightness of Mach lines for other barotropic fluids is stated, and the expansion curve for a hypothetical barotropic fluid is derived having straight Mach lines throughout.

J10. On the Linearized Supersonic Flow through Ducts. ALEXANDER WEINSTEIN, *Naval Ordnance Laboratory.*—The paper gives an analysis of the flow due to the distribution of sources along a skeleton cylinder. The results are compared with the corrected Beltrami's formulas for the flow of an incompressible fluid (*cf.* A. Weinstein, Bulletin American Mathematical Society **52**, 240 (1946)), and with the computation of Mack, Ludloff and Weiche (Journal of Applied Physics **18**, 681 (1947)).

J11. On the Differential Equations for Slip Flow.* C. TRUESDELL, *Naval Ordnance Laboratory.*—A fluid is defined as a continuum in which the dissipation function is a function of the following variables: a constant of dimension [mass]/[length][time]; a constant of dimension [length]^3/[time]^3/[temperature]; the mean pressure; the thermodynamic pressure, the temperature, the extraneous force, and their gradients up to (say) pth order; and finally the velocity gradients. The dissipation function is expanded in a power series in the velocity gradients of which each term is a power series in the gradients of the thermodynamic state. In the resulting expressions for the stress tensor terms involving tensors of rank 4 in the velocity gradients, tensors of rank 3 in products of the velocity gradients and state gradients, and tensors of rank 2 in the state gradients are retained. Expressions are then obtained for the stresses in slip flow of a rarefied gas which include those derived from kinetic theory by Burnett, Chapman-Cowling and Schamberg as a special case. The present derivation is based solely upon the principles of invariance, and therefore serves as a standard to which the results of a kinetic theory derivation must conform. The fact that the above-mentioned kinetic theory derivation produces equations less general than those derived indicates that a number of special assumptions, of which the Stokes relation is one, lie hidden in the kinetic theory development. The mathematical nature and physical implications of these special assumptions are discussed.

* Supported by O.N.R.

J12. On Methods of Deriving Three-Dimensional Gas Flow Patterns from Plane Flows. P. NEMENYI and R. PRIM, *Naval Ordnance Laboratory.*—Two questions are investigated: (1) From a plane rotational or irrotational flow pattern how can a flow pattern be obtained, all three components of which are different from 0, but depend only upon two variables? This investigation is a generalization of that of Poritsky who solved the problem for the special case where the third component is uniform throughout the field. (2) From a plane irrotational flow pattern how can a rotational flow be constructed the velocity vector of which is everywhere parallel to a common plane but dependent on all three coordinates? The problem was solved for incompressible fluids by Massotti. The present authors generalize Massotti's analysis to compressible fluids and apply their result to the special case of flow in horizontal layers along a winding surface with straight horizontal elements.

J13. Extension of Crocco's Theorems to Flows Having Non-Uniform Stagnation Enthalpy. R. PRIM, *Naval Ordnance Laboratory.*—Crocco's theorems relating the vorticity and pressure along streamlines of plane and of axially symmetric steady gas flows are generalized to include flows having non-uniform stagnation enthalpy by a reformulation in terms of the vorticity of the reduced velocity field. It is shown that Crocco's stream-function equations for steady-plane and axially symmetric gas flows remain valid if the restriction to flows having a uniform stagnation enthalpy is removed.

J14. Spark Shadowgrams of Spheres at Supersonic Speeds in Water.* J. HOWARD MCMILLEN AND R. L. KRAMER, *Naval Ordnance Laboratory.*—Spark shadowgrams have been taken of one-eighth inch steel spheres traveling through water at both transonic and supersonic speeds (above 5000 ft/sec). When a grid was placed between the sphere and the spark, the distortion of the grid shadow gave a qualitative picture of the pressure distribution around the sphere and in the region between the sphere and shock wave. At supersonic speeds, the usual concentration-of-light band which follows the absence-of-light band was replaced by a series of bands and fine lines covering an angular width of about 0.1 radian. By using masks to select beams from the spark, it was shown that these patterns were produced by rays passing near the shock-wave front. No simple optical explanation for these lines and bands, other than postulating certain pressure distributions within the shock wave, has been found. Spark shadowgrams were also obtained for fast spheres (7000 ft/sec) in air at Mach number 6.7. These showed temperature fronts paralleling the wake with the low temperature region on the trajectory side. Excitation of molecular vibration levels is offered as a possible explanation of these fronts.

* Supported by O.N.R.

J15. Measurement of Velocity Loss of Shocks Traveling in a Shock Tube. R. J. EMRICH, *Lehigh University* AND F. B. HARRISON, *Princeton University.*—The transits of a shock moving in a straight airfilled tube of 15-cm diameter past four stations have been measured within errors of less than ± 0.1 μsec. For shocks whose velocities at 25°C vary from 355 to 435 m/sec, the losses in velocity over 2.5 meters vary from 0.05 to 0.2 percent; repeated measurements on shocks of equal strength show a variation in the velocity loss of about the same magnitude as the velocity loss itself. Calculations, using the Rankine-Hugoniot relations applied to a normal shock in a perfect gas and measured values of sound velocity, indicate that for propagation into air of 70

percent relative humidity at 25°C shocks of strengths $(p_2-p_1)/p_1$ between 0.05 and 0.68 suffer decreases in shock strengths per meter of travel of about 0.5 percent. Of over 100 shock velocities measured, none showed a decrease in shock strength of more than 1.2 percent per meter of travel. A knowledge of the amount of decrease permits calculation of conditions in the gas at some desired point in a shock tube from a velocity measurement made ahead of the point. This work was supported by the U. S. Navy.

K1. Electrical Properties of Pure Silicon and Silicon Alloys. G. L. PEARSON AND J. BARDEEN, *Bell Telephone Laboratories.*—Electrical resistivity and Hall measurements have been made over the temperature range from 90°K to 900°K on pure silicon and on silicon alloys containing 0.0005 to 10.0 percent *P*-type impurity or *N*-type impurity. The resistivity curves in the intrinsic range indicate an energy level separation of 1.2-electron volts. In the transition region between the intrinsic and impurity ranges the Hall curves flatten and indicate that one free electron (or hole) is furnished by each impurity atom. The mobility and mean free path of both electrons and holes have been calculated as a function of temperature and impurity content. In the high temperature region where lattice scattering predominates the hole mobility is $5\times10^5T^{-1}$ cm²/volt-sec. and the mean free path is $2\times10^{-4}T^{-1}$ cm. At any given temperature the ratio of electron to hole mobility is 2.9. At lower temperatures the impurity atoms contribute to scattering so that the mobility and mean free path reach a maximum and decrease with further decrease in temperature as required by theory. In the impurity scattering region the mobility and mean free path are inverse functions of impurity content.

K2. Temperature Dependence of Work Function of Semiconductors. A. H. SMITH* AND P. H. MILLER, JR., *University of Pennsylvania.*—Samples of *P*-type and *N*-type silicon and of *N*-type germanium have been examined to determine the temperature dependence of the work function of these semiconductors as they are heated to near intrinsic temperatures. High temperatures of the semiconductors were obtained by passing current directly through the sample, and observations were made as the sample cooled. The method of determining change in work function was to observe the current *versus* voltage curves of photoelectrons emitted from a tantalum surface and arriving at the semiconductor surface. This experiment indicated negligible change in work function of semiconductors at high temperatures from that at 200°C. These results are consistent with the hypothesis of surface energy states. This work was supported in part by the U. S. Navy.

* Now at the University of Chicago.

K3. Deuteron-Bombarded Semiconductors.* K. LARK-HOROVITZ, E. BLEULER, R. DAVIS, AND D. TENDAM, *Purdue University.*—Pure germanium (resistivity of ~1 to 50Ω-cm) and *P*- and *N*-type germanium semiconductors have been bombarded with ~10-Mev deuterons. The resistivity of the pure samples decreases after bombardment. The resistivity of the *P*-type samples, measured both as bulk resistivity and as spreading resistance, also decreases. *N*-type samples show a tendency to a transformation into *P*-type, and the resistance, measured as spreading resistance, increases. These effects, observed immediately after bombardment, remain after the radioactivity of the sample has disappeared. Rectification and photo-effects change after bombardment with the change in sign of the carriers. From the measured radioactivity of the bombarded sample, the deuteron current and the number of recoils in the sample calculated from Coulomb scattering, the effect of new impurity centers, trapped hydrogen atoms, and lattice defects produced by recoil can be estimated.

* Assisted by Signal Corps and ONR contracts.

K4. Photoelectric Effects and Their Relation to Rectification at Metal-Semiconductor Contacts.* S. BENZER, *Purdue University.*—By illumination of a metal-semiconductor contact and observation of the photoelectric change in external current as a function of applied voltage, information may be obtained regarding the nature of the barrier layer. According to present rectification theories, a photocurrent flowing in the high resistance direction is expected at zero applied voltage, the photo-current saturating as voltage is applied in this direction. In the low resistance direction, the photo-current, which in this case is opposite to the dark current (photo-negative effect), should decrease in magnitude, approaching zero as the applied voltage reaches the barrier height. In these experiments, millisecond pulses of light were focused on the contact, producing current pulses in a series resistor which were amplified and observed on an oscilloscope. The photo-current as a function of bias was obtained in this manner for contacts of metal *vs.* various specimens of Ge and Si, and for contacts of the semiconductors *vs.* each other. While the results resemble the theoretical expectations in some aspects, there are marked anomalies. A non-rectifying contact, for example, may show large differences in photo-effect in the two directions.

* This work was assisted by a Signal Corps contract.

K5. Galvanomagnetic and Thermomagnetic Effects in Tellurium.[1] WAYNE SCANLON AND K. LARK-HOROVITZ, *Purdue University.*—The transverse Hall e.m.f. may be masked by other galvanomagnetic or thermomagnetic effects which also contribute to the measured e.m.f. In tellurium, the transverse effects are unusually large and were found to alter significantly the true Hall effect. The longitudinal effects were also investigated but were found to be so small that they did not alter the measured Hall e.m.f. appreciably. The Nernst effect was found to pass through a maximum value at about 130°C and was negligibly small at temperature below 30°C and above 300°C. This effect was eliminated from the Hall effect data by averaging results with both direction of sample current. The Ettingshausen effect in tellurium was found to pass through a maximum value at about 160°C, and decreased rapidly to zero on either side of the maximum. The sign of the effect was positive throughout the region of temperatures investigated. Since the thermo-electric power was found to be positive throughout this temperature range, the

Ettingshausen temperature difference produced an e.m.f. which was in the opposite direction to a positive Hall e.m.f. The maximum e.m.f. resulting from the Ettingshausen effect occurred in the region of temperatures where the apparent Hall coefficient showed the anomalous double reversal of sign from positive to negative and back to positive again. Upon correcting the Hall data for the Ettingshausen effect, no reversal of sign was observed.

[1] This work was supported by a Signal Corps contract.

K6. Theory of the Nernst and Ettingshausen Effects in Semiconductors at High Temperature.* V. A. JOHNSON AND K. LARK-HOROVITZ, *Purdue University.*—A large Ettingshausen effect exists in tellurium at high temperatures.[1] Earlier theories of galvanomagnetic and thermomagnetic phenomena in semiconductors are valid only in the impurity temperature range, whereas the present theory considers both electrons and holes. The Nernst coefficient, Q', is derived by calculating the transverse electric field, E, produced by thermal current flowing through a sample in a direction perpendicular to a magnetic field, H. The thermal current density, w, is evaluated under the assumption that there is no transverse temperature gradient, longitudinal electric field, nor transverse electric current. $Q'=E/(wH)$. The Ettingshausen coefficient P is calculated from the thermodynamic relation $P=Q'T$ and is expressed by quantities characteristic of the semiconductor:

$$\sigma\kappa P=\frac{9\pi kT}{16c}(n_1b_1^2+n_2b_2^2)+\frac{3\pi T^2}{8c}\left\{n_1b_1^2\frac{d}{dT}\left(\frac{\mu_1}{T}\right)+n_2b_2^2\frac{d}{dT}\left(\frac{\mu_2}{T}\right)\right\},$$

where σ, κ are electrical and thermal conductivities, n_1 number of electrons per cm^3, b_1 electronic mobility, μ_1 chemical potential for electrons, with subscript 2 pertaining to holes. The temperature behavior of P is in agreement with experiment.

* This work assisted by a Signal Corps contract.
[1] See preceding abstract.

K7. Temperature-Pressure-Conductivity Relations in Semiconductors. F. C. BROWN, *Cambridge 39, Massachusetts.*—Conductivity-temperature variations in semiconductors are interpreted as depending on number of electrons that have adequate thermal energy to enter conduction band against one or more field levels. The limited temperature range in selenium permits observation of only one level. Silicon and germanium have two. In hexagonal silicon crystals between room temperature and 400°K variation of conductivity is due to varying number of electrons having energy greater than 0.23 volt. With minute electrode contact area this value may vary because of nature of surface state with unbalanced electric field. Between 500°K and 1300°K the variation is largely due to the number of electrons having energy greater than 0.8 volt. By increasing pressure the work function is lowered for both levels. By pressure only at electrodes the low value work function can be reduced practically to zero, while conductivity through crystal lattice remains unchanged. Light sensitiveness corresponds to temperature effect. Thus radiation produces change of conductivity because of temperature rise at electrode contacts surfaces, and proportional to conductivity temperature coefficient. The proportional conductivity change by temperature (or radiation) is reduced by increased pressure, but within limits the absolute change of conductivity is increased by pressure.

K8. Structure and Conductivity in the VI$_b$ Group of the Periodic System.* A. VON HIPPEL, *Massachusetts Institute of Technology.*—In the sequence: oxygen, sulfur, selenium, tellurium, and polonium, a systematic change takes place from diatomic molecules, through ring and chain molecules, to a simple cubic lattice structure formed by atoms. This transition is paralleled by a modification in the electrical behavior from insulator (O, S), to semiconductor (Se, Te,) to metal (Po). The paper is concerned with this progressive change in structure and conductivity and with the interrelation of the two phenomena. It discusses first the stability of ring and chain molecules, considers next schematically the electronic conductivity of Se from the standpoint of the band picture, and, finally, suggests an alternative approach which connects structure and conductivity by extending qualitatively the concept of quantum-mechanical resonance from molecular structures to lattice structures.

* This work was supported by O.N.R. and the U. S. Signal Corps.

K9. Frequency Spectrum of Noise in Crystal Rectifiers.* WILLIAM MILLER, *University of Pennsylvania.*—The noise power generated by crystal rectifiers is found to have a $1/f$ spectrum for $10^3<f<10^6$ c.p.s.[1] A model has been investigated wherein noise represents a modulation of the crystal current by motion of impurity atoms in the semiconductor. The correlation function (hence the power spectrum) can be found by calculating probability after effects for the distribution of impurity atoms in the semiconductor, and then relating each distribution to a value of noise current. If one assumes that the noise is generated only by the impurity atoms in a thin layer near the surface of the semiconductor, then the calculated power spectrum is more complicated than the observed $1/f$ law, giving a $1/(f)^{\frac{1}{2}}$ dependence for $f\ll\lambda$, and $1/f^3$ for $f\gg\lambda$. (λ = average jumping frequency of an impurity atom.) The case of many layers, each with its own modulating factor, has been solved, but the result contains too many parameters to be useful at present without further assumptions.

* Assisted by the Office of Naval Research.
[1] P. H. Miller, Jr., Proc. I.R.E. Waves and Electrons **35**, 252 (1947).

K10. Theory of the Luminescence of Ionic Phosphors. FERD E. WILLIAMS,* *General Electric Company.*—The ionic radii of excited states of Tl^+ and Mn^{++} are computed approximately and, recognizing that the ions of a crystal are relatively incompressible compared to the lattice, potential energy curves are constructed for the normal and excited states of these ions in the KCl and ZnF_2 lattices, respectively. Corrections are applied for the Madelung, exchange repulsion, ion dipole, and van der Waals interactions. A single precise configuration coordinate, namely, the distance from the activator ion to the nearest neighbor, is used for all potential energy curves, but various assumptions are made as to the behavior of the rest of the lattice

for different processes. To compute peak absorption and emission energies it is shown to be reasonable and to result in moderately good agreement with experiment to assume that the entire lattice expands freely to accommodate the activator in whatever state it exists, whereas to compute the activation energy for the competing radiationless recombination, it is assumed that the next nearest neighbors are held rigid. A new origin of electron traps is suggested. On the basis of the analysis several criteria for luminescence are cited, and several significant experiments are proposed.

* Also Assistant Professor of Chemistry, University of North Carolina, Chapel Hill, North Carolina.

O1. Design Study for a 10-Bev Proton Synchrotron. M. STANLEY LIVINGSTON, *Brookhaven National Laboratory.**—The threshold for the production of pairs of nucleons by protons is believed to be 5.6 Bev,[1] and a preliminary design figure of 10 Bev has been chosen for the Brookhaven Accelerator Project. Orbit radius required for 10-Bev protons at 15 kilogauss is 80 ft., and economy prescribes a ring magnet and synchrotron acceleration. At 4-Mev injection energy the frequency is 180 kilocycles; at 10 Bev it is 2.0 megacycles. Such low frequencies allow pulse techniques for injection and ejection. Allowing 1 sec. for acceleration, the average voltage per turn is 5500 volts. Aperture requirements due to ion oscillations suggest a magnet gap 4 ft. wide and 1 ft. long, with a doughnut vacuum chamber between poles. The vacuum requirements to reduce gas scattering during acceleration are within practical limits. A "*C*" magnet constructed of ½-inch laminations to reduce eddy current losses will have 5×10^7 joules stored energy; rotating machinery and flywheels can reutilize stored energy and reduce power requirements. The frequency-modulated accelerating system may require straight sections and a "racetrack" magnet design. Model studies and component designs are in progress.

* Research carried out under the auspices of the Atomic Energy Commission.
[1] Feshbach and Schiff, Phys. Rev. **72**, 254 (1947).

O2. Induction Accelerator for a Proton Synchrotron. JOHN P. BLEWETT, *Brookhaven National Laboratory.**—The radiofrequency accelerating system for the proposed Brookhaven proton synchrotron must supply an average 5500 ev of energy per revolution to the ion beam, and must operate over the frequency range 180 kc to 2000 kc. Resonant structures of the sort used in electron synchrotrons would be very large and extremely difficult to tune over the frequency range. If operated untuned their impedance levels would be unreasonably low, calling for circulating currents of thousands of amperes. Higher impedance levels are attainable, however, in a "transformer" type of accelerating system. In one of the straight sections of a racetrack a ferromagnetic core surrounds the vacuum envelope. A winding on the core serves as primary, and the ion beam is the secondary. Reasonable impedance and power levels over the frequency range result from this procedure. The core will include several tons of laminated or powdered ferromagnetic material. Appropriate choices of dimensions and materials will be presented, and driving circuits will be discussed.

* Research carried out under the auspices of the Atomic Energy Commission.

O3. Ion Orbit Control for a Proton Synchrotron. G. K. GREEN, *Brookhaven National Laboratory.**—The magnetic guiding field of a proton synchrotron is shaped so as to provide stability in the vertical and radial betatron oscillations. Superposed on these "free" oscillations are the slow synchrotron oscillations, in phase and radius. The ion orbit oscillations set a lower limit on the doughnut aperture and consequently affect the magnet gap size and the magnet cost. In order to minimize the amplitude of the oscillations, to prevent particle loss by striking the walls, the injection must be very precisely controlled—and then the accelerating radiofrequency and magnetic field must be precisely synchronized. Three basic control methods are considered—programming, data computing, continuous control—of which a combination is indicated. Continuous control by means of pick-up electrodes can be applied to regulate the radiofrequency and to indicate the radial position of the beam. Computations indicate that stable control can be achieved. Various schemes will be tested in a 40-inch electron model, scaled to the proton velocities of a 10-Bev machine.

* Research carried out under the auspices of the Atomic Energy Commission.

O4. Magnetic Circuit for a Proton Synchrotron. WM. H. MOORE AND JOHN P. BLEWETT, *Brookhaven National Laboratory.**—Calculations have been made for a 10-Bev proton synchrotron magnet, considering both air core and iron core types. The air core magnet requires an unreasonably high stored energy and presents very difficult problems of mechanical support and fabrication. A new iron core magnet design uses shaping of the field coils to assist in maintaining the desired field configuration. The magnet is a poleless *C* structure open on the side farthest from the center. This will allow easy access for pumps and injection systems and will facilitate ejection of the accelerated protons. The poleless structure is economical in its iron requirements, since the return path for the flux is kept to a minimum. Electrical and magnetic characteristics will be described. A six degree arc of the magnet will be modelled at ¼ scale to confirm the conductor location and pole face shaping.

* Research carried out under the auspices of the Atomic Energy Commission.

O5. A Microwave Accelerator for Production of High Intensity Gamma-Rays. G. A. KOLSTAD, H. L. SCHULTZ, AND C. G. MONTGOMERY, *Yale University.*—Photo-nuclear disintegration experiments require intense monochromatic gamma-ray sources to bring the counts observed well above background. A microwave accelerator has been designed and is being built for this purpose. A coaxial re-entrant cavity of copper-plated steel has been designed to resonate

at 50 megacycles with a Q of 1.9×10^4 and a shunt resistance of 1.3 megohms. A 60-cycle a.c. resonance-charging spark-gap modulator forms pulses of 20 kilovolts and 250 microseconds in length. This pulse power of 1 megawatt drives a tuned-plate, tuned-grid, parallel-line oscillator which uses two Machlett ML-880 tubes. The radiofrequency pulses are magnetically coupled out of the oscillator and into the cavity through a coaxial line. The ions are to be formed by a source within the inner conductor and accelerated across a 1-inch gap by radiofrequency voltages of about 1.5 Mev. The short gap makes possible a high beam intensity, since focusing is unnecessary. The $Li^7(p, \gamma)\,2\,He^4$ reaction should yield a 17-Mev gamma-ray intensity of about 10^8 or 10^9 per second if 100 milliamperes average ion current can be obtained. A high current ion source is being constructed similar to the one described by Finklestein.[1]

[1] A. T. Finklestein, Rev. Sci. Inst. 11, 94 (1940).

O6. Preliminary Studies of Operation of the Yale Linear Electron Accelerator.* H. L. SCHULTZ, J. A. LOCKWOOD, R. L. MCCARTHY, AND P. J. RICE, *Yale University.*—Results of preliminary experiments using a single cavity resonator will be reported.[1] Electrons were injected at low energy into a seven inch long cylindrical cavity operating in the TM_{010} mode with peak r-f input power in excess of 500 kw. Using a thin lens beta-ray spectrometer, the energy spectra of emergent electrons under varied conditions of excitation power and injection voltage have been measured. Special problems associated with r-f circuit design will be discussed.

* Work assisted by the Office of Naval Research.
[1] Phys. Rev. 72, 346 (1947).

O7. The Clinton Pile Oscillator. J. I. HOOVER, W. H. JORDAN, C. D. MOAK, L. A. PARDUE,* H. POMERANCE, J. STRONG,** AND E. O. WOLLAN, *Clinton National Laboratory.*—The pile oscillator is an instrument for measuring thermal neutron absorption cross sections. In the form used here, it consists of a small beryllium boat which is made to oscillate in the region of the graphite reflector of a pile, with an amplitude of about 15" and a frequency of about 1 cycle per second. At the middle of the stroke the boat passes along the axis of a cylindrical boron-coated ion chamber. The depression of the neutron flux in the vicinity of the absorber produces an alternating current in the ion chamber which is then amplified, rectified, and integrated. The absorption cross section of an unknown sample is determined by comparing the charge accumulated in the integrating circuit with that obtained by a standard gold absorber. The instrument will detect a total absorption cross section of about 10^{-3} cm^2. One of the major difficulties in making this instrument reliable for absorption measurements has been that of eliminating the effects of scattering by the sample. In the present instrument no correction for scattering is necessary when the absorption cross section is greater than 1 percent of the scattering cross section.

* Now at the University of Kentucky, Lexington, Kentucky.
** Now at University of California, Berkeley, California.

O8. Helical Focusing Beta-Ray Spectrograph. C. S. WU, W. W. HAVENS, JR., R. ALBERT, AND G. GRIMM, *Columbia University.*—The solenoidal type beta-ray spectrograph of Columbia University has been re-installed for the investigation of beta-disintegration. Many components of this instrument have been redesigned in order to extend the study of the beta-spectra to very low energies. The counter used in connection with this work has an extremely thin collodion film, 0.1μ thick, supported by a metal grid. To reduce the pressure difference on the thin window, the counter is filled with alcohol vapor only. The characteristics and efficiency of the counter *vs.* alcohol vapor pressure for electrons of various energies have been carefully investigated. In order to distinguish between electrons and positrons, a simple modified baffle system has been used and is found to transmit particles of one sign only, introducing no detectable scattering. An electronic voltage regulator has been designed and built to regulate the current in the solenoid to within 0.3 percent of the fluctuations over a long period of time in the range from a few amperes to 600 amperes.

O9. The Focusing in Crossed Fields of Charged Particles at Relativistic Energies.* WALTER E. MILLETT, *Harvard University.*—The focusing of charged particles in crossed cylindrical electric and uniform magnetic fields, as formulated by Henneberg,[1] has been extended to include relativistic velocities. Where y equals the ratio of the electric to the centrifugal acceleration for the circular orbit $r=r_0$, the focusing angle $\Phi=\pi/(1+y^2(1-\beta^2))^{\frac{1}{2}}$ which for fixed $y\neq0$ diverges from classical values ($\beta\ll1$) by significant amounts for energies above ten percent of the particles' proper energy. The line width for a half-angle of divergence α is

$$B=-\alpha^2 r_0\frac{1+\frac{1}{2}y+y^2+3y^3+\frac{1}{2}y\beta^2(2-3y-\frac{7}{2}y^2)-\frac{3}{2}y^3\beta^4}{[1+y^2(1-\beta^2)]^3},$$

and the velocity dispersion

$$D=\frac{2r_0[1+y(1-\beta^2)]}{(1-\beta^2)[1+y^2(1-\beta^2)]}.$$

For the achromatic case $y=-1/1-\beta^2$. y has its usual values for the Wien, electric, and magnetic cases.

* Assisted by the U. S. Navy.
[1] W. Henneberg, Ann. d. Physik 19, 335 (1934).

O10. Detection of Beta-Rays by Scintillations. GEORGE B. COLLINS AND ROSALIE C. HOYT, *University of Rochester.*—The 1P21 photo-multiplier tube has been used in a manner similar to that described by Marshall and Coltman[1] to detect scintillations produced in various substances by beta-rays. The objective is a fast counter for low ionizing particles. A fast oscilloscope and amplifier with a resolving time of the order of 5×10^{-7} second was employed. $BaSO_4$+5 percent $PbSO_4$, anthracene, naphthalene, and diphenyl, when bombarded with beta-rays from radium, produced pulses on the oscilloscope whose maximum height was 15 to 7 times noise. The shapes of the individual pulses were observed on the oscilloscope by means of a triggered sweep

and a delay line. These shapes appeared to be fully explained in terms of the response time of the electrical circuit. It thus appears that the light emitted by these substances, following excitation by a beta-particle, occurs in a time less than 5×10^{-7} second, except for possible long period fluorescence with $\tau>5\times10^{-6}$ second which would not be observed. Under α-ray bombardment, ZnS and ZnO were found to decay in 5×10^{-6} second. Great differences were observed in the relative responses of various substances to alpha- and beta-rays. This work was supported by the Office of Naval Research.

[1] Fitz-Hugh Marshall and J. W. Coltman, Phys. Rev. 72, 528 (1947).

O11. Correlated Probabilities in Multiple Scattering.* W. T. SCOTT, *Smith College* AND H. S. SNYDER, *Brookhaven National Laboratory*.—We have used Fermi's distribution function for the scattering-produced probability of a certain lateral displacement, y, and a certain angular deflection, θ, of a particle passing through a length, t, of the gas of a cloud chamber,[1] to calculate the distributions of several quantities, including the following: θ at point P when the particle is known to pass through points P and Q, or through P, Q, and R; y at t' beyond Q for known passage through P and Q, and consequently the distribution in apparent curvature when observed at three points[2]; y at t' beyond R for known passage through P, Q, and R; curvature C_b of points Q, R, S for known C_a of points P, Q, and R (S either between Q and R or beyond R); the ratio C_b/C_a (both C_b and C_a variable, with S beyond R); the reduction in scattering error made by observing at 4 points (a factor $(15/16))^{\frac{1}{2}}$; the difference C_b-C_a. Results confirm and extend those of Bethe.[2] We find the ratio of C-type curves to S-type to be 1.4. Calculations on an accurate inclusion of the Born-approximation scattering law will be reported.

* This work was carried out at the Brookhaven National Laboratory under contract with the U. S. Atomic Energy Commission.
[1] See B. Rossi and K. Greisen, Rev. Mod. Phys. 13, 267 (1941).
[2] H. A. Bethe, Phys. Rev. 70, 821 (1946).

R1. Self-Diffusion of Sodium in Sodium Chloride.* DILLON MAPOTHER** AND ROBERT MAURER, *Carnegie Institute of Technology*.—The self-diffusion coefficient of sodium in sodium chloride has been measured within the temperature interval of 350°C to 700°C. The diffusion coefficient may be represented by the equation

$$D=D_0\exp(-\epsilon/kT)$$

for temperatures greater than 550°C. The values of the constants D_0 and ϵ are 3.13 cm²/sec. and 1.80 ev. Below 550°C the diffusion coefficient may be represented by the same equation, but the values of D_0 and ϵ are 1.6×10^{-5} cm²/sec. and 0.77 ev. The diffusion coefficient was measured by evaporating Na^{24} in the form of the chloride on a face of a single crystal of sodium chloride. After diffusion had proceeded for a known time at a known temperature the distribution of beta-activity within the crystal was determined. A comparison of measured diffusion coefficients with coefficients calculated from electrolytic conductivity data will be presented.

* This work was supported in part by the Office of Naval Research.
** duPont Fellow in Physics.

R2. Calculation of the Binding Energy of Self-Trapped Electrons in Potassium Chloride. KENNETH E. KEYES, *Carnegie Institute of Technology*.—A calculation of the binding energy of Landau's self-trapped electrons in potassium chloride was made assuming that the "potential hole" created by the distortion of the lattice is $V(r)=-(1/K_0-1/K)e^2/r$, where $r\geq a$, and

$$V(r)=-(1/K_0-1/K)e^2/a=V_e=V_K-V_{K_0}$$

when $r\leq a$, where V_K represents the potential energy at the trapping center due to the surrounding dipoles, and V_{K_0} represents the potential energy at a positive ion surrounded by undisplaced dipoles. V_K and V_{K_0} were calculated using methods developed by Mott and Littleton.[1] Since the ionic displacements depend on the average field of the trapped electron, we calculated a family of wave functions for a number of assumed values of V_e. From each wave function a value of V_e may be computed. Then a plot of the difference of the initial and final values of V_e *versus* the initial value of V_e determines V_e and therefore the binding energy. This binding energy turned out to be such that the absorption band due to the self-trapped electrons would lie in the near infra-red.

[1] N. F. Mott and M. J. Littleton, Trans. Faraday Soc. 34, 485 (1938).

R3. Binding Energy for a Self-Trapped Electron in NaCl.* J. J. MARKHAM, *University of Pennsylvania* AND F. SEITZ, *Carnegie Institute of Technology*.—A calculation (based on Born's theory of ionic crystals) has been made of the binding energy of a self-trapped electron in NaCl. The potential well, caused by the ionic displacements, was assumed to be a sawed-off Coulomb field, the sides being given by $(1/K_0-1/K)e/r$, where the K's are the dielectric constants. The depth of the well was calculated by the method of Mott and Littleton. Here, however, we require a self-consistent solution, i.e., the initial wave function assumed to calculate the depth of the hole must be identical to the one obtained by the variational method. The electron is smeared over a sphere whose radius equals approximately three interatomic distances. The outer displacements are calculated by a semicontinuum theory while the dipole on the three nearest ions are calculated from the conditions of equilibrium. The optical dissociation energy is 0.68 ev, whereas the thermal energy is 0.13 ev. The second value presumably explains why self-trapping has not been observed to date. The above energy should be about 1.5 times larger in LiF. These results suggest that self-trapping should be sought for at very low temperatures.

* This work was supported in part by Navy contract with the University of Pennsylvania.

R4. Activation Energy for the Migration of Paired Vacancies in KCl. G. J. DIENES, *Bakelite Corporation* AND FREDERICK SEITZ, *Carnegie Institute of Technology*.—The experiments of Leivo, Estermann, and Stern, on the changes in darkening and in density of KCl under intense x-ray irradiation, show that vacancies diffuse into the lattice at room temperature at a rate which indicates that the activation energy for diffusion of the migrating entities must be of the order of 0.5 ev or less. Since the

activation energies for migration of isolated ion vacancies is considerably larger than this, it has been suggested by Huntington that the migrating units could be coupled pairs of positive and negative ion vacancies which assist one another in a manner similar to that proposed by Johnson and Wagner for diffusion of a solute atom in substitutional alloys. In the present calculation the activation energy for migration of a pair of vacancies is calculated on the basis of the Born theory of ionic crystals. The calculations resemble closely those carried out by Mott and Littleton on the formation and migration of single vacancies. It is found that the activation energy for migration of the pair is about 0.38 ev. The calculation error is estimated at about 10 percent. It is possible, however, that the repulsive potentials employed in the calculation are in larger error than this. The theoretical calculations do not contradict the viewpoint that the vacancies migrate in the form of pairs.

R5. Domain Structure and Electric Response of Barium Titanate Single Crystals.* B. T. MATTHIAS AND A. VON HIPPEL, *Massachusetts Institute of Technology.*—$BaTiO_3$ single crystals have been grown and investigated microscopically, with x-ray diffraction and in their dielectric and piezoelectric response. It is possible to see directly the domains of the ferroelectric crystals and to change their number, size, and orientation. Wall displacements and the alignment of such domains, for which well-known indirect evidence exists in the case of ferromagnetics, have now been observed directly in both polarized and unpolarized light, and the influence of electric fields, temperature, and pressure have been studied. Untwinned crystals consisting of very few domains have been made, and their dielectric and piezoelectric response has been measured without and with biasing voltage. Conclusions can be drawn about the formation of the electric dipoles in the Ti-O_6 octahedra and about their mutual coupling. The crystals are not tetragonal below the Curie point.

* This work was supported by O.N.R. and the U. S. Signal Corps.

R6. Volume Electrostriction in Barium Titanate Ceramics. HANS JAFFE, *The Brush Development Company.*—The electrostrictive effects in barium titanate ceramics were studied by measuring the strain produced by strong alternating fields, and, conversely, the charge flowing onto a biased titanate plate when a stress was applied. It was found that barium titanate expands in the direction of the applied field and contracts in all directions at right angles to the applied field. The coefficient for the lateral contraction is about one-third of that for the parallel expansion. The volume change is given by the parallel expansion minus twice the lateral contraction. In case of an electric signal applied parallel to a bias d.c. field or a prepolarizing field previously applied,* there is a linear term in the relation between volume change and applied signal; correspondingly, a piezoelectric effect is observed if a hydrostatic pressure is applied to biased or prepolarized material. This piezoelectric effect is easily observed on titanate bodies immersed in oil subjected to alternating pressure, and serves conveniently as an indication of the piezoelectric activity of titanate ceramics in various states of previous electric treatment. A typical value for the hydrostatic piezoelectric constant, d_h, of prepolarized barium titanate is $50 \cdot 10^{-12}$ coulomb/newton.

* S. Roberts, Phys. Rev. 71, 890 (1947).

R7. On the Anomalous Dielectric Behavior of $BaTiO_3$ Near 0°K. J. M. RICHARDSON, *Bell Telephone Laboratories.*—The dielectric constant ϵ of $BaTiO_3$ has been measured by B. Wul[1] down to about 2°K. The temperature coefficient $d\epsilon/dT$ remains more or less constant as the temperature is dropped from, say, 100°K down to about 5°K, below which it begins to approach zero as required by the third law. On the basis of $\epsilon \sim 100 (T \sim 0°K)$ and reasonable assumptions about the effective charges and masses associated with the important normal modes in the polarization process, one estimates that the acoustical branches and some of the low frequency optical branches of the frequency spectrum will possess characteristic frequencies, at least one of which corresponds to a characteristic temperature $\Theta (= kT/\nu)$ of about 10°K. A theory of $d\epsilon/dT$ similar to Born's[2] theory of pyroelectricity shows the decrease becoming pronounced at $T \sim \frac{1}{4}\Theta$.

[1] B. Wul, J. Phys. 10, 64 (1945).
[2] M. Born, Rev. Mod. Phys. 17, 245 (1945).

R8. Breakdown Directions in Lithium Halide Crystals. J. W. DAVISSON, *Massachusetts Institute of Technology.*—Electrical breakdown paths in lithium halide crystals form star patterns which consist of 12 paths of the type $[xxy]$ where $x \geqslant y$. The paths lie within those acute sectors of the (110) planes bounded by the directions [110] and [111]. The star assumes the [110] orientation at low and tends to approach [111] with increasing temperature. Complex $[xxy]$ patterns showing radical changes in orientation of the paths as they proceed through the crystal, but following a definite sequence of directions, are obtained under excess voltage conditions. Although the breakdown paths apparently mark those directions for which electrons can be most rapidly accelerated by the applied field to the ionization potential of the lattice, it is shown that the star paths do not follow simply from an electron wave interaction with the lattice or from a statistical competition between the [110] and [111] directions.

* This work was supported by O.N.R. and the U. S. Signal Corps.

R9. Low Frequency Dispersion in Ionic Crystals.* R. G. BRECKENRIDGE, *Massachusetts Institute of Technology.*—A new region of anomalous electrical response has been observed at low frequencies in ionic crystals that have been treated to introduce relatively large numbers of lattice defects. The crystals thus far studied include various alkali halides and silver chloride. The effect is attributed to a jumping of the positive ions to vacant lattice sites under the influence of the applied field. This jumping is observed as an anomalous dispersion, producing a change in the dielectric constant which is small and frequently within the limits of error of measurement, and an associated peak

in the dielectric loss tangent which is readily measurable. This maximum of $\tan\delta$ has been studied both as a function of frequency at a fixed temperature and as a function of temperature at fixed frequency. From the magnitude of the peak and position on the frequency or temperature scales it is possible to calculate the number of lattice defects present in the sample and the activation energy for diffusion U of the positive ion in the crystal. A knowledge of U allows a separation of the activation energy for conduction, $(W/2)+U$, into its components, thus determining $W/2$, the activation energy for hole formation.

* This work was supported by O.N.R. and the U. S. Signal Corps.

R10. Some Characteristics of Bridges and Arcs between Separating Metallic Contacts. G. F. HULL, JR. AND H. SALTZMAN, *Dartmouth College.**—When metallic contacts carrying a current are separated, the contact may be bridged by a very small globule of metal, following which an arc may be formed. From cathode-ray oscillograms of the voltage across separating contacts, minimal length arc characteristics for gold and for platinum have been obtained, which lie between those found by Ives and Fink.[1] For currents and voltages below the minimal length arc characteristics metallic bridges are drawn out between the separating contacts. Oscillograms of these bridges show a rise in voltage to 0.42 volt, followed by a second rise to 0.9 volt for gold, and for platinum a rise to 0.65 volt and then to 1.44 volt. These voltages correspond to within 1 percent of the melting and boiling temperatures of gold and platinum, respectively, as given by contact theory.[2] These oscillograms also show evidence for the existence of transient arcs below the minimal length arc characteristics. Examination of all the oscillograms which contain arcs (about 800 in all) shows that an arc is always preceded by the formation of a metallic bridge. This suggests that the initial metallic vapor for the arc discharge is formed by the evaporation of a bridge.

* Assisted by the Office of Naval Research.
[1] H. E. Ives, J. Frank. Inst. 198, 437 (1924). H. P. Fink, Wiss. Veröff. a.d. Siemens-Werk 17, 45 (1938).
[2] R. Holm and E. Holm, Wiss. Veröff. a.d. Siemens-Werk 7, 217 (1929).

R11. Anomalous Plastic Deformation in Brass and Aluminum. ANDREW W. MCREYNOLDS, *University of Chicago.*—The curve for stress *vs.* strain in solids is usually found smooth, with slope constant in the elastic range and uniformly decreasing in the plastic range. Such deformation is explained as the sum of a large number of small independent slips. Measurements on 70-30 copper-zinc and 2S aluminum, made at room temperature and slow constant loading rate, show that deformation proceeds in steps of rapid flow followed by only elastic strain. Height and length of steps are approximately uniform, 270 p.s.i. and 0.0005 strain, respectively, in aluminum, and are independent of rate of loading over a wide range. The phenomenon is dependent on temperature and has been found not to occur in 2S aluminum below $-50°$C, nor in tests on copper, cadmium, and 99.99 percent aluminum at 20°C. Further tests indicate that the horizontal portions of the steps occur as the propagation of a wave of deformation through the stressed regions, and thus represent a cooperative effect between grains rather than the sum of independent slips. Consequent hardening of the entire lattice prevents plastic flow until arrival of another wave, and results in the vertical portions.

R12. The Photoelastic Constants of Cubic Crystals. E. BURSTEIN, P. L. SMITH, AND B. HENVIS, *Naval Research Laboratory.*—The stress-optic constants, Π_{ij}, of a number of alkali halides, MgO and TlCl, were determined by a combination of static[1] and ultrasonic diffraction measurements.[2] The latter was also employed to obtain the elastic constants of TlCl. The strain-optic constants, p_{ij}, were then calculated from Π_{ij} and the elastic constants, s_{ij}. Previous photoelastic data have only been completely reported for NaCl, KCl, CaF_2, and diamond. The results will be discussed in terms of Mueller's theory of the photoelastic effect of cubic crystals.[3] The theory, however, requires a knowledge of the ionic oscillator strengths and the change in ionic polarizability with strain. Since such information is not available, the results can only be compared qualitatively with the predictions of the theory. Preliminary results on a number of other cubic crystals will also be reported.

[1] K. Banerjee, Ind. J. Phys. 2, 195 (1927).
[2] H. Mueller, Zeits. f. Krist. (a) 99, 122 (1938).
[3] H. Mueller, Phys. Rev. 47, 947 (1935).

R13. Further Studies of the Rupture of Metal Foils. WALLER GEORGE, *Naval Research Laboratory.*—The mechanism of the rupture of notched metal foils under constant tensile load has been reviewed previously.[1] Generally, the process consists of the slow elongation of the notch normal to the direction of the applied tensile load until a critical length is reached. At this point the crack velocity increases rapidly. The critical length is shown to be influenced by certain grip designs. Rigid gripping systems minimize these head-controlled instabilities. The effect of a threefold change in scale of the areal dimensions of the system is reported, using rigid grips with the specimen and head thicknesses being kept constant. The areal size effects obtained are compared with volume size effects found in slow bend tests by workers at the University of North Carolina,[2] in terms of the work required per unit extension of the fracture.

[1] W. George and G. Irwin, Bull. Am. Phys. Soc. 1947 (Chicago meeting).
[2] P. Shearin, Proc. Bristol Conference, May 1947 (to be published Proc. Phys. Soc.).

R14. Application of the Method of Least Squares to X-Ray Crystal Structure Analysis.* W. J. TAYLOR, *The Ohio State University.*—The method of least squares has been applied to the refinement of atomic coordinates in x-ray crystal structure analysis by Hughes,[1] who, however, proceeded by numerical methods. In the present study the normal equations of least squares theory are obtained in an analytical form suitable for crystal structure analysis. The special equations applicable to the translation or rotation of a molecule or group of atoms as a rigid unit

within the unit cell are derived. The method of least squares is compared with the method of steepest descents recently proposed by Booth.[2] It is shown that the least squares method is of general applicability, not only for the refinement of atomic coordinates in the final stages of the analysis, but also to at least some extent as a substitute for the trial-and-error method in the initial stages of the analysis.

* Supported by the Office of Naval Research.
[1] E. W. Hughes, J. Am. Chem. Soc. 63, 1737 (1941).
[2] A. D. Booth, J. Chem. Phys. 15, 415 (1947).

R15. The Two Ways of Aging. HERBERT M. MEYER, *Newark, New Jersey.*—For twenty-five years the question has not yet been answered as to whether age-hardening is caused by a single, continuous phenomenon (precipitation of the secondary phase) or by two phenomena (distortion within the matrix at lower aging temperatures, and precipitation at higher temperatures). Merica advanced first the hypothesis of "critical dispersion" of secondary CuAl particles; Fraenkel suggested "cold and warm aging;" Honda assumed distortion of the solid solution (by means of an interlocked, strained structure) previous to precipitation. Two trends have developed so far: in Europe the writer and others confirmed Honda's hypothesis. Preston and Guinier detected with new x-ray methods minute inhomogenities forming upon preferential planes within the matrix, and at higher aging temperatures a local superlattice was observed before the metastable transition structure appears. This structure as well as the connection between the Widmanstaetten figures and precipitation upon preferential lattice planes were studied by Fink, Mehl and others in this country. Here the main school of thought returned to Merica's original "simple hypothesis," after microscopic particles had been observed at early aging stages; but these particles are not real (Gayler). Aging actually develops along two distinct ways according to temperatures applied, and both ways eventually may lead to precipitation.

S1. Distribution of He^3 Between Liquid and Vapor He^4.* HENRY A. FAIRBANK AND C. T. LANE, *Yale University,* AND L. T. ALDRICH AND ALFRED O. NIER, *University of Minnesota.*—The relative abundances of He^3 in the liquid and vapor phases of atmospheric helium have been studied as a function of temperature above and below the λ-point. The relative abundance of He^3/He^4 in the vapor (C_v) was determined by means of the mass spectrograph and the corresponding quantity for the liquid (C_L) computed from C_v and the mass balance and composition balance equations. From 5.2°K to the λ-point the ratio C_v/C_L increases as the temperature decreases, whereas below the λ-point this ratio sharply decreases to zero, showing that the vapor in equilibrium with superfluid helium contains no measurable amount of He^3. On the basis of these results a simple method of concentrating He^3 is suggested.

* The work at Yale University was assisted by the Office of Naval Research and that at the University of Minnesota by grants from the Research Corporation and the Graduate School.

S2. Experiments on the Isotopic Properties of Helium in the Liquid Phase.* J. G. DAUNT, R. E. PROBST, AND H. L. JOHNSTON, *Ohio State University.*—Experiments have been carried out on the process of filtration[1,2] of the rare isotope He^3 by superfluid flow through supra-surface films in contact with liquid helium II, using varying initial concentrations. Such films have been made to form semi-permeable membranes between two reservoirs of liquid helium II, permitting a flow of the He^4 isotope only (and allowing the formation of an osmotic pressure). The experimental arrangements employed and the preliminary results obtained will be described.

* This work was assisted by a contract with the Office of Naval Research.
[1] J. G. Daunt, R. E. Probst, H. L. Johnston, L. T. Aldrich and A. O. Nier, Phys. Rev. 72, 502 (1947).
[2] J. G. Daunt, R. E. Probst, and H. L. Johnston, J. Chem. Phys. 15, 759 (1947).

S3. Countercurrent Gaseous Exchange Method for the Enrichment of Isotopes. R. B. BERNSTEIN AND T. I. TAYLOR, *Columbia University.*—A method is described for the enrichment of isotopes by countercurrent gaseous exchange in a thermal diffusion column. The theory is derived for two cases of interest: diffusion limited and reaction-rate limited. Solutions of the equations are presented for the over-all separation at the steady state as a function of the following: single stage enrichment factor α; diffusion constant D or exchange rate constant k; length of column Z; and the convective flow L which in turn depends upon pressure, temperature, column dimensions, etc. The results may be expressed in the usual form $S=\alpha^N$. For the diffusion limited case $N=4\pi DcZ/L$ and for the reaction rate limited case $N=kA_Acz/L$ where c = moles of gas per cc and A_A = cross-sectional area of hot gas stream. The latter simplifies to the result that the number of theoretical plates per unit length is given by $N/Z=k/v$ where v is the convective velocity. Experiments are described in which C^{13} was concentrated by the exchange reaction $C^{12}O_2+C^{13}O=C^{13}O_2+C^{12}O$. The observed dependence of the over-all separation upon the operational variables is consistent with the theory.

S4. Thermal Diffusion with Neon. F. K. ELDER, JR.,* *Yale University.*—A two-stage, Clusius-Dickel hot wire thermal diffusion apparatus of six-meter length was designed and constructed for separation of neon isotopes. Discontinuous operation for a period of eight days produced 300 cc enriched in the heavier isotopes, and 1300 cc enriched in the lighter isotope (both volumes at two-thirds of an atmosphere pressure). Three liters (NTP) of spectroscopically pure neon were used, having as the initial relative concentration of neon 20, 21, and 22: 90.4 percent, 0.30 percent, and 9.27 percent, respectively. The final concentrations, given in the same order, were 56.4 percent, 0.80 percent, and 42.8 percent, at the heavy end; and 99.3 percent, 0.15 percent, and 0.51 percent, at the light end. The separation factor for neon 22:20 reached its maximum value of about 150 in 72 hours and maintained that value until the apparatus was shut down 115 hours later. The results on neon 21 concentration are somewhat inexact,

because of the small quantities of this isotope involved, but the indicated equilibrium separation factor for neon 21:20 is a little over nine, reached in approximately the same time as that for neon 22:20.

* Now at the University of Pennsylvania.

S5. Theory of Isotope Separation in Geological Processes. W. H. FURRY, *Harvard University.*—Isotope separation may occur in geological processes either because of differences in diffusion rates or because of differences in chemical equilibria. Both the fraction of the material affected and the changes in concentration produced must be small compared with results obtained in artificial processes of separation because of the absence of counterflow. Appreciable effects may be produced, however, on account of the very long times involved. Measurement of these effects could perhaps be useful as one source of evidence about the conditions which prevailed during certain geological processes. In some idealized cases the differential equations describing such effects possess simple solutions which show the dependence of the separation on the time and on quantities such as diffusion coefficient and rate of flow.

S6. Critical Fields of Superconducting Vanadium. ROBERT T. WEBBER AND J. M. REYNOLDS, *Yale University.**—The transitions into superconductivity and the critical fields have been investigated in two spheroidal globules of vanadium about $\frac{1}{4}''$ in diameter and of about 99.7 percent purity. An induction method was used in which a weak alternating magnetic field was superimposed on steady magnetic fields of intensities up to 9000 gauss. The e.m.f, generated in a small secondary coil wound around the specimens was amplified and continuously recorded. The transitions in the absences of the constant field were very broad, extending from approximately 4.2 to 3.5°K, and slightly lower than those reported by Meissner and Westerhoff.[1] The steady magnetic fields necessary to quench the superconductivity were very intense, increasing by about 5000 gauss per degree K below the beginning of the transition. The amount of shielding in the secondary agreed approximately with calculations, although hysteresis effects were observed and a preliminary measurement of the field distortion using a fine bismuth strip indicated little Meissner effect and some frozen in moment. A check on the alternating field induction method using a small sample of tin gave results in excellent agreement with the results of de Haas and Engelkes.[2]

* Assisted by the Office of Naval Research.
[1] W. Meissner and H. Westerhoff, Zeits. f. Physik **87**, 206 (1933).
[2] W. J. de Haas and A. D. Engelkes, Physica **4**, 325 (1937).

U1. The Al(αn) and Si(dn) Neutron Spectra. R. A. PECK, JR., *Yale University.**—A thin silicon target has been bombarded with 3.7 Mev deuterons, and a thick aluminum target with 7.6 Mev alpha-particles. In each case, the neutrons evolved have been studied and their energy distribution plotted following a conventional microphotographic method. The silicon spectrum was partly analyzable into the constituent isotopic reactions (target nuclei of masses 28, 29, 30). It has yielded mass values for P^{29}, Si^{29}, Si^{30}, and three nuclear excitation levels of P^{31}. The aluminum reaction, involving a single isotope target element, has provided a value for the mass of P^{30} and one level.

* This work was assisted by the Office of Naval Research.

U2. Neutron Diffusion in Hydrogenous Media.* C. W. TITTLE† AND CLARK GOODMAN, *Massachusetts Institute of Technology.*—Knowledge of the spatial distribution of neutrons in hydrogenous media is important in the design of radiation shields. Heterogeneous mixtures of Bi+H_2O, Pb+H_2O and Fe+H_2O have been studied by Munn and Pontecorvo.[1] Before extending this work, a comparison has been made between homogeneous and heterogeneous mixtures of carbon, hydrogen, and oxygen having the same C:H:O ratios per unit volume. Source: 150 mg Ra−α−Be; homogeneous mixture: furfural, $C_5H_4O_2$; heterogeneous mixture: Acheson graphite and water. Intensities of thermal and indium resonance neutrons were measured to distances of 54 cm and 30 cm, respectively, from the source using In and Cd−In−Cd foils. A checkerboard lattice consisting of rods of graphite (1.92 cm×1.92 cm) spaced 0.77 cm apart in water, when corrected for minor differences in atomic concentrations, gave distributions equivalent to the homogeneous mixture beyond 12–20 cm (12, indium resonance; 20, thermal). Slabs of graphite 1.92 cm thick spaced 1.83 cm under equivalent conditions gave the same distributions beyond 14–24 cm. At 4 cm the intensity ratios for thermal neutrons were 1.00:0.91:0.81:furfural:checkerboard:slab.

* This work was supported in part by the Office of Naval Research.
† Gulf Oil Corporation Fellow in Physics.
[1] Munn and Pontecorvo, Can. J. Research **25A**, 157–167 (1947).

U3. Transmission of Monoenergetic Slow Neutrons Through Solid Solutions and Mechanical Mixtures of TiC and WC. S. S. SIDHU, *Argonne National Laboratory.*—TiC and WC form continuous substitutional solid solutions at least up to 25 percent TiC+75 percent WC by weight when heated to 4000°F, TiC being the solvent and WC the solute. Total neutron scattering cross sections of a series of finely powdered solid solutions and corresponding mechanical mixtures of the two carbides were determined as a function of the mole percent of WC from the measured transmission of monoenergetic neutrons with energies 0.08138, 0.03479, 0.02056, and 0.01526 ev or wave-lengths $\lambda=1.004$A, $\lambda=1.536$A, $\lambda=1.998$A, and $\lambda=2.319$A, respectively. The cross sections of both the solutions and the mixtures increase with increasing mole percent of WC. For mixtures they are the same as the additive cross sections, each constituent scattering independently of the other. They are analogous to x-ray scattering from the mixtures in which each constituent gives its own diffraction pattern, and the patterns of the two constituents are superimposed. The neutron cross sections of solid solutions are lower than those of the mixtures at low percentages of WC but increase rapidly with the concentration of the solute molecules. They appear to be sensitive both to the structure of the solvent and the concentration of the substituting atoms.

U4. Laue Photography of Neutron Diffraction. C. G. SHULL, M. C. MARNEY AND E. O. WOLLAN, *Clinton National Laboratory.*—Using a collimated beam of thermal neutrons from the Clinton pile, it has been possible to photograph the Laue pattern produced by neutron diffraction in single crystals. The photography was accomplished with x-ray film placed next to a sheet of indium foil. Neutron capture in the indium foil produced beta-particle emission with resultant blackening of the x-ray film at the Laue spot positions. Typical Laue photographs will be shown and the sensitivity of the present method will be compared to the usual x-ray technique.

U5. Slow Neutron Velocity Spectrometer Studies of Fe, Ni, and Cu. L. J. RAINWATER, W. W. HAVENS, JR. AND C. S. WU, *Columbia University.*—According to a recent theory of Feshbach, Peaslee, and Weisskopf[1] the slow neutron scattering cross section of elements should be $\sigma_{scatt} \sim 4\pi R^2$ when the neutron energy is not near (relative to the level spacing) that of a resonance. This was shown to apply for most elements[1] with the particular exceptions of Fe, Ni, and Cu which have unusually large scattering cross section in the thermal region. On the basis of this theory[1] large scattering cross sections are observed for energies just above resonance energies, so there should be virtual levels spaced near to zero energy (relative to the level spacing). The scattering cross section should then decrease with neutron energy in a well defined manner related to the level spacing and the position of the virtual level. For Fe the cross section below 300 ev is well matched by $\sigma=(11.0+0.35E^{-\frac{1}{2}})$ neglecting low energy crystal interference effects. Below 60 ev the Ni cross section is well matched by $\sigma=(17.0+0.77E^{-\frac{1}{2}})$ and a resonance is observed near 100 ev. Below 20 ev the Cu cross section is well matched by $\sigma=(7.8+0.54E^{-\frac{1}{2}})$. The cross sections decrease at higher energies.

[1] Feshbach, Peaslee, Weisskopf, Phys. Rev. 71, 145 (1947).

U6. Slow Neutron Velocity Spectrometer Studies: Crystal Interference and Molecular Binding Effects at Low Energies. W. W. HAVENS, JR., L. J. RAINWATER, AND C. S. WU, *Columbia University.*—The slow neutron cross section of H in paraffin changes from about (20.6 ± 1) above 1 ev to $\sim$76 at 0.005 ev showing the effective increase in the (n, p) reduced mass caused by chemical binding. Below 0.05 ev the results are in good agreement with Bethe's theoretical curve.[1] The cross section of D_2O increases from 10.5 above 1 ev to $\sim$20 at 0.005 ev caused by reduced mass binding effects. The cross section is in fair agreement with $(10+0.72E^{-\frac{1}{2}})$ over the region studied. Optical crystals of quartz and calcite were studied to determine the degree of transparency at low energies, the value of the additive cross section at higher energies, and the shape of the curves in the transition region. The SiO_2 cross section is nearly constant at 9.0 above 0.57 ev and at 1.25 below 0.01 ev with a mid-value of 5.0 at 0.1 ev. Similarly, the $CaCO_3$ cross section is nearly constant at 19.8 above 0.9 ev and at 3.5 below 0.009 ev with a mid-value of 11 at 0.08 ev. Other results will be shown.

[1] Bethe, Rev. Mod. Phys. 59, 127 (1937).

U7. Slow Neutron Cross Sections of Oxygen, Nitrogen, Argon, and the Proton in Methane, Ethane, *n*-Butane, Ethylene, and 1,3 Butadiene, as Measured with a Neutron Beam Spectrometer.[1] EDWARD MELKONIAN, *Columbia University.*—The samples were in the gaseous phase. The theoretical interpretation of the scattering of neutrons by O_2 molecules must include magnetic scattering.[2] The free oxygen atom cross section was found to be 3.68×10^{-24} cm^2. In the thermal region, the N_2 and A cross sections can be represented by:

N_2: $[9.60+0.48E^{-\frac{1}{2}}]\times10^{-24}$ cm^2 per atom
A: $[0.640+0.123E^{-\frac{1}{2}}]\times10^{-24}$ cm^2 per atom

where E is the neutron energy in ev. The proton cross section between 2.5 and 15 ev neutron energy was found to be essentially constant, and the average of all results gave as the free proton cross section $19.96\pm0.2\times10^{-24}$ cm^2 per proton. Above 15 ev the resolution width used caused an appreciable effect by fast neutrons. Below 2.5 ev chemical binding effects became important, and all the curves differed, showing the effect of binding in different molecules.

[1] Rainwater, Havens, Wu, and Dunning, Phys. Rev. 71, 65 (1947).
[2] Halpern, Phys. Rev. 72, 746 (1947).

U8. Thermal Neutron Absorption Cross Sections of Separated Isotopes. H. POMERANCE AND J. I. HOOVER, *Clinton National Laboratory.*—The thermal neutron absorption cross sections of small samples of enriched isotopes have been measured in the Clinton pile oscillator. Some of the values (in barns) to be reported are as follows:

Ag^{107}	Ag^{109}	Ni^{58}	Ni^{60}	Fe^{54}	Fe^{56}	Fe^{57}
30.0	83.7	4.3	2.7	2.1	3.1	0.5

Normal isotopic mixtures of these metals were run in conjunction with the measurements on the separated isotopes as a check on the consistency of the results. Preliminary data on Mo indicate that about 80 percent of its cross section is due to Mo^{95}. The values given above were obtained by comparing the unknown sample with a gold sample, for which a σ_a of 95 barns was assumed. Corrections for the isotopic impurities were made where possible. The separated isotopes were supplied by the *Y*-12 Isotope Development Department under the supervision of C. P. Keim. We wish to acknowledge our indebtedness to this group.

U9. Cross Section Measurements Using Fast Continuous Energy Neutrons. V. L. PARSEGIAN,* L. V. TITONE, AND C. W. VAN DER MERWE, *New York University.*—The total cross section $\sigma_t(E)$ of a scatterer for fast neutrons is usually determined by transmission measurements, using a series of "monoenergetic" neutron beams. In the absence of suitable neutron sources a method is proposed by which $\sigma_t(E)$ may be determined using continuous energy neutrons, such as from Ra–Be mixtures. It has been shown by Baldinger, Huber and Staub that the energy distribution $S(E)$ of a neutron beam may be determined by measuring the number-energy distribution $H(E)$ of nuclear recoils occurring in an ionization chamber. According to the proposed method for determining $\sigma_t(E)$, it is shown that

if the recoil distribution is determined with and without an intercepting scatterer, the relation $\exp(-n\sigma_t(E)x) = [dH(E)/dE]/[dH_0(E)/dE]$ holds, in which $dH(E)/dE$ and $dH_0(E)/dE$ are the slopes of the recoil distributions at neutron energy E, for the distributions obtained with and without the scatterer, respectively (n is the atoms per cm^3 and x the length of scatterer). $\sigma_t(E)$ may then be obtained from the ratio of slopes of the two distributions over the entire range of the neutron source. The method offers means for determining other than total cross sections, including possibly resonance effects, and may prove useful in connection with neutrons obtained from atomic piles.

* Present address: The Kellex Corporation, New York, New York.

U10. Angular Dependence of Coincidences Between Fission Neutrons. S. DeBENEDETTI, J. E. FRANCIS, JR., W. M. PRESTON, AND T. W. BONNER, *Clinton National Laboratory.*—Coincidences between fission neutrons were measured at angular separations of 30°, 60°, 90°, 135°, and 180°. The source was a sample of U^{235} irradiated in a beam from the Clinton Pile. The neutrons were detected with two proportional counters containing hydrogeneous material in the form of 20 polythene films perpendicular to the wires. The counters were located in a plane perpendicular to the beam and were connected to a coincidence circuit of 3×10^{-7} sec. resolving time. The spurious coincidences measured with a PoBe source of the same strength as our fission sample, consisted of random coincidences (considerably more numerous than the desired effect) and of coincidences arising when the same neutron produced a recoil in both counters (important only at 30°, where they about equaled in number the true coincidences). After subtraction of the spurious coincidences the final results are affected by a statistical error of about 10 percent. The number of coincidences is constant from 30° to 90° and increases by a factor 2 from 90° to 180°. Using the hypothesis of neutron emission from fragments in motion, this result shows that when more than one neutron per fission is emitted both fragments contribute to neutron emission.

U11. Angular Correlation of γ-Rays. EDWARD L. BRADY AND MARTIN DEUTSCH, *Massachusetts Institute of Technology.*—The study of the angular correlation of successive γ-rays[1] has been continued with improved equipment which will be described. The results for Co^{60} gave the following values for ϵ_θ, defined as the true coincidence counting rate at the angle θ minus the true coincidence rate at $\theta=90°$ divided by the rate at 90°: $\epsilon_{180}=0.216\pm0.025$; $\epsilon_{135}=0.075\pm0.026$; $\epsilon_{120}=0.048\pm0.025$; $\epsilon_{60}=0.002\pm0.022$. The fact that the lifetime of the intermediate state is short compared to the precession period of the nucleus in the field of its own electrons was established by the observation that the anisotropy is not affected within the statistical error by the application of a magnetic field of about 10,000 gauss. This work was supported in part by the Office of Naval Research.

[1] E. L. Brady and M. Deutsch, Phys. Rev. 72, 870 (1947).

U12. Relative Yields of Some X-Ray Induced Nuclear Reactions. G. FRIEDLANDER AND M. L. PERLMAN, *General Electric Company.*—The yields of a number of nuclear reactions induced by x-rays from the 100 Mev betatron have been compared by measurement of the radioactivities of product nuclei. In addition to the (γ, n) reactions previously investigated,[1] (γ, p) reactions on Si^{30}, Ni^{62}, Mo^{98}, and Ru^{102} and $(\gamma, 2n)$ reactions on F^{19} and Cu^{63} have now been studied. At 100 Mev maximum energy, the values of the four (γ, p) yields show a spread of about 50 percent and are comparable to those of the (γ, n) yields among elements below nickel. The abrupt increase observed in the neighborhood of $Z=29$ for (γ, n) yields[1] was not found for the (γ, p) yields. Each of the two $(\gamma, 2n)$ reactions studied was found to be approximately one tenth as probable at 100 Mev maximum energy as the (γ, n) reaction on the same nuclide. It is hoped that further results will be available at the time of the meeting.

[1] M. L. Perlman and G. Friedlander, Phys. Rev. 72, 1272 (1947).

U13. X-Ray Yield Curves for γ-*n* Reactions. G. C. BALDWIN AND G. S. KLAIBER, *General Electric Company.*—Yield curves for the reactions $C^{12}(\gamma, n)C^{11}$ and $Cu^{63}(\gamma, n)Cu^{62}$ have been taken with x-rays up to 100 Mev. The induced radioactivity at each energy is plotted per unit x-ray intensity as measured by an r-meter thimble jacketed by $\frac{1}{4}$" of Pb. Both yield curves are similar to the photo-fission yield curves,[1] the x-ray yield increasing to a maximum and then slowly decreasing as the x-ray energy is increased. With simple assumptions regarding the generation of ionizing secondaries in the Pb walls of the monitor and assumption of a constant intensity x-ray spectrum, these curves can be analyzed. The relative cross section is found to have a maximum at approximately 22 Mev for Cu^{62} and 30 Mev for C^{11}, decreasing to negligible values at high quantum energies. This decrease in cross section can be attributed to competition from multiple disintegrations. These reactions provide detectors sensitive only to part of the x-ray spectrum. Absorption curves have been taken in Pb using uranium photo-fission and in Cu and Pb using the $Cu^{63}(\gamma, n)Cu^{62}$ reaction as detectors. The resulting absorption coefficients compare favorably with theoretical values.

[1] G. C. Baldwin and G. S. Klaiber, Phys. Rev. 71, 3 (1947).

X1. Mass Spectrometric Study of Some Deuterated Hydrocarbons. RICHARD E. HONIG, *Research and Development Department, Socony-Vacuum Laboratories.*—If deuterated hydrocarbons are to be used as stable tracers in studying chemical reactions, preliminary investigations of their behavior in the mass spectrometer are of interest. The following compounds were synthesized from D_2O (atom percent D>99) and studied: CH_3D, CD_4, C_2D_2, C_3H_5D, $CH_3CH_2CH_2D$, and CH_3CHDCH_3. Mass spectra, obtained with 50-volt electrons, of CD_4 and C_2D_2 resemble closely those of CH_4 and C_2H_2, whereas the singly deuterated compounds show significant deviations from the regular patterns which may be explained by differences in bond strengths. The deuterium position in the two propane isomers is accurately reflected by their respective spectra. Intensities/pressure (sensitivities) of the parent ions are the same within the experimental uncertainty for deuterated and regular hydrocarbons. A 13 percent difference observed for $CH_3CH_2CH_2D$ and C_3H_8 appears to be caused by

impurities contained in the former. Ionization potentials, measured reproducibly to ±0.02 volt, could not distinguish between deuterated and regular compounds. Only for CD_4 and CH_4 was a significant difference of 0.17±0.04 volt observed, which may be explained by shifts in the zero-point energies of the two molecules.

X3. Use of Mechanical Synthesizer to Determine Characteristics of Non-Dissipative Electric Wave-Filters. S. LEROY BROWN AND JAMES M. SHARP, *University of Texas.**—The mechanical harmonic synthesizer may be used to plot polynomials after they have been reduced to an equation in harmonic functions of θ by a substitution of the form $x=R\cos\theta$ where R is an arbitrary modulus. Since, in any electrical network containing both L and C components, the expression for the reactance reduces to the ratio of two polynomials in ω ($2\pi\times$frequency), the synthesizer may be utilized to determine, indirectly, the variation of reactance with frequency. The method employed is to plot with the synthesizer the first polynomial, the numerator, and then the second, the denominator of the expression for the reactance. The numerical value of the reactance in ohms is then the ratio of respective ordinates read from the two curves corresponding to any particular value ω (plotted as abscissa). This method is extended to plotting the important quantity in filter circuits $X_1/-4X_2$ from which the cut-off frequencies, attenuation, phase shift, and iterative impedance are determined.

* Assisted by Office of Naval Research.

X4. Work, Heat, and Temperature Concepts in Thermodynamics and an Examination of the Temperature Scale. J. L. FINCK, *The J. L. Finck Laboratories.*—In this paper the concepts of work, heat, and temperature are examined from the standpoint of a complete equation* for the internal energy of a system. In an incomplete system energy necessarily remains with the system, which results in the inefficiency of a process. This inefficiency is, of course, appreciable for processes taking place at a finite speed, but is not necessarily eliminated by means of a quasi-static process. The Kelvin temperature scale is shown to be based on an incomplete equation for the internal energy and therefore offers certain difficulties. A temperature scale based on a complete equation is shown to have advantages over the Kelvin scale, and it is further shown that the temperature of absolute zero as based on a complete equation is lower than that on the Kelvin scale.

* Bull. Am. Phys. Soc. 22, 28 (1947), p. 16, T1.

X5. Measurement of Rocket Flame Velocity by Doppler Shift. F. P. BUNDY, *General Electric Company.*—Rocket flame velocity is usually deduced from measurements of the thrust force and mass flow rate made on the rocket motor. In response to a need for an independent absolute measurement of the flame velocity, a method has been developed which is based on the Doppler shift of the sodium D-line radiation from the flame. The small shift of wave-length is measured from interference patterns formed by a Fabry-Perot interferometer. Because the spectral line width is greater than the Doppler shift it is necessary to photograph separate interference patterns using upstream and downstream light and then compare the positions of the fringes. The accuracy of the method with the present apparatus is within ±10 percent. With the improved apparatus which is being set up it is expected to bring the accuracy to within less than ±5 percent. Some of the optical and mechanical problems encountered in the development will be discussed. A few interesting spectroscopic effects produced by rocket flames will be presented.

X6. A Simple Temperature Controller. J. C. MOUZON, *The Brown Instrument Company.*—A simple temperature controller has been developed which permits thermostating of equipment to closer limits than is possible with ordinary on-off control. The sensitive element is a resistance thermometer which is employed in a 60-cycle a.c. bridge. The output of the bridge is amplified by one-half of a dual triode and is fed to the grid of a thyratron. The other half of the dual triode is used as a rectifier to supply d.c. to the amplifier stage. The plate circuit of the thyratron includes the heater load. A.c. power is supplied to the thyratron and heater circuit. The use of a.c. on the bridge and thyratron makes the control essentially independent of line voltage. By shunting the heater load with a condenser or by using a parallel resistance and capacity in the cathode of the thyratron it is possible to obtain proportional action in which the power supplied to the heater is a function of the departure of the temperature from the desired value. This action minimizes the cycling that accompanies on-off control.

X7. Scattering and Transmission Cross Sections of Circular Disks and Apertures for Sound and Electromagnetic Waves. R. D. SPENCE,* *Yale University.*—This note reports the results of calculations on the scattering cross section of a circular disk for normally incident sound waves and on the transmission cross section of circular apertures for sound and electromagnetic waves. The calculations were made by separating the wave equations in oblate spheroidal coordinates. Numerical results have been obtained in the range

$$0<\frac{2\pi}{\lambda}a<5,$$

where a is the radius of the disk or aperture.

* Now at Michigan State College.

X8. The Development of a Combustion Wave in a Flowing Gas.* R. J. DERY, *Bureau of Mines.*—A flame front is propagated in a flowing gas with a velocity which is the resultant of the flame-propagation velocity in the direction of the normal to the flame front and the velocity of the unburned gas. The case of a combustion wave in a gas in Poiseuille flow in a cylindrical tube has been investigated theoretically for an ideal system with constant burning velocity, constant volume, and null lateral expansion of stream tubes. The equation of motion of points on the flame surface in an axial plane relative to a point moving with the velocity v_m of the gas on the axis of the cylindrical jet is then $\vec{u}=a\vec{n}-(r^2/R^2)v_m$, where $\vec{n}$ is the outer normal to the

flame surface and R the radius of the jet. Schlieren photographs of the initial stages of spark-ignited flames in gas issuing from a tube are in agreement with the theory.

* Assisted by the U. S. Navy.

X9. The Approximate Small Signal Theory of Electron Beam Wave Interaction in a Wave Guide with a Filament Beam. PHILIP PARZEN, *Federal Telecommunication Laboratories.*—The small signal electron beam wave interaction in a wave guide is characterized by an axial propagation constant h, which may be obtained from the constants, h_n, for the cold guide by considering the beam as a source of forced vibrations, periodic in space, of the fields, which are expanded in the normal modes of the cold guide. For a filament beam, h is given by

$$1=\frac{(k^2-h^2)}{(\beta-h)^2}R\,\Sigma_n\frac{B_n}{h_n^2-h^2},$$

where $k=2\pi/\lambda$, $\beta=\omega/v_0$, v_0 is d.c. velocity of beam, R is $10^6 I_0$ (amps)$/V_0^{\frac{1}{2}}$ (volts) and $B_n=|E_n|^2/N_n$, where E_n is the longitudinal electric field of the nth cold mode at the beam and $N_n=\int|E_n|^2dA$ over the guide cross section.

X10. Further Report on High Pressure Experiments on Ultrasonic Propagation.* GERALD J. HOLTON, *Harvard University.*—The experimental arrangement and some of the results for measurements of sound velocity and attenuation in liquids at high pressures have been presented recently.** Further data and a summary of the theoretical conclusions are now given. Included are discussions of specific heats, relaxation times, and molecular association in liquids like water; for instance, it can be shown that the absorption at 15 mc/sec. approaches the classical value at pressures from a few hundred to several thousand atmospheres, depending on the temperature.

* Assisted by the U. S. Navy.
** A. P. S. Meeting, November 1, 1947.

Y1. Disintegration of Isomers of Ba^{133}. FU-CHUM YU AND J. D. KURBOTOV, *The Ohio State University.*—By the activation of barium with slow neutrons a radioactive isotope of barium of half-life of over 20 years has been obtained. After sufficient time is allowed for the 12-day Ba^{131} to disintegrate, long-life barium was found to emit gamma-rays of energy of 310 kev, conversion electrons, and x-rays. Independently by activation of cesium with deuterons followed by chemical separation of barium, radiations emitted by two isomers of Ba^{133} (1) of the previously known half-life of 38.8 hours and (2) of a long life have been studied. From the evidence of the accumulation of gamma-ray intensity of a long-life isomer during the disintegration of the 38.8-hour isomer, the genetic relationship between these two isomers was established. A scheme of disintegration of the isomers of Ba^{133} will be proposed.

Y2. Radiations from Antimony (124).* M. V. SCHERB AND C. E. MANDEVILLE, *Bartol Research Foundation.*—The characteristic radiations of Sb^{124} have been re-investigated.[1,2] The hard gamma-ray was found to have an energy of 1.67 Mev as measured by coincidence absorption. This value agrees well with the many earlier determinations. The beta-rays, measured by aluminum absorption, had a maximum energy of 1.62 Mev, agreeing fairly well with earlier absorption measurements of the Indiana group,[1] but differing from subsequent spectrometric data by as much as 0.83 Mev. The genuine beta-gamma coincidence rate decreased from an extrapolated value of 0.92×10^{-3} coincidence per beta-ray at zero absorber thickness to 0.38×10^{-3} coincidence per beta-ray at 0.11 g/cm² in aluminum. The inner beta-ray group then has an end point at about 0.5 Mev. A gamma-gamma coincidence rate of $(0.59\pm0.03)\times10^{-3}$ coincidence per gamma-ray was also observed.

* Assisted by the Office of Naval Research.
[1] Mitchell, Langer, and McDaniel, Phys. Rev. **57**, 1107 (1940).
[2] Meyerhof and Scharff-Goldhaber, Phys. Rev. **72**, 273 (1947).

Y3. Beta- and Gamma-Radiations from Antimony.* BERNARD D. KERN, DANIEL J. ZAFFARANO, AND ALLAN C. G. MITCHELL, *Indiana University.*—A source of antimony obtained from the Oak Ridge pile was investigated, with respect to its beta- and gamma-rays, by the use of a thin lens magnetic spectrometer. Gamma-ray energies of the 60-day Sb^{124} were determined from photoelectric lines produced with a thin lead radiator and also from Compton electrons produced in copper. The energies of the strongest lines are 0.603 and 1.708 mv. Three weaker lines have energies 0.650, 0.714, and 2.064 mv. The beta-ray spectrum was measured using a source of surface density 5.5 mg/cm² on a backing of 1 mg/cm². The spectrum is complex, and a Fermi plot of the data gives groups with the following end points: 2.32, 1.58, 0.98, 0.63, and 0.47 mv. An internal conversion line was found at 0.571 mv, corresponding to the gamma-ray of energy 0.603 mv. A measurement of the gamma-rays of Sb^{122} (2.7 days), taken before the source was aged, gives a gamma-ray of energy 0.568 mv.

* Supported by the Office of Naval Research.

Y4. Beta- and Gamma-Radiation of Antimony.* C. SHARP COOK AND LAWRENCE M. LANGER, *Indiana University.*—Measurements on the beta- and gamma-rays emitted by antimony bombarded by slow neutrons at Oak Ridge have been made with a high resolution, 40-cm radius of curvature, shaped field magnetic spectrometer.[1] The beta-spectrum of 60-day Sb^{124} was determined after all 2.8-day Sb^{122} had decayed and after chemical separation. A source of 1 mg/cm² plated onto a 0.010″ graphite backing was used. The counter window had a low energy cut-off of 2.0 kev. The spectrum is complex and by means of the Fermi plot may be resolved into five groups having maximum energies at 2.37, 1.50, 0.98, 0.68, and 0.50 Mev. An internal conversion line was observed at $H\rho=1050$ gauss-cm, corresponding to a gamma-ray energy of 0.121 Mev. Compton and photoelectrons ejected from a Pb radiator yield lines corresponding to gamma-rays of 2.14, 1.708, and 0.608 Mev. Additional weak lines were observed, which, if caused by K electrons ejected by Sb gamma-rays, correspond to gamma-ray energies of 0.732 Mev and 0.654 Mev. Runs, taken when the source was fresh, yield K and L lines corresponding to a gamma-ray of Sb^{122} of 0.568 Mev.

* This research was supported by the Frederick Gardner Cottrell Fund of the Research Corporation and the Office of Naval Research.
[1] L. M. Langer and C. S. Cook, Rev. Sci. Inst., in press.

Y5. Coincidence Measurements in Sb^{124}. E. T. JURNEY AND ALLAN C. G. MITCHELL, *Indiana University.**—The disintegration of Sb^{124} has been re-investigated,[1,2] using coincidence counting methods. The beta-ray absorption in aluminum was measured, using a single counter with a thin window, and the curves analyzed by the method of Bleuler and Zünti.[3] Two intense groups were found with end points at 2.24 and 0.51 mv. Beta-gamma and gamma-gamma coincidences were measured. When the number of beta-gamma coincidences per beta-ray is plotted against absorber thickness, the curve is practically flat from the highest absorbers used up to a thickness of 168 g/cm², corresponding to the energy of 0.47 mv, where a sharp rise sets in, indicating the presence of a low energy group of electrons. The high energy portion is being investigated further for evidence of additional groups.

* Supported by the Office of Naval Research.
[1] A. C. G. Mitchell, L. M. Langer, and P. W. McDaniel, Phys. Rev. 57, 1107 (1940).
[2] W. E. Meyerhof and G. Scharff-Goldhaber, Phys. Rev. 72, 273 (1947).
[3] E. Bleuler and W. Zünti, Helv. Phys. Acta 19, 375 (1946).

Y6. Absorption Curve of Be^{10} Beta-Rays. WILLIAM E. STEPHENS AND A. M. BOTTOMS, *University of Pennsylvania.*—The aluminum absorption curve of the beta-rays from beryllium[10] [1] has been measured. The results are in agreement with those of McMillan[2] and indicate an apparent end point between 185 and 190 mg/cm² of aluminum. Attempts are being made to reduce the tail (presumably bremsstrahlung) by the use of beryllium holders and absorbers.

[1] Beryllium target fragments supplied by Professor A. L. Hughes and Professor F. N. D. Kurie of Washington University.
[2] E. M. McMillan, Phys. Rev. 72, 591 (1947).

Y7. The C^{14} Beta-Ray Spectrum. MARGARET N. LEWIS AND MIRIAM PAUL, *University of Pennsylvania.*—Further studies of the C^{14} beta-ray spectrum[1] with a permanent magnet spectrograph have been made. The apparent end point is 152±5 kev. Scattering has been reduced by use of a thin source and support. The energy sensitivity calibration of the film in the region of the end point was made with the use of the line spectrum of Ra *B*.

[1] W. E. Stephens and Margaret N. Lewis, Phys. Rev. 72, 526 (1947).

Y8. Positron-Electron Ratios in Cu^{64}. L. CRANBERG AND J. HALPERN, *University of Pennsylvania.*—The work of Backus[1] on Cu^{64}, which gives positron-electron ratios in excess of values predicted by theory at energies below 50 kv, is compared with earlier work of Tyler[2] and Townsend.[3] Although spectral shapes from Tyler's work deviate from straight-line Kurie plots at 350 kv for positrons and 320 kv for electrons, positron-electron ratios agree with theory down to energies of approximately 100 kv. This suggests that source scattering of positives and negatives can be treated symmetrically when spectral shapes are similar. Such a situation no longer holds at energies below 50 kv. When Backus' results are compared with ratios taken at the upper end of the spectrum, the discrepancy from theory is greater than was indicated. The low energy region, however, is particularly sensitive to inelastic scattering effects, which will be discussed in detail.

[1] Backus, Phys. Rev. 68, 59 (1945).
[2] Tyler, Phys. Rev. 56, 125 (1939).
[3] Townsend, Proc. Roy. Soc. (London) **A177**, 357 (1941).

Y9. Neutron Induced Activities in Erbium. B. H. KETELLE AND W. C. PEACOCK, *Clinton National Laboratory.*—Two erbium activities were produced in ion-exchange[1] separated erbium, by n, γ reactions and were studied with beta-ray spectrometer and coincidence techniques. (1) A 9.4±0.2-*d* β^- emitter has been found. It emits no gamma-rays and has a beta-ray end point of 0.33±0.01 Mev. (2) A 7.5±0.2-*h* β^- emitter has also been found. It has three alternate modes of β^- decay. 71±5 percent of the betas have an energy of 1.05±0.03 Mev and are followed by two gammas of 0.305±0.010 and 0.113±0.005 Mev in cascade. The 0.113-Mev gamma-ray is highly converted and has a half-life of 2.5 μsec. (see following abstract). 6±1 percent of the betas have an energy of 1.49±0.05 Mev and decay directly to the ground state of Tm. 22 percent of the betas have an energy of 0.67±0.03 Mev and are followed by a 0.805±0.025-Mev gamma. From the disintegration energies it appears that the 7.5-h period should be assigned to Er^{171} and the 9.4-d period to Er^{169}. A Tm activity of 500±100-d was shown to grow from the activated Er samples; this is probably Tm^{171} daughter of 7.5-h Er^{171}.

[1] B. H. Ketelle and G. E. Boyd, J. Am. Chem. Soc. November 1947.

Y10. Short-Lived Isomers in Tm^{169} and Tm^{171}. F. K. MCGOWAN AND S. DEBENEDETTI, *Clinton National Laboratory.*—Using a technique previously described, delayed coincidences were observed with sources of 33-days Yb^{169} (*K* capture to Tm^{169}).[1] The delayed rays are conversion electrons from a state of around 1 μ-sec. half-life and about 0.2-Mev excitation energy. 30 percent of the immediate pulses are due to x-rays from *K* capture and the rest to conversion electrons from other γ-rays. This proves that at least in some instances the short-lived isomeric state is preceded by the emission of immediate γ-rays. No delayed coincidences were detected with sources of 9.4-days Er^{169},[2] which leads by β^- decay to the same final nucleus as Yb^{169}. Sources of 7.5-hours Er^{171} (β^- decay to Tm^{171})[2] also give delayed coincidences corresponding to a half-life of 2.5 μ-sec. and 0.113-Mev excitation energy. In this case the number of conversion electrons per disintegration is about 0.4.

[1] W. Bethe, Zeits. f. Naturf. 1, 173 (1946).
[2] See preceding abstract.

Y11. The Beta- and Gamma-Spectra of Ga^{72}.* S. K. HAYNES, *Clinton Laboratories and Vanderbilt University.*—The experimental curves obtained in an investigation of the beta- and gamma-ray spectra of Ga^{72} with a thin lens spectrometer are presented and discussed. Evidence is given for the existence of beta-particle groups with maximum energies of 3.15 Mev, (9.5 to 20 percent) 2.5 Mev, (8 to 18.5 percent) 0.955 Mev, (32 percent) and 0.64 Mev, (40 percent). The photoelectron spectrum indicates gamma-rays of the following energies: 2.51 Mev (26 percent), 2.21 Mev (31.5 percent), 1.87 Mev (7.5 percent), 1.59 Mev (4.5 percent), 1.05 Mev (4.5 percent), 0.84 Mev (100 percent), 0.63 Mev (18.5 percent), and possibly a weak gamma-ray at 1.25 Mev (2 percent). A conversion line appears at 0.68 Mev in the beta-ray spectrum, but no

corresponding line can be identified with certainty in the photoelectron spectrum. The conversion coefficient is probably between ten and fifty percent, indicating an isomeric state of considerable duration. A partial decay scheme of Ga^{72} is presented.

* This work was performed under contract with the Atomic Energy Commission.

Y12. Radiations from Mo^{99} and Tc^{99}.* C. E. MANDEVILLE AND M. V. SCHERB, *Bartol Research Foundation.*—The 67-hour activity was induced in Mo_2O_3 irradiated by slow neutrons at the Clinton pile. Separations were made for the removal of calcium, iron, phosphorous, and columbium as possible impurities. The energy of the hard beta-rays of Mo^{99} was measured by aluminum absorption and was found to have an end point at 1.03 Mev. Coincidence measurements indicated that no gamma-rays are coupled with the high energy spectrum. A low energy group of beta-rays is present in Mo^{99}, having a maximum range of 0.057 g/cm² in aluminum. This spectrum is coincident with gamma-radiation. The gamma-rays have a maximum energy of 0.71 Mev as measured by coincidence absorption. A small gamma-gamma coincidence rate, 0.085×10^{-3} coincidence per gamma-ray, was detected in Mo^{99}. The electrons of the highly converted gamma-ray of the 6-hour metastable state of Tc^{99}, separated from Mo^{99}, were found to be non-coincident with gamma-radiation. Also, no gamma-gamma coincidences were observed in the technetium fraction. The conversion electrons had a range of 0.022 g/cm² in aluminum. A disintegration scheme will be proposed.

* Assisted by the Office of Naval Research.

Y13. The 7-Second Au^{197} Isomer. H. FRAUENFELDER, P. C. GUGELOT,† O. HUBER, H. MEDICUS, P. PREISWERK, P. SCHERRER, AND R. STEFFEN, *Swiss Federal School of Technology.*—The decay of the two isomeric states of Hg^{197},[1] produced by the $Au^{197}(p, n)Hg^{197}$ reaction, has been investigated to study the 7-sec. Au^{197*}.[2] Both decay by electron capture. The 25-h activity excites a 0.3-Mev state of gold, from which a cascade of a 0.165-Mev—and a 0.135-Mev γ-ray leads to the ground state. The 65-h activity excites a level of 0.077-Mev above the ground state. No indication of a genetic relation between both periods was found. Coincidence measurements showed that none of these Au levels had an appreciable lifetime. To determine the radiations of the 7-sec. Au^{197*}, we bombarded gold with Be+D neutrons. The half-life was found to be (7.4±0.3) sec. This excited level decays by a *ca.* 0.250-Mev converted γ-ray, which is followed by a *ca.* 0.07-Mev converted γ-ray. By distilling active mercury we obtained this Au activity and found that *ca.* 4 percent of the decay of 25-h Hg^{197} yields this isomeric state. The measured half-life was (7.4±0.2) sec. Absorption curves of the conversion electrons agreed with those obtained by n, n excitation. A tentative energy-level scheme will be given.

† Now at Princeton University.
[1] G. Friedländer and C. S. Wu, Phys. Rev. 63, 227(1943).
[2] M. L. Wiedenbeck, Phys. Rev. 68, 1 (1945).

Z1. The Mass-Energy Relation.* W. F. G. SWANN, *Bartol Research Foundation.*—Relativity serves only to predict the relation for those portions of the mass and energy which are dependent upon the velocity. Electromagnetic theory comes near to providing for the rest mass in terms of ordinary electrostatic energy, but with the well known discrepancy amounting to a factor of four-thirds. For uncharged particles, electromagnetic theory does nothing. A hypothesis is developed according to which the whole of the rest mass arises from internal motions of the particles in a form consistent with the required behavior of the particles in respect to the apparent forces which they exert. The line of thought is analogous to that of the whole philosophy which sought to see all potential energy as a manifestation of kinetic energy. It has, moreover, the advantage of unifying the concepts of rest energy and kinetic energy in a form which gives the mass-energy relation a more clear-cut meaning. The development is carried out along classical lines following the general idea that in seeking ultimately to develop consistent quantum theory in relation to these matters it is good to start by seeking consistent classical representation.

* The work constitutes a theoretical contribution to the general nuclear physics program supported at the Bartol Research Foundation by the Office of Naval Research.

Z2. A Simplified Notation in Classical Mechanics. H. C. CORBEN, *Carnegie Institute of Technology.*—In non-relativistic classical mechanics, a dynamical system may be specified by N coordinates q_k and the conjugate momenta p_k, i.e. by a point in $2N$-dimensional phase space $Q_i=\{q_k, p_k\}$. If one defines an orthogonal $2N$-vector $P_i=\{p_k, -q_k\}$ all of the canonical equations for a conservative holonomic system may be written in the form $\dot{Q}_i=\partial H/\partial P_i$. The Poisson and Lagrange brackets of two dynamical variables X, Y become simply $(X, Y)=(\partial X/\partial Q_i)(\partial Y/\partial P_i)$ and $[X, Y]=(\partial Q_i/\partial X)(\partial P_i/\partial Y)$ respectively, and all of the P.B. and L.B. relations are contained in $(Q_i, P_j)=[Q_i, P_j]=\delta_{ij}$. The infinitesimal contact transformation generated by $S(P_i)$ leads to $\delta Q_i=\partial S/\partial P_i$. This simplified notation is easily extended to special relativity theory, where for the motion of a single particle $N=4$. By introducing a metric G_{ij} in phase space it may be further extended to general relativity theory, where the corresponding P.B. relations are $(Q_i, P_j)=G_{ij}$. It then follows that in general the Poisson brackets of two coordinates or of two momenta of a particle do not vanish, being proportional to the antisymmetrical off-diagonal 4×4 tensors of G_{ij}. In the corresponding quantum theory it would be necessary to represent the position of a particle by operators which do not commute.

Z3. On Multiple Excitation of an Elastic System. G. S. BENNETT, *Michigan State College.*—Approximate solutions to the non-linear differential equations are used to evaluate the importance of possible combination frequency resonances where two sinoidal forces are applied to a one degree of freedom elastic system which has a force function expressible as a power series in displacement. It is shown that such resonances exist, but that the maximum ampli-

tudes at resonance are generally much less than the "static" displacement due to one of the exciting forces, and so can be disregarded as a source of trouble in vibration problems. The same method is used and the same general remarks made for the case when the damping function is expressible as a power series in velocity.

Z4. Symmetric Energy-Momentum Tensor of Iwanenko-Sokolow Field. C. KIKUCHI, *Michigan State College.*—The Lagrangian

$$L=\tfrac{1}{2}\{\kappa_1^2\kappa_2^2\varphi_\alpha\varphi_\alpha+\tfrac{1}{2}(\kappa_1^2+\kappa_2^2)F_{\alpha\beta}F_{\alpha\beta}+F_{\alpha\beta,\gamma}F_{\alpha\beta,\gamma}\}$$

which leads to the Iwanenko-Sokolow[1] field equations $(\Box-\kappa_1^2)(\Box-\kappa_2^2)\varphi_\alpha=0$ will be used to indicate how the symmetric energy-momentum tensor can be derived for fields whose Lagrangian depends upon the derivatives of the field quantities. The method due to F. J. Belinfante[2] will be used.

[1] D. Iwanenko and A. Sokolow, J. of Phys. USSR 8, 54, 358 (1944).
[2] F. J. Belinfante, Physica 6, 887 (1939).

Z5. First Passage Time Moments for Certain Markoffian Random Functions. A. J. F. SIEGERT, *Northwestern University.*—Let $y(t)$ be a stationary Markoffian random function for which the moment conditions are fulfilled, so that a Fokker-Planck equation is satisfied by the probability density $P(y_0/y, t)$.[1] We define $p(y_0/t', a)dt'$ as the conditional probability that $y(t)$ passes the value $a>y_0$ for the first time between $t'>0$ and $t'+dt'$, provided that $y(0)=y_0$. From the equation

$$P(y_0/y, t)=\int_0^t p(y_0/t', a)P(a/y, t-t')dt'$$

for $y>a>y_0$ and its Laplace transform we then obtain the recursion formula for the moments $t_n(y_0, a)$ of the first passage time:

$$t_n(y_0, a)=2n\int_{y_0}^{a} dz[B(z)W(z)]^{-1}\int_{-\infty}^{z} W(x)t_{n-1}(x, a)dx$$

with $t_0(y_0, a)=1$, where $W(z)=P(y_0/z, \infty)$ and $B(z)$ is defined in the reference p. 331, Eq. (38).

[1] M. C. Wang and G. E. Uhlenbeck, Rev. Mod. Phys. 17, 323, 331, 332 (1945).

Z6. Observable Effects of the Quantum Fluctuations of the Electromagnetic Field. T. A. WELTON, *Massachusetts Institute of Technology.*—Under the action of the zero-point fluctuations of the electromagnetic field a free charged particle will exhibit forced oscillations about its mean position. The mean square amplitude of this fluctuation in position can be simply calculated in the non-relativistic limit. This fluctuation is too small to be observable in a macroscopic experiment but, for an electron in a hydrogen atom, the fluctuation in position will give rise to a change in the effective potential energy. The alteration will be proportional to the mean square displacement and the Laplacian of the potential energy. It is easily seen that the sign of the change is such as to weaken the effect of the potential energy. In this way, a simple, reasonably quantitative explanation is given of the displacement of the $2S$ level of hydrogen recently observed by Lamb. Similarly, a simple discussion can be given of the higher order corrections to such processes as elastic scattering. The same methods can be used to calculate the fluctuation in direction of a free spin. This effect is closely related to the anomalies in Zeeman and hyperfine splittings observed in recent molecular beam experiments. A discussion will be given of this point.

Z7. On the Method of Virtual Quanta. M. LAX, *Syracuse University* AND H. FESHBACH, *Massachusetts Institute of Technology.*—A quantum analogue of the classical Weizäcker-Williams method has been derived in which it is shown that, in the Born approximation, the electromagnetic field of a charged particle whose energy is large compared to its rest mass, can be replaced by an equivalent spectrum of transverse and longitudinal photons. The range of applicability is that of the Born approximation and thus may include the case of close impacts involving high energy virtual quanta. In the procedure used, the electromagnetic field generated when the charged particle changes its momentum by p and its energy by ν_0 is approximated by the Moller formula. The denominator $(p^2-\nu_0^2)^2$ insures that the scattered particle comes off in essentially the forward direction for high energy particles. Integration over all directions of the scattered charge and comparison of the charged induced cross section with the photon induced cross section with the approximation $p=\nu_0$ yields the desired equivalent photon distribution. Criteria for the general validity of the $W-W$ method may now be given. The inclusion of the longitudinal photon spectrum increases its range of applicability. An extension of this procedure to meson theories permit the derivation of an equivalent meson spectrum of a nucleon.

Z8. The Electromagnetic Level Shift. H. A. BETHE, *Cornell University.*—The shift of the energy levels of a bound electron, due to its interaction with electromagnetic radiation, is calculated relativistically. No numerical result has yet been obtained, but it has been shown that the result is finite, and is of the same order of magnitude as that of the previous non-relativistic theory. To obtain this result, it is necessary to subtract from the self-energy of the bound electron, the self-energy of a packet of free electron waves which agrees in shape with the bound wave function. Alternative subtraction procedures will be discussed but rejected. One difficulty in the relativistic calculation is that at first sight the level shift seems to be of order αV where $\alpha=e^2/\hbar c$ and V is some average of the potential energy; moreover, this term still diverges logarithmically at high frequency. However, actually the term of order αV vanishes identically because the bound wave function satisfies the Dirac equation. There remain then terms of order $\alpha^2 V$, as in non-relativistic theory. The most important term depends on the wave function at the origin and shifts the s-levels only, but the spin-orbit coupling ($P_{3/2}-P_{1/2}$ splitting) is also changed, and levels like $d_{3/2}$ and $P_{3/2}$ in hydrogen will no longer coincide exactly.

Z9. The Electromagnetic Level Shift. F. J. DYSON, *Cornell University.* (Introduced by H. A. Bethe.)—Following a suggestion of Bethe, the shift of the energy levels of a one-electron atom due to the interaction of the electron with the radiation field has been calculated, using relativistic mechanics but ignoring the spin of the electron. The electron is represented as a particle of spin zero satisfying the relativistic Klein-Gordon wave-equation. Using Bethe's method of subtracting the self-energy of a free particle from that of the bound particle, the calculations give finite values for the level-shifts; owing to a certain arbitrariness in the subtraction prescription, these values are not uniquely defined, but the limits of ambiguity amount to only a small percentage of the predicted shifts. For the $2s-2p_{1/2}$ separation in hydrogen, the most plausible subtraction prescription gives a value of 1034 megacycles, in close agreement with Bethe's non-relativistic estimate and with experimental evidence. The calculations are less formidable than those for a Dirac electron; this is principally because the current operator of a slowly moving Klein-Gordon particle is uniformly small, whereas the Dirac α-operator always gives some matrix elements of magnitude comparable with unity. The quantities to be calculated are expanded in eigen-functions of the Klein-Gordon equation, and the non-orthogonality of these eigen-functions causes much less trouble than was anticipated.

Z10. On the Electromagnetic Shift of Energy Levels. JULIAN SCHWINGER, *Harvard University,* AND VICTOR WEISSKOPF, *Massachusetts Institute of Technology.*—A relativistic calculation of the electromagnetic shift of atomic energy levels, as observed by Lamb,* can be carried out on the basis of the hole theory of the positron. Two different methods are being used whose fundamental idea consists in the elimination of the infinite self-energy either by suitable subtraction of the free electron mass or by modifying the Hamiltonian to unite the electromagnetic mass with the mechanical mass of the electron. The effect of the polarization of the vacuum by the Coulomb field must be included in this calculation; however, the previous treatment of this effect by Uehling did not consider exchange effects. The two methods are equivalent and give rise to a finite value of the level shifts, the order of magnitude being the same as conjectured by Bethe.**

* Lamb and Retherford, Phys. Rev. 72, 241 (1947).
** H. A. Bethe, Phys. Rev. 72, 339 (1947).

Z11. Equations of the Neutrino. NATHAN ROSEN, *University of North Carolina.*—The neutrino, regarded as a particle having zero charge, zero rest-mass, and spin $\frac{1}{2}$, is usually described by means of the Dirac equations. This means that a neutrino field is described by complex functions. However, one would expect a wave field composed of neutral particles to be described by means of real functions. It is found that one can obtain a self-consistent formalism involving only real functions by means of a transformation from the usual Dirac formalism.[1] It appears that, with the description of the neutrino field by means of real functions, one can remove the difficulty in the neutrino theory of light associated with the arbitrariness of the phases of the complex functions used in the past.[2]

[1] I have learned that essentially the same thing was first done by E. Majorana, Nuovo Cimento 14, 171 (1937).
[2] M. H. L. Pryce, Proc. Roy. Soc. A165, 247 (1938).

Z12. Tensor Forces and the Binding Energy of the Triton. W. RARITA, *Brooklyn College,* AND H. FESHBACH, *Massachusetts Institute of Technology.*—The success of tensor forces in explaining the two body phenomena leads one to hope that the three particle nuclear problems can also be fitted into the theory. An important such problem is the triton binding energy. An initial attack was made by Gerjuoy and Schwinger,[1] using Gaussian wave functions. Instead we have introduced the more flexible Hylleraas expansion for the trial wave function which allows a more systematic improvement of the binding energy sought. Because of the sharp discontinuity in the rectangular potential the variational method here used may not be entirely reliable. Tests of the procedure used were made by applying it to the binding energy problem of the deuteron with tensor forces and also to the binding energy of the triton with a square well potential but without tensor forces. We estimate that the present theory assuming the same range and rectangular shapes for all the potentials will give at most but 60 percent of the experimental triton binding energy. We are investigating the sensitivity of this result to range and potential well shape.

[1] E. Gerjuoy and J. Schwinger, Phys. Rev. 61, 138 (1941).

Z13. Molecular Systems Containing a Positron. AADNE ORE,* *Princeton University.*—Recently Wheeler[1] has envisaged the existence of atomic or molecular systems which contain a positron, e.g., e^+Cl^-. Since the ordinary approximate methods of molecular or atomic theory are not well adapted to the problem of the dynamic stability of the new systems, information about this stability that can be obtained without elaborate calculations has been sought, (1) from experimental data descriptive of hydrides and molecular hydrogen and, (2) from previous calculations of the energy of light poly-electrons. Procedure (1) corresponds essentially to a variational treatment utilizing exact molecular wave functions. This method is refined by modifying these functions according to the virial theorem. While no molecular wave function is explicitly known the necessary matrix elements can be obtained from available spectroscopic data. The treatment suffices to guarantee stability only when the positron is replaced by a positive meson of mass of the order of twenty electron masses or more. Procedure (2) allows a lowering of these approximate minimum mass values, in a special case (e^+H^-) to a few electronic masses. The results do not exclude the systems envisaged by Wheeler.

* Frank B. Jewett Fellow.
[1] J. A. Wheeler, Ann. New York Acad. Sci. 48, 219 (1946).

Z14. Light *versus* Matter. GERTRUDE SCHWARZMANN.—The basic difference between the motion of light and that of matter is the independency existing between frequency and speed of light compared to the functional interdependency existing between frequency and speed of material entities. Conjoint to the speed v of electrons and protons are the frequencies $v^2 \cdot b/7.3$ and $252v^2 \cdot b$, respectively, where b stands for $\{(c^2-1^2)/(c^2-v^2)\}^{\frac{1}{2}}$. The speed of light c is an unattainable upper limit of the speed of particles and particle waves as the particle speed c is conjoint to the particle frequency infinite, unattainable upper limit of the frequencies of both, light and matter. From the viewpoint of this paper, based on the same assumptions as "Actual Mass and Inert Mass" in this issue, the mass equivalent to the energy of a produced or materializing photon is on one hand its own inert mass, on the other hand the inert mass of the dematerializing or produced particle pair. The variation of the frequency of material entities with b is prerequisite to a universe built up of four kinds of material entities and to the conservation of linear momentum on materialization and dematerialization respectively.

SUPPLEMENTARY PROGRAMME

SP1. A Precision High Voltage Vacuum-Tube Voltmeter.[1] * LUKE C. L. YUAN, *Princeton University.*—A vacuum-tube voltmeter circuit is described which is capable of measuring voltages within the range of from 0 to -5000 volts with an accuracy of 0.05 percent and a linear characteristic over the entire range. The input impedance is greater than 5×10^{10} ohms. The circuit was developed for the purpose of measuring accurately high voltage sources of extremely low current drain which were employed for cosmic-ray studies. It is based on a null method using a vacuum tube having a high amplification factor as one arm of a balanced circuit and a constant current source as the other arm. The negative terminal of the measured voltage is applied to the plate of the tube and the grid voltage is varied to maintain the same grid current which balances the current from the constant current source. Linearity results from the negligible varying space-charge effect at constant grid current, and high precision measurements are obtained by means of a special circuit for measuring the change in grid voltage. By setting the grid current equal to a value of $1/\mu$, where μ is the amplification factor of the tube, the meter can be made to read directly the measured voltage.

[1] This work was supported by the Office of Naval Research.
* To be called after Session H if time permits.

SP2. Electronic Polarizability of O^{--} in Presence of Ti^{+4}.* W. SHOCKLEY, *Bell Telephone Laboratories.*—Berberich and Bell[1] demonstrated that the high dielectric constant of TiO_2 does not require enormously high values for either electronic or atomic polarizabilities. However, the electronic polarizability, $\alpha(O^{--})$, is anomalously high in Ti compounds compared to other oxides. If $\alpha(O^{--})$, obtained from $(n^2-1)/(n^2+2)$ by subtracting Pauling's[2] cation values, is plotted *versus* volume per O^{--} ion, then values for Al, Be, Mg, Li, Ca, Sr, and Ba oxides fall near one line; Zn, Cd, and Hg about 20 percent higher and TiO_2 and $CaTiO_3$ about 80 percent higher. Data on dispersion indicates that the high values are not due to a small energy gap, but instead to a large sum of matrix elements; this large sum probably arises from the fact that optical excitation involves wave functions aroung the Ti^{+4} ion which can be made up of eight components involving $3d$, $4s$, and $4p$ of about the same energy, whereas for the other cases only four components such as $4s$, $4p$ are available.

* To be called after Session R if time permits.
[1] L. J. Berberich and M. E. Bell, J. App. Phys. 11, 681 (1940).
[2] L. Pauling, Proc. Roy. Soc. 114A, 181 (1927).

SP3. Reflection and Transmission of Electromagnetic Waves by Thin Curved Shells.* JOSEPH B. KELLER, *New York University.*—The equations and boundary conditions for the determination of the electromagnetic field in an infinite homogeneous medium containing a homogeneous obstacle of different material are transformed into two integro-differential equations for the electric and magnetic fields. These equations contain integrals over the obstacle surface and volume. When the obstacle is a shell of constant thickness the fields are expanded in powers of the thickness. The lowest order terms are just the incident fields, and recursion formulae can be obtained for the higher terms. The first-order terms, which give the field scattered by a thin shell, are obtained as surface integrals involving the incident field. These integrals are evaluated approximately, yielding explicit formulae for the scattered field. From the results the law of reflection is derived for curved shells; geometrical optics is obtained in the limit of zero wavelength; the mirror law, the focal length of a curved shell, and the conditions for the occurrence of point images and foci are deduced; the change of phase at a focus is found; the Rayleigh scattering law is obtained when the wave-length is long, etc. The result is compared with various exact solutions, and with the solutions of geometrical optics and of the Kirchhoff method.

* To be called after Session X if time permits.

SP4. Reflection and Transmission of Electromagnetic Waves by a Spherical Shell.* HERBERT B. KELLER AND JOSEPH B. KELLER, *New York University.*—Exact, explicit expressions are obtained for the field of a radiating periodic point dipole in medium 1 at the center of a spherical shell of medium 2, which is bounded by medium 3. The values of ϵ, μ, σ, and the shell radii are arbitrary. The reflected and transmitted fields are examined in various special cases.

When the shell radii become infinite, the thickness remaining constant, the fields agree with those obtained by R. K. Luneberg for the case of plane waves normally incident on a flat plate of medium 2 between media 1 and 3. When the radii are infinite and media 2 and 3 identical, the Fresnel formulae for normal incidence of plane waves on a plane interface between two half-infinite media are obtained. When the radii are finite, media 2 and 3 identical, and $\mu_1 = \mu_3$ the results of C. T. Tai are obtained. For finite radii, media 1 and 3 identical, and the shell thickness small compared to a wave-length, the fields check with the approximate results of J. B. Keller for the fields reflected and transmitted by a thin shell of any shape, when his results are specialized to the present case.

* To be called after session X if time permits.

SP5. Actual Mass and Inert Mass.* GERTRUDE SCHWARZMANN.—The corpuscles are pictured as thin rings of mass $m\mu^*$ and radius r^* spinning about one of the rings' diameter as spin axis so that their moments of inertia equal $\frac{1}{2}m\mu^* \cdot r^{*2}$. Interpretation of spin motion as full-fledged motion allows of introducing a kinetic energy of spin equal to that of linear motion of the independent corpuscles and of expressing the units of action (h in the case of matter, $(2h)$ in the case of light) as spin quanta. From these assumptions and those previously listed[1] the following conclusions may be drawn: Today's rest masses of electrons and protons are not their actual masses, but the inert masses of electrons and protons proceeding at velocity 1 cm/sec. The inert masses are quantities of motion, $h \cdot f/v^2$ and $(2h) \cdot f/c^2$ in case of particles and photons, respectively. Attributing to all corpuscles equal radius, to all particles equal mass, to all photons the mass of particle pairs, makes the ratio of the frequency to the linear velocity square the actual bearer of the particular particle nature of materiel entities in both corpuscle and wave state.

* To be called after session Z if time permits.
[1] G. Schwarzmann, Phys. Rev. **72**, 536 (1947).

TO BE READ BY TITLE

RT1. The Nature of Low Energy Radiation. BENJAMIN LIEBOWITZ, *350 Fifth Avenue, New York.*—The Birmingham conference last July " . . . made abundantly clear that the fundamental idea essential for further progress in physical theory is still lacking." (Quotation from Pryce, Nature **160**, 628.) I suggest that some currently accepted ideas might be profitably re-examined, particularly the corpuscular concept of radiation. Aside from theoretical difficulties arising from this concept, there is sound experimental evidence against it, for example, the "forgotten" photo-ionization of gases and vapors by *sub*energetic radiation. Furthermore, Schwinger's classical prediction of the betatron light and its recent experimental confirmation support the classical theory of *emission* from free electrons right into the visible region. The nub of the difficulty, therefore, lies in *absorption*. To account for absorption processes I have proposed a *post-concentration* conception according to which radiant energy before absorption is undulatory, i.e., *not* concentrated in "corpuscles"; but it becomes concentrated *after* absorption by rapid interchanges of energy among many electrons which, initially, are only feebly excited by the light. As a result of these interchanges, some electrons acquire sufficient energy to make transitions and/or to escape as photoelectrons. The possibility of such electronic interactions seems already implied in quantum statistics. At present, these remarks apply only to low energies.

RT2. The Effective Path Length through a Vertical Cosmic-Ray Telescope.* ENOS E. WITMER, *University of Pennsylvania,* AND MARTIN A. POMERANTZ, *Bartol Research Foundation.*—Previously reported calculations of the average path length traversed by a cosmic-ray particle through a vertical coincidence counter train have been extended to include the more general case of trays of any dimensions.[1] The earlier results were valid only for cosmic-ray telescopes in which the width of the individual trays was negligible in comparison with the length. Formulas have been obtained for the following distributions of cosmic-ray intensity with zenith angle θ: $\cos^2\theta$, $\cos\theta$, isotropic. From these, families of curves of $\bar{L}/L$ *vs.* l/L, with w/L as parameter have been plotted. Here $\bar{L}$ is the average path length, L is the separation between extreme trays, l is the length, and w the width of a tray. As an example, when $L = l = w$, $\bar{L}/L$ has a value of 1.094 for a $\cos^2\theta$ distribution. Details will be published shortly.

* Supported in part by Office of Naval Research.
[1] E. E. Witmer and M. A. Pomerantz, Bull. Am. Phys. Soc. (November 1947), Houston Meeting, Abstract F10.

RT3. Theory of the Damped Non-Linear Oscillator. M. AVRAMY MELVIN, *Columbia University.* Concrete examples are: loaded viscously damped non-linear springs, heavy gyros, a sliding boulder, avalanche, or skier on icy ground, automatic control systems, here considered more generally than in an earlier paper.* Steady states of zero motion and the approaches to them are described. Within the region of faithfulness to a given equilibrium position, the history of the oscillator is represented by a spiral in the velocity-position plane. This spiral may be bounded between two readily calculable comparison spirals beginning at the same initial point. In this way follow criteria for oscillation and over-damping, and the possible existence of any finite number of oscillations in the transient state of non-linear oscillators. A method is given by which the velocity-position plane may be sectioned into successive characteristic *oscillation number regions*, i.e., from which the number of oscillations to the steady state takes on successive half-integer values. Methods for setting upper and lower bounds of the number of oscillations and times required for the deviation to fall to any desired value are described. Several applications are given.

* M. Avramy Melvin, J. App. Phys. **18**, 704 (1947).

Author Index to Papers Presented at the New York Meeting

Alburger, David E.—No. D1
Allis, W. P.—See page 1239
Anderson, C. D.—See page 1238
Apker, L.—See page 1238
Arnold, Robert D. and Arthur F. Kop—No. F6
Arnott, E. G. F.—See page 1239
Arons, A. B.—No. J3
Bacher, R. F.—See page 1238
Baldwin, G. C. and G. S. Klaiber—No. U13
Benedict, D. L.—No. E15
Bennett, G. S.—No. Z3
Benzer, S.—No. K4
Bernstein, R. B. and T. I. Taylor—No. S3
Bethe, H. A.—No. Z8
Blatt, John M.—No. H4
Blewett, John P.—No. O2
Brady, Edward L. and Martin Deutsch—No. U11
Bragg, J. K.—No. G10
Breckenridge, R. G.—No. R9
Breit, G., A. A. Broyles, and M. H. Hull—No. D6
Brown, F. C.—No. K7
Brown, Harrison—No. D9
Brown, Sanborn C.—No. C4
Brown, S. Leroy and James M. Sharp—No. X3
Bundy, F. P.—No. X5
Burstein, E., P. L. Smith, and B. Henvis—No. R12
Callen, H. B.—No. F11
Clark, K. C.—No. G11
Cobine, J. D. and C. Gallagher—See page 1239
Collins, George B. and Rosalie C. Hoyt—No. O10
Cook, C. Sharp and Lawrence M. Langer—No. Y4
Coor, T. and G. A. Snow—No. H6
Corben, H. C.—No. Z2
Cox, E. F.—See page 1239
Cranberg, L. and J. Halpern—No. Y8
Danforth, W. E. and W. E. Ramsey—No. E7
Danielson, G. C.—No. F10
Daunt, J. G., R. E. Probst, and H. L. Johnston—No. S2
Davis, Kenneth E. and Everett M. Hafner—No. D7
Davison, Perry W.—No. D2
Davisson, J. W.—No. R8
DeBenedetti, S., J. E. Francis, Jr., W. M. Preston, and T. W. Bonner—No. U10
Dery, R. J.—No. X8
Deutsch, Martin—No. C6
Dienes, G. J. and Frederick Seitz—No. R4
DuBridge, L. A.—No. P1
Dyson, F. J.—No. Z9
Edwards, James W., Rudolph Speiser, and Herrick L. Johnston—No. G14
Elder, F. K., Jr.—No. S4
Emrich, R. J.—No. J15
Estermann, I.—See page 1239
Fairbank, Henry A., C. T. Lane, L. T. Aldrich, and Alfred O. Nier—No. S1
Farley, B. G.—No. C5
Finck, J. L.—No. X4
Fraunfelder, H., P. C. Gugelot, O. Huber, H. Medicus, P. Preiswerk, P. Scherrer, and R. Steffen—No. Y13
Friedlander, G. and M. L. Perlman—No. U12
Franck, James—See page 1238
Furry, W. H.—No. S5
Galginaitis, S. V.—No. E11
George, Waller—No. R13
Green, G. K.—No. O3
Havens, W. W., Jr., L. J. Rainwater, and C. S. Wu—No. U6
Haynes, S. K.—No. Y11
Heineman, M.—No. J8
Hereford, Frank L.—No. C3
Herlin, Melvin A. and Sanborn C. Brown—No. E10
Herring, Conyers—See page 1238
Hershberger, W. D.—No. G7
Herzfeld, K. F.—See page 1239
Hess, Victor Francis and J. Donald Roll, S.J.—No. C1
Hiller, James—See page 1239
Holstein, T.—No. E12
Holton, Gerald J.—No. X10
Honig, Richard E.—No. X1
Hoover, J. I., W. H. Jordan, C. D. Moak, L. A. Pardue, H. Pomerance, J. Strong, and E. O. Wollan—No. O7
Hubbell Harry H., Jr.—No. G13
Hughes, D. J. and C. Eggler—No. D8
Hull, G. F., Jr. and H. Saltzman—No. R10
Hulsizer, Robert I.—No. H9
Jacobs, Harold, George Hees, and Walter Crossley—No. E6
Jacobs, Harold and Armand P. LaRocque—No. E5
Jaffe, Hans—No. R6
Jen, C. K.—No. G2
Johnson, J. B.—See page 1238
Johnson, T. H., and R. P. Shutt—No. C8
Johnson, V. A. and K. Lark-Horovitz—No. K6
Jurney, E. T. and Allan C. G. Mitchell—No. Y5
Keller, Herbert B. and Joseph B. Keller—Nos. J7, SP4
Keller, Joseph B.—Nos. J6, SP3
Kern, Bernard D., Daniel J. Zaffarano, and Allan C. G. Mitchell—No. Y3
Ketelle, B. H. and W. C. Peacock—No. Y9
Keyes, Kenneth E.—No. R2
Kikuchi, C.—No. Z4
Kip, Arthur F. and Robert D. Arnold—No. F5
Kolstad, G. A., H. L. Schultz, and C. G. Montgomery—No. O5
Lachenbruch, S. H.—No. E4
Lark-Horovitz, K., E. Bleuler, R. Davis, and D. Tendam—No. K3
Lax, M. and H. Feschbach—No. Z7
Leverenz, H. W.—See page 1238
Lewis, Margaret N. and Miriam Paul—No. Y7
Liebowitz, Benjamin—No. RT1
Lindsay, R. B.—See page 1239
Livingston, M. Stanley—No. O1
Lord, J. J. and Marcel Schein—No. H3

McConaghie, Virginia M. and Harald H. Nielsen—No. G9
McGowan, F. K. and S. DeBenedetti—No. Y10
McKay, K. G.—See page 1238
McMillen, J. Howard and R. L. Kramer—No. J14
McReynolds, Andrew W.—No. R11
Mandeville, C. E. and M. V. Scherb—No. Y12
Markham, J. J. and F. Seitz—No. R3
Mapother, Dillon and Robert Maurer—No. R1
Marton, L.—No. E2
Matthias, B. T. and A. von Hippel—No. R5
Meaker, C. L., C. S. Wu, and L. J. Rainwater—No. C7
Melkonian, Edward—No. U7
Melvin, M. Avramy—No. RT3
Merritt, F. R. and C. H. Townes—No. G4
Meyer, Herbert M.—No. R15
Miller, William—No. K9
Millett, Walter E.—No. O9
Moore, Wm. H. and John P. Blewett—No. O4
Morse, P. M.—See page 1238
Mouzon, J. C.—No. X6
Munk, M. M.—No. J9
Nafe, John E. and Edward B. Nelson—No. D11
Nemenyi, P. and R. Prim—No. J12
Nesbitt, E. A. and H. J. Williams—No. F1
Nottingham, W. B.—See page 1238
Opatowski, I.—No. J1
Ore, Aadne—No. Z13
Pake, G. E.—No. F9
Parker, W. L.—See page 1239
Parsegian, V. L., L. V. Titone, and C. W. van der Merwe—No. U9
Parzen, Philip—No. X9
Pearson, G. L. and J. Bardeen—No. K1
Peck, R. A., Jr.—No. U1
Perl, W.—No. J5
Pollard, Ernest, and Perry W. Davison—No. D3
Pollock, H. C., F. R. Elder, and R. V. Langmuir—See page 1238
Pomerance, H. and J. I. Hoover—No. U8
Pomerantz, Martin A.—No. H10
Posin, D. Q.—No. E9
Pound, R. V.—No. F8
Power, A. D.—No. E14
Prim, R.—No. J13
Rainwater, L. J., W. W. Haven, Jr., and C. S. Wu—No. U5
Ramsey, Norman F.—No. D12
Ramsey, W. E. and W. E. Danforth—No. E13
Rarita, W. and H. Feshbach—No. Z12
Raymond, Richard C. and Wayne Webb—No. G1
Reverdin, D. L., L. Marton, and S. H. Lachenbruch—No. E3
Richardson, J. M.—No. R7
Rose, M. E.—No. D5
Rosen, Nathan—No. Z11
Rothstein, Jerome—No. E8
Safford, Richard W.—No. C9
Sard, R. D. and E. J. Althaus—No. H1
Scanlon, Wayne and K. Lark-Horovitz—No. K5
Schaaf, S. A. and R. R. Cyr—No. J2
Schein, Marcel—No. C2
Scherb, M. V. and C. E. Mandeville—No. Y2
Schultz, H. L., J. A. Lockwood, R. L. McCarthy, and P. J. Rice—No. O6
Schwarzmann, Gertrude—Nos. Z14, SP5
Schwinger, Julian—See page 1238
—— **and Victor Weisskopf**—No. Z10
Scott, W. T. and H. S. Snyder—No. O11
Seitz, Frederick—See page 1239
Shapiro, Maurice M. and John R. Barnes—No. D13
Shockley, W.—Nos. F2, SP2
Shull, C. G., M. C. Marney, and E. O. Wollan—No. U4
Sidhu, S. S.—No. U3
Siegert, A. J. F.—No. Z5
Sleator, William, Jr., J. M. Blair, E. E. Lampi, and J. H. Williams—No. D4
Smith, A. H. and P. H. Miller, Jr.—No. K2
Smith, Lloyd P.—See page 1238
Smoluchowski, R.—See page 1239
Snoek, J. L.—See page 1239
Sommers, H. S., Jr., P. R. Weiss, and W. Halpern—No. E1
Spence, R. D.—No. X7
Spitzer, Lyman, Jr.—See page 1239
Stalder, J. R. and David Jukoff—See page 1239
Stephens, William E. and A. M. Bottoms—No. Y6
Strandberg, M. W. P. and T. Wentink, Jr.—No. G5
Swann, W. F. G.—No. Z1
Sydoriak, S. G.—No. F4
Taylor, W. J.—No. R14
Tittle, C. W. and Clark Goodman—No. U2
Townes, C. H., B. D. Wright, and F. R. Merritt—No. G3
Truesdell, C.—No. J11
Tsien, Hsue-Shien—See page 1239
Turkevich, John and Harry H. Hubbell, Jr.—No. G12
Uhlenbeck, G. E.—See page 1239
Valley, G. E.—No. H2
Van Vleck, J. H.—No. G8
von Hippel, A.—No. K8
Webber, Robert T. and J. M. Reynolds—No. S6
Weinstein, Alexander—No. J10
Welton, T. A.—No. Z6
Wentink, T., Jr., M. W. P. Strandberg, and R. Hillger—No. G6
Wheeler, J. A.—No. H8
Wilchinsky, Zigmond W.—No. G15
Williams, Ferd E.—No. K10
Williams, H. J.—See page 1239
—— **and R. M. Bozorth**—No. F3
Williams, Robert W.—No. H5
Witmer, Enos E.—No. D10
—— **and Martin A. Pomerantz**—No. RT2
Wu, C. S., W. W. Havens, Jr., R. Albert, and G. Grimm—No. O8
Yager, W. A.—No. F7
Yennie, D. R. and A. B. Arons—No. J4
Yu, Fu-Chum and J. D. Kurbotov—No. Y1
Yuan, Luke C. L.—No. SP1